TASMANIAN SLOPE TROPHODYNAMICS: FINAL REPORT

J.PARSLOW, J.A.KOSLOW, F.B. GRIFFITHS, L. CLEMENTSON

C.RATHBONE, P.BONHAM, D.MCKENZIE

CSIRO DIVISION OF FISHERIES

FRDC PROJECT 91/17

CSIRO
AUSTRALIA

DIVISION OF **FISHERIES**

SUMMARY

This study was designed to improve understanding of the ecological basis of the deep water stocks, especially orange roughy, fished on the continental slope in Tasmanian waters. The study was designed to identify and quantify the food chain linking deep water stocks to surface production, and to study seasonal and interannual change in the ocean environment, and its effects on surface production and the links to the demersal fisheries.

A series of 4 cruises were conducted on the slope south of Tasmania, thought to be the major feeding site for orange roughy stocks. On each cruise, 2 to 3 oceanographic transects (oriented south-west, central and south-east) were conducted from the outer shelf across the slope to deep water (Fig. 1). Measurements along each transect mapped the physical and chemical structure of the water column, and phytoplankton biomass and production. At a trawl site near the 1000 m contour on the central transect, repeated tows with opening-closing plankton nets and midwater trawls, and a demersal trawl, were used to monitor diel changes in the vertical distribution of the mesozooplankton and micronekton communities, and to sample the demersal community. Moored and free-floating sediment traps measured the vertical flux of particulate material at the trawl site.

A set of ca 3000 satellite images were processed to produce monthly composite sea surface temperature images over the period 1990-1993, to identify seasonal and interannual changes in circulation and water properties and provide a context for the cruises. The summer pattern (Jan, Feb, Mar) is dominated by a flow of warm, "East Australia Current" (EAC) water south along the slope on the east coast. This warm water generally leaves the slope south-east or south of Tasmania, is entrained into mesoscale eddies, and can be carried well south of Tasmania, reaching 47°S. Mesoscale or large scale circulation can bring cool subantarctic water to the slope and shelf in the south-west and south. Autumn months (Apr, May, Jun) see seasonal cooling, and the retreat of the EAC warm tongue. The Zeehan Current, which brings warm water down the west coast of Tasmania in winter, is generally established by June, and is usually present throughout winter (Jul, Aug, Sep). In spring, temperatures increased in November and December due to local warming and southward movement of warm EAC water on the east coast.

Interannual variation during 1990-1993 was dominated by a cold period from October 1991 to November 1992. This cold period was characterised by broad cooling over the ocean around Southern Tasmania, and a weakened influence of both the EAC and Zeehan Currents in the study area.

Below 300 m, the physical oceanographic sections across the slope were dominated by SubAntarctic Mode Water (typically 300m to 700 m) and Antarctic Intermediate Water (typically 800 m to 1200 m). The depth, thickness and properties of these layers varied significantly across cruises, and substantial changes in deep current direction and magnitude were indicated by changes in the slope of density contours.

Above 300 m, the ocean environment showed large seasonal changes. The structure in winter (Jul, 1991) was dominated by the Zeehan Current, present as a core of deeply mixed saline water, concentrated on the shelf break in the south-west, but expanding inshore and offshore as a broad pool in the south-east. In spring (Nov, 1994), seasonal stratification produced shallow mixed layers with high nutrients, leading to a spring bloom throughout much of the study area. In summer (Feb, 1992), nutrients and chlorophyll were still high in the south-west, but a pool of saline EAC water with low nutrients and chlorophyll covered much of the central transect. In autumn (Apr, 1993), seasonal cooling had deepened the mixed layer and increased surface nutrients, leading to a modest autumn bloom throughout the study area. Mesoscale features affected nutrient and chlorophyll distributions in all seasons, and there was often evidence of upwelling at the shelf break.

Estimated phytoplankton production was minimum in winter (about 300 mg C m^{-2} d^{-1}) and maximum in spring (up to 2 g C m^{-2} d^{-1}). These maximum values, associated with the spring bloom, compare well with highly productive coastal upwelling systems. The estimated annual production (ca 300 g C m^{-2} y^{-1}) was 3 times higher than historical estimates for these waters. The sediment traps indicated relatively low export efficiencies through 200 m (ca 10% of net primary production), but similar fluxes through 650 m. A moored sediment trap showed much lower absolute fluxes reaching the bottom, with peak fluxes during the spring and autumn blooms.

A simple trophodynamic model based on phytoplankton, zooplankton and micronekton indicated a balanced ecosystem, with secondary production of ca 15 gC m^{-2} y^{-1} and tertiary (micronekton) production of ca 0.5 gC m^{-2} y^{-1}. Sinking particulates, seasonal migration of zooplankton (Neocalanus), and diel migration of micronekton appeared to be equally effective in supporting tertiary production below 500 m. This production is sufficient to support the demands of the local demersal biomass at the trawl site (ca .05 gC m^{-2}). However, the orange roughy stock (pre-fishery), distributed over the slope south of Tasmania, has an average density ca 100 times this figure. The roughy stock, distributed as dense aggregations on pinnacles, feeds on mesopelagic micronekton advected past pinnacles. Our data indicate that the stocks on the slope must draw on advected micronekton representing tertiary production from an ocean area 10 to 100 times the area of the continental slope. The surrounding ocean waters (part of the Sub-Tropical Convergence Zone) are known to be productive: our offshore primary production estimates were similar in magnitude to those obtained on the slope.

One might expect stock-stock competition to be less intense in an open system of this kind, than in a system depending on local production. One might also expect orange roughy to respond to interannual changes in broad-scale ocean production and/or circulation patterns around and across the continental slope.

BACKGROUND.

This project was conceived in 1990, when the orange roughy fishery was in an early stage of high exploitation, and many aspects of the stock structure and dynamics were still controversial. The mid-slope component of the South-east Fishery (SEF) has changed substantially over the last five years. Long-term sustainable quotas for the orange roughy fishery have been imposed, based on biomass surveys and stock assessment carried out by CSIRO Division of Fisheries. There is still some uncertainty about the size and extent of orange roughy stocks, and the link between the winter spawning aggregations off St Helens and the summer feeding aggregations on the slope south of Tasmania. As orange roughy quotas have been reduced, there has been increased targeting of other mid-slope stocks such as dories.

In 1990, very little was known about the ecological or trophodynamic basis of these mid-slope fisheries. There had been studies of the slope ecology on the east coast of Tasmania (Bulman and Blaber, 1986; Young and Blaber, 1986; Blaber and Bulman, 1987; May and Blaber, 1989), intensive studies at a site in Storm Bay on the south-east shelf (Clementson *et al*, 1989; Harris *et al*, 1991), and studies of oceanography and blue grenadier on the west coast of Tasmania (Gunn *et al*, 1989), but little or no work on the slope south of Tasmania, except for observations obtained during the original orange roughy trawl survey (Bulman and Koslow, 1992). In a comprehensive study, one would ideally like to understand the oceanographic environment of the fishery, and its seasonal and interannual variation, the way in which this oceanographic forcing affects primary production and the ecosystem in the upper water column over the shelf and slope, and the coupling between this ecosystem and the mid-slope community supporting commercial stocks. A comprehensive study of this kind would require many research scientists, and a large amount of ship time.

This study has addressed the ecological basis of the mid-slope stocks south of Tasmania, using relatively limited resources, by piggy-backing on biomass assessment cruises. It was originally proposed to conduct comparable studies on the slope north-east of Tasmania, as well as south of Tasmania, but given limited ship-time and resources, it was decided to restrict work to the slope south of Tasmania. The region south of Tasmania appears to be the primary centre for feeding aggregations of orange roughy.

The slope south of Tasmania arguably represents one of the most complex oceanographic environments in Australia. The ocean surrounding Tasmania forms part of the Sub-Tropical Convergence Zone, a broad frontal region between the subtropical gyres and the waters of the Southern Ocean (Harris *et al*, 1992, 1993). It is characterised by intense oceanographic fronts (the Subtropical Front(s) and SubAntarctic Fronts) which have basin or circumglobal extent (McCartney, 1977; Harris *et al*, 1993). There is strong mesoscale variation

associated with meandering of these fronts (Harris *et al*, 1993). This is a region with a temperate as opposed to sub-tropical seasonal cycle: there is a strong seasonal cycle in mixed-layer physics and chemistry, with deep mixing and elevated surface nutrients in winter, and summer stratification (Harris *et al*, 1987). This is also a region of strong interannual variability, apparently associated with changes in wind forcing and frontal positions (Harris *et al*, 1988).

The oceanography on the shelf and slope is further complicated by two boundary currents. On the east coast of Tasmania, a stream of warm saline water, thought to be an extension of the East Australian Current (EAC), flows south along the slope, reaching further south in summer. On the west coast, a winter current (the Zeehan current, sometimes referred to as an extension of the Leeuwin Current) transports warm, saline water south along the shelf break. The slope south of Tasmania can be expected to see an influence of these two warm currents, combined with offshore water, all subject to stirring by mesoscale features associated with ocean fronts and bathymetry, as well as seasonal and interannual variation.

This study has adopted a trophodynamic approach, focusing on primary production in shelf and slope waters, and the food chains which transfer this production to the demersal fisheries on the mid-slope. At the beginning of the study, we quoted general regional estimates of annual primary production of about 100 gC m^{-2} y^{-1} (Harris *et al*, 1987). Studies conducted as part of the Southern Program found very high biomasses of nekton (500 g m^{-2} wet weight myctophids: May and Blaber, 1989) and benthic invertebrates (50 g m^{-2} wet weight of brittle stars: Blaber *et al*, 1987) on the upper slope east of Tasmania. These biomass densities seemed very large compared with annual primary production estimates, given typical food chain transfer efficiencies.

Similar discrepancies arose in preliminary assessments of orange roughy biomass and energy requirements. Early estimates suggested a pre-fishery spawning biomass of ca 1 to 200000 tonnes. Distributed over the east coast Tasmanian slope between 700 and 1500 m, this represents a biomass of ca 30 g m^{-2}, much higher than observed on orange roughy grounds in New Zealand (ca 3 g m^{-2}). Moreover, preliminary evidence (since confirmed) suggested that orange roughy do not have the low metabolic rates that might be expected of fish living at 1000 m. Organic matter can reach the slope community from the surface production zone either by vertical flux of sinking organic matter, or by transfer through a series of vertically migrating predators. By either route, one would not normally expect a high transfer efficiency from the surface to the bottom at mid-slope.

NEED

Part of the need described in the original study was to use trophodynamic calculations to provide a guide to the potential productivity and sustainable yield of orange roughy. This has largely been overtaken by developments in terms of acoustic biomass assessment, ability to age roughy, and the refinement of stock dynamics models for roughy (eg 1995 SEF Stock Assessment Report). This study should now be seen primarily as providing strategic information towards the ecologically sustainable development of the mid-slope fishery. This contribution falls into three major areas. It was not clear a priori to what extent the slope community is supported by local surface production. This has been addressed by quantifying production in surface waters, and the pathways and efficiency involved in its transfer to depth. The fishery occurs in a region of strong seasonal and interannual variability, but the effect of these on slope ecosystems was unclear. The study has documented seasonal and interannual changes in the oceanographic environment, providing an improved basis for interpreting any observed changes in fish abundance, distribution and community composition. The slope fishery is a classic multi-species fishery, with potential for stock-stock interactions, especially as the fishery targets a range of stocks. An understanding of the overall energetic constraints on the community, and diets and trophic interactions among species within the community, provides a basis for consideration of stock-stock interactions.

The study has addressed these needs for both oceanographic and trophodynamic knowledge by conducting a series of 4 seasonal cruises over the continental shelf and slope south of Tasmania. On these cruises, we measured physical, chemical and biological variables along three sections oriented onshore to offshore. We have used sea surface temperature (SST) images to interpret and interpolate among the *in-situ* data, and to examine interannual variability. We have sampled zooplankton and nekton in a depth-stratified manner on all cruises, and examined links via diet. We deployed multi-sample moored sediment traps, and free-floating sediment traps to look at the vertical flux between the surface and deep water.

OBJECTIVES.

The original objectives were:
1. To identify and quantify the food chain supporting deep-water stocks of the South-East Trawl.
2. To assess the implications of the trophodynamic system, and its dependence on oceanographic forcing, for impacts of climate variability and climate change on stock dynamics, and for stock-stock interactions, in the SET.

As noted above, the study, and therefore domain of the objectives, have been restricted to the slope south of Tasmania.

13 July 1991   20-22 Feb 1992
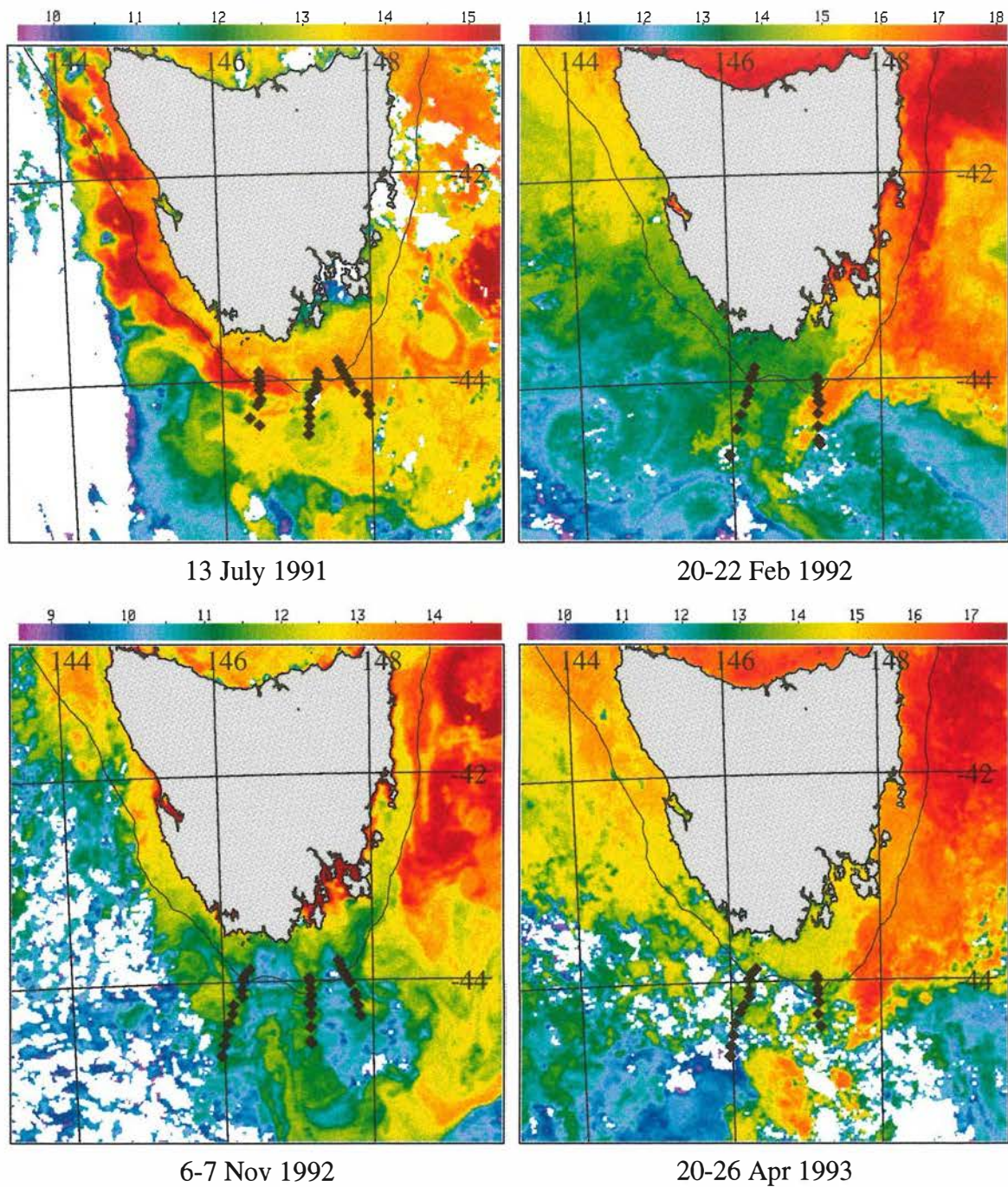
6-7 Nov 1992   20-26 Apr 1993

Fig. 1. Satellite composite SST images for the 4 cruises: (A) SS2/91 (B) SS1/92 (C) SS4/92 (D) SS3/93. Black diamonds indicate station positions on oceanographic transects. Note that the temperature scale differs among images.

METHODS.

The overall strategy of the study was to combine data from cruises, from moorings and from satellite sensors. Four cruises were conducted on FRV *Southern Surveyor* in July 1991 (SS2/91), February 1992 (SS1/92), November 1992 (SS4/92) and April 1993 (SS3/93). We expected considerable mesoscale variation within the study region (Harris et al, 1993), and the oceanographic sampling within cruises was designed to resolve this variation as well as possible within the constraints of ship time. On each cruise, we attempted to carry out 3 transects from the outer shelf to beyond the 2500 m contour, with 8 to 10 stations on each transect. These transects are referred to as the western transect, through the Matsuuyker region, the central transect (through the Pedra Blanca region) and the eastern transect (see Fig. 1). Loss of time due to bad weather meant that the eastern transect was dropped in February 1992 and April 1993. The western transect was shifted further west and extended after the first cruise, so that it joined up to the northern end of the Southern Ocean WOCE SR3 transect conducted on *Aurora Australis*. The station positions for each cruise are indicated in Fig. 1.

A trawl site at 44°12'S, 147°10'E, at ca 1000 m depth on the Pedra Blanca transect, was occupied on all four cruises. A 24 h study of diel variation in photosynthesis parameters was conducted there, and on the last 2 cruises, a free-floating sediment trap array was deployed at this station for 24 h. Stratified oblique tows from near bottom to the surface were conducted with a multiple opening-closing (EZ) zooplankton net, and a multiple opening-closing midwater trawl. Plankton and nekton samples were analyzed for total biomass, taxanomic and size composition, and a subset of the dominant nekton species were reserved for gut analysis. These plankton and nekton tows/trawls were repeated over a 24 h period to look for evidence of diel vertical migration, and diel variation in feeding.

A sediment-trap current-meter array was deployed near the trawl site. The traps were McLane Parflux multiple-sampling traps with rotating collector able to acquire up to 18 sequential samples over a 12 month period. The mooring was deployed on three separate occasions. Between February 1992 and November 1992, the mooring was deployed with one sediment trap (at 700 m) and two current meters. The mooring was fouled during that deployment, and both current meters failed. The sediment trap also failed, due to an electronic fault in manufacture. The array was redeployed in November 1992, with one new trap at 950 m, and the old trap at 200 m. The new trap (at 950 m) worked during this period, but unfortunately the fault in the original trap was only reported to us after this deployment. Both traps were recovered, repaired and redeployed in April, 1993, and scheduled for recovery in February 1994. This mooring was

lost. The net outcome of these attempts was ca 6 months of sediment flux data at 950 m between November 1992 and April 1993.

NOAA AVHRR satellite data received in Hobart over the period 1990 to 1993 was processed to sea surface temperature on a standard map projection, and composited to provide "cloud-free" monthly SST images (Fig. 2). Images collected over a shorter period during each cruise were composited to provide a background for the *in situ* data (Fig. 1).

Detailed methods describing the collection and analysis of field samples, and the statistical analysis of data, are given below.

CTD SAMPLING

Water samples were collected using a General Oceanics rosette equipped with 8 litre Niskin bottles and a NBIS Mk. IIIB CTD with 16 channel digitiser and altimeter. At least 2 Niskin bottles were equipped with reversing thermometers for each CTD profile. At primary production stations, profiles of downwelling photosynthetically available irradiance (PAR) and *in situ* fluorescence were obtained using a Biospherical Instruments QSP-200 underwater 4π quantum sensor and a SeaTech *in-situ* fluorometer respectively. Both instruments were mounted on a frame along with a Seabird SBE-19 CTD, and deployed from the hydro winch, generally within 30 minutes of the corresponding CTD cast.

SALINITY AND DISSOLVED OXYGEN

Samples for dissolved oxygen were preserved with Winkler reagents on collection and analysed later during the cruise. Both salinity and dissolved oxygen were measured using the methods of Major *et al.* (1972).

NUTRIENTS

Unfiltered nutrient samples were collected in 15 ml polypropylene tubes with screw caps (Disposable Products, Australia). The tubes were used as received from the manufacturer and rinsed twice with sample seawater. All samples were analysed during the cruise using a Tecnicon AA-II auto-analyser. To maintain consistency in the analysis procedure all samples were initially frozen (-20°C) for 24 - 48 hours before analysis. Full details of the analytical methods used for inorganic phosphorus and silicate can be found in Airey and Sandars (1987).

Filtered nutrient samples were pressure filtered through acid-washed 0.45 µm (47 mm Millipore HA) filters, using acid-washed polycarbonate filter units. Approximately 250 ml of sample was filtered and discarded before a further aliquot of sample water was filtered and retained for analysis. All nutrient samples were stored in acid-washed high-density polyethylene bottles at -20°C

until analysed by flow injection analysis. Full details of the analysis for inorganic N and P can be found in Clementson *et al.* (1989) and for total N and P in Harris *et al.* (1991).

CHLOROPHYLL

At least 4 litres of sample seawater was filtered through a 47 mm glass-fibre filter (Whatman, GF/F). For samples collected during cruises SS2/91 and SS1/92 the filters were then folded in half, wrapped in aluminium foil and stored at -20°C and -70°C respectively, until analysis. Samples from cruises SS4/92 and SS3/93 were folded in half and stored in cryo-tubes in liquid nitrogen until analysis. Samples from all cruises, except SS1/92, were extracted in 90% acetone and analysed using the spectrophotometric equations of Jeffrey and Humphrey (1975) with a Shimadzu UV-240 spectrophotometer. Samples collected during SS1/92 were extracted in 90% acetone and analysed using the HPLC method of Wright *et al.* (1991) with a Waters 660E system controller and 990 photo-diode array detector and a Gilson 401 dilutor and sample controller and 232 sample injector.

PARTICLE SIZE SPECTRA.

Samples for particle size analysis were taken from the same Niskin bottles as the samples for chlorophyll analysis and primary production estimates. Size spectra were determined within 2 hours of the rosette coming on deck, and samples were stored in the dark in insulated containers until analysed. The size distribution and abundance in each size class were obtained using a Hiac Royco model 320, 9 channel particle size analyser, an automatic bottle sampler and a HR 60 sensor using the same procedures as Harris *et al* (1987). The size class midpoints (equivalent spherical diameters, esd) were 2.68, 3.92, 5.75, 8.45, 12.40, 18.21, 26.73 and 39.23 µm esd. Particulate carbon was calculated for particles $< 5.57 \mu m$ and > 5.75 µm equivalent spherical diameter (esd) (Chavez, 1989) using a conversion factor of 0.142 pg C μm^{-3} of phytoplankton volume (Jorgenson, 1979). As the particle size technique does not distinguish detritus from phytoplankton, the carbon estimates should be taken as indicative only.

MOORED SEDIMENT TRAP

Samples were collected using McLane PARFLUX Mark 7G-21 time-series sediment traps. Before deployment, sample containers on each trap were acid washed (10% HCl), rinsed three times with "Milli-Q" water and filled with 10% NaCl solution which contained 400 mg/L $HgCl_2$ (3 mM $HgCl_2$) .

The sediment traps were deployed on 9 November 1992 at 44°12.25´S, 147°05.35´E. The traps were placed on a single mooring at 305 and 952 m below the surface in a water column 1022 m deep. The shallower of the two

traps malfunctioned and did not collect any samples. The deeper trap collected all samples and the dates and duration of the sampling periods are given in Table 1.

Upon recovery of the traps (10 April 1993), sample containers were removed, sealed and stored at 4°C until the samples could be split. Prior to splitting each sample, 2/3 of the density/preservative solution was syphoned off and retained for washing the sample during the splitting process. The sample and remaining density solution was then wet sieved through a 1 mm mesh nylon sieve resulting in two fractions, <1 mm and >1 mm. Material in the >1 mm size fraction was picked from the sieve with forceps and sorted by size into 4 replicates. Each replicate was stored in the original preservation solution in a pre-combusted glass scintillation vial at 4°C till analysis. Immediately prior to an analysis "swimmers" were removed from the samples and stored in Steedman's preservative solution. The samples were then washed three times with "Milli-Q" water, to remove residual salt and $HgCl_2$, dried, weighed and analysed.

TABLE 1. THE SAMPLE PERIODS AND DURATIONS FOR THE MOORED SEDIMENT TRAP.

TRAP PERIOD	OPEN DATE	CLOSURE DATE	DURATION (D)
1	9/11/92	16/11/92	6.77
2	16/11/92	22/11/92	6.77
3	22/11/92	29/11/92	6.77
4	29/11/92	6/12/92	6.77
5	6/12/92	13/12/92	6.77
6	13/12/92	20/12/92	6.77
7	20/12/92	26/12/92	6.77
8	26/12/92	2/1/93	6.77
9	2/1/93	9/1/93	6.77
10	9/1/93	16/1/93	6.77
11	16/1/93	22/1/93	6.77
12	22/1/93	29/1/93	6.77
13	29/1/93	5/2/93	6.77
14	5/2/93	12/2/93	6.77
15	12/2/93	19/2/93	6.77
16	19/2/93	25/2/93	6.77
17	25/2/93	4/3/93	6.77
18	4/3/93	11/3/93	6.77
19	11/3/93	18/3/93	6.77
20	18/3/93	25/3/93	6.77
21	25/3/93	31/3/93	6.77

After the >1 mm fraction was sorted, the sieve was washed with the original preservation solution and the washings added to the <1 mm fraction, which was then wet split into 4 replicates using a McLane PARFLUX wet sample divider. Three of these replicates were then each split again into 4 replicates. All replicates were stored in original preservative solution in acid-washed polycarbonate sample bottles (30 ml) at 4°C until analysis. Immediately prior to an analysis the samples were washed three times with "Milli-Q" water, to remove residual salt and $HgCl_2$, dried and weighed.

FREE-FLOATING SEDIMENT TRAPS

The free-floating sediment traps used were similar to the "MULTITRAPS" described in Knauer *et al.* (1979) and Martin *et al.* (1987). The traps consisted of 8 identical polycarbonate cylinders (ca 4.5 L capacity) without a baffle system in the top of the cylinder and with conical shaped collection cups, mounted on a stainless steel crossframe.

Prior to deployment the traps were washed with a 0.1% solution of "Triton X-100" detergent, rinsed well with "Milli-Q" water before a further washing with 10% HCl. The traps were then rinsed at least 3 times with "Milli-Q" water and capped with specially made polycarbonate lids, until needed. Within 6 hours prior to deployment each cylinder was filled with density solution (270 g NaCl in 4 L of filtered seawater).

The free-floating sediment traps were deployed on two occasions with details of deployment summarized in Table 2. Upon retrieval of the traps, cylinders were removed from the crossframe and placed on racks. The contents of each cylinder was then vacuum filtered through a precombusted, preweighed 47 mm glass-fibre filter (Whatman, GF/F), except for the SEM sample which was collected on a polycarbonate membrane filter (Poretics, 0.4 µm). Samples collected for carbonate, reactive P, total C and N and SEM analysis were stored flat in clean polycarbonate filter holders at -20°C. Samples for pigment analysis were stored in liquid nitrogen.

TABLE 2. DETAILS OF DEPLOYMENT AND RECOVERY FOR FREE-FLOATING SEDIMENT TRAPS.

DATE OF DEPLOYMENT	DATE OF RETRIEVAL	DURATION OF DEPLOYMENT	POSITION OF DEPLOYMENT	POSITION OF RETRIEVAL	DEPTH OF TRAPS (M)
7/11/92	8/11/92	25 h	44°11.5´S, 147°01.7´E	44°09.3´S, 147°18.7´E	200, 650
18/4/93	20/4/93	43 h	44°09.05´S, 147°11.2´E	43°53.07´S, 146°21.08´E	200, 650

CHEMICAL ANALYSES OF SEDIMENT TRAP SAMPLES

Carbonate/organic matter samples were decalcified using 0.5 M HCl as described in Honjo (1980). Washed and dried samples were analysed for total C and total N using a Perkin Elmer 240C Elemental Analyser. Samples were analysed for reactive P and biogenic opal using the methods described in Honjo and Manganni (1992).

PHOTOSYNTHESIS VS IRRADIANCE STUDIES

Primary production estimates were made using a small bottle technique modified from Lewis and Smith (1983). Two different procedures were used. At the central Trawl Site, four or five casts were made ca 6 h apart over 24 h to obtain diel coverage. From each cast, samples were taken from 6 depths, and triplicate subsamples incubated at each of 7 nominal light intensities ranging from zero to between 350-600 μmoles m^{-2} sec^{-1}, to obtain a photosynthesis vs irradiance (PvsI) curve. In this report, these experiments are called "full" PvsI incubations. On the cross-shelf transects, a "short" PvsI incubation at three depths and four light intensities was carried out because of the short time interval between stations. In the short PvsI incubation, triplicate samples were incubated in the dark, and one at each of the 6 lowest light intensities (range 5-30 μmoles m^{-2} sec^{-1}) to obtain an estimate of α, the initial slope of the P-I curve. Triplicate subamples were incubated at a higher light intensity (range 160-300 μmoles m^{-2} sec^{-1}) to obtain estimates of P_m, the light-saturated rate of carbon fixation. Otherwise, samples in both short and full PvsI experiments were treated as described below.

The incubator used was constructed of white acrylic, and used Cool Daylight fluorescent tubes (Philips TLD 36W/54) as a light source. The incubator was made in three sections. The light bank formed the base of the incubator, with the tubes running lengthwise along the incubator. The middle section was clear perspex with channels along it to hold neutral density strips (Roscosun 50 % neutral density filter) which served to attenuate the light intensity nearly equally across all wavelengths. The top section was a water-cooled box, separated into 7 channels lengthwise, with each section sitting above a fluorescent tube. Each channel had 21 acrylic cups glued into the top panel. These cups protruded down into the channel and were immersed in running surface seawater to control the temperature during the incubation. Each channel was at a different nominal light intensity which was adjusted by varying the number of neutral density strips in the middle section. The light intensity in each cup was measured by immersing the 4π sensor from a Biospherical Instruments QSL-100 quantum meter into a scintillation vial containing 7 ml of seawater in each position. Because of the white acrylic used in the construction, and the reflection of light from the sides of the channels and the top of the incubator, each vial would have received nearly omnidirectional light. The nominal intensities used for the normal P-I incubations were 8, 15, 30, 60, 160, and >350 μmoles m^{-2} sec^{-1}. One additional channel was completely light-tight, and served to act as the dark control for each incubation. The nominal light intensities for the short incubations have been detailed above. The temperature in a vial during the incubations was within 1.0 °C of sea surface temperature.

At primary production stations, water samples for nutrients, chlorophyll determinations, particle size distribution and carbon fixation rates were taken from Niskin bottles at three to six depths. The Niskin bottles used the standard General Oceanics neoprene o-rings and tubing: they had not been retrofittted with silicone o-rings and tubing (Chavez and Barber, 1987).

Water samples were gently siphoned from the Niskin bottles into 500 ml polycarbonate jars, and immediately placed in a closed, insulated box. Great care was taken to minimise agitation of the samples in an attempt to reduce damage to fragile phytoplankton which can lead to increased uptake of ^{14}C in the dark (Harris et al. 1989). All laboratory manipulations were done in dim light. In the laboratory, sodium ^{14}C bicarbonate, (Amersham, initial specific activity 53 mCi mmol^{-1}, initial concentration 2.0 mCi ml^{-1}) was filtered through 0.22 μm Dynagard filters immediately before use. For each depth, 162 μCi of the filtered sodium ^{14}C bicarbonate solution was added to 162 ml of sample contained in a polycarbonate jar. This was gently mixed 10 times to disperse the isotope, and then 7 ml aliquots were dispensed into scintillation vials. These vials, which were not specially cleaned prior to use (Cullen *et al*, 1992), were immediately placed into the incubator. The total time between sampling the Niskin bottles and samples being placed in the incubator was typically less than 1 hour. Two time zero samples for each depth were dispensed at the same time

as the incubated samples, 0.25 ml of 6M HCl were added with 1 minute (and within 3 minutes of the isotope being added) and the samples were then immediately placed into a Paton Scientific Model OP1412 orbital shaker, and shaken at 180 revolutions per minute for two hours to remove unfixed ^{14}C. Two 100 µl aliquots were also taken from each sample at each depth, added to 7.0 ml of 0.1M NaOH in seawater, shaken gently, and then 10 ml Dupont Aquassure liquid scintillation cocktail was added. These samples were immediately counted to determine the total amount of isotope added to each sample. Three replicate vials at each of 6 light intensities (plus 3 dark vials) were incubated from each depth for 1 hour. They were then removed from the incubator, 0.25 ml of 6M HCl was added, and then placed in the shaker and shaken as described above for 2 hours. Ten ml of Dupont Aquassure liquid scintillation cocktail was added to each vial, and they were counted in a liquid scintillation counter within 24 hours.

STATISTICAL ANALYSIS.

An outline of the statistical procedures and other analyses applied to the data is given below.

MIXED LAYER DEPTHS

Mixed layer depths were calculated from CTD temperature and salinity profiles as the shallowest depth for which either the absolute change in temperature ΔT over 10 m exceeded 0.1 °C, or the absolute change in salinity ΔS over 10 m exceeded 0.05. For some stations on the first two cruises, CTD data were lost, and mixed layer depths were calculated from Seabird CTD profiles. Standard mixed layer depths were also compared with mixed layer depths calculated using a weaker temperature criterion ($\Delta T > 0.05$ °C). Depths calculated using the two criteria were generally similar. Exceptions occurred primarily on the winter cruise (SS2/91), where very weak shallow stratification occurred overlying deep winter mixed layers.

FLUORESCENCE-CHLOROPHYLL CALIBRATION.

This is complicated by the fact that the fluorometer was not attached to the rosette CTD, and so fluorescence from in-situ Seatech profiles must be calibrated against chlorophyll from Niskin bottle samples taken at slightly different times. Chlorophyll values were compared with fluorescence values averaged over a 4 m bin centred on the bottle sample depth. Chlorophyll was then regressed on fluorescence, and the regression equation subsequently applied to the rest of the fluorescence profile to obtain a continuous calibrated chlorophyll profile.

At first, an attempt was made to fit a single line through all data for one cruise. Two kinds of systematic problems were noted. Individual outliers, with standardized residuals greater than 2.5, occurred where bottle stations had been taken in strong vertical fluorescence gradients: these were assumed to be due to misregistration of depths, due to the time interval between CTD and fluorescence profiles, and rejected. It then became clear that there were systematic differences in the chlorophyll-fluorescence relation among stations, with all depths on individual stations falling consistently above or below the mean regression line. The stations were subsequently divided into groups, and regressions by group led to a highly significant reduction in the unexplained variance. The R^2 values for station groups ranged from 0.91 to 0.92 for SS3/93, 0.95 to 0.98 for SS4/92, 0.93 to 0.97 for SS1/92, and 0.71 to 0.81 for SS2/91. The highest R^2 values occurred in spring, where the range in chlorophyll was large. The lowest occurred in winter, where the chlorophyll range was low. The standard deviation of residuals may be of more interest as a guide to the errors incurred in predicting chlorophyll from fluorescence within groups. These were lowest in winter (ca 0.03 μg Chla l^{-1}) and largest in spring (0.13 to 0.2 μg Chla l^{-1}), and generally less than 10% of chlorophyll values. The calibrated fluorescence profiles were used primarily as a basis for primary production modelling (discussed below).

LIGHT ATTENUATION.

The PAR profiles from the Biospherical sensor attached to the Seabird CTD were used, along with the calibrated fluorescence profiles, to infer a relationship between chlorophyll and the bulk attenuation coefficient for downwelling irradiance (PAR), Kd. PAR profiles were log-scaled, and smoothed by a moving window of depth 10 m. The gradient of the smoothed profile was then calculated at 10 m intervals as the change in (smoothed) log PAR over 10 m, divided by 10 m. This gradient is influenced by PAR values over a 20 m interval, and was compared with the mean chlorophyll fluorescence value over the same interval. Two possible relationships between Kd and Chl a were considered: a linear relationship:

$$Kd = A + B . Chla$$

and a non-linear relationship based on an equation first proposed by Riley (1956):

$$Kd = A + 0.0088.Chla + 0.054.Chla^{0.67}.$$

In linear regressions, R^2 values were generally low, except for SS4/92, where the range of chlorophyll values was large. For SS1/92, and SS4/92, the Riley relationship gave a better fit, with lower mean square residual. For SS3/93, the linear regression and Riley equation give similar residual variance, but the Riley

equation had an unrealistically low intercept. No PAR data were obtained on SS2/91, and the relationship obtained for SS4/92 was assumed to apply. The derived relationships used in subsequent production modelling were:

SS1/92:
   Kd = .0443 + .0088 . Chl a + .054 . Chl $a^{.67}$, std. dev. residuals = 0.0114.

SS4/92 (and SS2/91):
   Kd = .0284 + .0088 . Chl a + .054 . Chl $a^{.67}$, std. dev. residuals = 0.0125.

SS3/93:
   Kd = .0186 + .0659 . Chl a, std. dev. residuals = 0.010.

It is interesting that the intercept is much higher for the summer cruise (SS1/92) than for the spring cruise (SS4/92), indicating a higher level of non-chlorophyll absorption, possibly degradation products or humics of coastal origin.

ESTIMATION OF P VS I PARAMETERS.

NORMAL P VS I INCUBATIONS

After standardising the primary production rates to Chl a, a non-linear parameter estimation routine was used to fit the P vs I models of Platt *et al*, (1980) to the data. If no photoinhibition was seen, the model used was:

$$P_I^B = P_m^B [1-\exp(-\alpha.I/ P_m^B)] + c.$$

where:
   P_I^B = production (mg C (mg Chl a)$^{-1}$ h^{-1}) at irradiance I (μmol m^{-2} s^{-1}),
   P_m^B is the maximum photosynthetic rate (mg C (mg Chl a)$^{-1}$ h^{-1}) at light saturation.
   α is the initial slope (mg C (mg Chl a)$^{-1}$ h^{-1} (μmol m^{-2} s^{-1})$^{-1}$)
   c is the intercept at zero light.

If photoinhibition was seen, then the model used was

$$P_I^B = P_s^B [1-\exp(-\alpha I/ P_s^B)] \exp(-\beta I/ P_s^B) + c.$$

where:
   β is the photoinhibition parameter (mg C (mg Chl a)$^{-1}$ h^{-1} (μmol m^{-2} s^{-1})$^{-1}$).

On SS 2/91, SS 1/92, and SS 3/93 the dark samples were included in the curve fitting procedures. The darks were omitted from the curve fitting on SS 4/92 because of a pronounced sigmoid shape to the uptake curve at very low light intensities. We believe this is partly due to a seasonal effect (spring bloom period) and changes in algal physiology during this spring bloom. The effect of omitting the darks from the calculation was to increase the initial slope, α, of the fitted curves.

SHORT P vs I INCUBATIONS

The initial slope, α, of the PvsI curve was found by fitting a linear regression through the uptake in the dark samples and the uptake measured at the lowest 6 light intensities (a total of 9 samples). The intercept of the regression was not constrained to pass through zero. The P_m values were estimated by taking the mean of three values at light intensities between ca. 160-250 μmoles m^{-2} sec^{-1}. These intensities were chosen because virtually all of the normal PvsI curves exhibit light saturation but not photoinhibition at these light intensities. The α values obtained by this procedure tended to be less than those obtained by the curve fitting procedure. For the modelling of column production estimates, the α and P_m values obtained from the short PvsI incubations have been corrected to values expected if sufficient samples had been available for the normal non-linear, least squares procedures to be utilised. The correction value was obtained by regressing the α values obtained from the full PvsI incubation procedure against α values obtained from the same experiment, using only light intensities corresponding to the short incubations, and the short incubation parameter estimation. Similarly, the P_m correction was obtained from a regression of curve fitted P_m vs the short incubation Pmax. The regression results are shown in Table 3.

TABLE 3. REGRESSION RESULTS FOR PARAMETERS FROM FULL VS SHORT INCUBATION EXPERIMENTS.

CRUISE	PARAMETER	SLOPE	INTERCEPT	R^2
SS2/91	P_m	1.27	-.425	.95
SS2/91	α	1.38	.012	.74
SS1/92	P_m	1.14	-.322	.97
SS1/92	α	1.43	.01	.96
SS4/92	P_m	1.40	-.37	.98
SS4/92	α	1.15	.016	.67
SS3/93	P_m	1.28	-.44	.97
SS3/93	α	1.22	.008	.63

Note that the R^2 values are very high for P_m; ie the estimate obtained from the "short" incubation subset is a good predictor of the estimate obtained from the

"full" incubation experiment. This is not so true for α. This may be partly because estimates of α (the initial slope) are intrinsically less accurate, and partly because of systematic departures in the data from the classical PvsI equation (the sigmoidal behaviour referred to above). These departures will be analysed in a future paper.

STATISTICAL ANALYSIS OF SEDIMENT TRAP RESULTS

Results for dry weight, carbonate, organic matter, total C, total N, reactive P and biogenic opal were obtained from analyses on 1/16 aliquots of the total < 1mm fraction. All results were the average of at least 2 replicate analyses. In this study 9 of the 16 aliquots were weighed for each trap period and therefore the mean weight of the < 1mm fraction for each trap period was calculated as the mean weight of the weighed aliquots multiplied by the total number of aliquots, as shown in equation (1).

weight/trap period = mean of weighed aliquots x 16   (1)

The standard error (SE) associated with the total dry weight per trap period was calculated from the standard deviation of the individual dry weights SD(W) as shown in (2).

$$SE(A) = N.SD(A).(1 - n/N)^{0.5}/n^{0.5}   (2)$$

where
      A is the mean dry weight per trap period
      n is the sample size (9 in this study)
      N is the population size (16 in this study)
and the factor $(1-n/N)^{0.5}$ represents the "finite population correction".

Results for each element per trap period and their corresponding standard errors were calculated as shown in equations (3) and (4) respectively.

$$C (mg) = B.A/1000   (3)$$

$$SE(C) = (SE(A)^2 . B^2 + SE(B)^2 . A^2 + SE(A)^2.SE(B)^2)^{0.5} / 1000   (4)$$

where
      C (mg) is the weight of element per trap period
      B (mg/g) is the weight of element per unit dry weight
      A (mg dry wt) is the dry weight per trap period as calculated in (1)

The standard errors of ratios such as C:N, N:P and N:Si were calculated as shown in (5).

$$SE(X/Y) = ((SE(X) / \mu_Y)^2 + (\mu_X.SE(Y)/\mu_Y^2)^2)^{0.5} \quad (5)$$

DETAILED RESULTS

ANALYSIS OF SATELLITE SST IMAGES: SEASONAL AND INTERANNUAL PATTERNS.

SUMMER (JANUARY, FEBRUARY, MARCH) (FIG. 2A,B).

The summer pattern is dominated by a flow of warm, "EAC" water south along the slope on the east coast. This warm water generally leaves the slope south-east or south of Tasmania, and can be entrained into mesoscale eddies and carried well south of Tasmania, reaching 47°S. Temperatures and temperature patterns in the study area typically depend on the interaction between this warm intrusion, and mesoscale or large scale circulation bringing cold subantarctic water to the slope and shelf. Along the west coast, temperatures are also warmer on the shelf and slope than further offshore: however, the evidence for a flow of warm water from the north-west in summer is not so clear. Temperatures in February are consistently warmer than those in January, due to seasonal heating, while temperatures in February and March are similar.

In 1990, warm water (>16°C) extended down the east and west coasts along the shelf and slope, and meandered well south of 45°S, in all three months. Shelf and slope temperatures in the study area were typically 16-17°C throughout the period. Water temperatures off north-east Tasmania were maximum (ca 20°C) in March.

In 1991, warm water (ca 18°C) penetrated down the east coast along the slope from January through March, but did not extend south of 44°30'S or west of 147°E. The area south of Tasmania was dominated by the effects of two counter-rotating eddies, centred on 46°S, which drew cold water (ca 13°C) from the south-east and south-west over the slope through the study area. Water was also noticeably cooler, ca 14 to 16°C, over most of the Southern Tasmanian shelf.

1992 was a particularly cold year. The north-east shelf water warmed to ca 16°C in January, but warm EAC water did not penetrate along the slope south of 43°S until February. In February, this warm tongue (ca 18°C) extended south and west to ca 45°S, 147°E, but retreated somewhat in March. Away from this tongue, the shelf and slope in the study area stayed quite cold (ca 13-14°C) through January and February, although the shelf water warmed to ca 15°C in March.

Fig. 2. Composite SST images of the ocean around Tasmania by month and year for the period 1990 to 1993. A. Summer (Jan, Feb, Mar), 1990-1991. B. Summer (Jan, Feb, Mar), 1992-1993. C. Autumn (Apr, May, Jun), 1990-1991. D. Autumn (Apr, May, Jun), 1992-1993. E. Winter (Jul, Aug, Sep), 1990-1991. F. Winter (Jul, Aug, Sep), 1992-1993. G. Spring (Oct, Nov, Dec), 1990-1991. H Spring (Oct, Nov, Dec), 1992-1993).
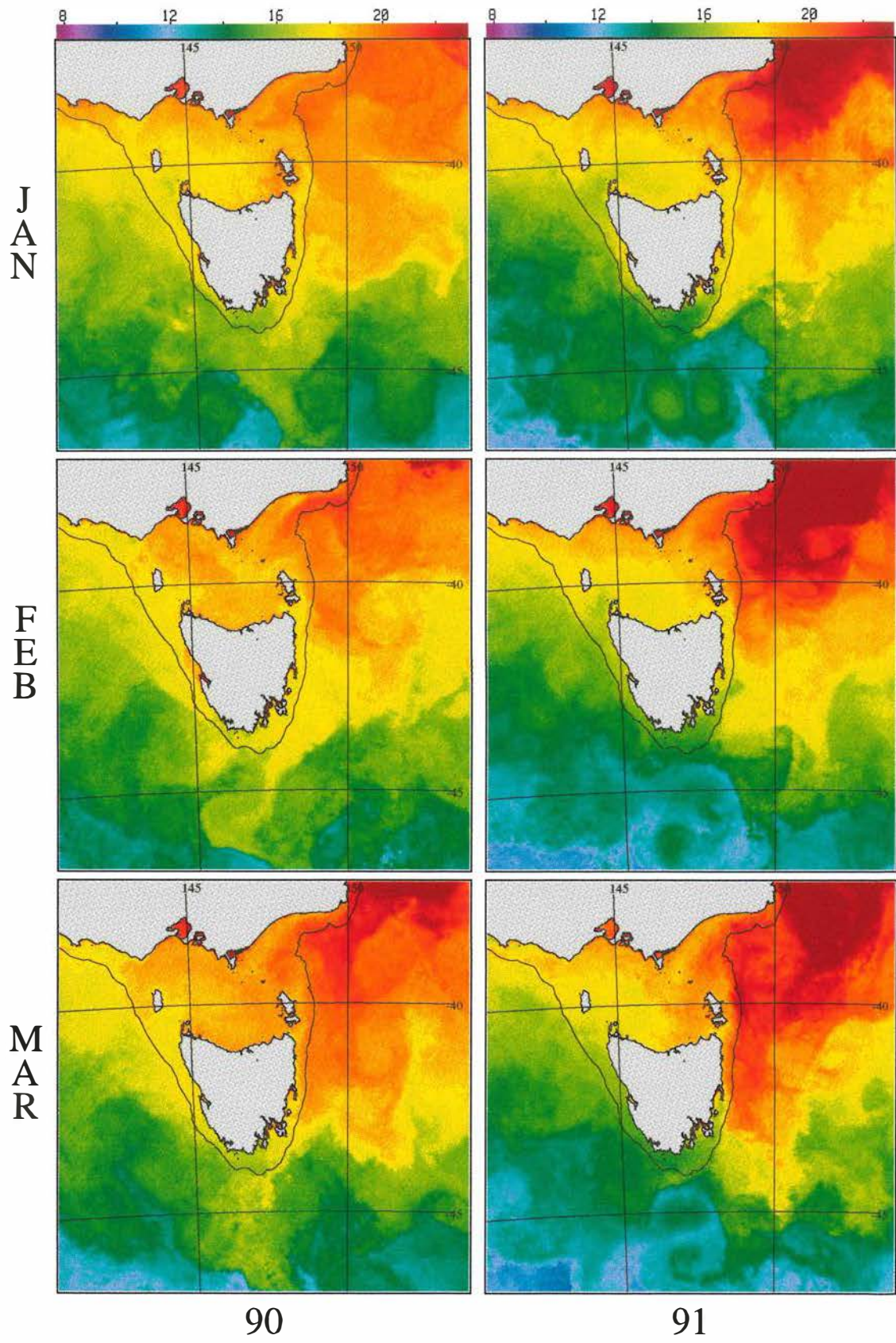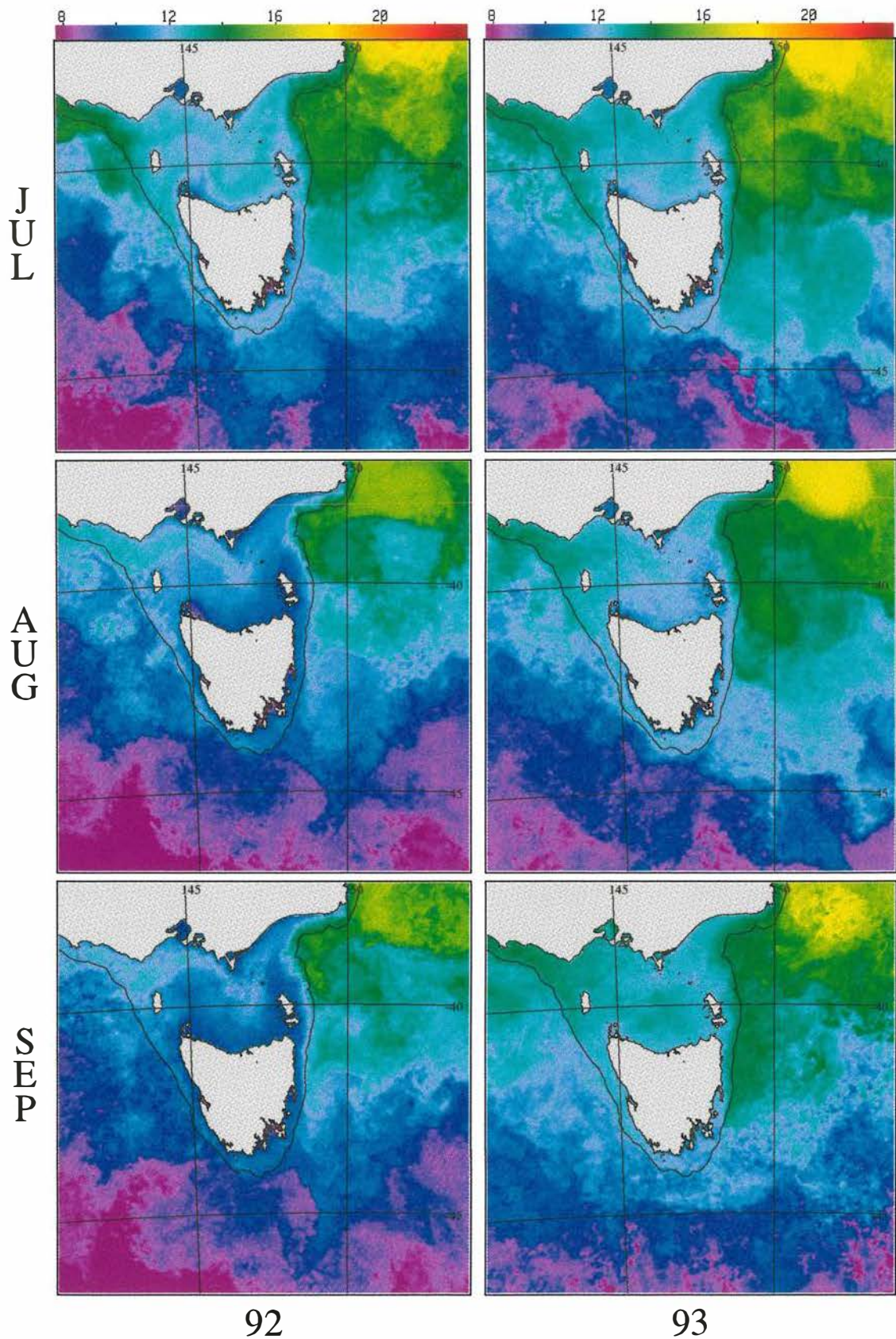
Fig. 2A
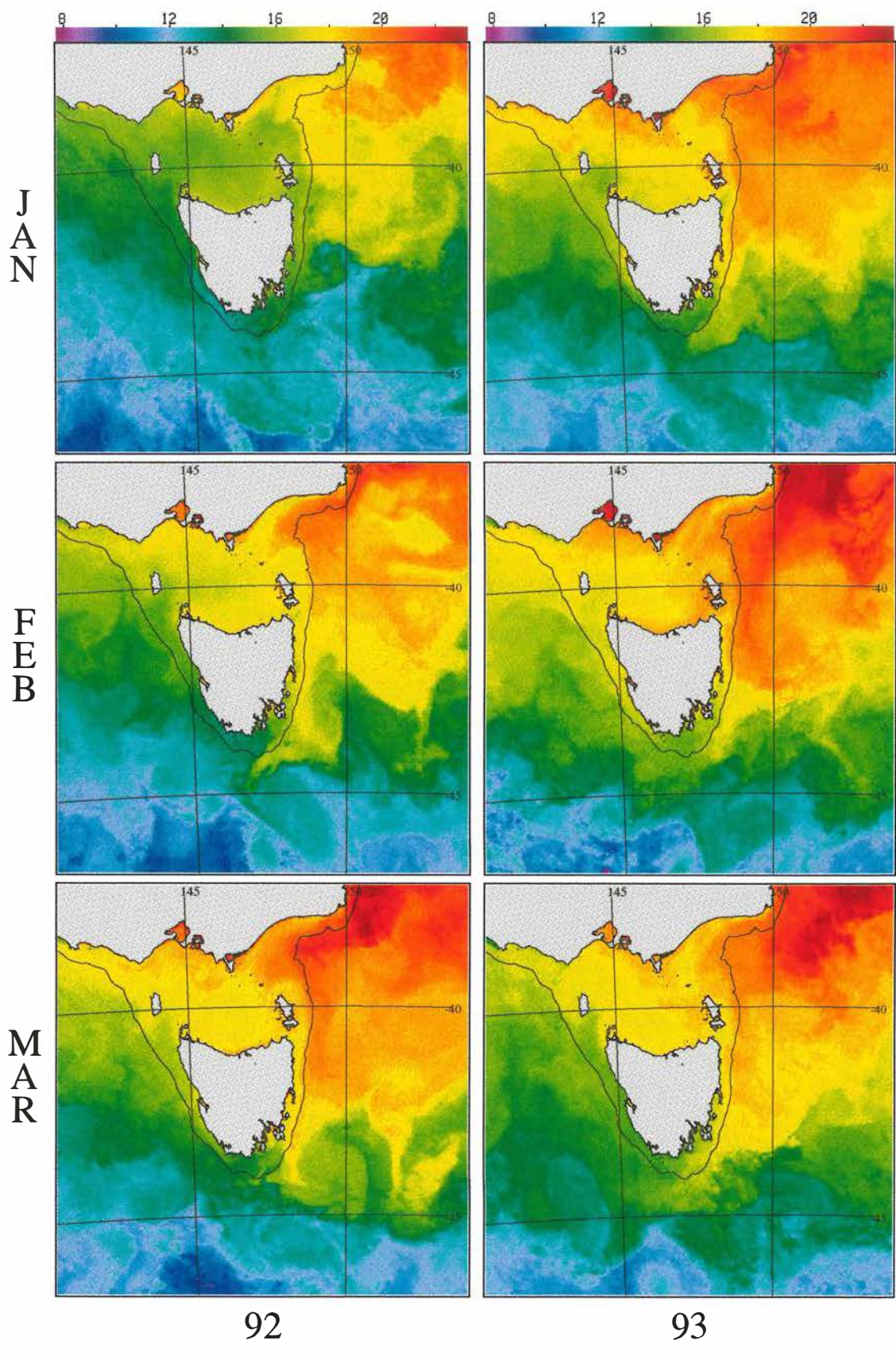
Fig. 2B

Fig. 2C

Fig. 2D

Fig. 2E

JUL

AUG

SEP

92

93
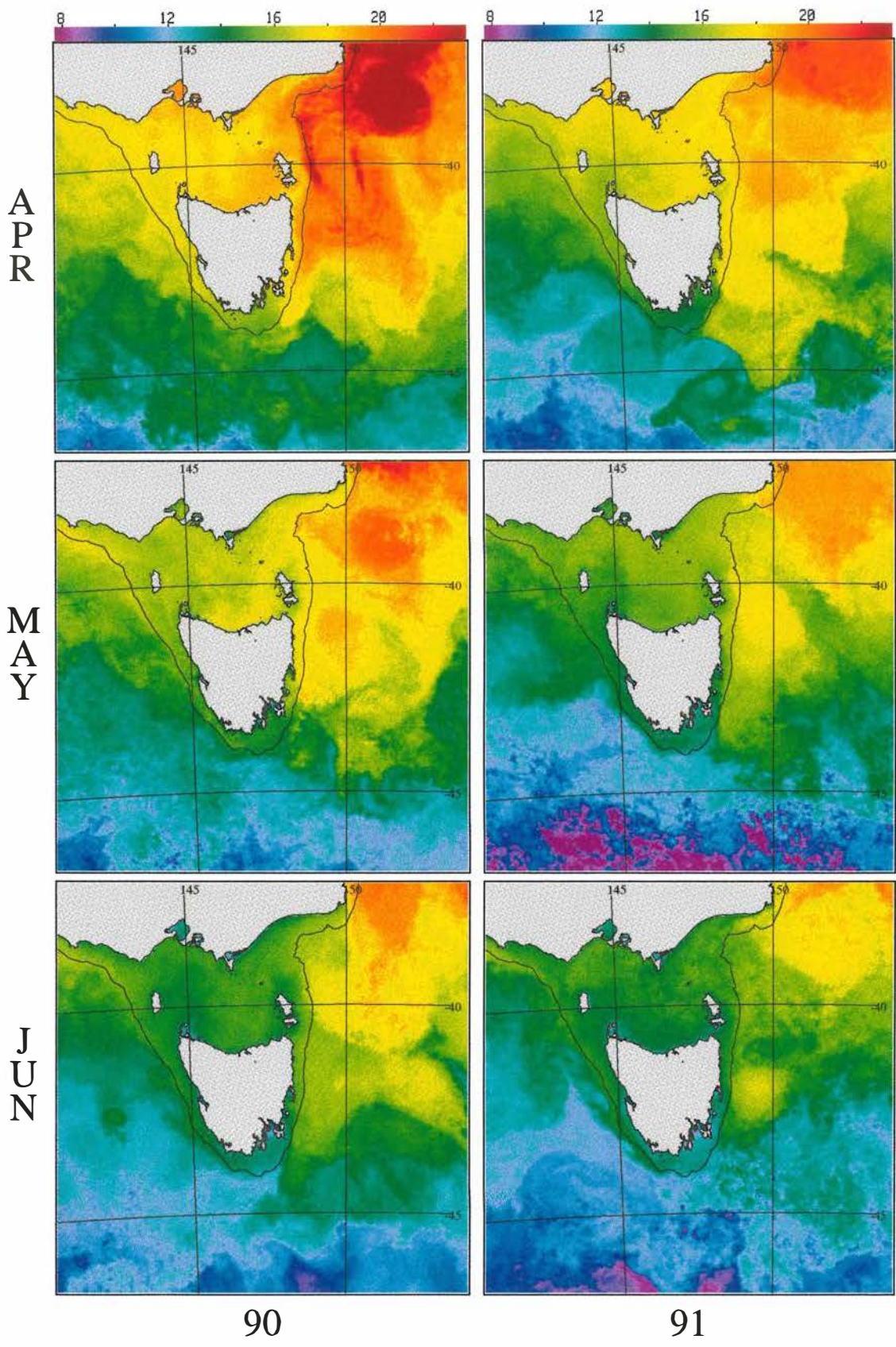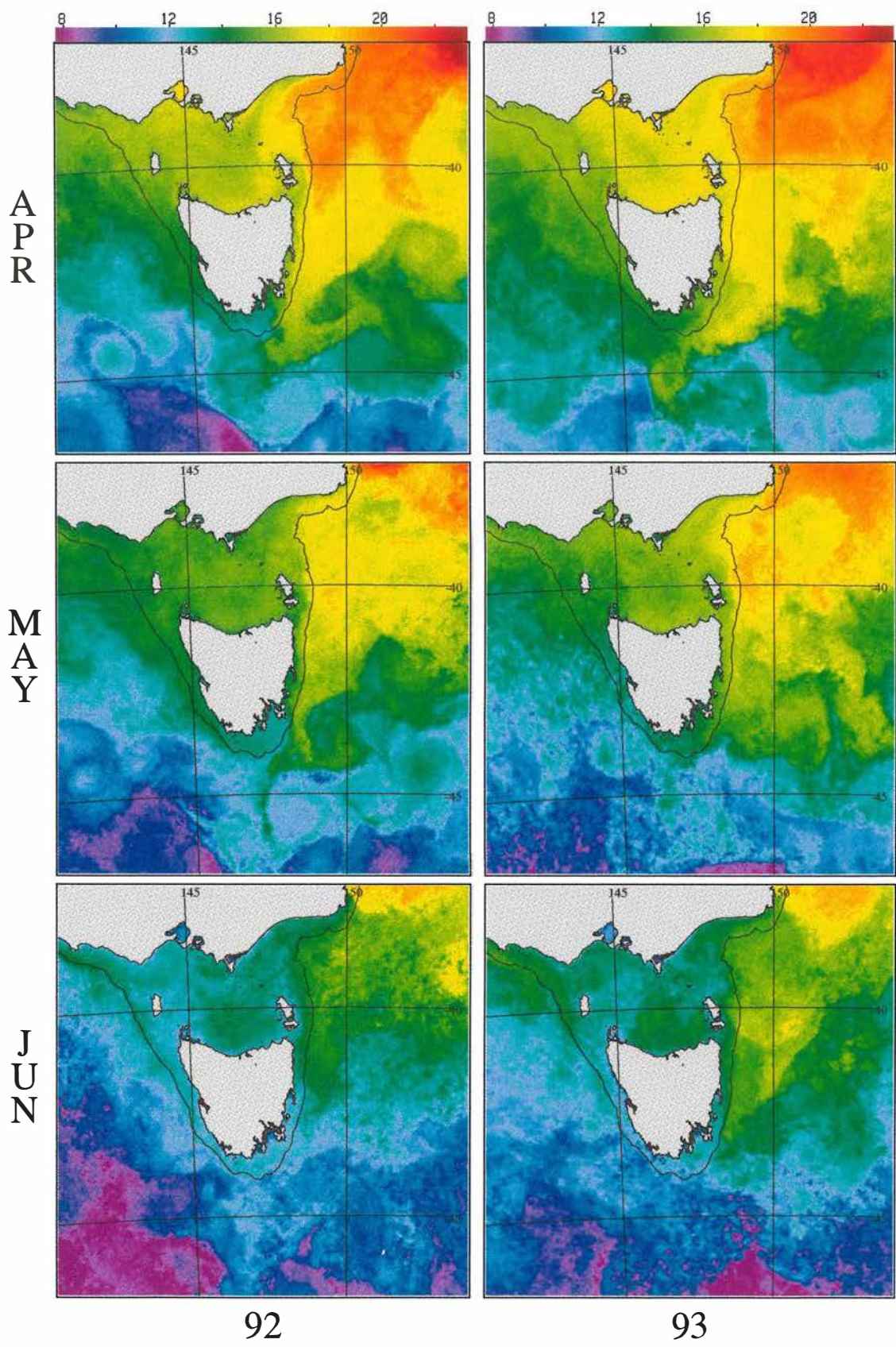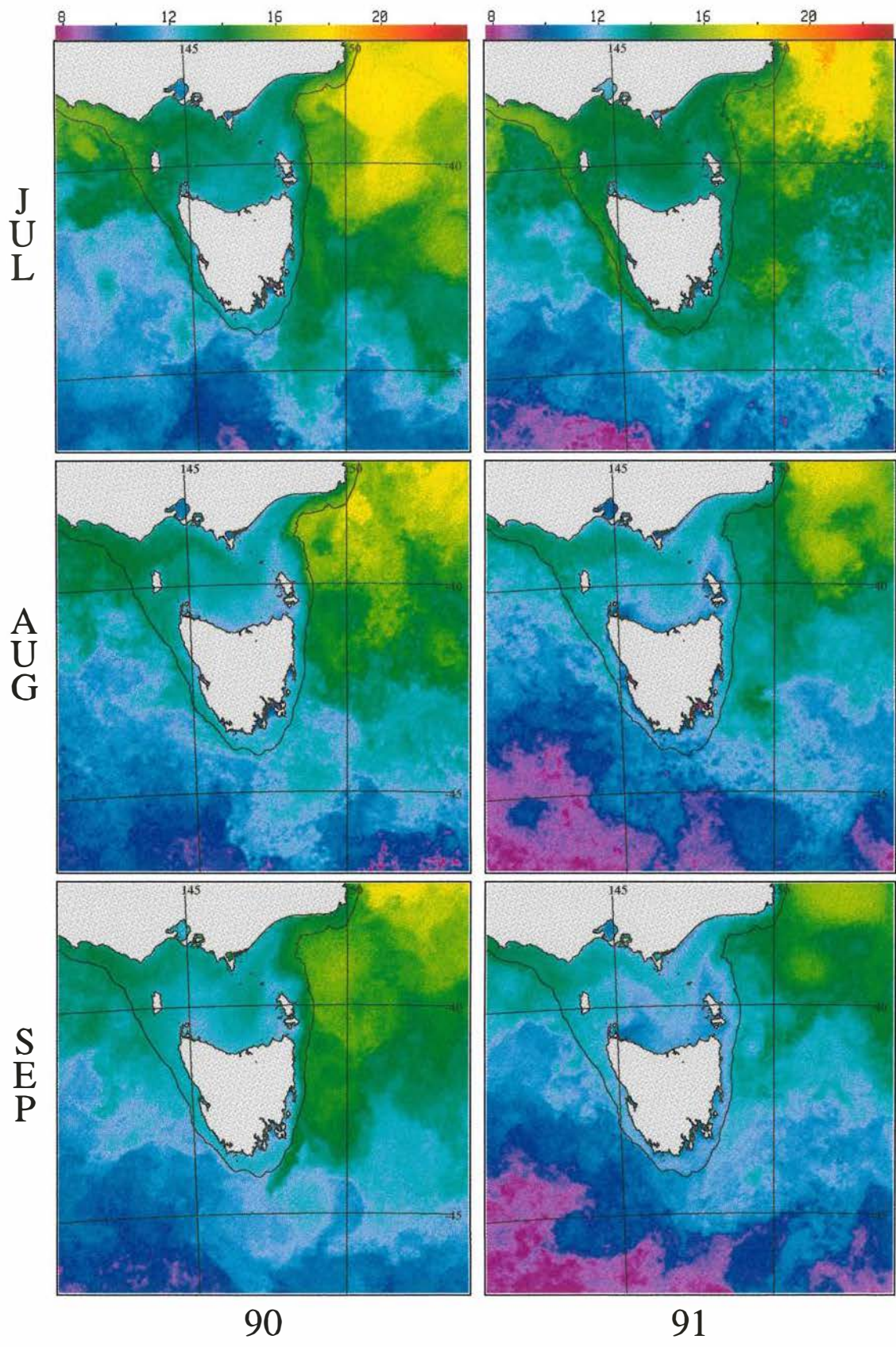
Fig. 2F
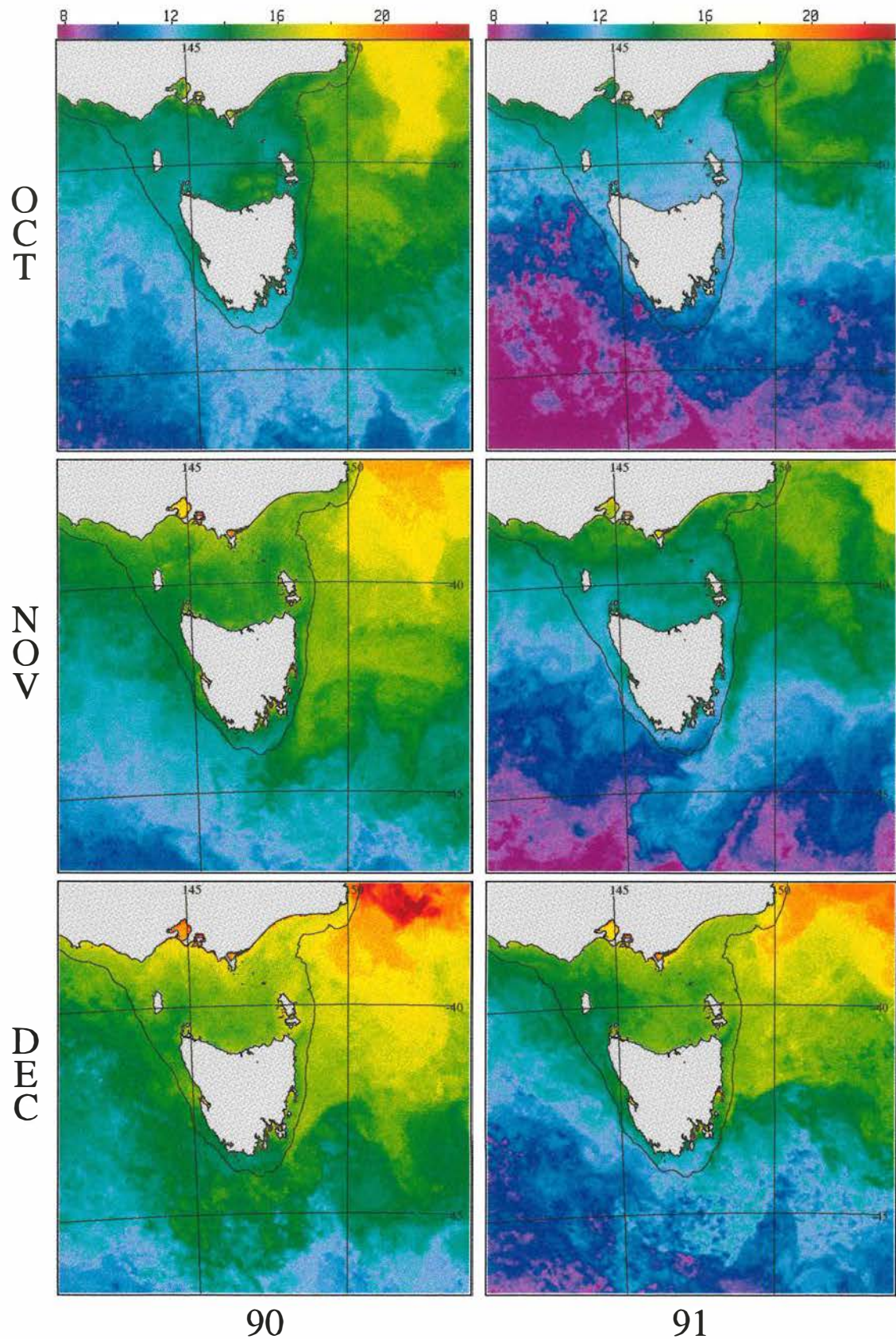
Fig. 2G
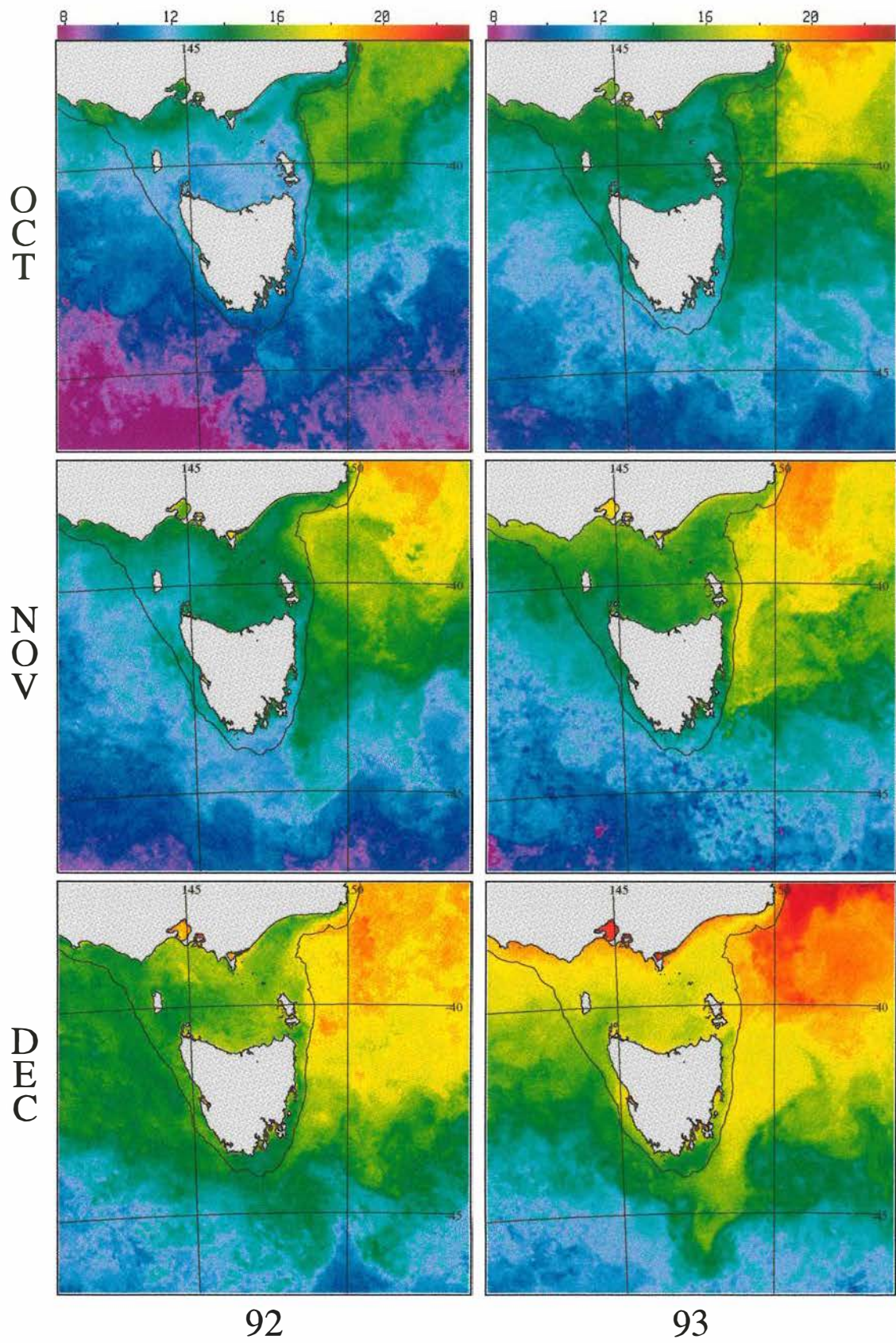
Fig. 2H

1993 saw a return to warmer conditions, although temperatures south of 45°S stayed quite cold (12°C and less) throughout the summer. Warm water (ca 16-18°C) penetrated well south along the eastern slope in January, while the slope south and south-west of Tasmania was still 12-14°C. In February and March, the shelf and slope throughout the study region were flooded with warm (16°C) water.

The interannual signal in summer was dominated by the particularly warm conditions in 1990, and particularly cold conditions in 1992. The west-east contrast in southern Tasmania waters between the EAC influence on the east coast, and cold offshore waters impinging on the west coast, was much more marked in 1991 and 1992. The summer cruise, in February 1992, took place in unusually cold conditions, with a minimum influence of EAC water in the study area.

AUTUMN (APRIL, MAY, JUNE). (FIG. 2C,D)

Autumn months see seasonal cooling, and the retreat of the EAC warm tongue. Cooling begins in April, but strong cooling takes place in May and June. The Zeehan Current, which brings warm water down the west coast of Tasmania in winter, is generally established by June.

In 1990, there was only slight cooling in April, and temperatures on the shelf still exceeded 16°C. The warm water tongue retreated north along the east coast in May and June, but there was still a pool of 16°C water lying offshore along the east coast. Strong cooling occurred over the slope south of Tasmania in May and June, and temperatures dropped to 12°C by June. Temperatures on the shelf in June were coolest in the south-east (ca 13°C), but remained warmer in the south-west, fed by the flow of warm (15-16°C) Zeehan Current water along the slope from the north-west.

In 1991, water on the slope and south-east shelf was already considerably cooler in April (ca 13 and 14°C respectively). Water on the slope cooled to 12°C in May and June, while water on the south-east shelf cooled to 13°C in June. The Zeehan Current along the slope on the west coast was clearly visible in June, and it maintained temperatures of ca 14°C on the shelf in the south-west and south.

In 1992, the warm water off the eastern coast was entrained into eddies south of Tasmania, and did not retreat northward until June, so that temperatures off the slope on the south-east coast remained warm until May. However, the shelf

27

and slope in the south and south-west were already cool (ca 13°C) in April. The Zeehan Current did not appear to penetrate south of Macquarie Harbour in 1992, and by June the entire shelf over the southern half of Tasmania had cooled to 12°C, and some areas over the slope had cooled to ca 10°C. A large tongue of very cold (8°C) water extended northward to 43°S west of Tasmania.

In 1993, warm EAC water (ca 17°C) still covered the slope south of Tasmania in April, with cooler (14°C) water spreading over the shelf from the west. The warm water retreated northward rapidly between May and June, and the slope cooled to 12-13°C in May, and to 10-12°C by June. The shelf had cooled to ca 12°C over the southern half of Tasmania by June. Again, the Zeehan Current did not appear to penetrate south of Macquarie Harbour.

In autumn, there was strong interannual variation in the timing of retreat of EAC water, and the southward penetration of Zeehan Current water. The cold years, 1992 and 1993, were marked by a weakening of the influence of the Zeehan Current. The autumn cruise took place in April 1993, with warm EAC water still relatively far south over the slope in the east and south, and cooler water intruding over the slope and shelf from the SW.

WINTER (JULY, AUGUST, SEPTEMBER). (FIG. 2E,F).

Cooling on the shelf generally continued throughout the winter period, whereas cooling offshore slowed after July, possibly due to the formation of deep winter mixed layers.

In 1990, the shelf around Tasmania had cooled to 13°C by July, and 12°C by August/September, except along the west coast, where the Zeehan maintained warmer temperatures (ca 14°C) in July and August. The Zeehan Current retreated in September, and the EAC water mass seemed to advance at the same time, sending a tongue of warm (16°C) water southward along the slope to 44°S. The slope water south of Tasmania was around 12°C throughout the winter, but tongues of colder (ca 10°C) water from the south intruded over the slope from the south and south-west in July and September.

In 1991, the Zeehan was still very pronounced in July, bringing 15-16°C water along the slope in the west and south-west. The influence of both Zeehan and EAC water retreated well northward in August and September; the shelf then cooled to 12°C and the slope in the west and south to 10°C.

In 1992, the shelf cooled to 12°C around Tasmania by July, and to 10°C by August and September. The Zeehan Current was evident on the western slope, particularly in August, but its temperature had fallen to 12°C. The water over the slope cooled to 8 to 9°C in August and September.

In 1993, shelf temperatures were ca 12°C throughout the winter. Temperatures over the slope ranged from ca 9 to 11°C, with some warming in September. There was no evidence of any Zeehan Current stream on the west coast.

Interannual variation in winter seemed to be dominated by shifts in broadscale temperature, with temperatures in 1992 typically 2°C colder than in other years at all latitudes. There was also strong interannual variation in the southward extent of the Zeehan Current. Overall, winter temperatures were warmest in 1990. However, the winter cruise (July, 1991) took place in a period when the Zeehan Current was running very strongly, with the warmest July temperatures on the shelf of the 4 years studied.

SPRING (OCTOBER, NOVEMBER, DECEMBER). (FIG. 2G,H)

Appreciable warming (and presumably stratification) has generally occurred by November. In addition to local warming, there appears to be southward movement of warm EAC water on the east coast during November and December, although the timing and extent varied from year to year. There was evidence in November and December in all years of intense local warming along the west coast, presumably associated with stratification due to spring runoff.

In 1990, the shelf and slope in the study area were still cold (ca 12°C) in October. Warming occured over the slope in the south-east in November, and in the south-west and south-east in December, as EAC water moved south and west. Warming also occurred on the inner shelf, with minimum temperatures over the outer shelf.

In 1991, temperatures in October were very cold, with 10°C water over the shelf, and 8 to 10°C water over the slope. In November, water over the inner shelf, and offshore to the SE, had warmed to 12°C, but the outer shelf and slope to the south and south-west was still 9-10°C. By December, water on the shelf on the west and east coasts had warmed to 14°C, but the shelf and slope in the study region were still ca 12°C.

In 1992, the situation in November was very similar to that in 1991. The shelf and slope in the study area had warmed to 12°C by November, and there was strong warming by December, with temperatures on the shelf and slope reaching 14 to 15°C, and warm EAC water (16°C) streaming along the south-east slope.

In 1993, temperatures on the shelf were already 12°C in October, but there was only slight warming (to about 13°C) on the shelf, and virtually no warming offshore, in November. There was substantial warming in December, with strong penetration of warm EAC water over the slope to the south and south-

east, and local warming on the shelf in the south-west. The shelf in the south-east had warmed to ca 14°C.

October 1991 marked the beginning of the particularly cold year, which arguably ended in November 1992. 1990 and 1993 spring temperatures were very similar. The spring cruise took place in November 1992. This was a period of sudden warming after an exceptionally cold winter, but was not characterised by a strong influence of EAC water.

CRUISE RESULTS: PHYSICAL OCEANOGRAPHY.

CRUISE SS2/91: JULY 1991

CTD stations on the western transect extended to only 1000 m (Fig. 3), so reached but did not penetrate below the salinity minimum of ca 34.4 associated with Antarctic Intermediate Water (AAIW). Salinities were less than 34.5 below 800 m (Fig. 3B). Temperature and salinity contours were almost horizontal below 400 m, indicating relatively weak geostrophic currents. The broadening of the 8-10 °C isotherms between 400 and 700 m is characteristic of SubAntarctic Mode Water (SAMW: McCartney, 1977; McCartney, 1982). There was strong doming of the temperature and salinity contours above 400 m over the continental slope, with contours sloping up sharply from the upper slope to the surface over the mid-slope region. In the upper 200 m (Fig. 4B), there was an increase in salinity from 35.1 over the inner shelf to a maximum of 35.5 at the shelf break, and a decrease across a fairly sharp front to a minimum of 35.1 over the mid-slope. Salinity then increased slightly to 35.2 offshore. Temperature behaved in a parallel manner, with a minimum of 13.6 °C at the inner shelf, a maximum of 14.6 °C over the upper slope, and a minimum of 12.7 °C over the mid-slope (Fig. 4A). The warm, saline core over the shelf-break and upper slope appears to be Zeehan Current water (see comments below).

Vertical stations on the central transect extended through AAIW, as evidenced by the salinity minimum between contours of 34.5 at ca 800 and 1200 m (Fig. 5B). The salinity, temperature and density contours sloped strongly upwards from inshore to offshore below 300m, indicating eastward flow (Fig. 5). SAMW was evident between 400 and 700 m. Within the top 200 m, the temperature cooled from ca 14 °C onshore to 12.7 °C offshore, and salinity decreased from 35.4 on the shelf to 35.2 offshore (Fig. 6). There was a broad temperature and salinity front, and a strong density front over the shelf break and upper slope, which intensified below 150 m. The warm, high salinity water inshore appears to be Zeehan Current water. The water column was well-mixed vertically on the shelf, and to ca 100m over the upper slope, but less deeply offshore.

On the eastern transect, mode water was strongly evident with temperatures of 8 to 10 °C between 500 and 800 m (Fig. 7). Temperature, salinity and density

contours generally sloped upward from onshore to offshore, but there was a maximum thickness of mode water at station 70, ca 30 km offshore of the shelf break. Inshore of station 70, and in and below mode water, contours sloped downward onshore to offshore. There was evidence of strong vertical mixing over the shelf and upper slope, with temperature and salinity being uniform to the bottom or ca 200 m (Fig. 8). This mixed layer constituted a broad pool of saline (35.4) and warm (13.9 °C) water, bounded offshore by a front associated with strongly sloping isopycnals. Surface temperature and salinity dropped to 13 °C and 35.2 at the offshore station, and the mixed layer depth decreased to 60 to 80 m.

Station Number
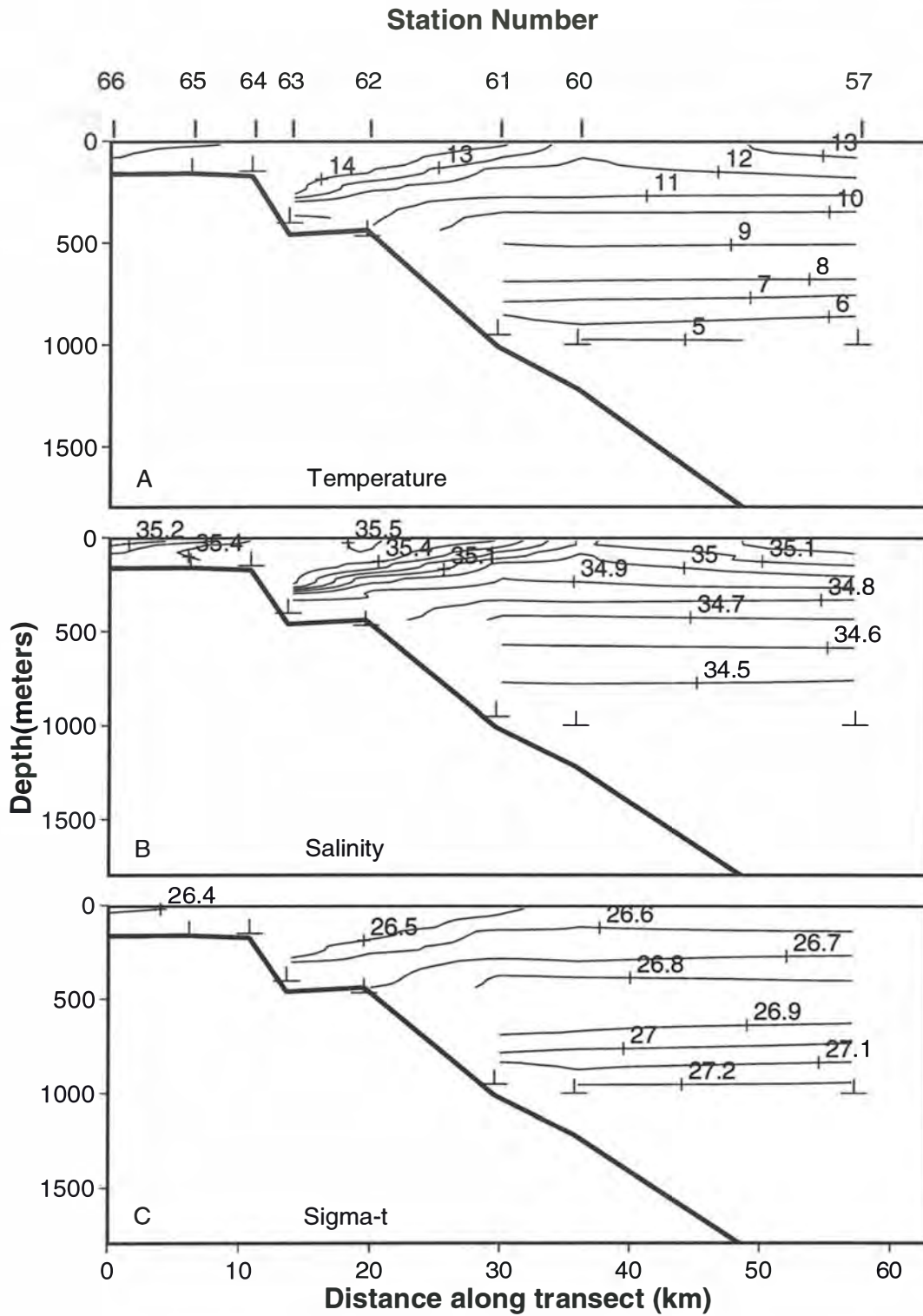
Fig. 3. Contours of (A) temperature (°C), (B) salinity and (C) sigma-t on vertical sections along the western transect, cruise SS2/91, July 1991.
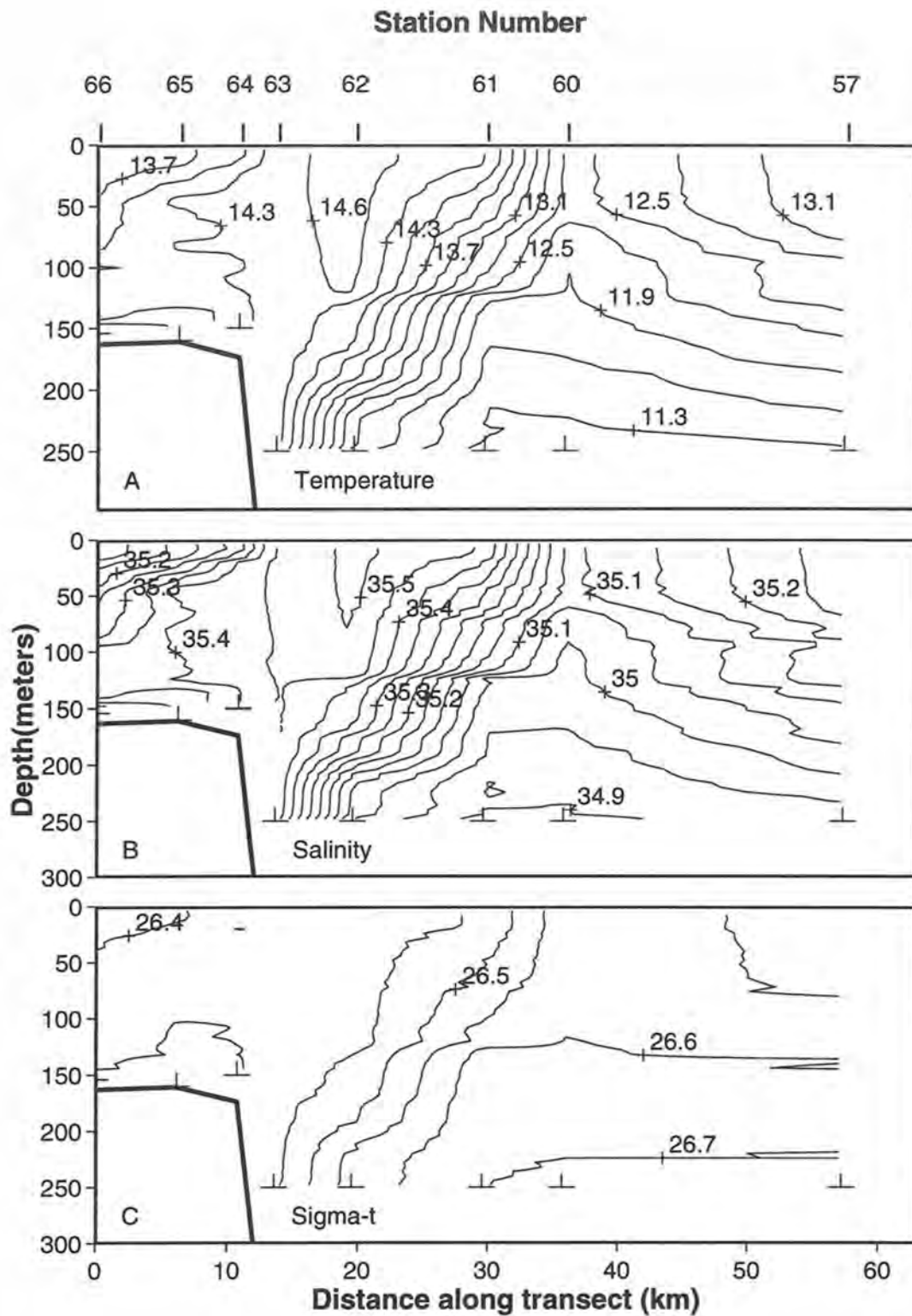
Fig. 4. Contours of (A) temperature (°C), (B) salinity and (C) sigma-t on vertical sections (0 - 250 m) along the western transect, cruise SS2/91, July 1991.
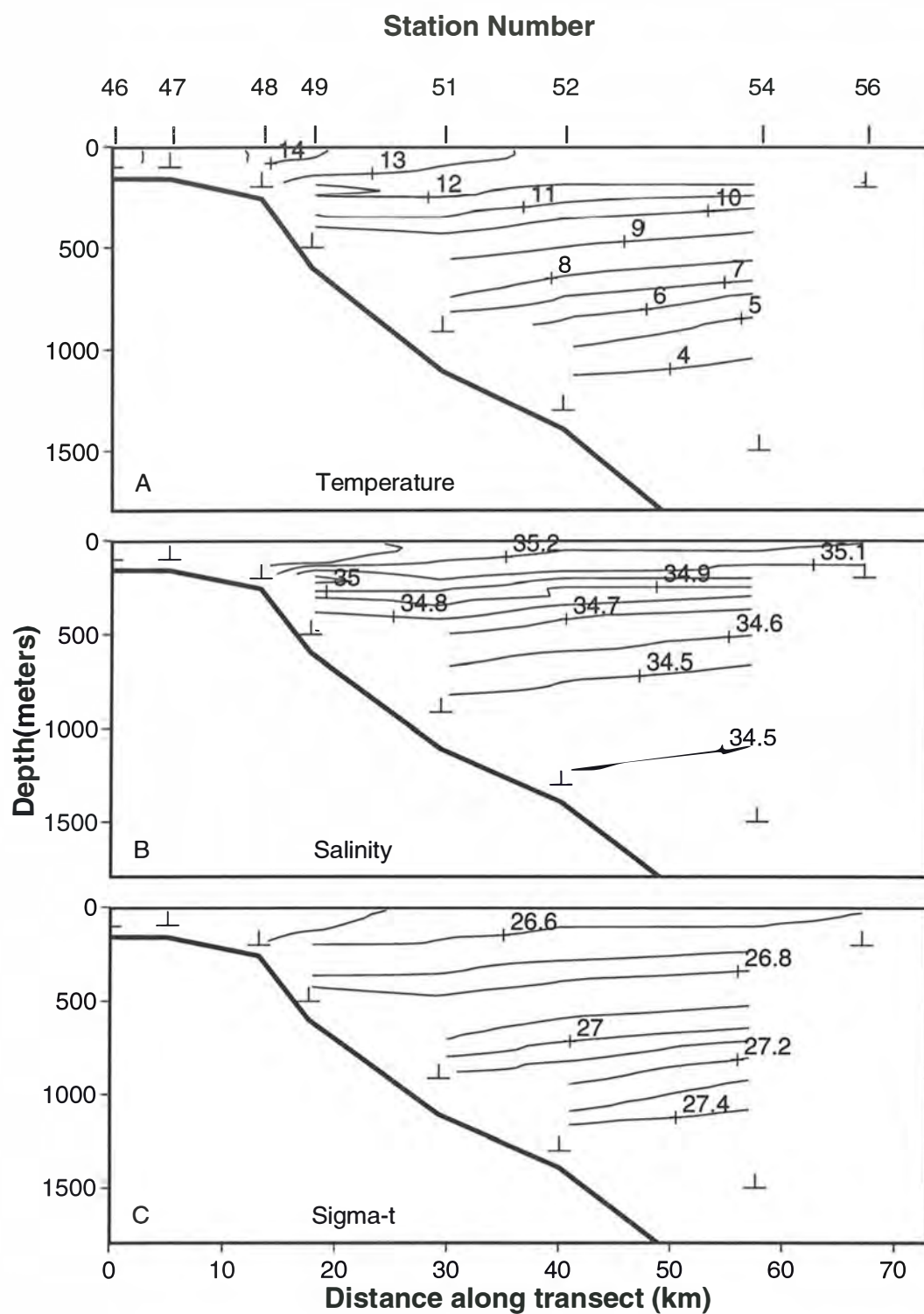
Fig. 5. Contours of (A) temperature (°C), (B) salinity and (C) sigma-t on vertical sections along the central transect, cruise SS2/91, July 1991.

Station Number
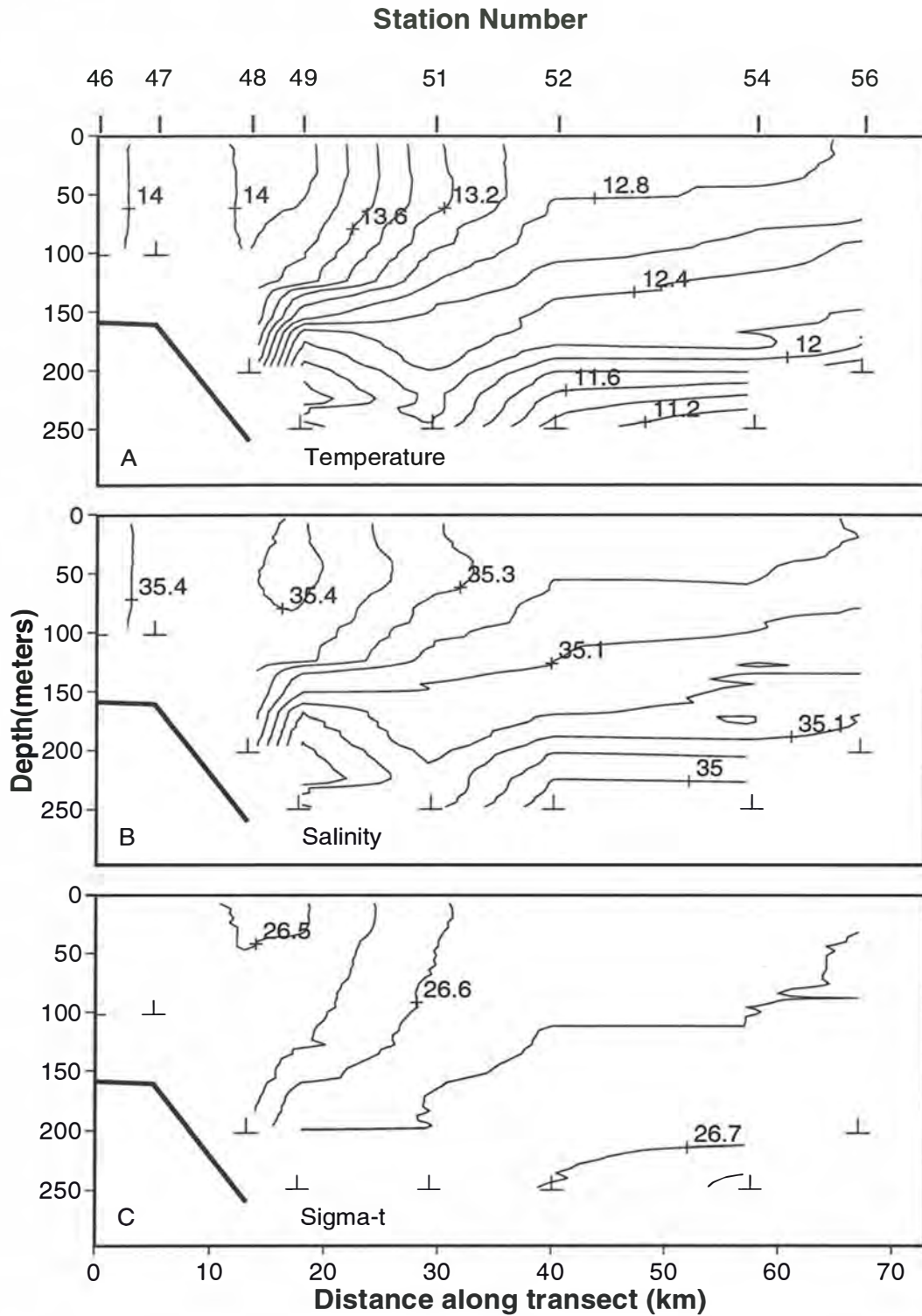
Fig. 6. Contours of (A) temperature (°C), (B) salinity and (C) sigma-t on vertical sections (0 - 250 m) along the central transect, cruise SS2/91, July 1991.
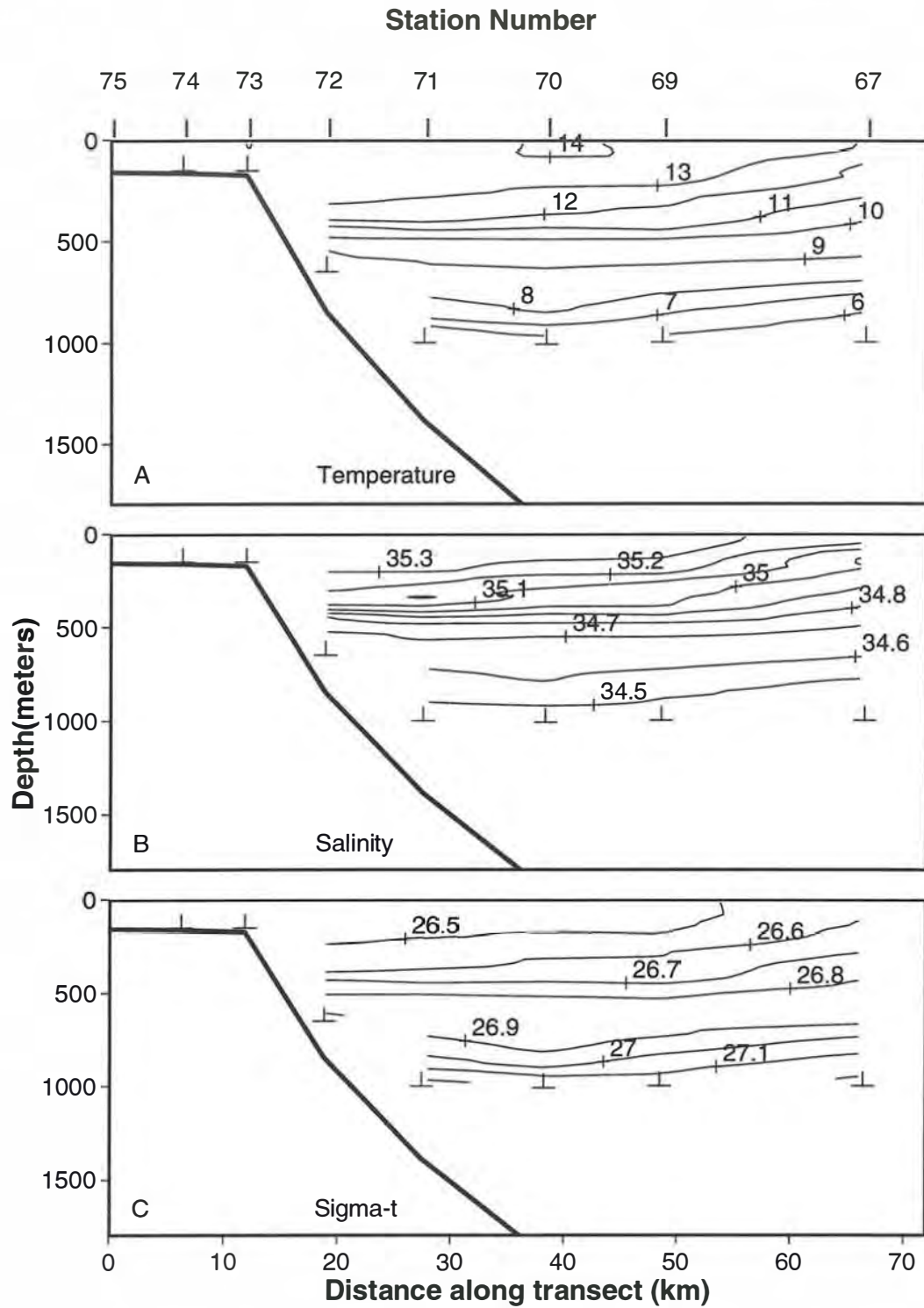
Fig. 7. Contours of (A) temperature (°C), (B) salinity and (C) sigma-t on vertical sections along the eastern transect, cruise SS2/91, July 1991.
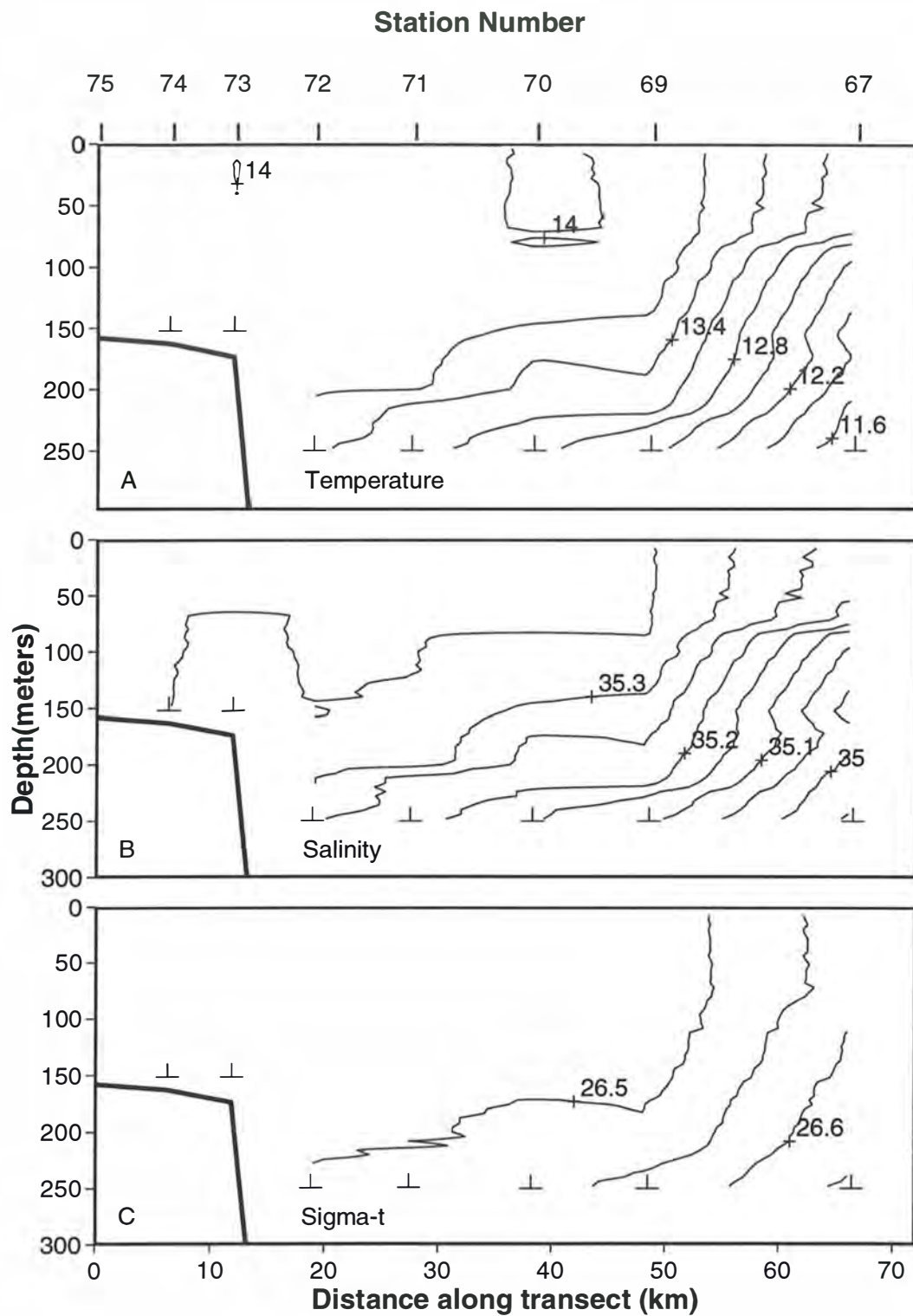
Fig. 8. Contours of (A) temperature (°C), (B) salinity and (C) sigma-t on vertical sections (0 - 250 m) along the eastern transect, cruise SS2/91, July 1991.

All three transects were dominated by a pool of warm, saline water over the outer shelf and upper slope. The temperature and salinity in this core decreased from 14.6 °C and 35.5 to 14 °C and 35.4 from the western transect to the eastern transect. On the western transect, the core was relatively narrow and situated above the shelf-break/upper slope, with lower salinity water inshore on the shelf. On the central transect, the core extended further inshore, onto the shelf. On the eastern transect, the core was deeply mixed, and extended over the shelf and a broad region offshore.

On all three transects, at the furthest offshore station, the surface salinity was ca 35.2 and, in the case of the western and eastern transects, the surface temperature was ca 13 °C. The surface temperature offshore was cooler on the central transect. On the western transect, a cold low salinity upwelling feature separated the warm core from offshore waters. Water in the core and on the shelf was much more deeply mixed than offshore waters, and most deeply mixed on the eastern transect. It seems likely that this was due to convective overturn driven by high rates of heat loss from the warm surface water, and the high density of the saline water mass after cooling.

The strongly sloping isopycnals on the outer edge of the saline core indicate shallow transport from west to east across all three sections, and are consistent with the core being an extension of the Leeuwin Current. However, the slope of the isopycnal surfaces on the continental slope below 800 m was reversed on the eastern transect, possibly indicating deep flow to the south and west on the south-east Tasmanian coast.

A satellite composite SST image during the period of the cruise (13 July, 1991) shows a pronounced tongue of warm water extending south along the west coast of Tasmania, and concentrated on the shelf break (Fig. 1A). This tongue appears to extend around the bottom of Tasmania and on to the shelf and slope on the south-east coast. Sea surface temperatures in the tongue are ca 14 to 14.5 °C in the study area, in agreement with the in-situ data. EAC water appears to extend southward to the east of Tasmania, but well offshore from the shelf break, and outside the study area. Offshore surface temperatures in the study area are ca 13 °C, also in agreement with in situ data. The cold upwelling feature on the western transect is apparent in the image. Successive SST images around the period of the cruise show dynamic mesoscale features in this region, although their interpretation is complicated by cloud effects in the composite. Overall, the SST images support the interpretation that water mass distribution on this cruise is dominated by the effects of the Zeehan Current.
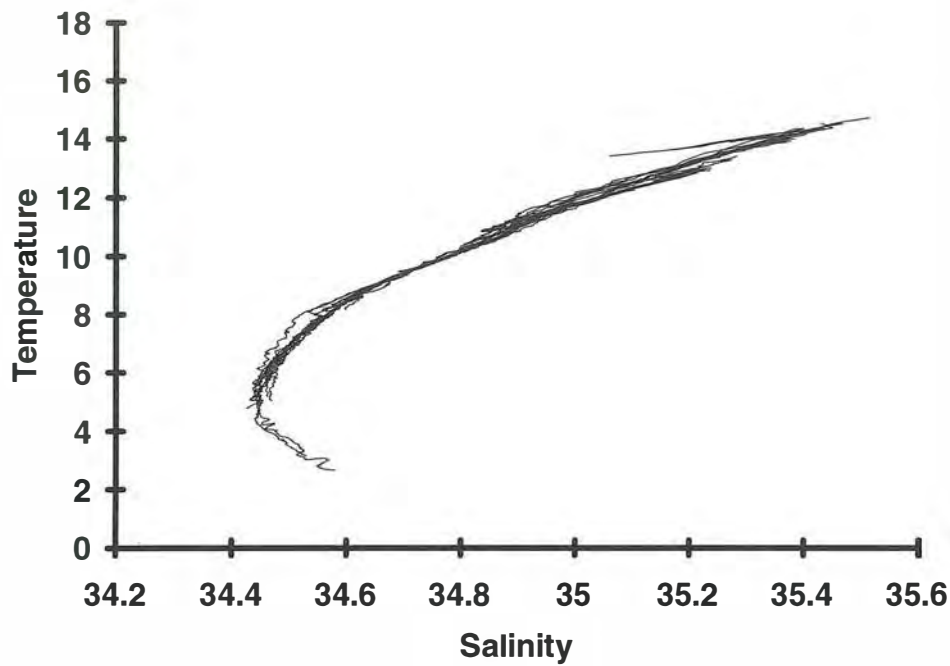
Fig. 9. Temperature (°C) vs salinity plots for CTD profiles from SS2/91.

The temperature vs salinity (T-S) diagrams for stations on this cruise were all tightly grouped (Fig. 9). The salinity minimum (AAIW) occurred at ca 34.43 and 5 °C. The T-S curves were almost linear between 8 °C, 34.6 (lower mode water) and the warm saline (14 °C, 35.5) water of the Zeehan Current. The low salinity warm water on the inner shelf on the western transect appears as a "hook" at the surface.

CRUISE SS1/92: FEBRUARY, 1992.

On the western transect, temperature and salinity contours generally sloped downward from onshore to offshore below 200 m (Fig. 10). There was a broad, shallow SAMW layer from 8 to 10 °C between 300 and 600 m. There was also evidence for doming upwards of temperature and salinity contours above 400 m over the upper slope, and at the shelf break. Mixed layer temperatures were maximum (ca 14.5 °C) over the upper slope, and isotherms in the thermocline sloped up onto the shelf inshore of this maximum (Fig. 11A). Salinity was highest (ca 35.1) in the warm temperature core, and lower on the shelf and offshore (Fig. 11B). A subsurface salinity maximum, also about 35.1, at 100 m depth, occurred offshore from the surface salinity maximum.

On the central transect, the salinity minimum (AAIW) was clearly distinguished by the 34.4 contour at ca 1000 m (Fig. 12B). Temperature and density contours sloped downwards from onshore to offshore below 500 m, but upwards above 500 m (Fig. 12A, C). There was some evidence for SAMW between 400 and 600 m, and for doming of contours at station 19 (offshore) above 500 m. Both SAMW and AAIW weakened over the slope, inshore of station 18, indicating that the EAC signature reaches deep in the watewr column. In the top 200 m, a pool of warm saline water (17 °C, 35.5) extended from the shelf-break to mid-slope (Fig. 13). This pool was bounded inshore and offshore by a strong salinity and temperature front. Surface temperatures were ca 14 °C on the inner shelf and offshore. Density contours sloped upwards inshore and offshore of the light warm, saline pool.

In the upper 200 m, both western and central sections were dominated by a warm, saline pool over the mid-slope. However, this pool was much warmer and more saline on the central transect than on the western transect (35.5, 17 °C vs 35.1, 14.5 °C). The offshore salinities and temperatures were similar on both transects (ca 14 °C and 35.0). The slope of the isopycnals indicated flow to the west at depth on both transects, with a possible reversal of this flow in the top 500 m offshore on the central transect. The data are consistent with a strong penetration of EAC water as far as the central transect, and a relatively weak influence of this water on the western transect.

Satellite SST composites for the period of the cruise (20-22 February) show a tongue of warm (EAC) water (ca 17 °C) extending over the central transect from the east, bounded inshore by the 200 m contour (Fig. 1B). Interestingly, in images just a few days earlier, this tongue was much narrower, located offshore of the shelf-break, and showed more mesoscale structure. The satellite image shows cooler temperatures (ca 14 to 14.5 C) on the shelf and throughout the western transect. The image sequence suggests that the slightly warmer, higher salinity water on the western transect is connected to the EAC tongue, and may represent the effects of mixing, cooling, and possibly subduction. Cooling and

subduction could explain the relatively rapid disappearance of the mesoscale
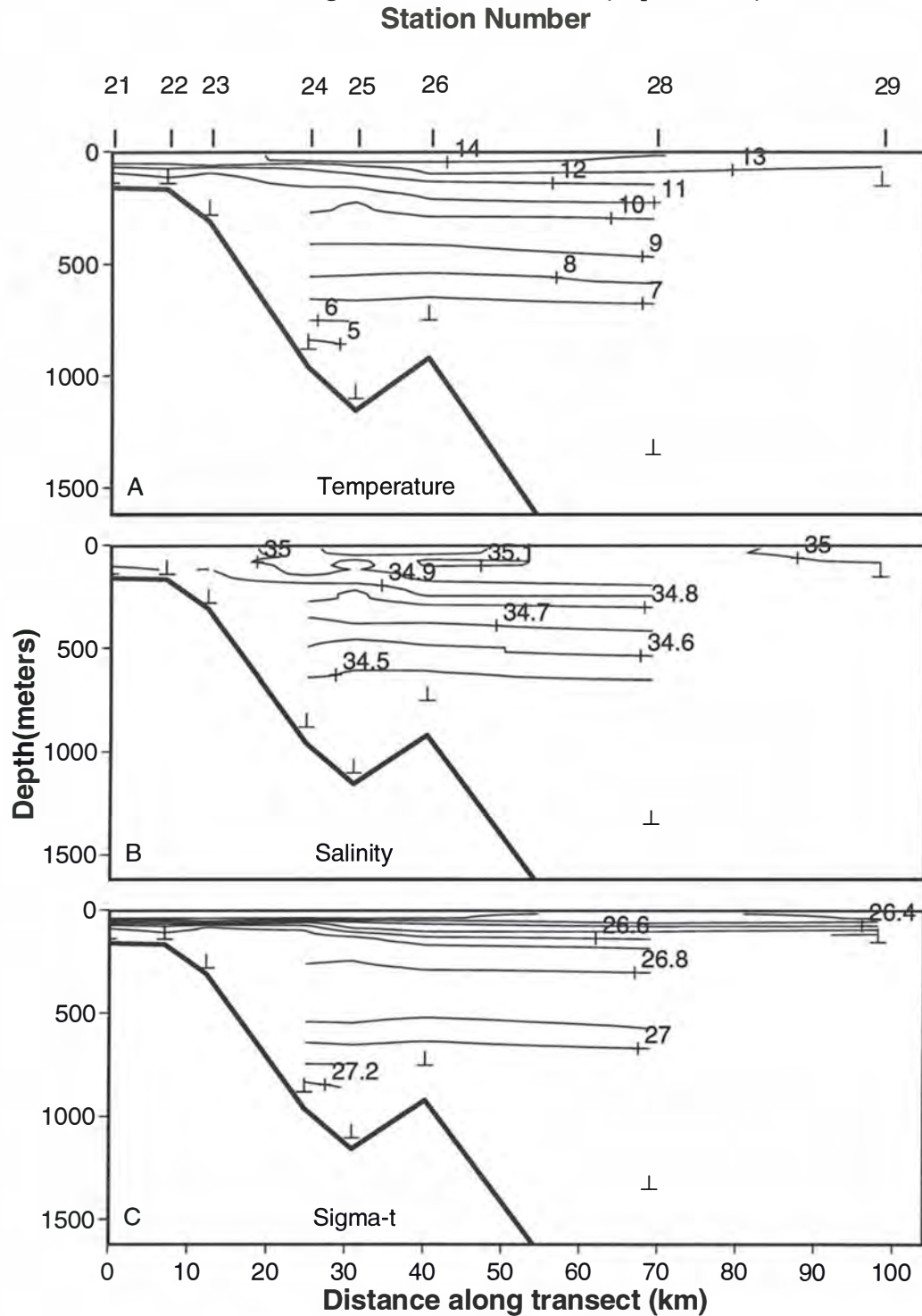structure in the warm tongue observed a few days previously.

Station Number

Fig. 10. Contours of (A) temperature (°C), (B) salinity and (C) sigma-t on vertical
sections along the western transect, cruise SS1/92, February, 1992.

Station Number
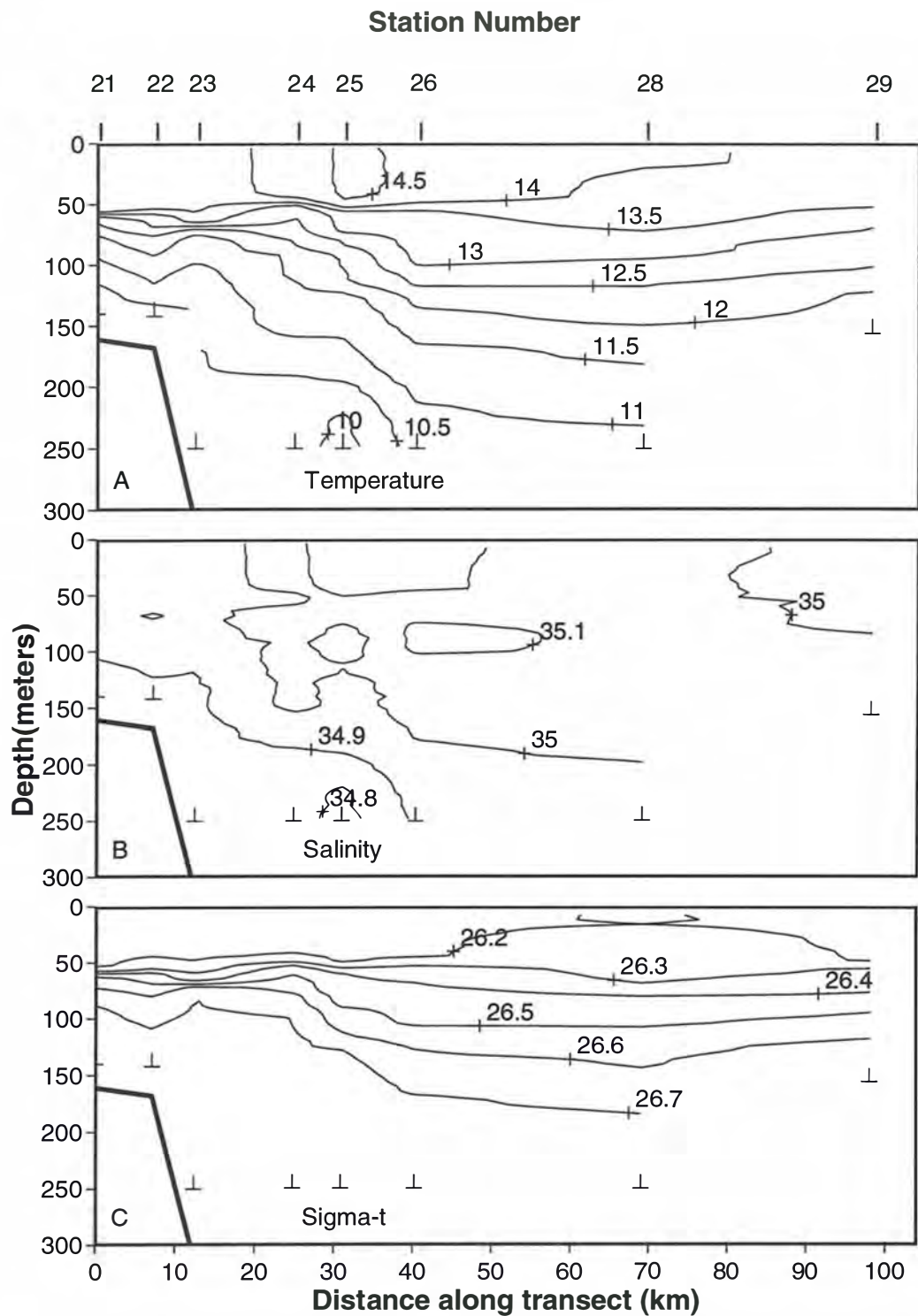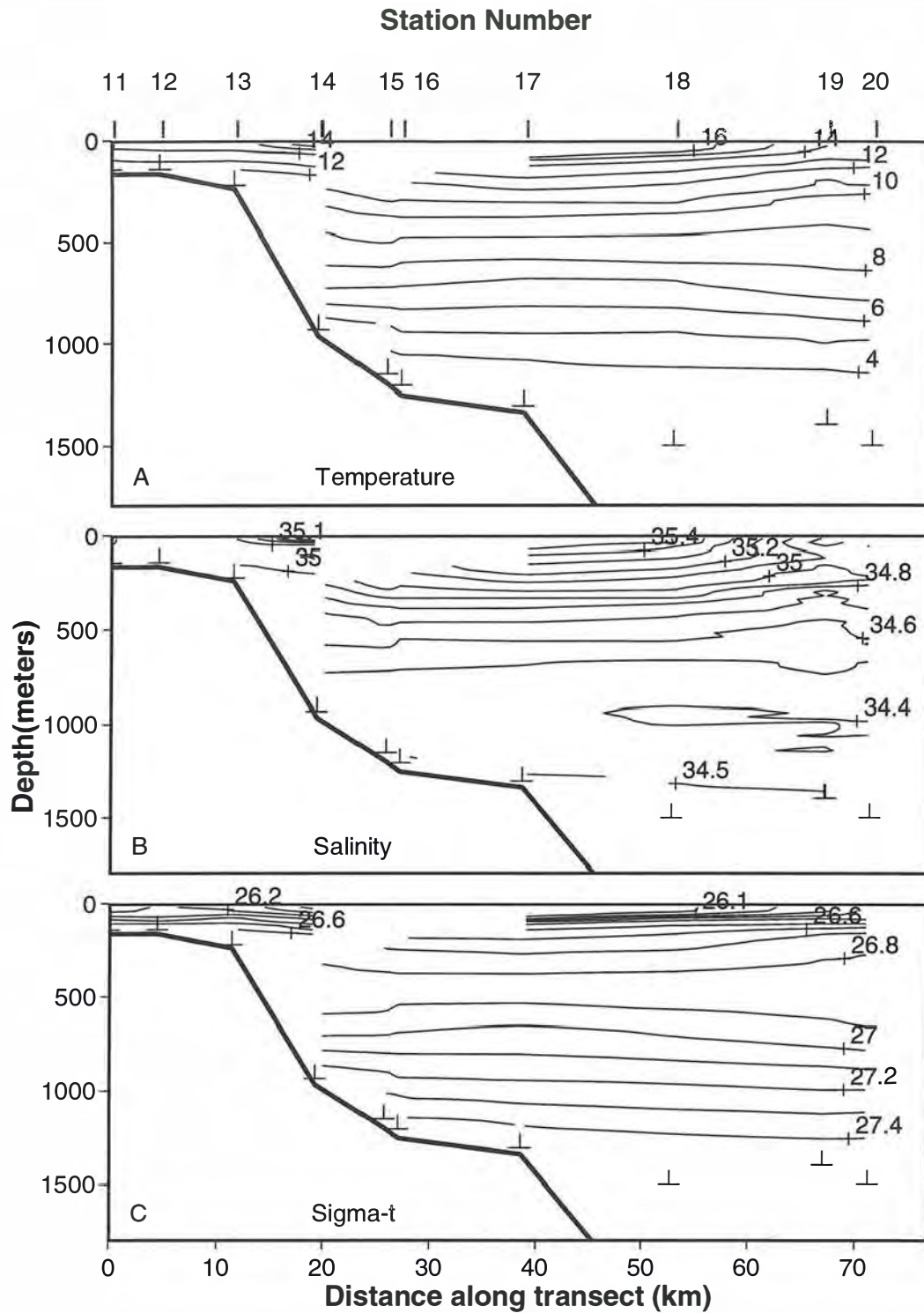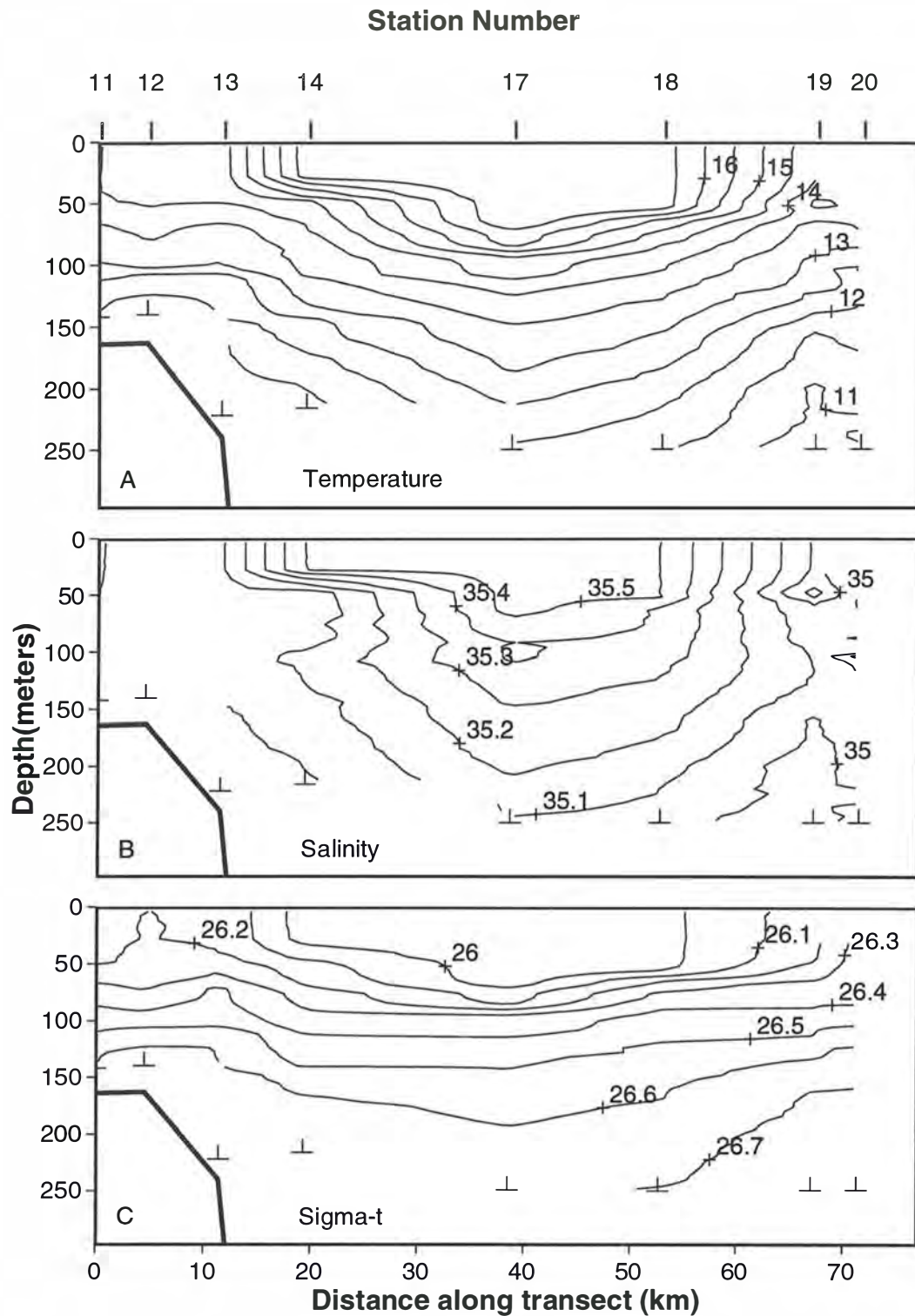

Fig. 11. Contours of (A) temperature (°C), (B) salinity and (C) sigma-t on vertical sections (0-250 m) along the western transect, cruise SS1/92, February, 1992.

Station Number

Fig. 12. Contours of (A) temperature (°C), (B) salinity and (C) sigma-t on vertical sections along the central transect, cruise SS1/92, February, 1992.

Station Number

Fig. 13. Contours of (A) temperature (°C), (B) salinity and (C) sigma-t on vertical sections (0-250 m) along the central transect, cruise SS1/92, February, 1992.
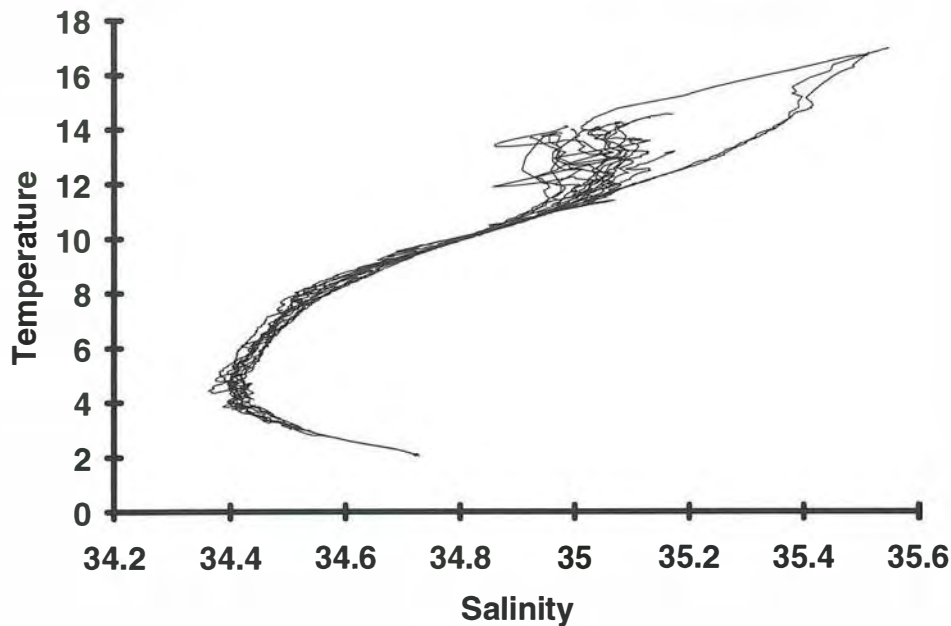
Fig. 14. Temperature (°C) vs salinity plots for CTD profiles on cruise SS1/92.

The T-S diagrams for SS1/92 were generally rather tightly clustered below the upper layer (T < 10 °C), although there was some indication of small salinity anomalies at the salinity minimum (Fig. 14). The salinity minimum was fresher than in July, 1991: ca 34.40 at 5 °C. In the upper layer, there were two characteristic water masses: the high salinity, high temperature water associated with the EAC (35.5, 17 °C), and a more typical upper layer with temperatures ranging from 11 to 14 °C, and salinity from 34.9 to 35.1. The properties of this pool were consistent with seasonal warming of the winter water masses formed by mixing between either EAC or Zeehan water and SAMW. The numerous reversals in T-S plots suggest mixing and isopycnal interleaving of water properties within this seasonal layer, and in one case between this pool and EAC water.

CRUISE SS4/92: NOVEMBER, 1992.

On the western transect, a salinity minimum of ca 34.4 shoalled towards the slope from ca 1100 m to 850 m (Fig. 15B). There was some broadening of the 8 - 10 °C isotherms between 300 and 600 m (SAMW) (Fig. 15A), but it was not as pronounced as that observed east of Tasmania (Fig. 19A). Isotherms and isopycnals generally shallowed from offshore to onshore at all depths. A small eddy-like structure, involving doming of the temperature, salinity and density

contours between 100 and 500 m, was centred on station 9, approximately 50 km from the shelf break.

Surface temperatures were mostly greater than 12 °C, and surface salinities as high as 35.2 (Fig. 16A,B). The peak surface temperatures and salinities occurred in two broad shallow pools extending from 10 to 30 km from the shelf break, and again from 50 to 80 km from the shelf break. Temperatures and salinities were lower on the shelf, and in a narrow gap between the warm pools over the eddy feature at station 9. The mixed layer was shallow (less than 40 m) throughout the section.

On the central transect, the AAIW salinity minimum occurred at ca 900 m (Fig. 17B). There was some evidence of SAMW in a slight broadening of the 8 to 10 °C isotherms below 250 m, and strong evidence of an isothermal 10 °C layer between 80 and 200 m which was presumably the remnant of the winter mixed layer. Temperature, salinity and density contours sloped upward from onshore to offshore below 600 m, but the slope was reversed above 600 m, with a corresponding spreading of temperature and salinity contours between 400 and 600 m over the slope (Fig. 17).

Within the top 200 m, a warm saline pool extended from the shelf break to ca 40 km beyond the shelf break (Fig. 18A,B). Maximum temperature and salinity (ca 35.05 and 11.8 °C) occurred out to 20 km from the shelf break, bounded offshore by a strong subsurface temperature and salinity front at 60 m. There was some indication of an increase in temperature and salinity at the furthest station offshore (60 km from the shelf break). The doming of temperature, salinity and density contours at 40 km from the shelf break could be contiguous with the feature observed on the western transect, except that the former does not show any expression below 200 m in the temperature and salinity fields.

On the eastern transect, there was much stronger evidence for SAMW, with broad 8 to 10 °C isotherms between 300 and 700 m, as well as a remnant winter mixed layer from 100 to 250 m (Fig. 19A). There was a marked dome feature in temperature and salinity located at stations 34 and 35, ca 30 km offshore off the shelf break, between 300 and 600 m (Fig. 19). Density contours sloped upward from onshore to offshore. In the top 200 m, a pool of warm saline water extended from the shelf break to ca 35 km offshore of the shelf break (Fig. 20). Peak surface temperatures at stations 34 and 35 exceeded 12 °C.

All three transects showed evidence of AAIW, although the depth of the salinity minimum layer appeared to vary both east to west and onshore to offshore. The slope of isopycnals also varied from east to west, suggesting flow to the north-west in the west, and flow to the north-east in the east, relative to 1500 m. The SAMW was only well defined on the eastern transect. The remnant winter

mixed layer was also poorly defined on the western transect, but well-defined in the central and eastern transects.
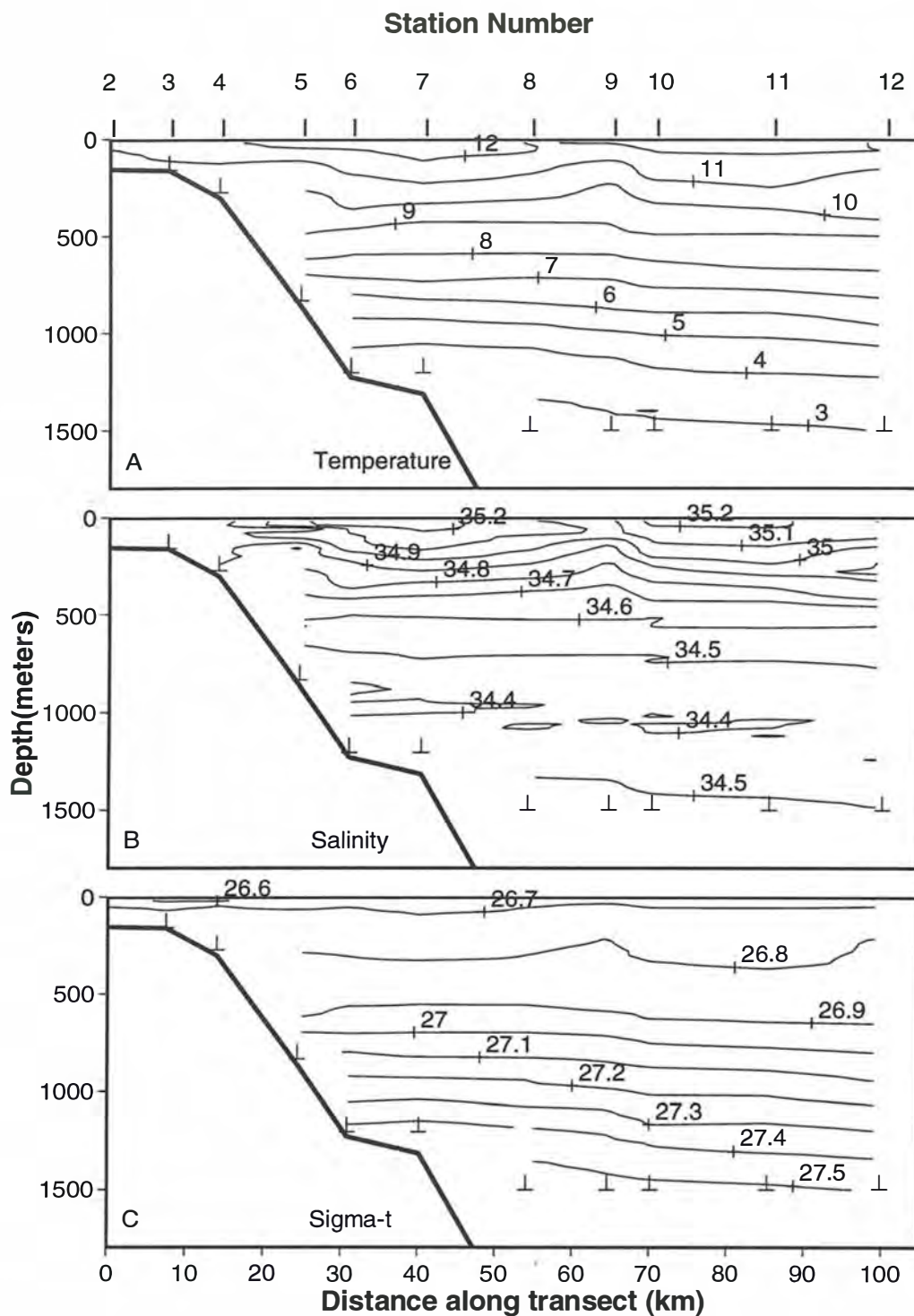

Fig. 15. Contours of (A) temperature (°C), (B) salinity and (C) sigma-t on vertical sections along the western transect, cruise SS4/92, November, 1992.
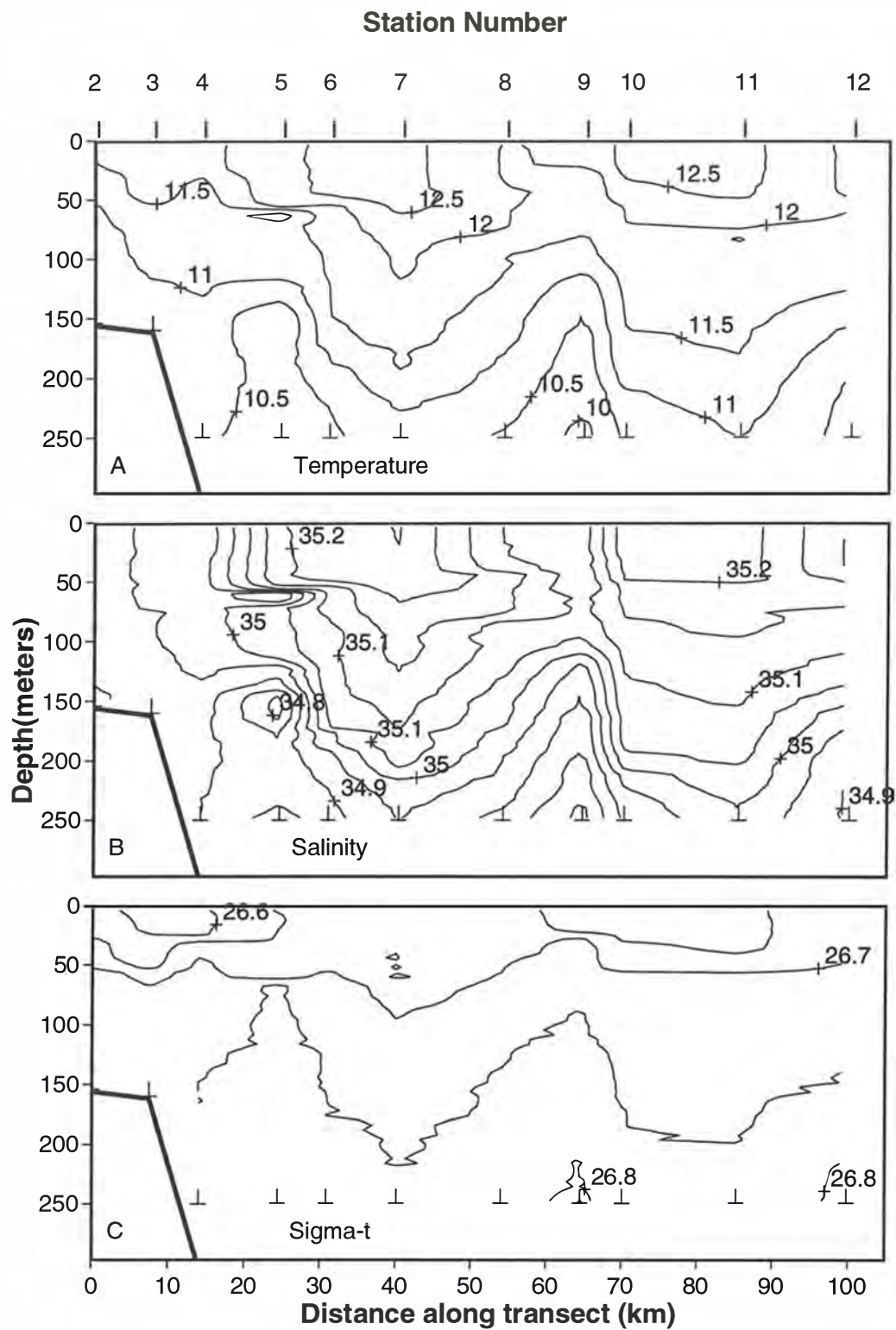
47

Fig. 16. Contours of (A) temperature (°C), (B) salinity and (C) sigma-t on vertical sections (0-250 m) along the western transect, cruise SS4/92, November, 1992.
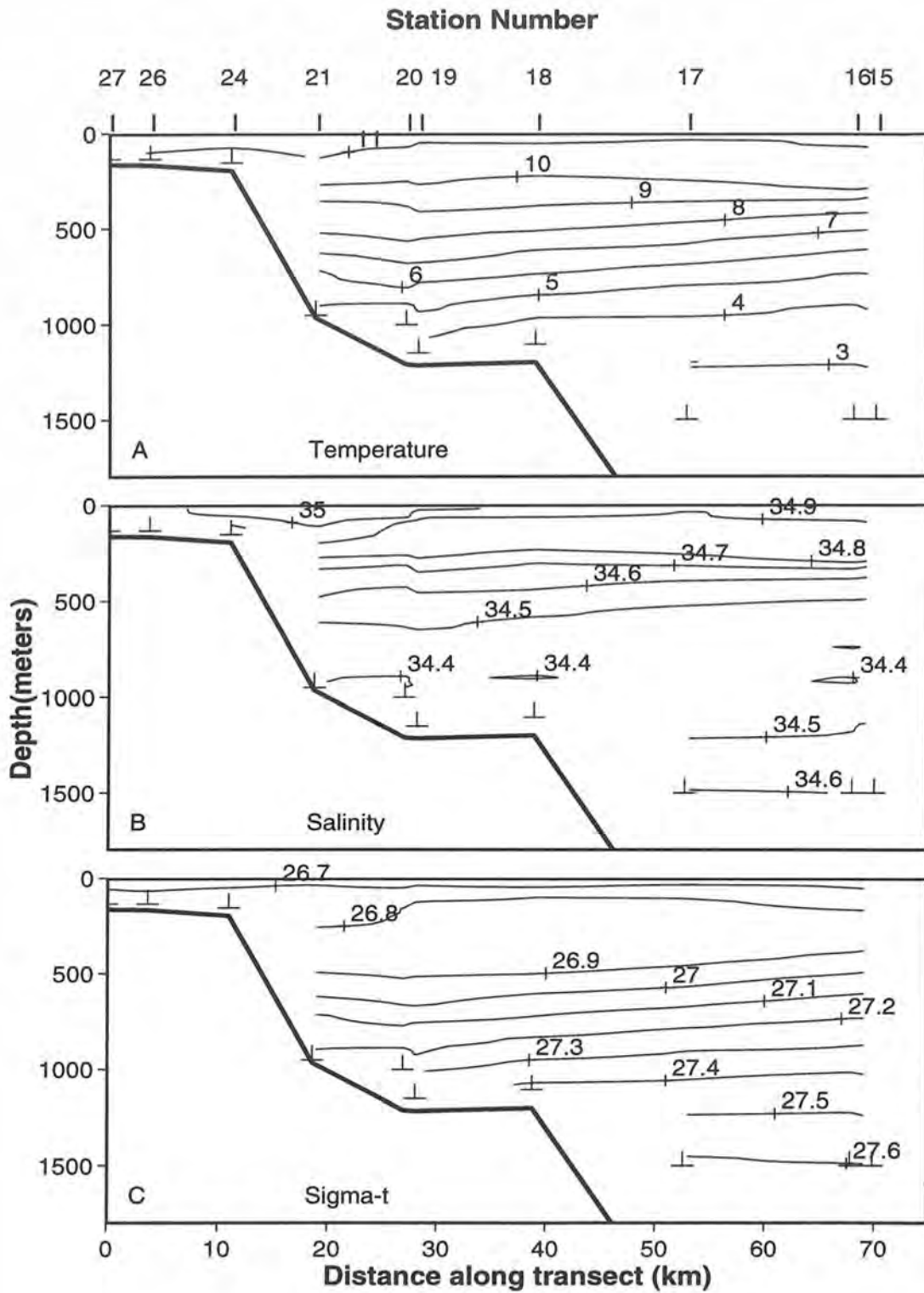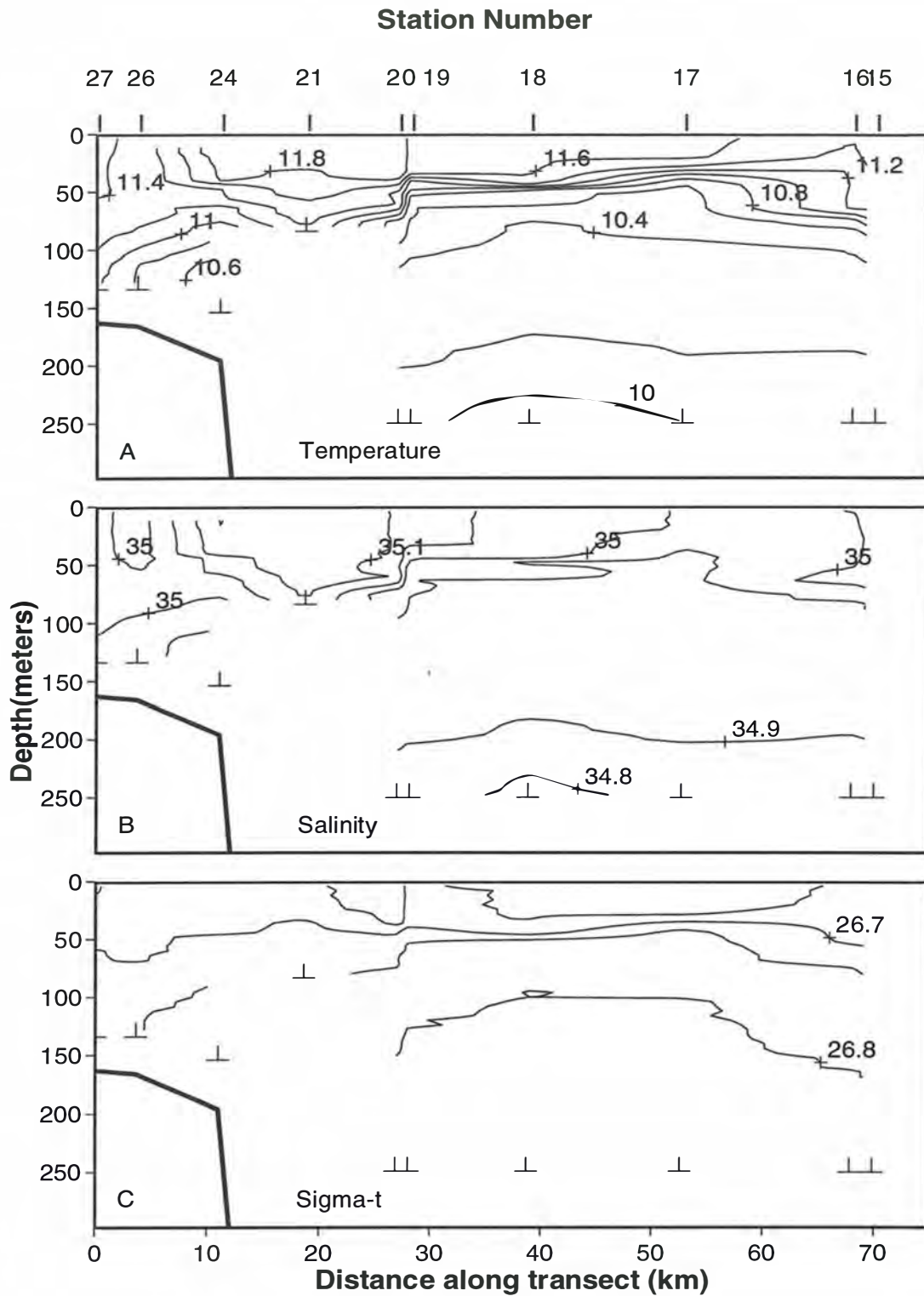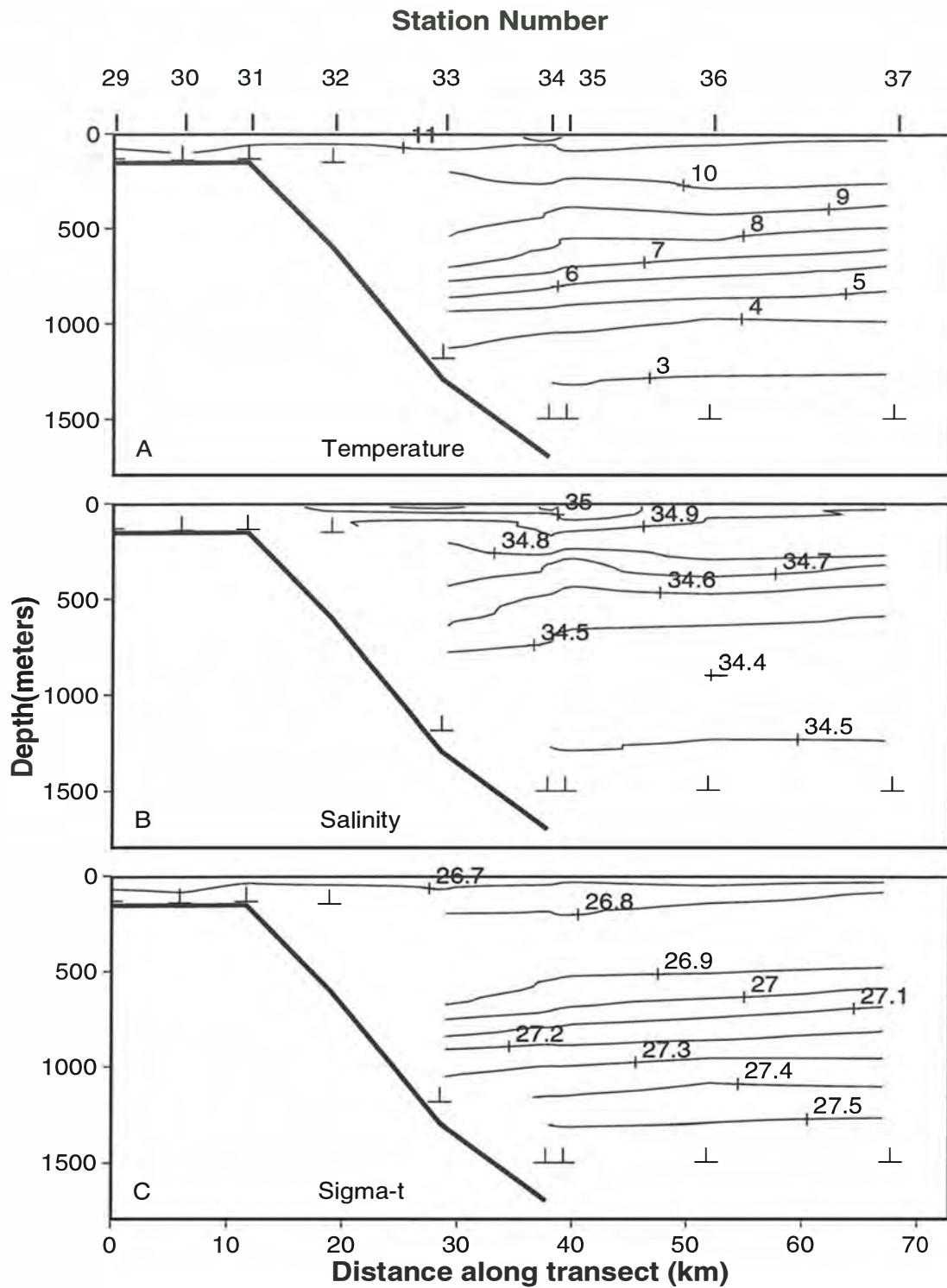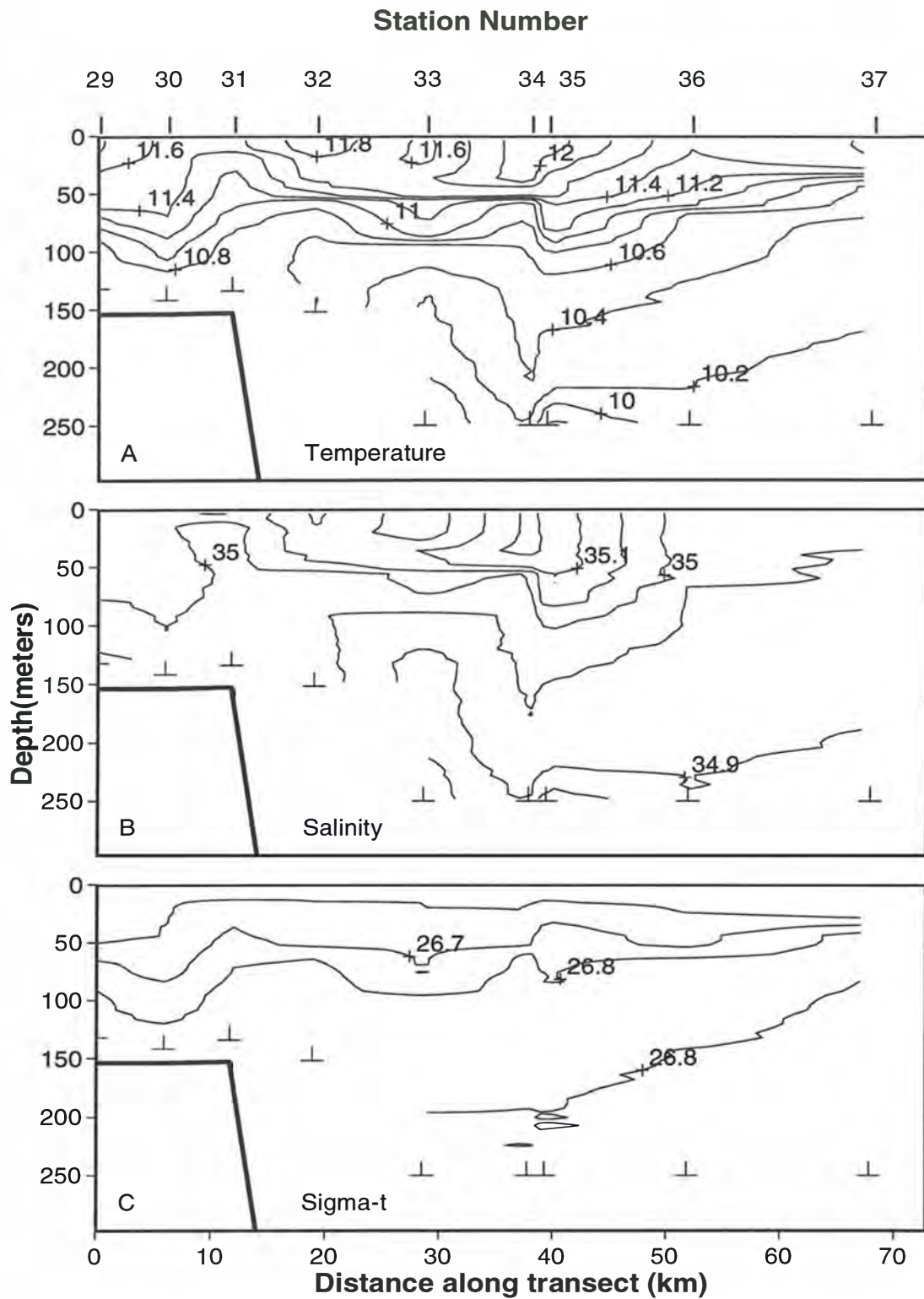
Fig. 17. Contours of (A) temperature (°C), (B) salinity and (C) sigma-t on vertical sections along the central transect, cruise SS4/92, November, 1992.

Station Number

Fig. 18. Contours of (A) temperature (°C), (B) salinity and (C) sigma-t on vertical sections (0-250 m) along the central transect, cruise SS4/92, November, 1992.

Fig. 19. Contours of (A) temperature (°C), (B) salinity and (C) sigma-t on vertical sections along the eastern transect, cruise SS4/92, November, 1992.

Fig. 20. Contours of (A) temperature (°C), (B) salinity and (C) sigma-t on vertical sections (0-250 m) along the eastern transect, cruise SS4/92, November, 1992.
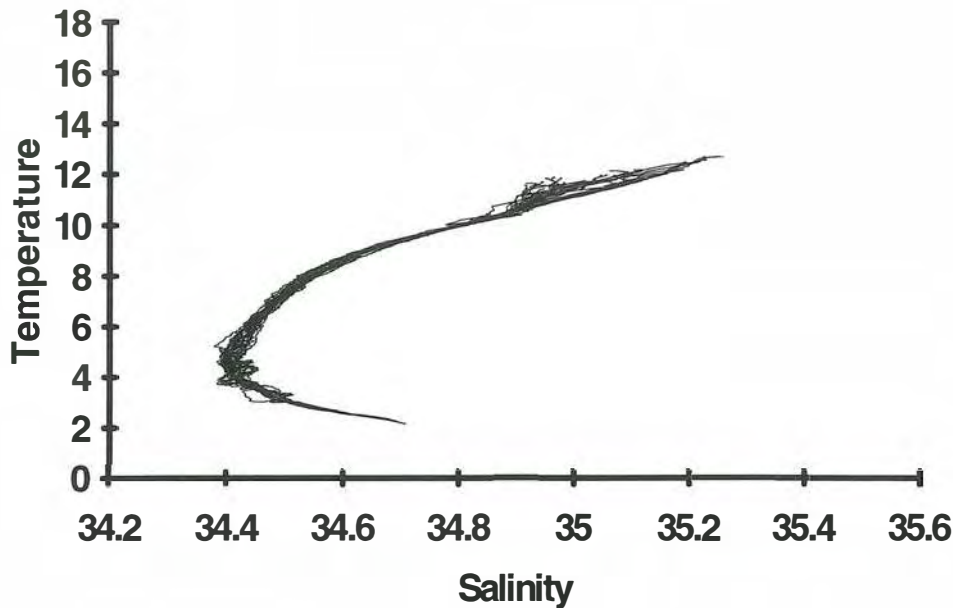
Fig. 21. Temperature (°C) vs salinity plots for CTD profiles on SS4/92.

In the top 200 m, on all three transects, a clearly defined pool of warm saline water was situated over the upper slope, just off the shelf edge. This pool was warmest and most saline on the western transect. All three transects also showed evidence of upwelling just offshore of the shelf break. The eastern and western transects showed evidence of upwelling or domed contours above 500 m respectively 30 and 50 km offshore of the shelf break. On the western transect, there was a second pool of warm saline water offshore of this feature.

The satellite SST images for the period of this cruise were cloud affected even after compositing. The image composites suggest that SST in the study area was generally about 12 to 12.5 C, with some cooler features which are difficult to distinguish from cloud effects (Fig. 1C). Warm EAC water extended south and east of the study area, but appeared to leave the shelf break off Tasman Peninsula. The image seems consistent with the hypothesis that the warmer more saline water in the study area was remnant Zeehan Current water.

The T-S plots for this cruise showed some layering of AAIW of different salinities, ranging from 34.38 to 34.43 within the broad salinity minimum (Fig. 21). The plots were almost linear between 9 °C, 34.63 and 12 °C, 35.3, with evidence for slight warming of ca 0.5 degrees in surface waters. The deep data (S < 34.9) closely overlay data obtained in February 1992.

CRUISE SS3/93: APRIL, 1993.

On the western transect, the deep temperature and salinity sections showed a pronounced SAMW layer, with temperatures of 8 to 10 °C, and salinities of 34.5 to 34.8, between 300 and 600 m, but shallowing to ca 100 m offshore beyond a strong surface front between stations 24 and 25 (Fig. 22). The SAMW lay below a strong thermocline and halocline, concentrated close to 100 m. The AAIW salinity minimum occurred at ca 1000 m, but the layer less than 34.4 broadened abruptly offshore beyond station 24. There was some indication of weak mesoscale structure in the top 800 m over the outer slope, and temperature, salinity and density contours sloped downward at the continental slope, indicating an eastward current along the slope.

Over most of the transect, the surface mixed layer was quite deep (ca 65 m) and relatively warm and saline (> 14 °C, > 35.0) (Fig. 23). The major feature in the top 200 m was a very intense surface front at the offshore end of the transect, ca 85 km from the shelf break. Here, temperature and salinity dropped from 14.5 to 11 °C, and 35.0 to 34.2, in the space of 10 km. The satellite composite for April 1993 showed a cold mesoscale feature and a strong surface front in this vicinity. There were strong temperature and salinity inversions in the top 100 m at stations near the front, but relatively little density signal. The mixed layer was slightly fresher, cooler and lighter over the upper slope and shelf. Temperature, salinity and density contours between 60 and 200 m all showed evidence of broad upwelling over the slope, with downwelling at station 19.

On the central transect, the SAMW layer, between 400 and 650 m, was thinner and deeper than on the western transect (Fig. 24). Surface mixed layers were deep (> 80 m) over the lower slope, and ca 40 to 60 m over the upper slope and at the offshore station (Fig. 25). A deep, warm, saline pool occurred over the slope, with peak temperatures of ca 16.5 °C and salinity > 35.4. Temperature and salinity decreased inshore on the shelf, and offshore. The warm saline pool was almost certainly EAC water, and the satellite composite for April showed a tongue of EAC water wrapped around the southern slope of Tasmania as far as this transect. Temperature, salinity and density contours all showed strong subsurface upwelling at the shelf break.

Temperature, salinity and density distributions on this cruise were distinguished by the effects of autumn cooling and mixing, which produced deep mixed layers above a sharp pycnocline. There was a strong contrast between western and central transects: the western transect showed relatively low temperatures and salinities (14 °C, 35.0), characteristic of offshore waters, with a striking front at the offshore stations, where the transect extended into a tongue of cool (11 °C), fresh (<34.4) water. Surface salinities below 34.4 are normally found in the SubAntarctic Front near 50 °S.

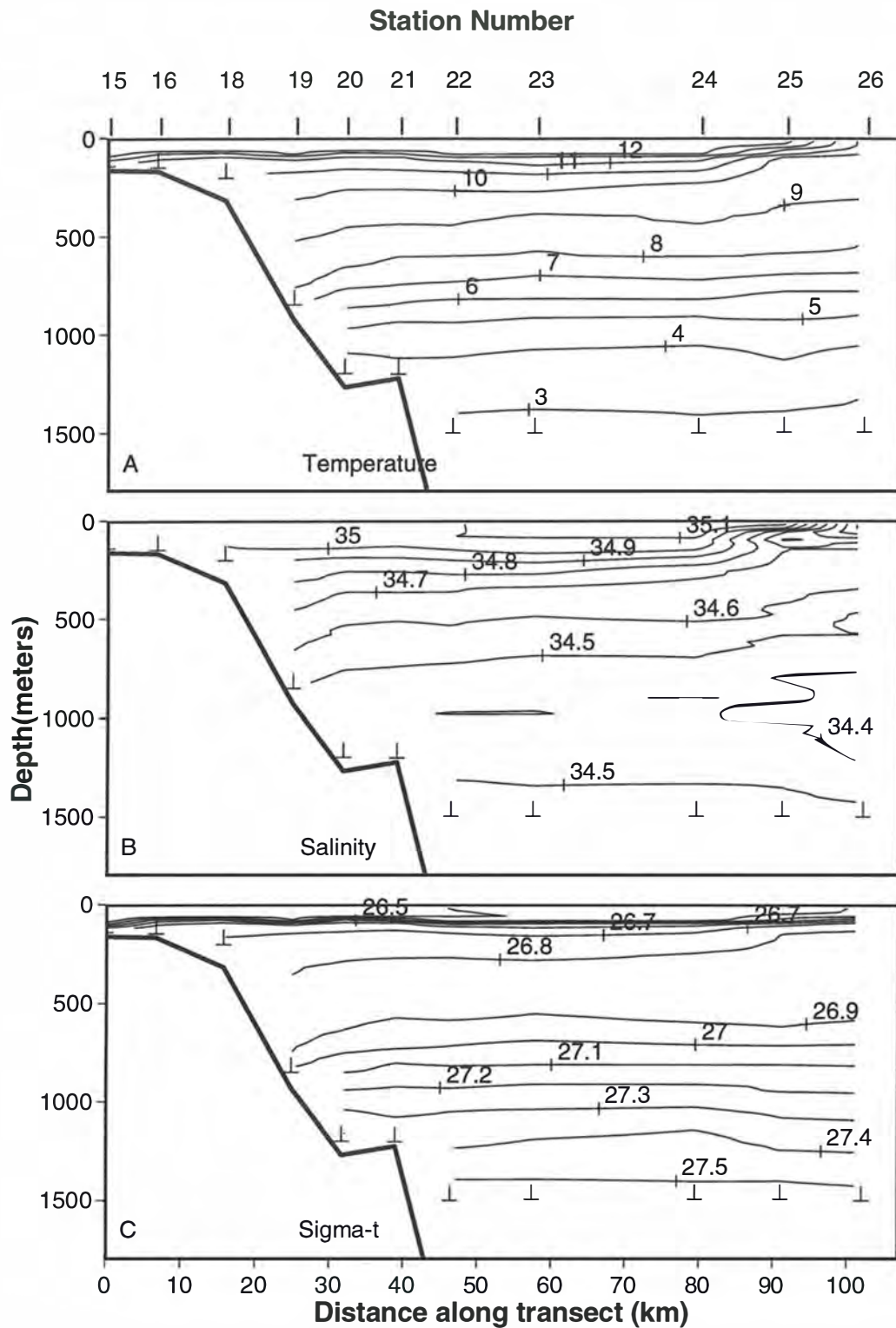**Station Number**

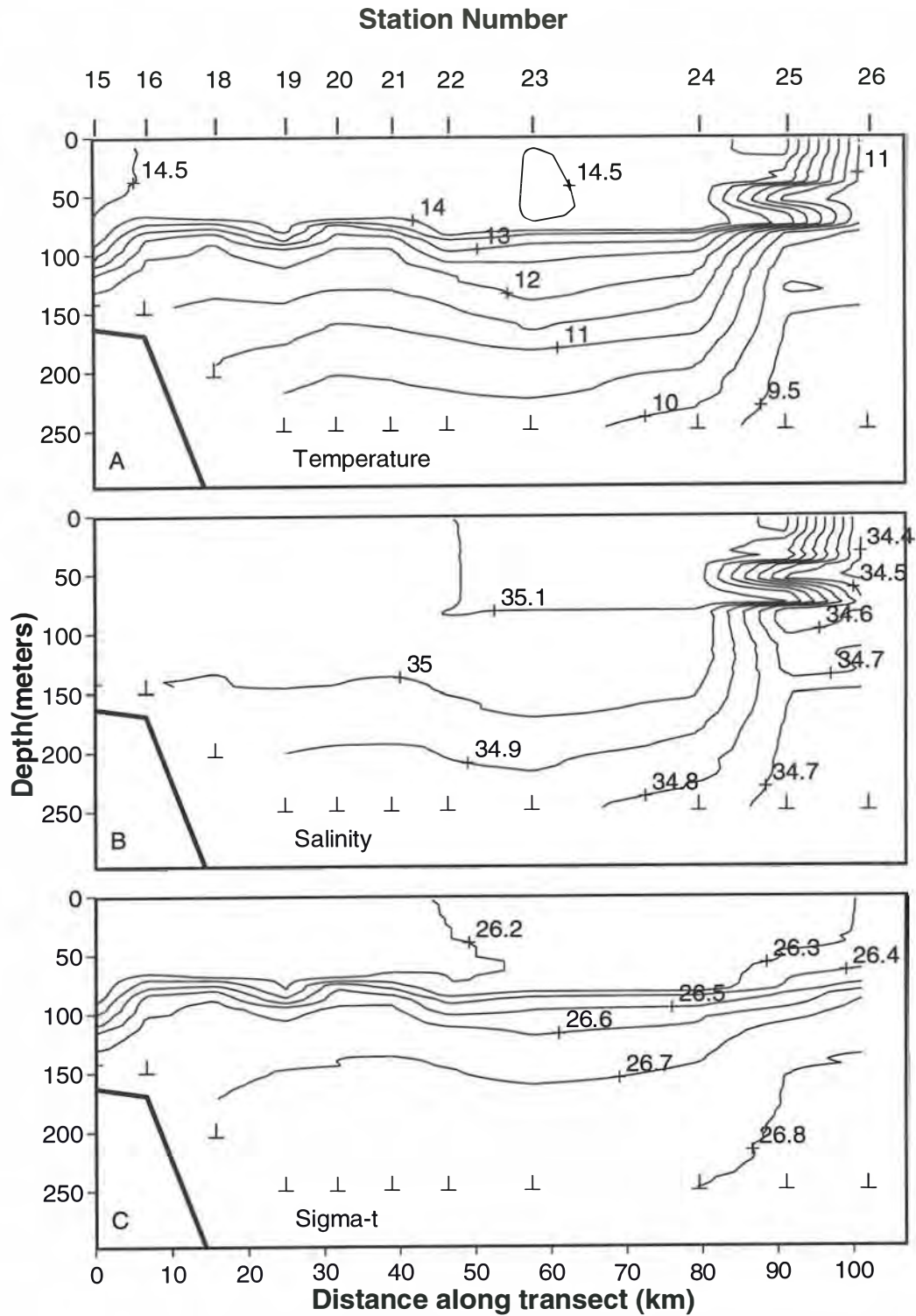Fig. 22. Contours of (A) temperature (°C), (B) salinity and (C) sigma-t on vertical sections along the western transect, cruise SS3/93, April, 1993.

Fig. 23. Contours of (A) temperature (°C), (B) salinity and (C) sigma-t on vertical sections (0-250 m) along the western transect, cruise SS3/93, April, 1993.
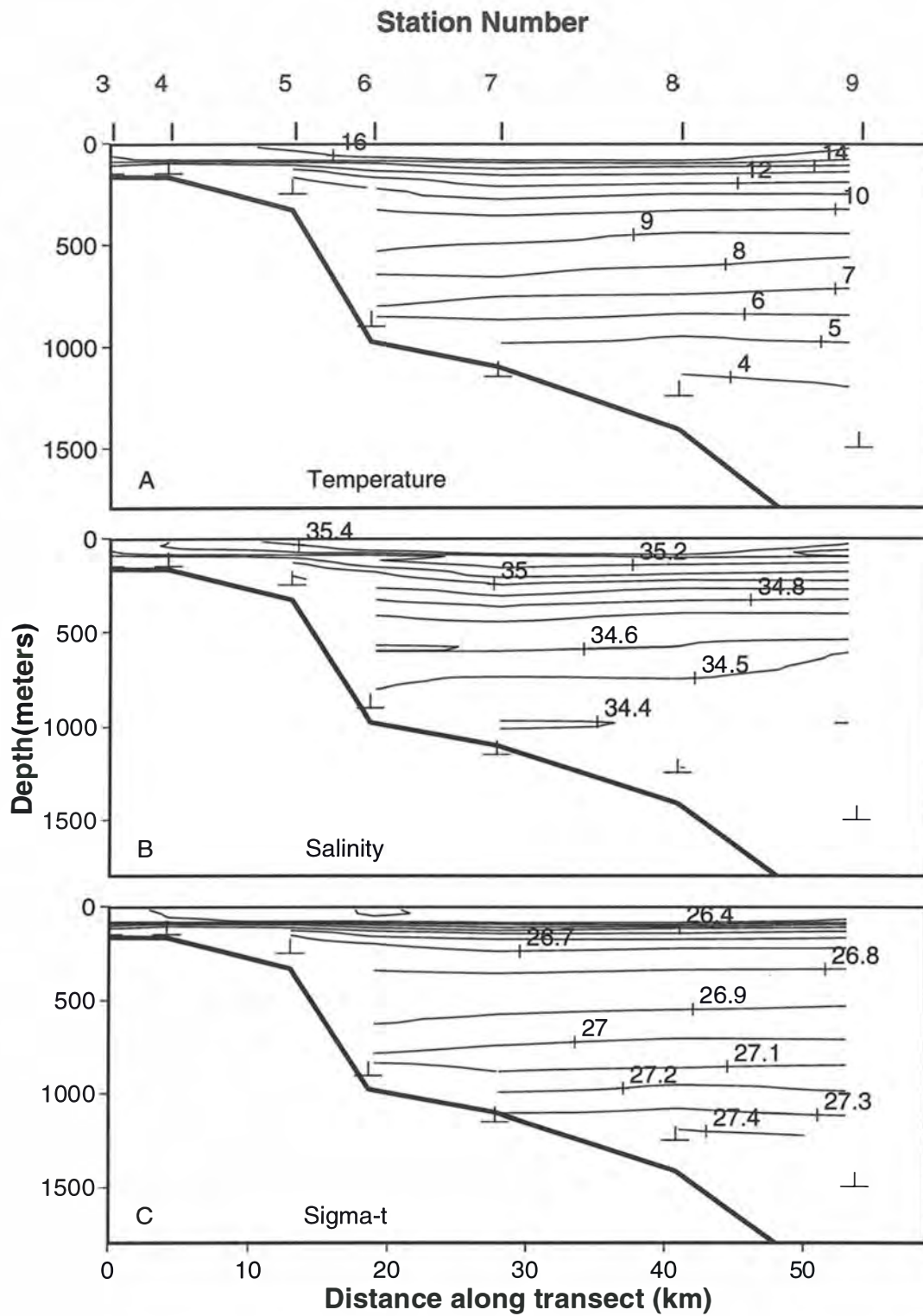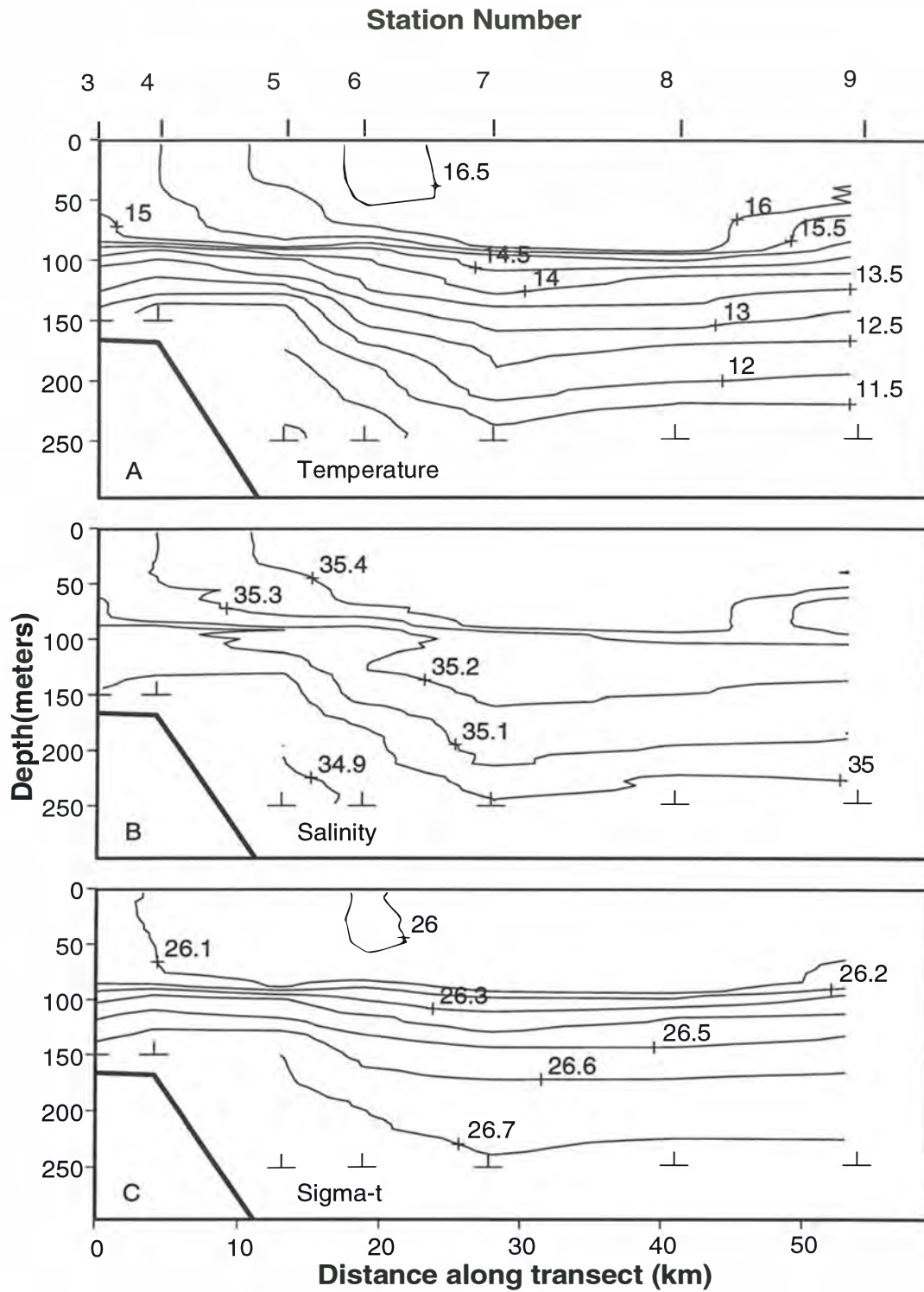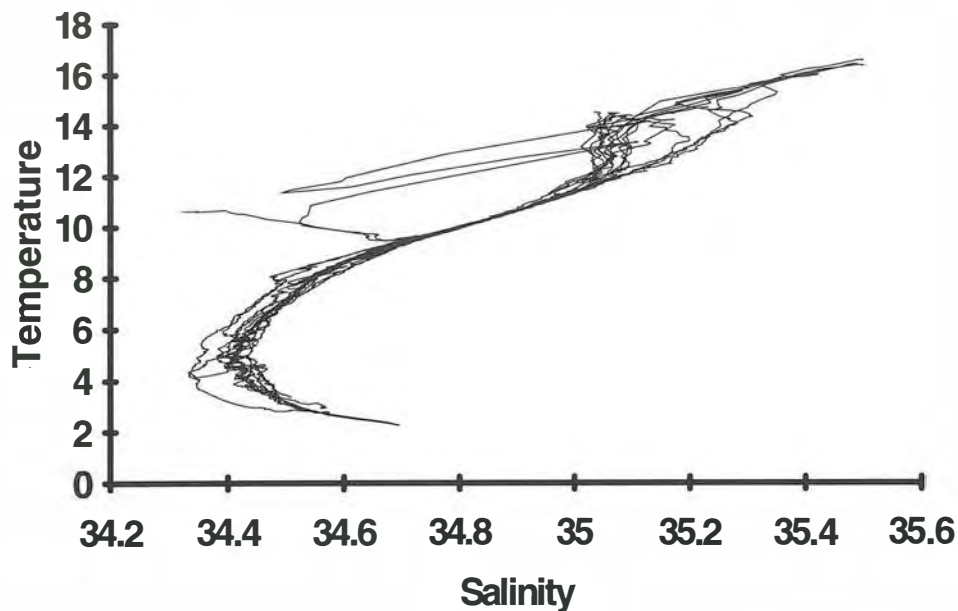
Station Number

Fig. 24. Contours of (A) temperature (°C), (B) salinity and (C) sigma-t on vertical sections along the central transect, cruise SS3/93, April, 1993.

Fig. 25. Contours of (A) temperature (°C), (B) salinity and (C) sigma-t on vertical sections along the central transect, cruise SS3/93, April, 1993.

Fig. 26. Temperature (°C) vs salinity plots for CTD profiles on SS3/93.

The central transect was dominated by EAC water, with mixed layer salinities and temperatures of 35.4 and 16.5 °C, extending from the shelf break almost to the offshore station.

The satellite images for April were again affected by cloud, but confirmed the intrusion of a tongue of cold water from the south-west, and the presence of warm EAC water from the east (Fig. 1D). Satellite images preceding the cruise suggested that autumn cooling and mixed-layer deepening took place rapidly during April. A SST image from 7-10 April showed a tongue of warm EAC water (ca 15.5 °C) apparently entrained in an eddy, extending over the western transect, and very warm EAC water (ca 17 °C), entrained in an eddy located over and south-west of the central transect. This water mass may have been displaced from the western transect by the cold tongue of Subantarctic Frontal water, as it moved north-east.

The T-S diagrams for most of the stations on this cruise were consistent with seasonal warming of the upper layer over the summer (Fig. 26). Most stations belonged to one of two groups: those in EAC water, with surface salinities up to and exceeding 35.4, and those outside EAC water, with surface salinities around 35.05. There were two remarkable T-S profiles (Fig. 26), corresponding to the two offshore stations on the western transect, located in SubAntarctic Frontal water. The frontal station showed evidence of interleaving and mixing between

the two water masses. At both these stations, the deep salinity minimum was much fresher (and shallower) than at the inshore stations. This means that the intruding tongue of SubAntarctic Frontal water was a deep feature, potentially affecting water mass properties at 800 to 1000 m on the slope.

SEASONAL CYCLE IN MIXED LAYER DEPTHS.

Maximum mixed layer depths were observed in winter (July, 1991), as might be expected (Fig. 27A). However, winter mixed layer depths varied considerably throughout the study region, being quite shallow (<20 m) inshore on the western transect, moderate (50 to 100 m) offshore on all three transects, and deep (100 to 250 m) in Zeehan Current water over the shelf and slope on all three transects. It seems reasonable to assume that these deep mixed layers are a result of cooling and convective mixing of warm, saline Zeehan Current water as it is advected south and east.

In spring (November, 1992), mixed layer depths were all less than 100 m, and in many cases quite shallow (10 to 30 m: Fig. 27B). The deepest mixed layers were observed on the shelf on the central and eastern transects. The shallow mixed layers were clearly the result of recent seasonal stratification. On the central and eastern transects, over the slope and offshore, the seasonal pycnocline lay above an isothermal, isohaline layer extending from ca 60 - 80 m to 200 - 300 m. This appears to be a "fossil" winter mixed layer. Interestingly, on the western transect over the slope and offshore, the water mass below the seasonal pycnocline was generally not isothermal or isohaline, but showed a weak but steady gradient to 200 m or deeper, except for one station on the upper slope. Stations on the shelf on the western transect were well-mixed below the seasonal thermocline. The pattern of "fossil" winter mixed layer depths evident on this cruise generally corresponded to the pattern observed on the winter (July) cruise, except that there was evidence for deep winter mixed layers offshore on the central and eastern transect. These may form in the period of convective cooling between July and October.

In summer (February, 1992), the seasonal thermocline was well established, and mixed layer depths were relatively uniform throughout the western and central transects, most in the range 40 - 60 m (Fig. 27C). In autumn, mixed layer depths had generally deepened to 60 - 90 m, and the pycnocline at the base of the mixed layer had sharpened, reflecting the early stages of autumn cooling and erosion of the seasonal thermocline (Fig. 27D).
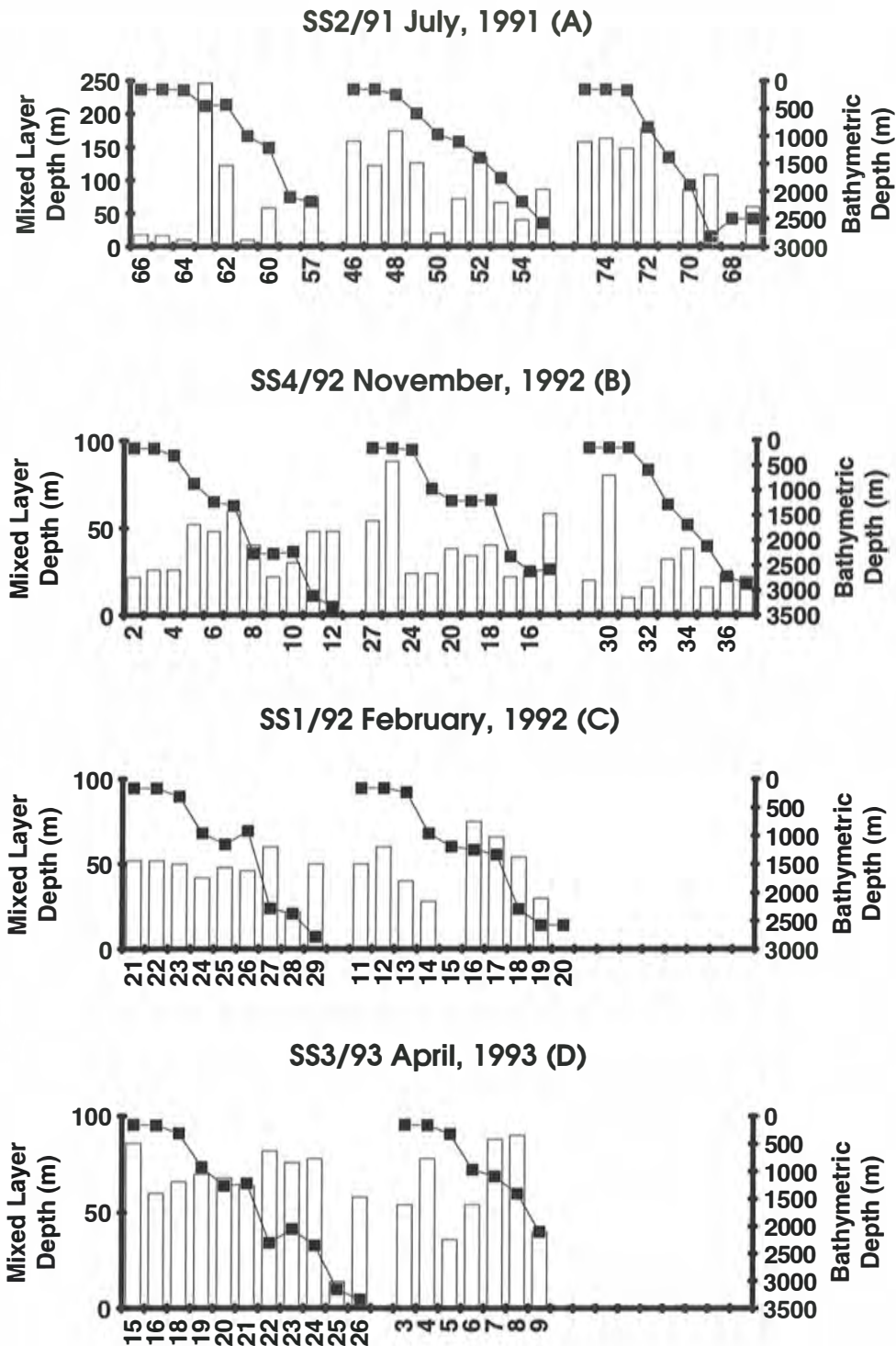
Fig. 27. Mixed layer depths (bars) and bathymetric depths (lines) for CTD stations by cruise and transect. Transects are presented as western, central and eastern (where available) from left to right.
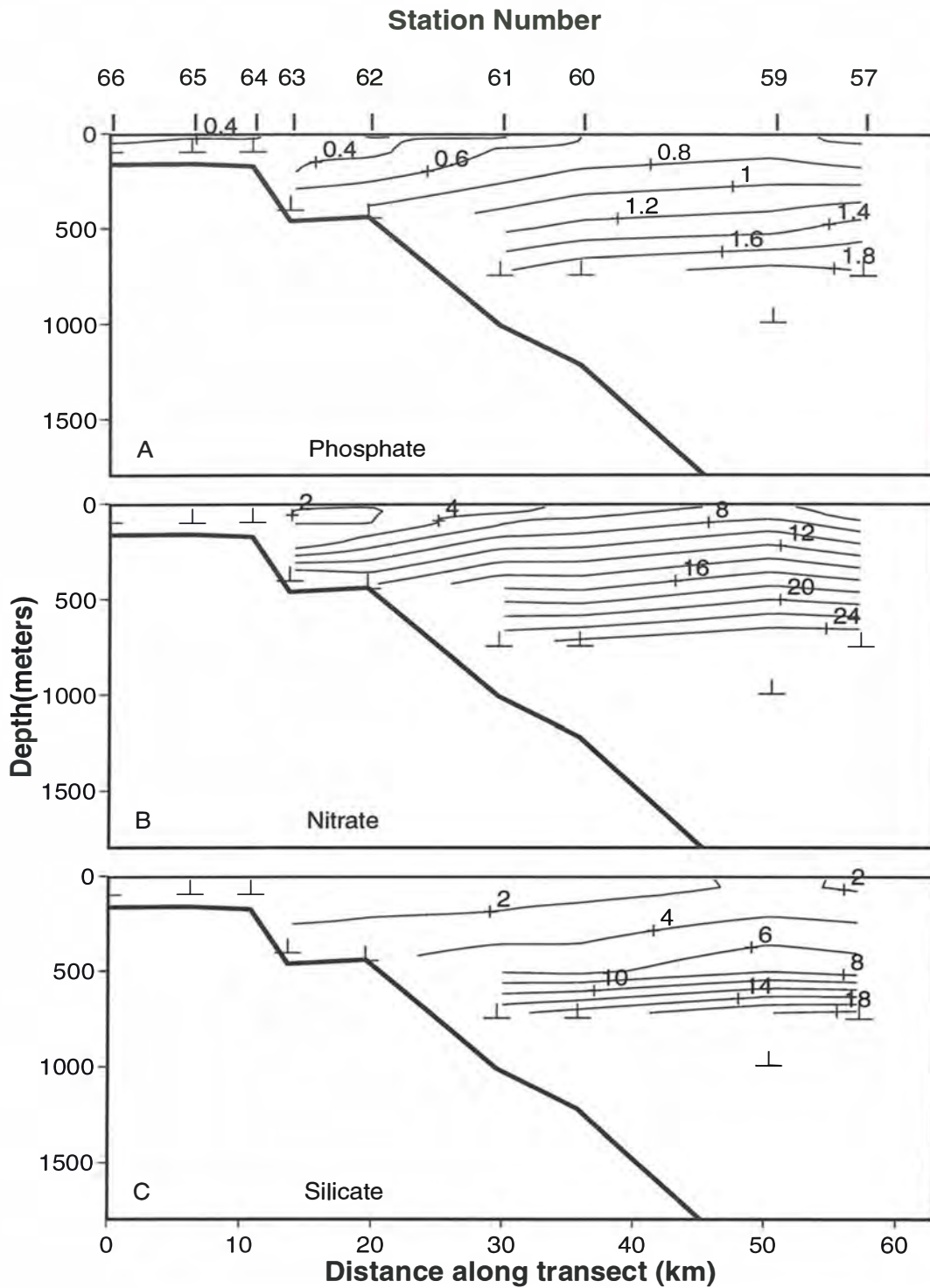
Fig. 28. Contour plots of (A) Phosphate (μM), (B) Nitrate (μM), and (C) Silicate (μM), on a vertical section along the western transect, cruise SS2/91, July 1991.

CRUISE RESULTS: NUTRIENTS, DISSOLVED OXYGEN AND BIOMASS.

CRUISE SS2/91: JULY, 1991.

On the western transect, nitrate and phosphate increased rather uniformly with depth between 200 and 900 m (Fig. 28A,B). Silicate increased rather slowly through SAMW, but increased rapidly into AAIW (Fig. 28C). Dissolved oxygen (DO) remained relatively high down to 500 m, especially over the upper slope, but decreased rapidly below 500 m (Fig. 29). At most stations on this transect, there were no nutrient samples taken between 100 and 250 m. Within the top 100 m, nitrate was uniform over the shelf and upper slope (ca 2 μM) and increased to ca 6 μM at the surface offshore (Fig. 30B). Offshore, nitrate values increased by 1 to 2 μM between the surface and 100 m depth. Phosphate increased from ca 0.4 μM on the shelf to 0.6 μM offshore (Fig. 30A), and silicate from 1.2 μM to 2 μM (Fig. 30C).
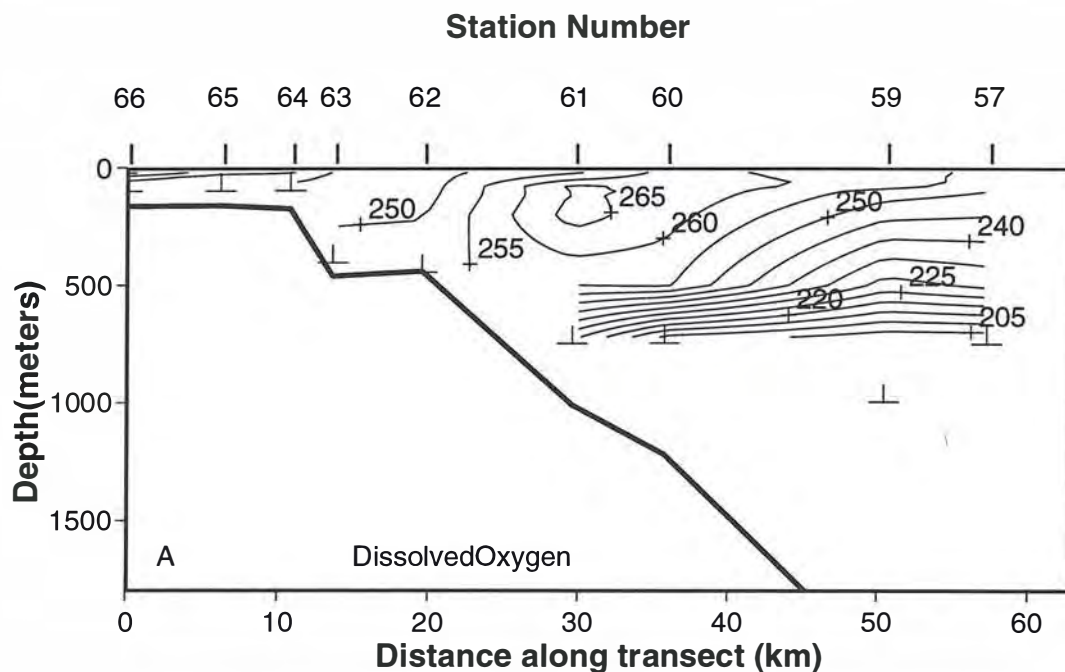

Fig. 29. Contour plots of Dissolved Oxygen (μM) on a vertical section along the western transect, cruise SS2/91, July 1991.
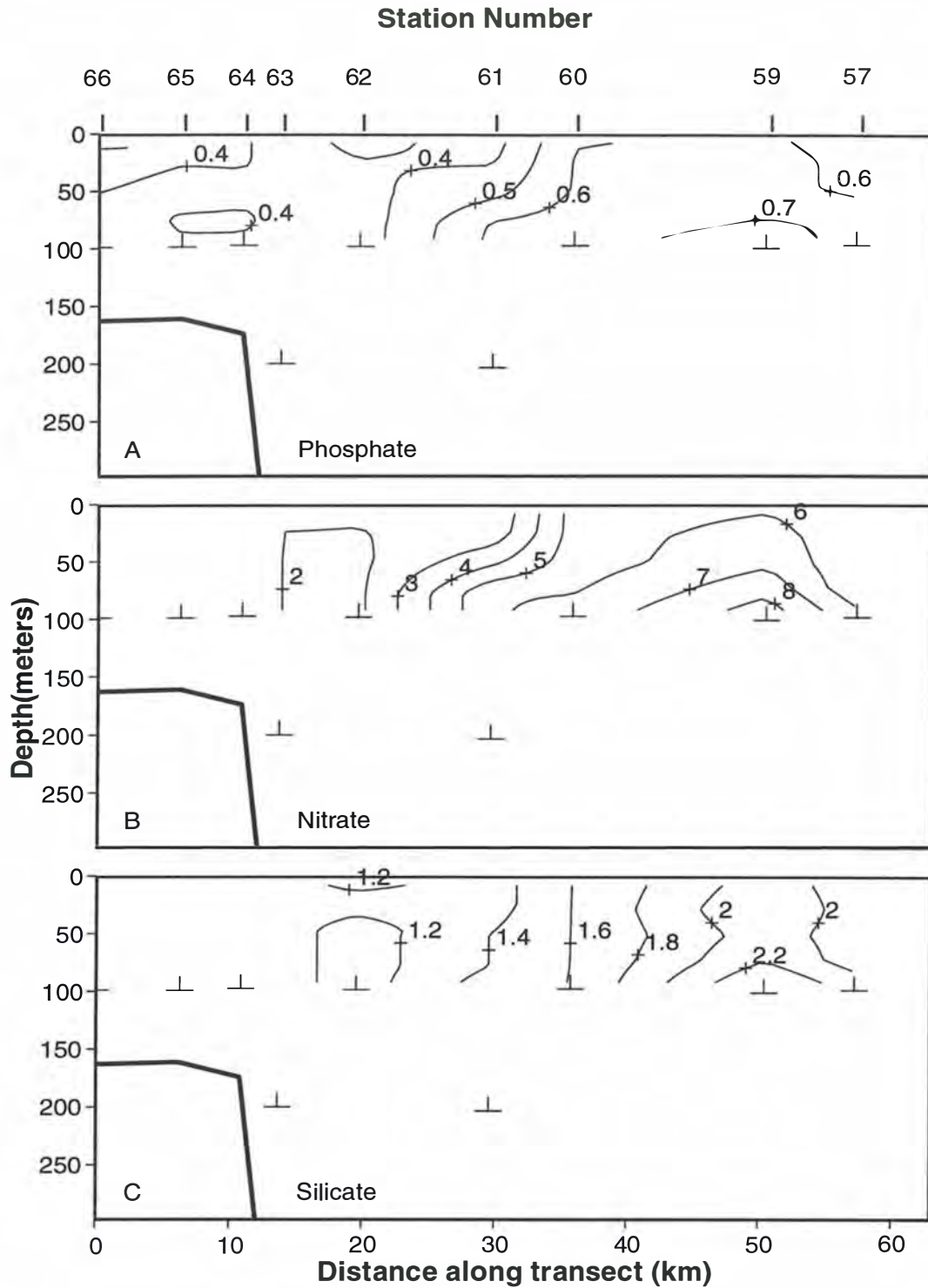
Fig. 30. Contour plots of (A) Phosphate (μM), (B) Nitrate (μM), and (C) Silicate (μM), on a vertical section (0-250 m) along the western transect, cruise SS2/91, July 1991.

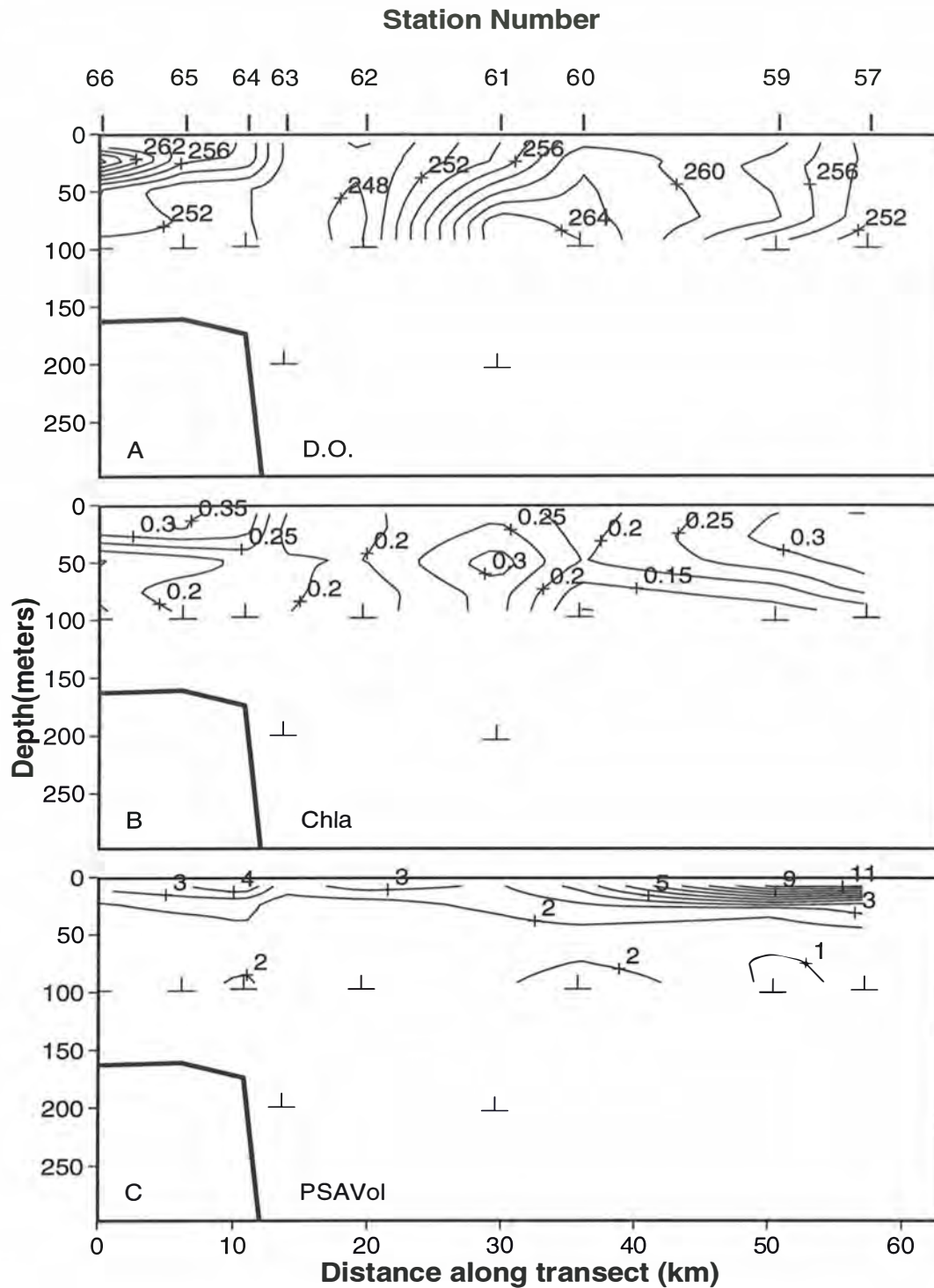Fig. 31. Contour plots of (A) Dissolved Oxygen (μM), (B) Chlorophyll a (μg L^{-1}) and (C) PSA Total Particle Volume (10^5 μm^3 L^{-1}), on a vertical section (0-250 m) along the western transect, cruise SS2/91, July 1991.
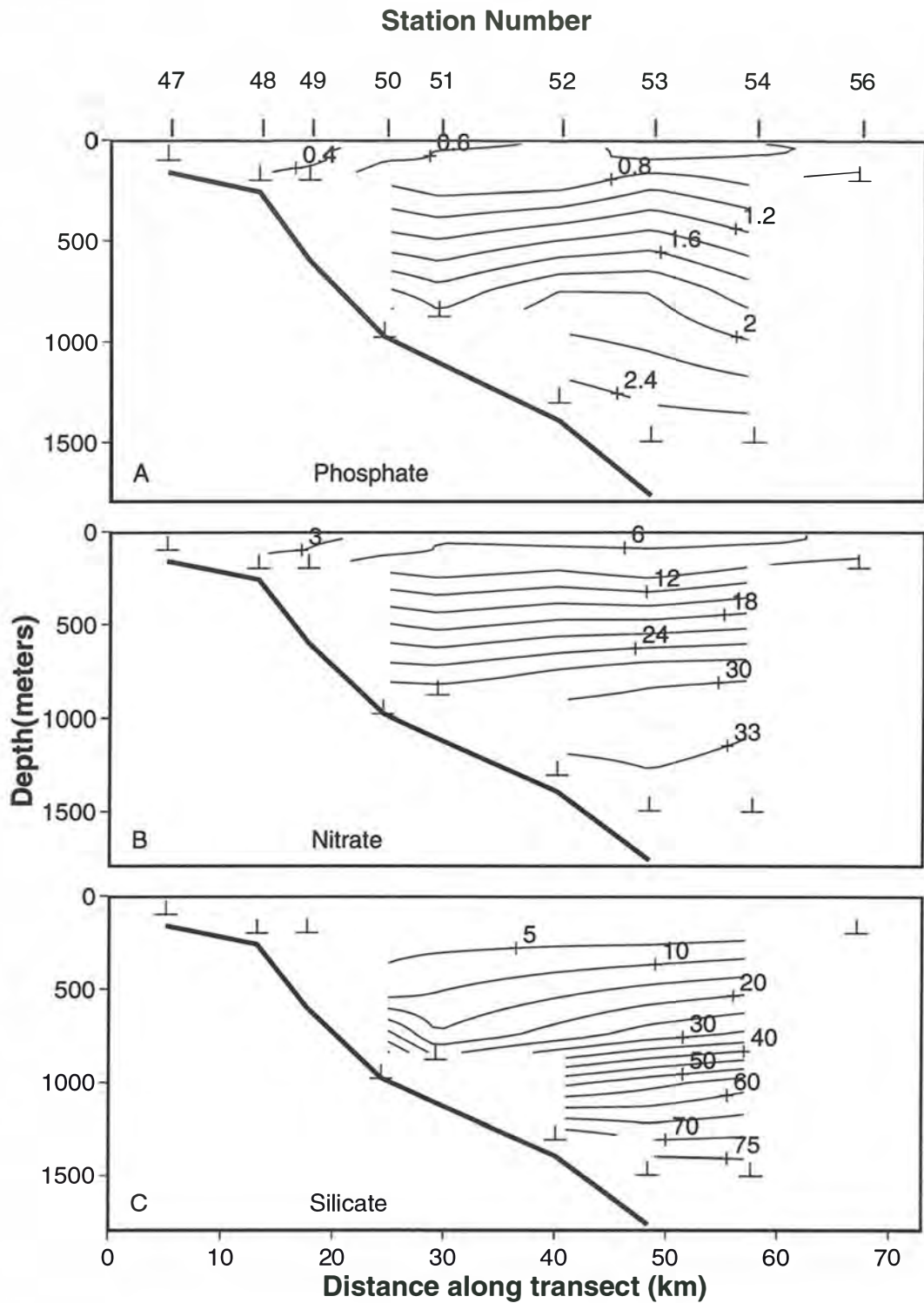
Fig. 32. Contour plots of (A) Phosphate (μM), (B) Nitrate (μM), and (C) Silicate (μM), on a vertical section along the central transect, cruise SS2/91, July 1991.

Surface chlorophyll was higher over the shelf and offshore (> 0.3 μg L^{-1}), with a minimum (<0.2 μg L^{-1}) over the upper slope (in the high salinity core), and in the low salinity core at station 60 (Fig. 31B). There was a subsurface maximum (ca 0.3 μg L^{-1}) in the stratified frontal waters separating the surface salinity maximum and minimum. DO showed a maximum in the cooler water on the inner shelf, and over the mid-slope, with a minimum in the warm, saline core (Fig. 31A). The DO distribution appeared to be controlled primarily by temperature. The PSA total particle volume was relatively low at 1.10^5 to 3.10^5 μm^3 L^{-1} throughout the region, except for a small increase at the surface associated with high chlorophyll over the shelf break, and a disproportionate increase to 11.10^5 μm^{3}L^{-1} at the surface offshore (Fig. 31C).

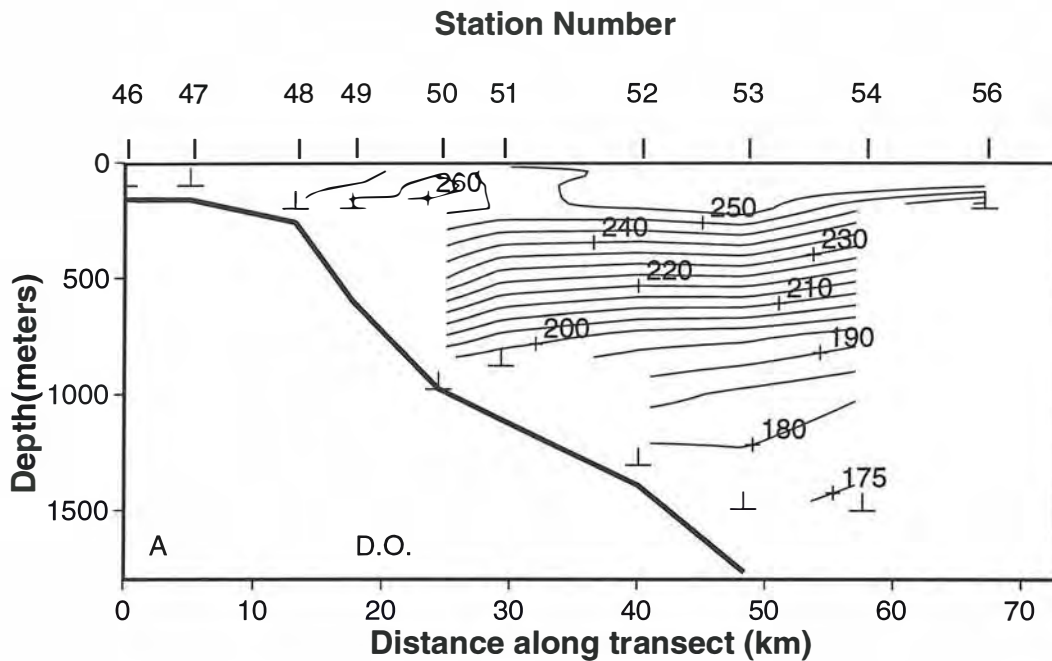Fig. 33. Contour plots of Dissolved Oxygen (μM) on a vertical section along the central transect, cruise SS2/91, July 1991.
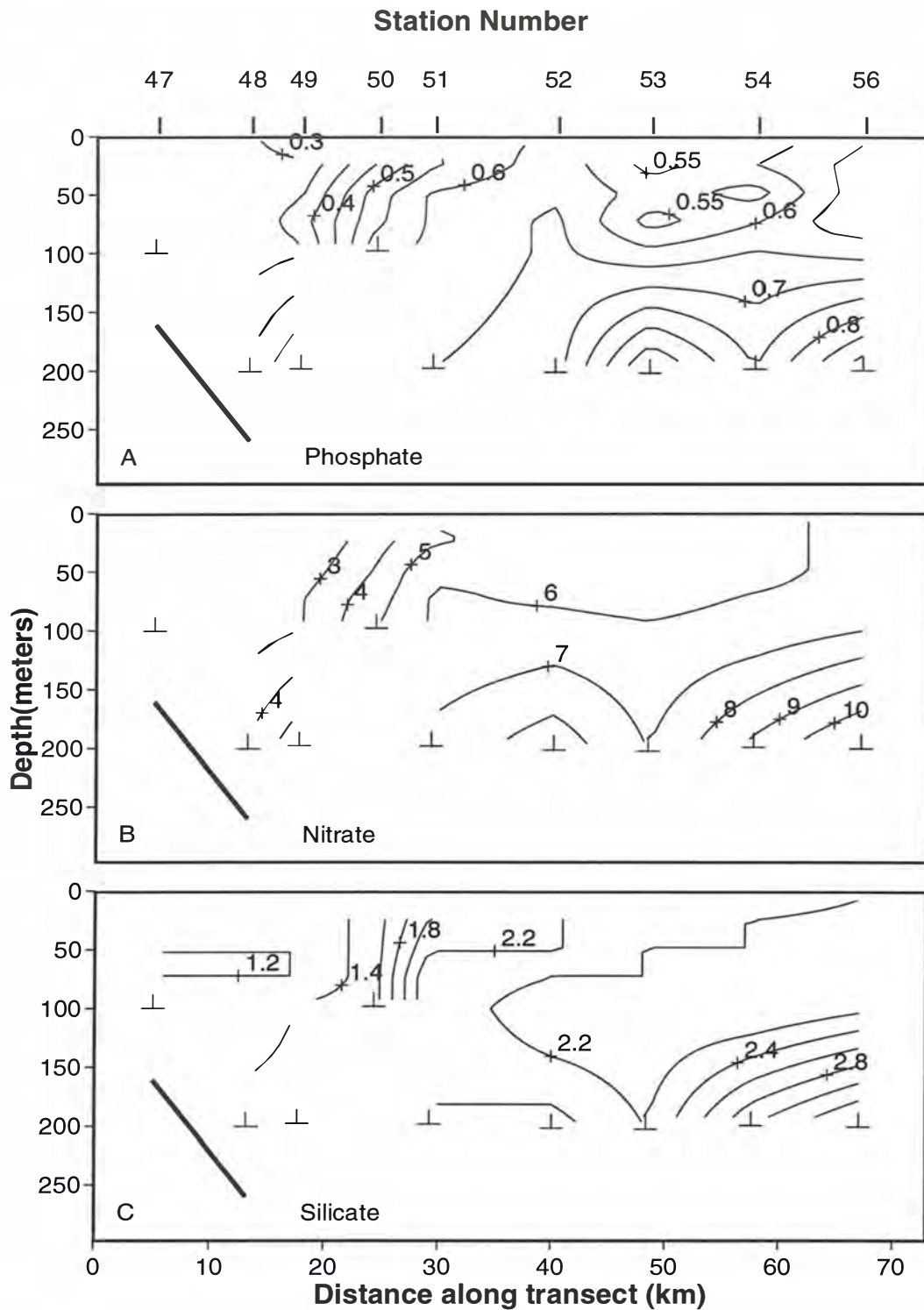
Fig. 34. Contour plots of (A) Phosphate (μM), (B) Nitrate (μM), and (C) Silicate (μM), on a vertical section (0-250 m) along the central transect, cruise SS2/91, July 1991.

Fig. 35. Contour plots of (A) Dissolved Oxygen (μM), (B) Chlorophyll a (μg L^{-1}) and (C) PSA Total Particle Volume (10^5 μm^3 L^{-1}), on a vertical section (0-250 m) along the central transect, cruise SS2/91, July 1991.

On the central transect, nitrate and phosphate increased rapidly with depth from 200 to 700 m, and relatively slowly in AAIW below 700 m (Fig. 32 A,B). Silicate behaved in an opposite manner, decreasing slowly through SAMW and rapidly through AAIW to reach 75 μM at 1500 m (Fig. 32C). DO decreased rapidly from 250 μM at 200 m to 200 μM at 800 m, and decreased much more slowly through AAIW (Fig. 33). Within the top 200 m, nitrate was low and vertically uniform on the shelf, and surface nitrate increased from ca 3 to 5 μM across the front between Zeehan Current water and subantarctic water (Fig. 34B). Offshore, nitrate increased with depth below 100 m, reaching 10 μM at 200m. Phosphate showed a similar distribution, increasing from ca 0.4 μM on the shelf to 0.6 μM offshore, and to 1 μM at 200 m (Fig. 34A). Silicate also behaved similarly, increasing from 1.4 μM on the shelf to 2 μM in surface waters offshore, and to 3 μM at 200 m (Fig. 34C).

Chl a was relatively low (ca 0.2 μg L^{-1}) and uniform on the shelf, and increased to a maximum of ca 0.4 μg L^{-1} at offshore stations (Fig. 35B). Offshore, Chl a decreased below 60 m, but was still about 0.2 μg L^{-1} at 100 m, and 0.1 ug L^{-1} at 150 m. DO was lowest in the warmer water inshore, and increased offshore (Fig. 35A). There was little vertical gradient in DO in the top 100 m, but it decreased strongly below 100m at offshore stations. The PSA total particle volume was again generally low, with elevated surface values on the inner shelf, and 40 to 50 km offshore (Fig. 35C). A strong subsurface maximum at 100 m at station 54 occurred below a local chlorophyll maximum at 30 m.

On the eastern transect, there were no nutrient or DO data below 200 m. Within the top 100 m, nitrate was low (< 1.7 μM) within the saline pool, and increased offshore to ca 5 μM in the mixed layer, and 6 μM at 100 m (Fig. 36B). Phosphate and silicate were distributed similarly, increasing from 0.4 μM to 0.6 μM, and 1.2 μM to 1.6 μM respectively (Fig. 36A,C). Chl a was especially low within the inshore warm pool, with values between 0.15 and 0.2 μg l^{-1} (Fig. 37B). Values increased to ca 0.27 to 0.3 μg l^{-1} offshore. DO was low and uniform in the warm pool, and increased from 255 μM inshore to 263 μM offshore, with no vertical structure in the top 100 m (Fig. 37A). PSA total particle volume was generally low, except for a surface maximum at shelf stations. This maximum occurred in waters that appeared well-mixed in terms of salinity and temperature.
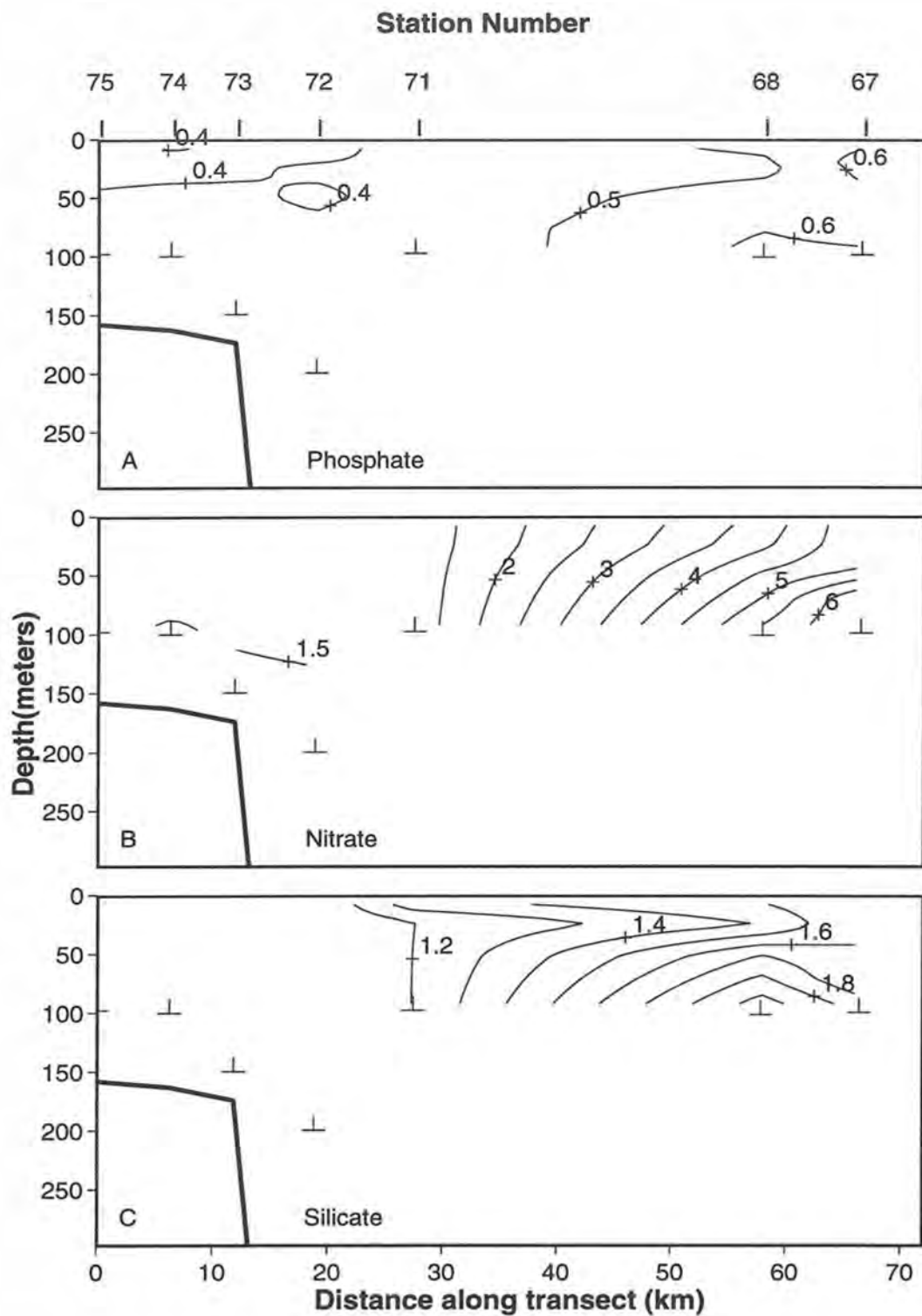
Fig. 36. Contour plots of (A) Phosphate (μM), (B) Nitrate (μM), and (C) Silicate (μM), on a vertical section (0-250 m) along the eastern transect, cruise SS2/91, July 1991.
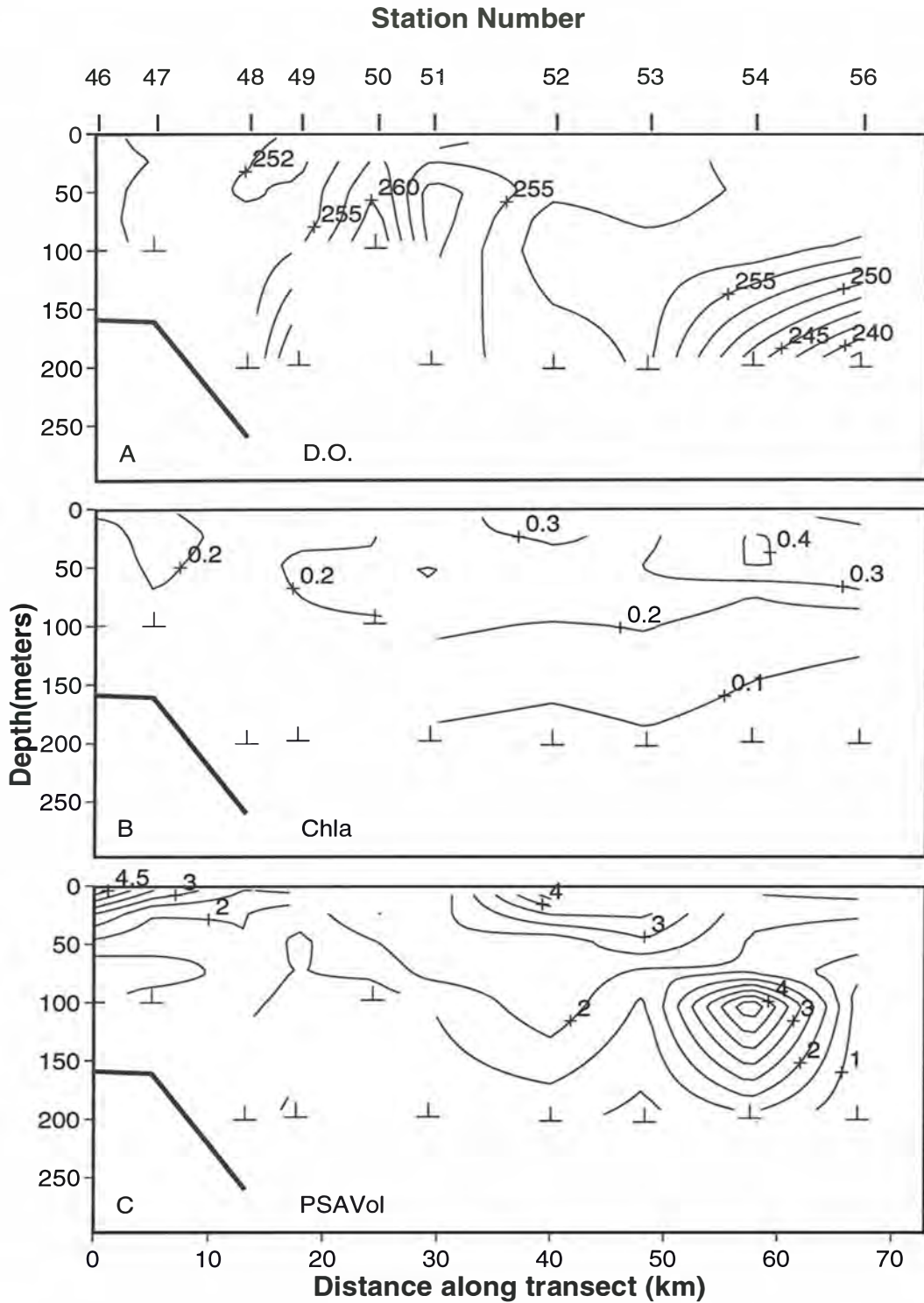
Station Number

Fig. 37. Contour plots of (A) Dissolved Oxygen (μM), (B) Chlorophyll a (μg L^{-1}) and (C) PSA Total Particle Volume (10^5 μm^3 L^{-1}), on a vertical section (0-250 m) along the eastern transect, cruise SS2/91, July 1991.

Nutrients (nitrate, phosphate, silicate) were all low in the warm, saline core, and increased in the cooler, fresher water offshore. Core nitrate values were slightly lower (ca 1.7 μM) in the deep broad mixed layer on the eastern transect than in the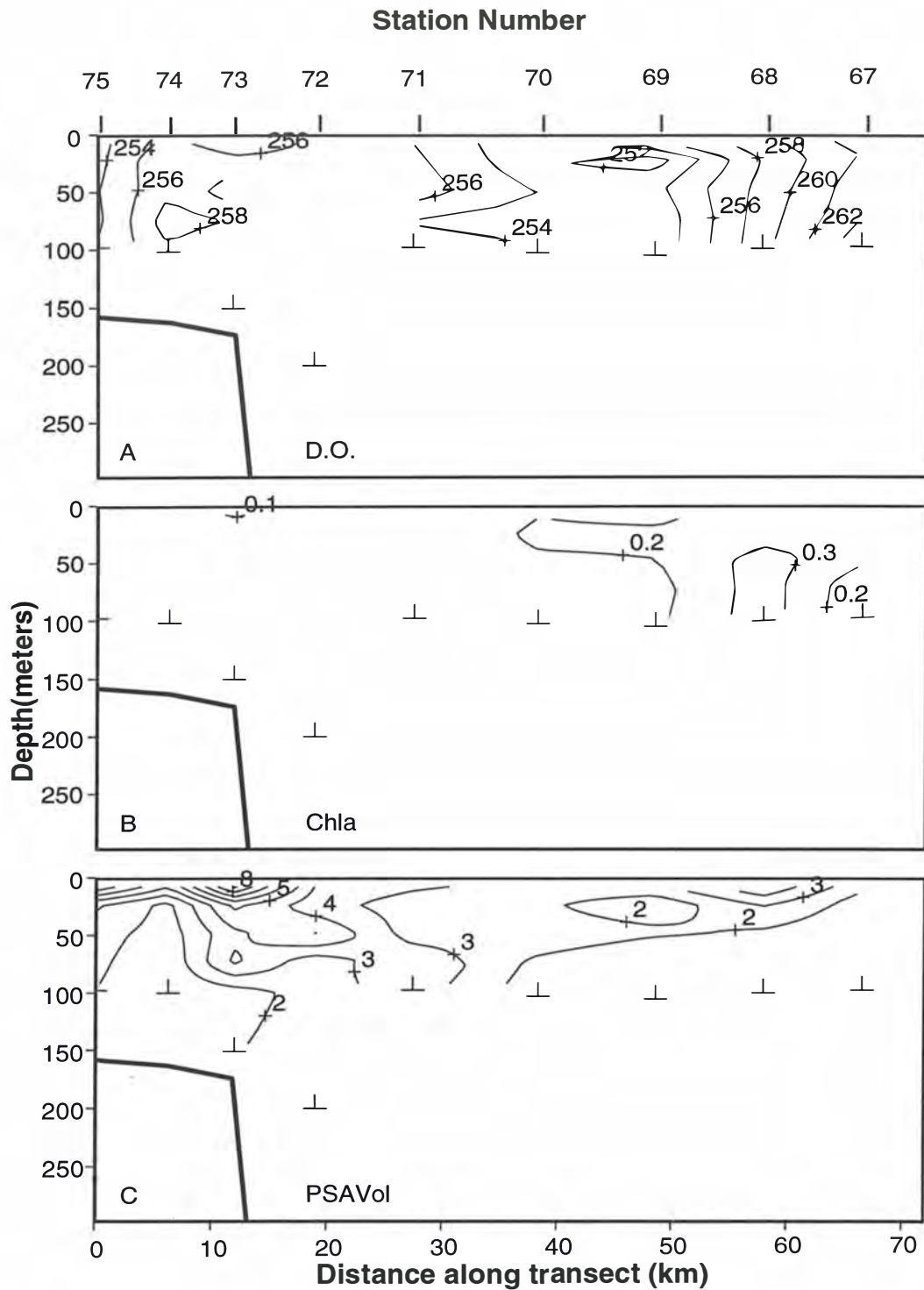 central or western transects (2-3 μM). Chl a values were low in the warm core, generally around 0.2 μg L^{-1}, and especially low in the deep mixed layers on the eastern transect. Chl a levels increased offshore, to ca 0.3 μg l^{-1}, and were generally elevated down to 100 m. Dissolved oxygen values generally reflected mixed layer temperatures, being higher in cooler offshore waters. In general, it appears that DO and nutrient values were controlled predominantly by physical transport and mixing at this time.

CRUISE SS1/92: FEBRUARY 1992.

On the western transect, nitrate and phosphate increased steadily below 200 m to reach values of 33 μM and 2.2 μM respectively in AAIW (Fig 38A,B). Silicate increased rapidly below 500 m to reach 85 μM at 1500 m (Fig. 38C). DO decreased slowly to ca 600 m, rapidly between 600 and 800 m (from 220 to 200 μM) and slowly through AAIW (Fig. 39). Mixed layer nitrate was between 1 and 2 μM throughout the western transect, and the nitracline varied between 40 and 70 m (Fig. 40B). The nitracline was much steeper over the shelf and upper slope, with 100 m nitrate values ranging from 11 μM on the shelf to 6 μM over the mid-slope. This indicates upwelling of high salinity, high nitrate water at the shelf break, and onto the shelf. The phosphate and silicate distributions showed the same pattern, with elevated subsurface values above the upper slope (Fig. 40). Surface silicate was less than 1.3 μM throughout.

Chlorophyll a was quite high throughout the transect, with mixed layer values greater than 0.8 μg l^{-1}, and peaking around 1 μg l^{-1} inshore and offshore from the warm pool (Fig. 41B). Chlorophyll a declined steeply below 50 m, decreasing to < 0.1 μg l^{-1} below 80 m, except offshore where it extended to ca 100 m. Mixed layer DO was minimum in the warm core, and maximum over the shelf break and offshore (Fig. 41A). There was a region of low DO at 100 m above the upper slope, again associated with shelf break upwelling. PSA total volume showed a similar distribution to chlorophyll a, declining steeply below 50 m to < 2.10^5 μm^3 L^{-1}, and increasing to 9.10^5 μm^3 L^{-1} in the surface chlorophyll maximum over the shelf break.

The general distribution of phosphate, nitrate and silicate between 200 and 1000 m on the central transect matched that on the western transect (Fig. 42). Phosphate and nitrate, but not silicate, showed doming at station 19 comparable with that observed in the temperature and salinity fields (Fig. 12, 42). The DO field between 200 and 800 m showed considerable horizontal variation, with high values (240 μM) extending to 500 m above a sharp oxycline inshore, a weak gradient between 200 and 700 m from 15 to 40 km from the shelf break,

and deep penetration of high oxygen over a sharp oxycline associated with the physical and nutrient doming observed at station 19, offshore (Fig. 43).

Nitrate was generally low (< 1 µM) and in some cases undetectable in the surface layer throughout the central transect (Fig. 44B). The nitracline was shallowest on the inner shelf and offshore, and deepest (ca 80 m) in the warm, saline core. Nitrate values were generally around 10 µM at 200 m. Phosphate values showed a similar distribution, being less than 0.25 µM in the mixed layer, and ca 0.7 to 0.8 µM at 200 m (Fig. 44A). Silicate was less than 1 µM in surface waters, and ca 4 µM at 200 m (Fig. 44C). Mixed layer chlorophyll a concentrations were maximum on the shelf and offshore (ca 0.7 and 0.9 µg L^{-1}), and lowest in the warm saline pool (ca 0.4 µg L^{-1}), although chlorophyll extended deeper in this zone (Fig. 45B). Mixed layer DO was higher on the inner shelf and offshore, and lowest in the warm core (Fig. 45A). DO contours between 100 and 200 m domed upwards on the outer edge of the warm pool, while there was a downward intrusion of high DO values along sloping isopycnals on the inshore edge of the warm pool. PSA total particle volume showed a similar distribution to Chl a, with surface maxima offshore, and at the shelf edge (Fig. 45C).

Surface nitrate values appeared to be depleted, or nearly depleted, on the central transect, but higher (ca 1 µM) on the western transect. There was evidence on the western transect for upwelling at the shelf-break, inshore of the warm pool, with very high nitrate values at 100 m on the shelf. Surface silicate was also strongly depleted throughout both transects, with lower values (<0.8 µM) on the central transect. Chl a values were quite high (> 0.8 µg L^{-1}) throughout the western transect and much of the central transect, and low (ca 0.4 µg L^{-1}) in the high salinity pool on the central transect. Mixed layer DO values were highest offshore on both transects (ca 269 µM) and lowest in the warmer water on the central transect (<248 µM).

On this cruise, physical and chemical properties were primarily determined by the distribution of EAC water over the middle and upper slope. Mixed layer nitrate and silicate had been depleted, or almost depleted, throughout the area, as one might expect in summer. Despite this, mixed layer Chl a was generally quite high, and showed little evidence of a subsurface maximum, except in the warm core on the central transect. This may reflect the effects of resupply of nitrate to the surface layer by wind mixing or shelf-break upwelling. It is not clear that the conditions observed on this cruise represent "typical" summer conditions, given that satellite images suggest 1992 was an anomalously cold year.
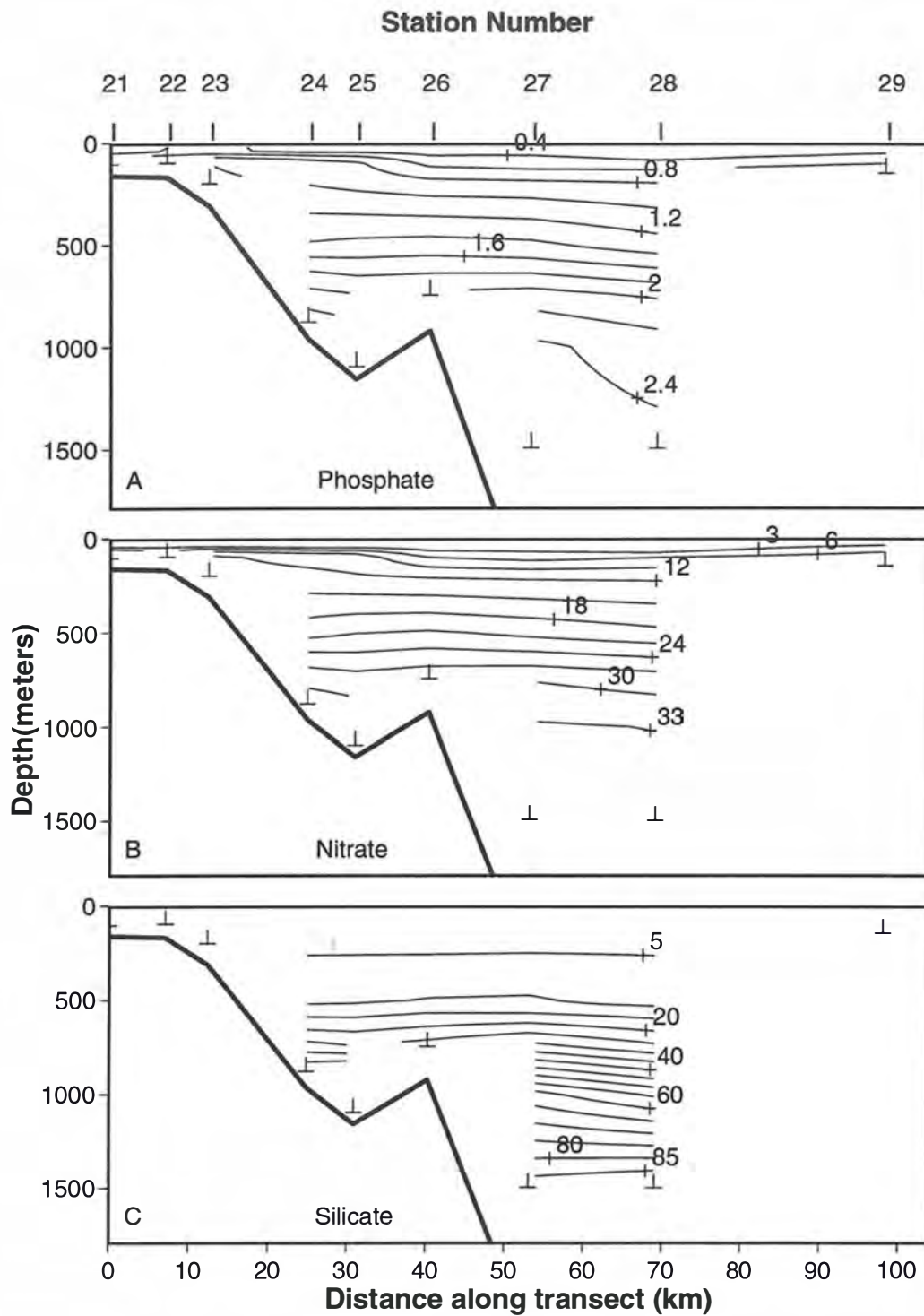
Fig. 38. Contour plots of (A) Phosphate (μM), (B) Nitrate (μM), and (C) Silicate (μM), on a vertical section along the western transect, cruise SS1/92, February 1992.

Fig. 39. Contour plots of Dissolved Oxygen (μM) on a vertical section along the western transect, cruise SS1/92, February 1992.

Station Number

Fig. 40. Contour plots of (A) Phosphate (μM), (B) Nitrate (μM), and (C) Silicate (μM), on a vertical section (0-250 m) along the western transect, cruise SS1/92, February 1992.

Station Number

Fig. 41. Contour plots of (A) Dissolved Oxygen (μM), (B) Chlorophyll a (μg L^{-1}) and (C) PSA Total Particle Volume (10^5 μm^3 L^{-1}), on a vertical section (0-250 m) along the western transect, cruise SS1/92, February 1992.
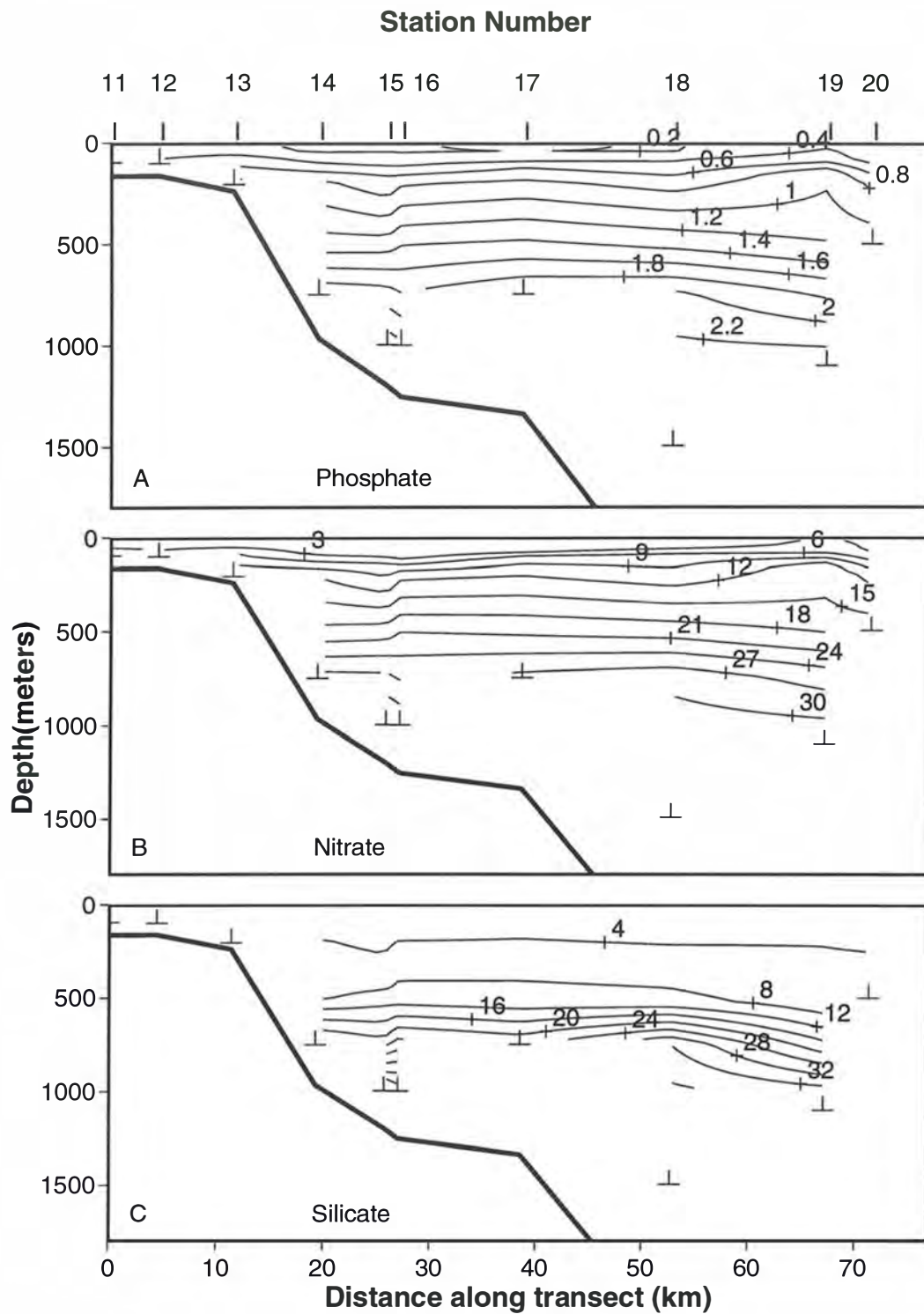
Fig. 42. Contour plots of (A) Phosphate (μM), (B) Nitrate (μM), and (C) Silicate (μM), on a vertical section along the central transect, cruise SS1/92, February 1992.
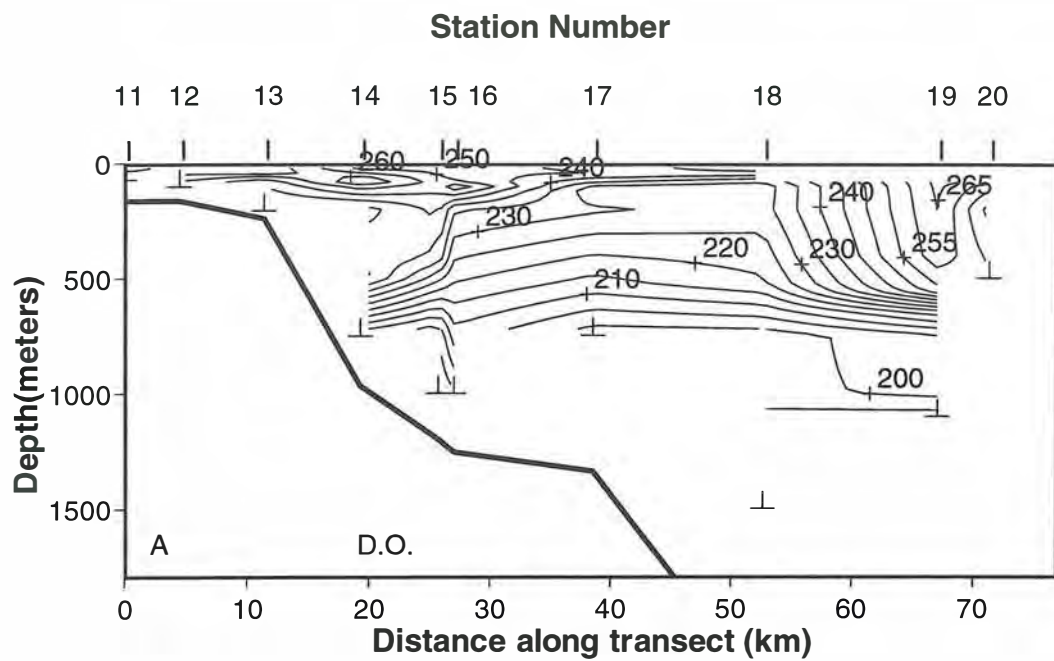
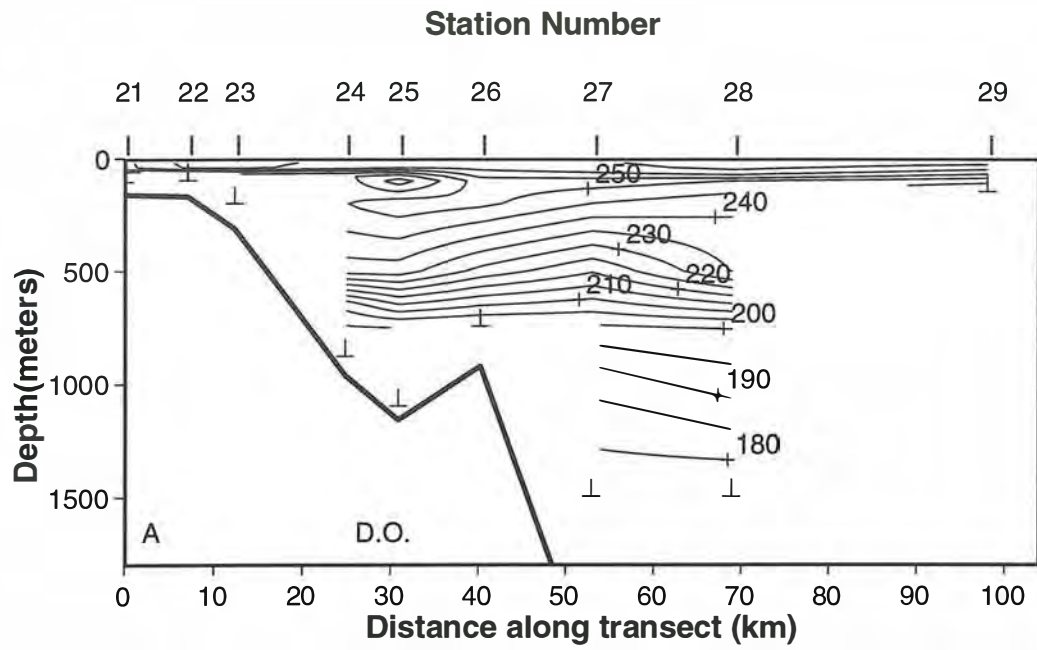Fig. 43. Contour plots of Dissolved Oxygen (μM) on a vertical section along the central transect, cruise SS1/92, February 1992.

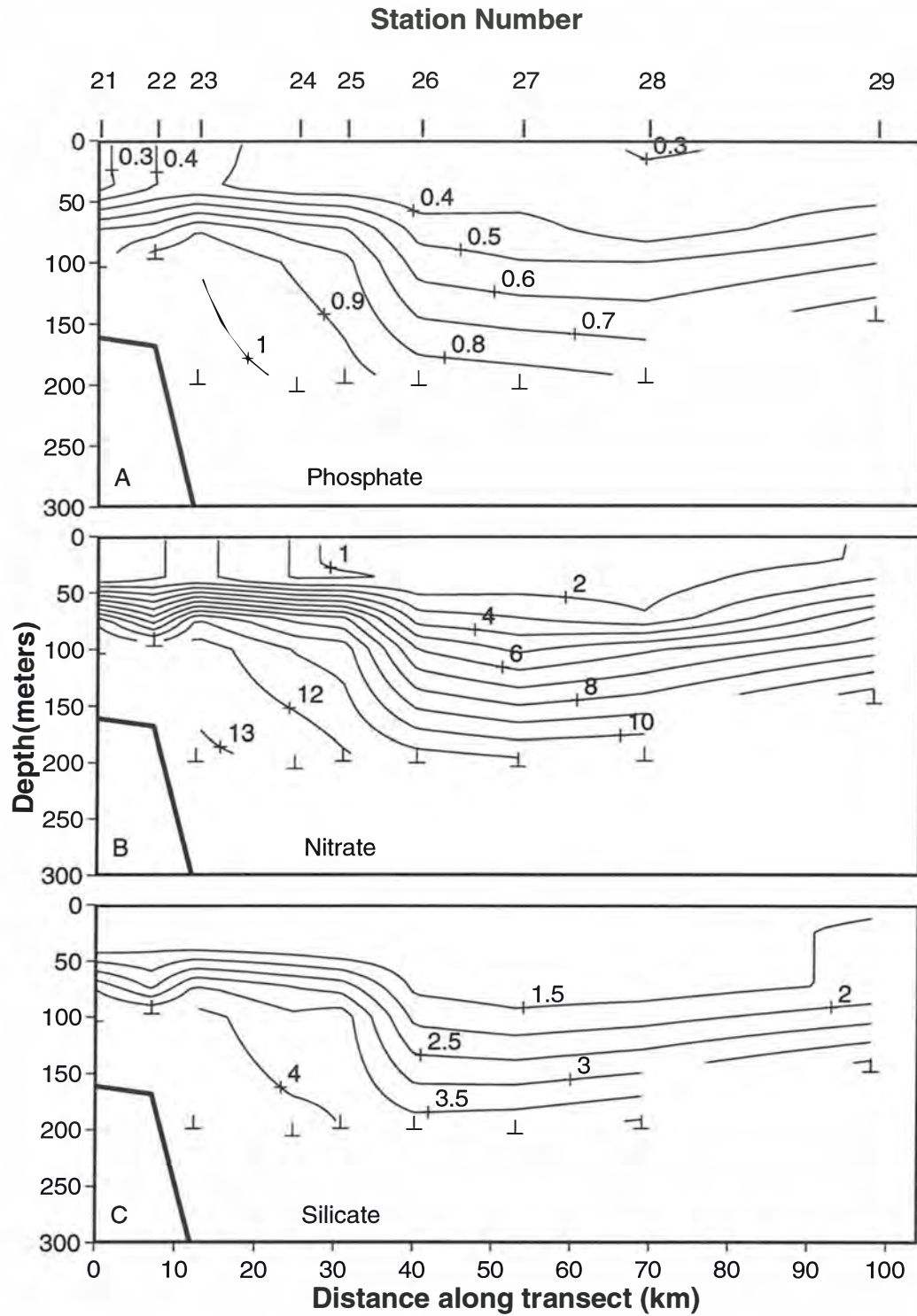Fig. 44. Contour plots of (A) Phosphate (μM), (B) Nitrate (μM), and (C) Silicate (μM), on a vertical section (0-250 m) along the central transect, cruise SS1/92, February 1992.

Station Number

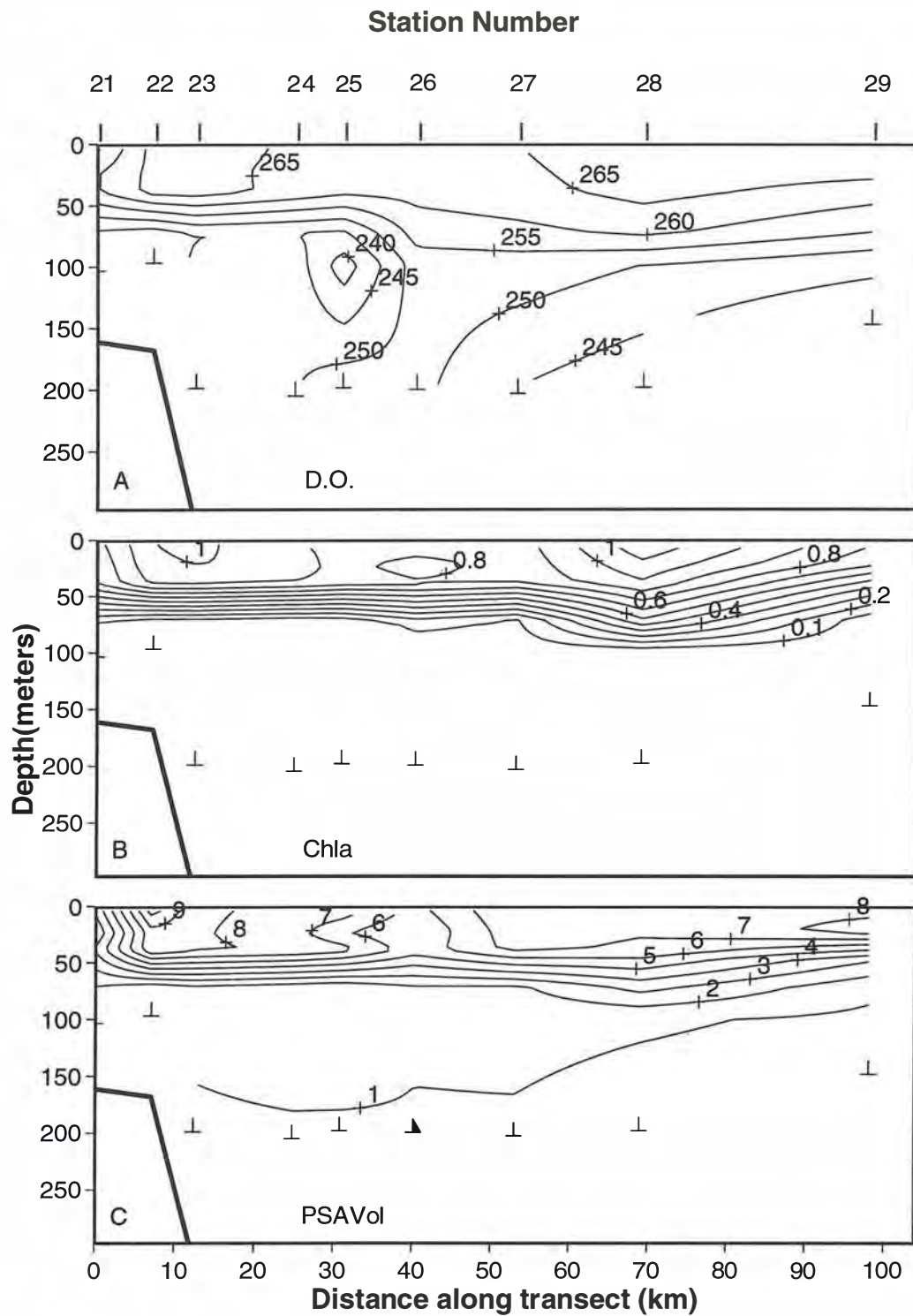
Fig. 45. Contour plots of (A) Dissolved Oxygen (μM), (B) Chlorophyll a (μg L^{-1}) and (C) PSA Total Particle Volume (10^5 μm^3 L^{-1}), on a vertical section (0-250 m) along the central transect, cruise SS1/92, February 1992.

CRUISE SS4/92: NOVEMBER 1992.

On the western transect, dissolved oxygen values were low in AAIW, and there was a strong gradient in DO from 500 to 800 m (Fig. 46). A broad band of intermediate DO (230 to 240 μM) from 100 to 500 m lay in and above the weak SAMW water mass from 300 m to 600 m. Nitrate and phosphate increased rather uniformly with depth below 100 m, and increased above the cold feature at station 9 (Fig. 47A,B). Silicate was low (< 10 μM) above 500 m, but increased to 40 μM at 1000 m and continued to increase strongly to 70 μM at 1500 m (Fig. 47C).

Fig. 46. Contour plots of Dissolved Oxygen (μM) on a vertical section along the western transect, cruise SS4/92, November 1992.

Station Number

Fig. 47. Contour plots of (A) Phosphate (μM), (B) Nitrate (μM), and (C) Silicate (μM), on a vertical section along the western transect, cruise SS4/92, November 1992.
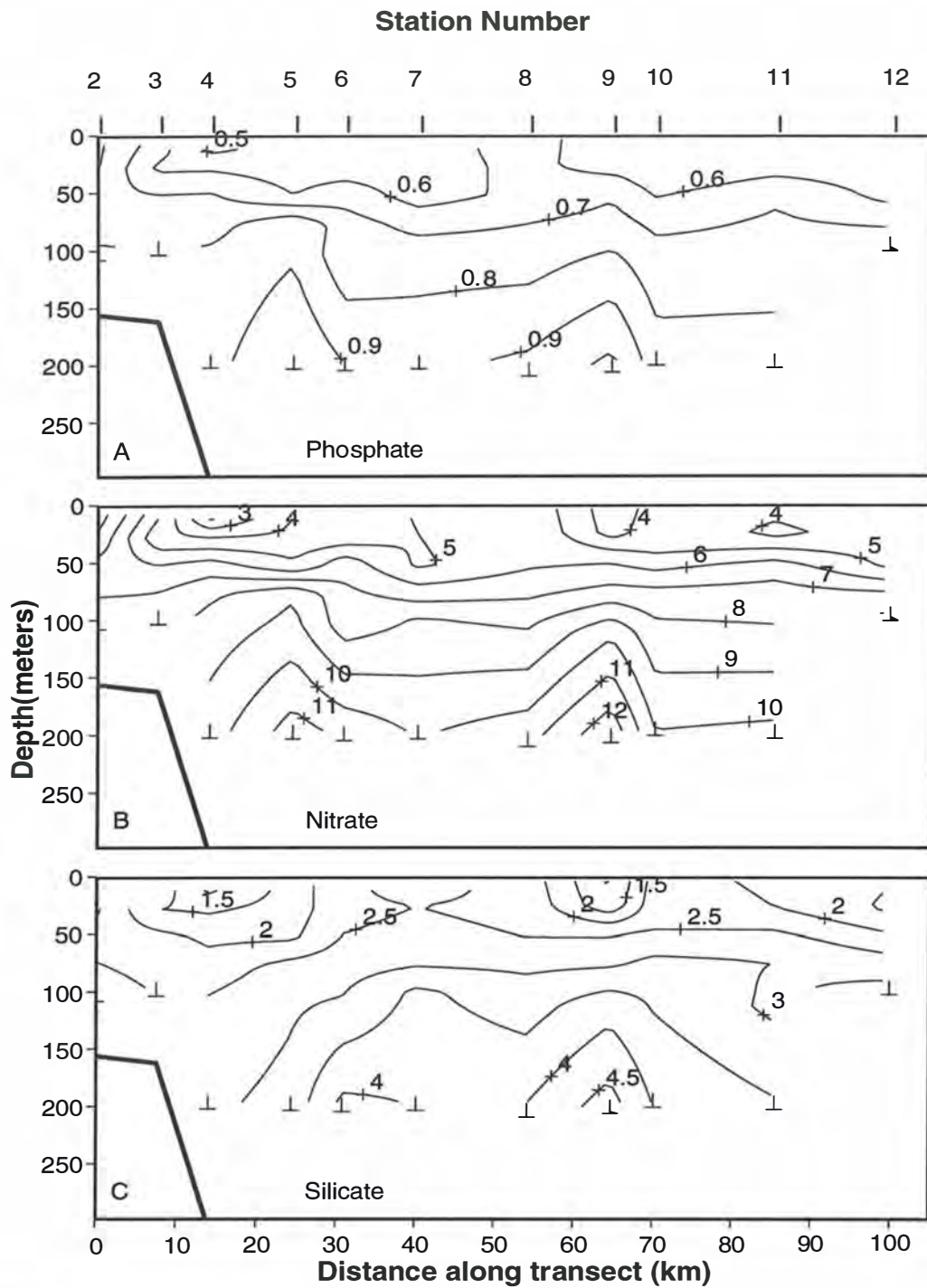
Fig. 48. Contour plots of (A) Phosphate (µM), (B) Nitrate (µM), and (C) Silicate (µM), on a vertical section (0-250 m) along the western transect, cruise SS4/92, November 1992.

Station Number
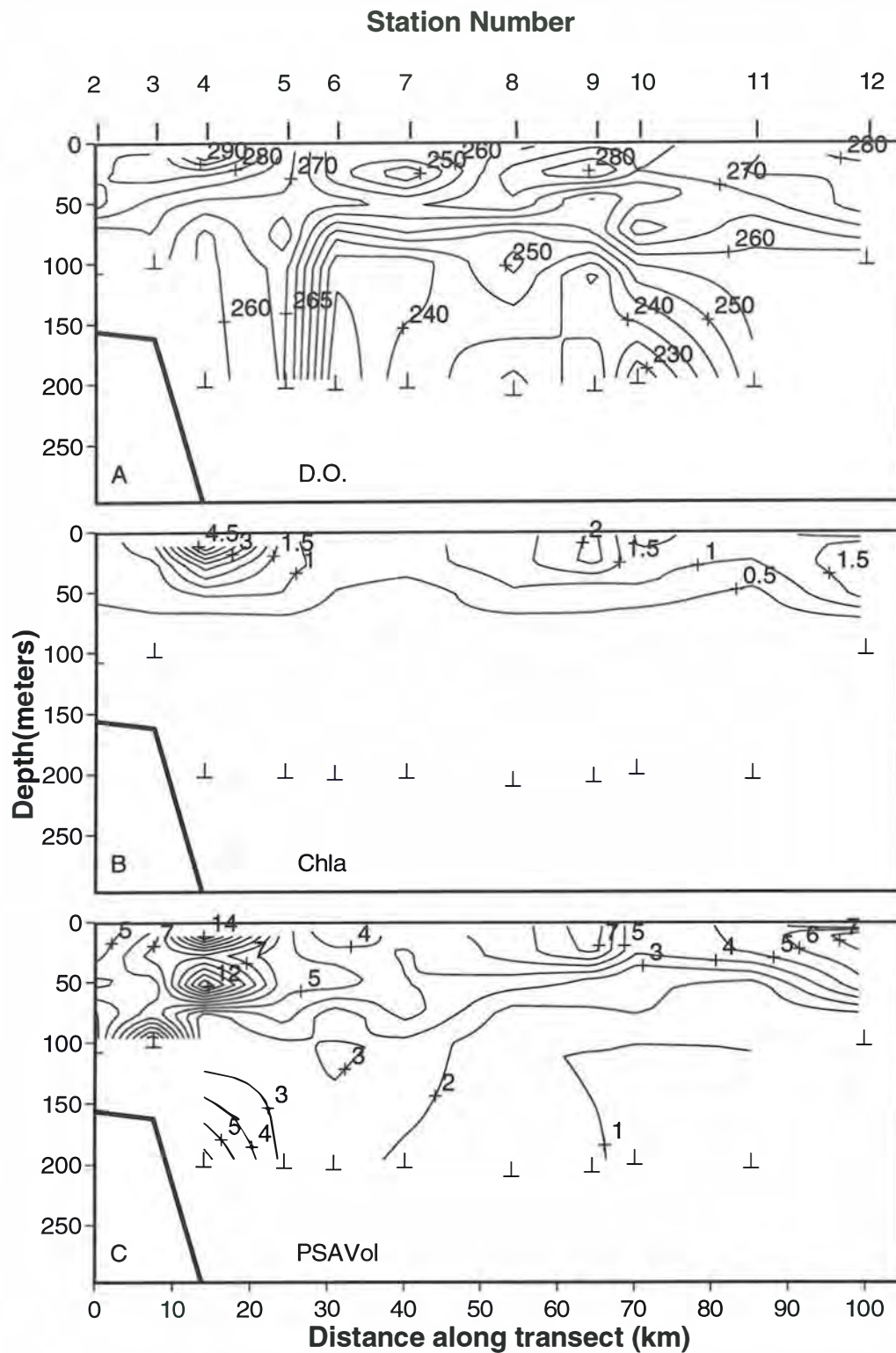
Fig. 49. Contour plots of (A) Dissolved Oxygen (μM), (B) Chlorophyll a (μg L^{-1}) and (C) PSA Total Particle Volume (10^5 μm^3 L^{-1}), on a vertical section (0-250 m) along the western transect, cruise SS4/92, November 1992.

Within the top 200m, there were two major processes affecting nutrient and DO distributions. Below 50m, there was a marked minimum in DO (Fig. 49A) and maximum in nutrients (Fig. 48) above the eddy feature at station 9. There was a similar DO minimum and nutrient maximum just offshore of the shelf break, below a salinity front between cool, fresh shelf water and the warm, saline pool over the slope (Fig. 16). Within the top 50 m, DO and nutrient distributions appear to be strongly affected by phytoplankton production. Maximum chlorophyll a occurred in two regions: one centred over the eddy feature at station 9, with peak values ca 1.8 μg L^{-1}, and one just inshore of the shelf-break front (Fig. 49B). There was also an increase in chlorophyll a at the furthest offshore station. Nutrients were depleted, and DO elevated, in these high chlorophyll areas (Fig. 48, 49). Peak DO values (>280 μM) may indicate supersaturation (Fig. 49A). Nitrate drawdown appeared to be as much as 2 μM in high chlorophyll areas (Fig. 48B), if we assume mixed-layer nitrate values were uniform pre-bloom. Silicate was strongly locally depleted to ca 1 μM in blooms (suggesting diatom blooms), but was greater than 2 μM throughout much of the surface layer (Fig. 48C). PSA total particle volume maxima in the surface layer coincided with chlorophyll maxima, but particle volume was also high below the surface layer under chlorophyll maxima (Fig. 49C).

On the central transect, there was a very strong DO gradient between 200 and 400 m offshore, which broadened and deepened over the slope (Fig. 50). DO values were generally high (>260 μM) throughout the capped winter mixed layer, and further elevated in surface waters. Deep nitrate, phosphate and silicate contours generally reflected temperature and salinity distributions (Fig. 51).

Nutrient and DO properties in the top 200 m (Fig. 52, 53) were again affected by circulation and phytoplankton production. There was evidence of strong upwelling of high-nutrient, low oxygen water at station 21, just beyond the shelf break. Surface DO was high (>280 μM) over most of the transect inshore and offshore of this feature (Fig. 53A). However, surface nitrate, silicate and phosphate showed strong depletion at the station just offshore and weak depletion at the station inshore of this upwelling site (Fig. 52). These nutrients were also strongly depleted at the station furthest offshore. Chlorophyll a concentrations reached maximum values just offshore of the shelf break upwelling (>2.3 μg L^{-1}), and at the furthest offshore station (>1.4 μg L^{-1}) (Fig. 53B). Peak PSA total particle volume values also occurred at the peak chlorophyll concentrations, just offshore of the shelf break upwelling (Fig. 53C).

Station Number

Fig. 50. Contour plots of Dissolved Oxygen (μM) on a vertical section along the central transect, cruise SS4/92, November, 1992.

Station Number
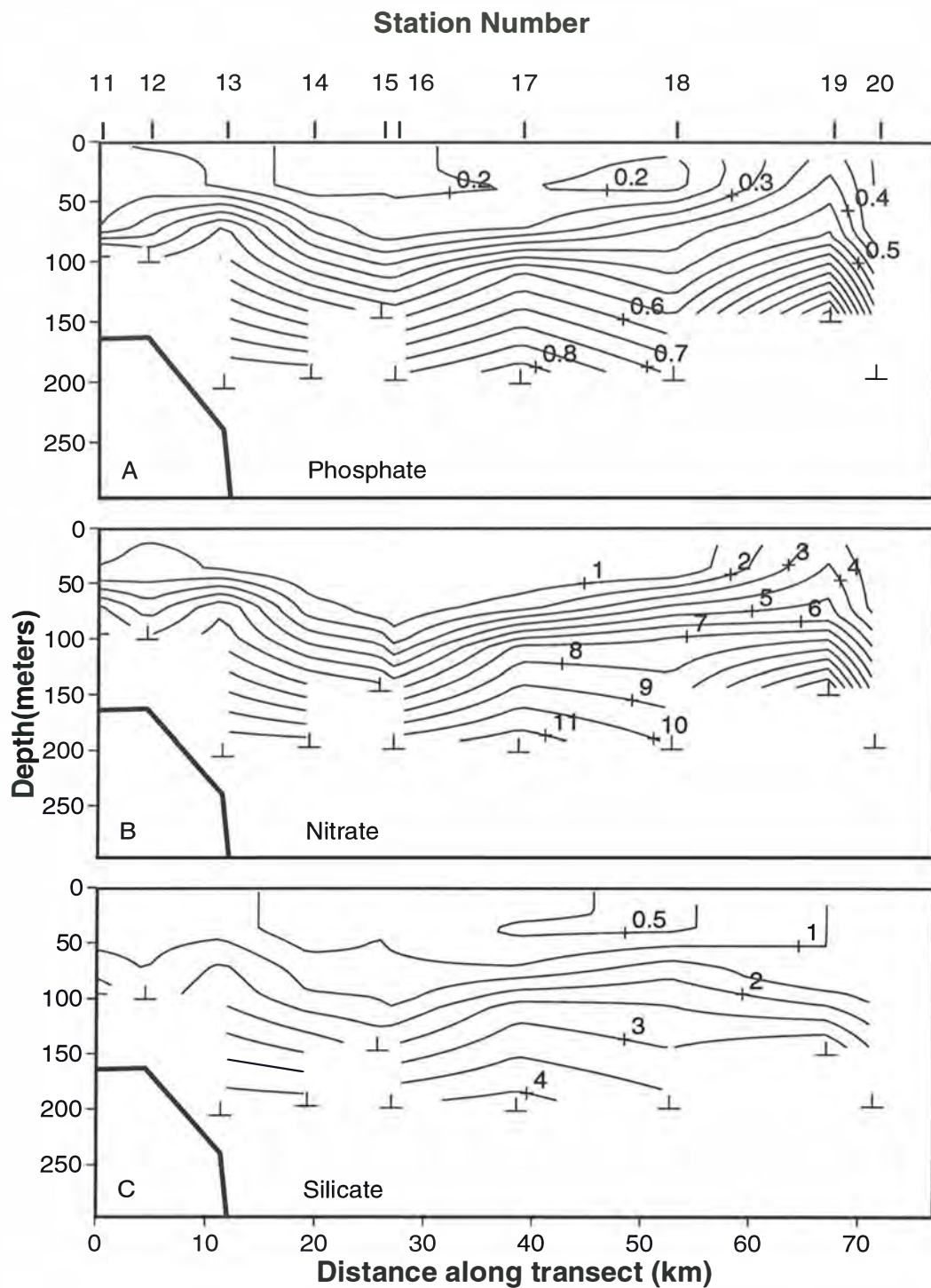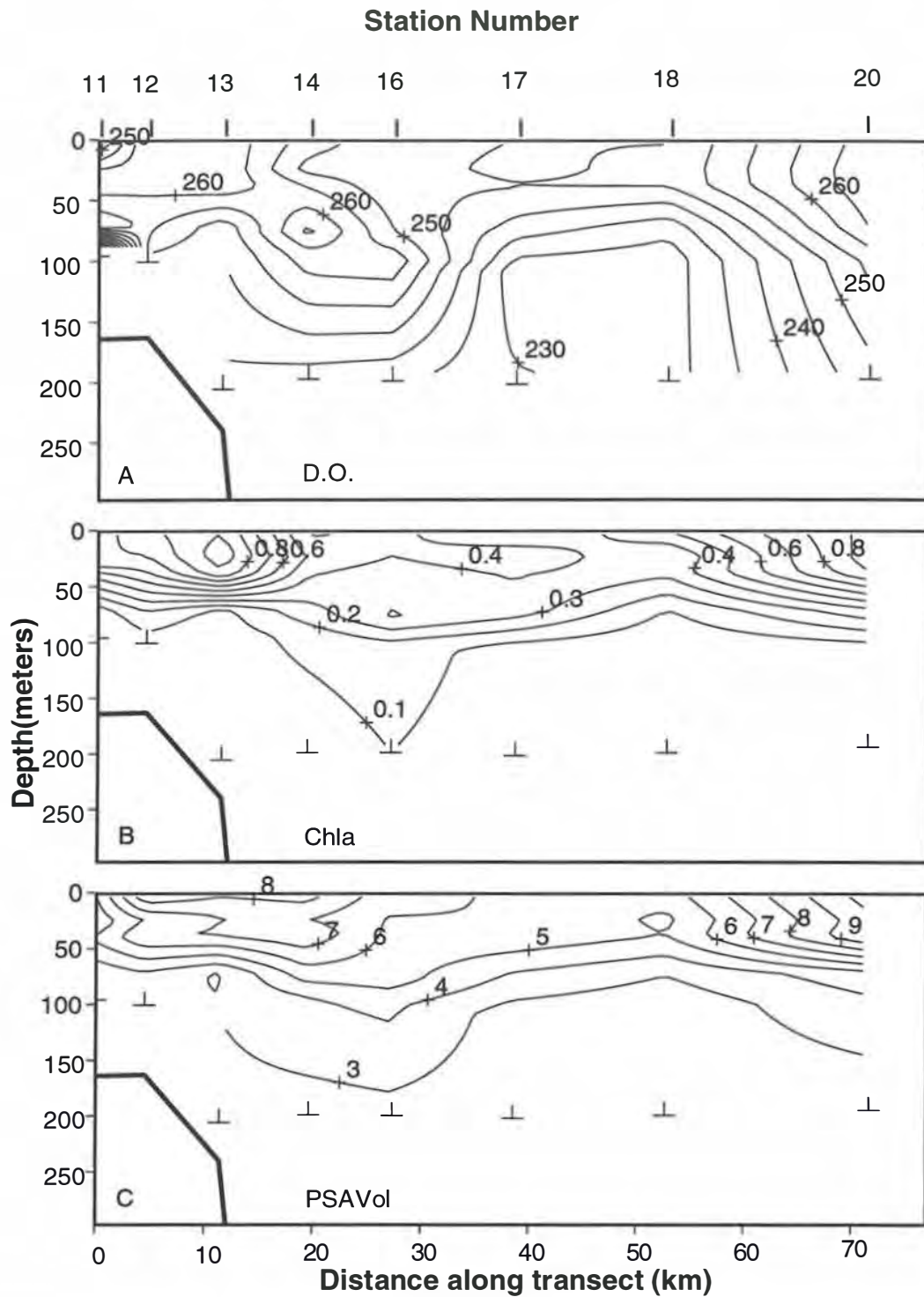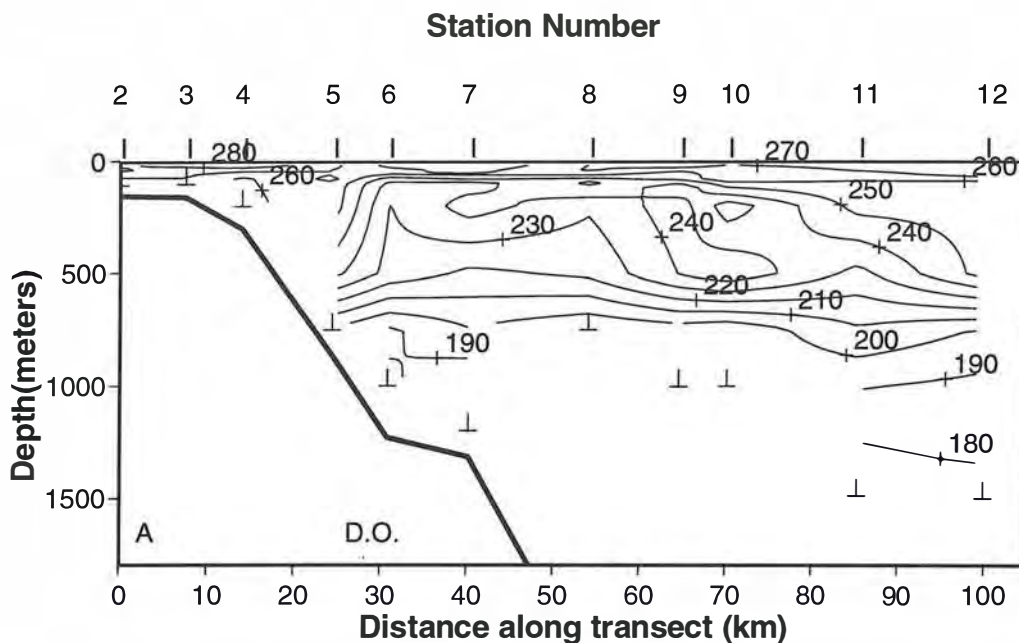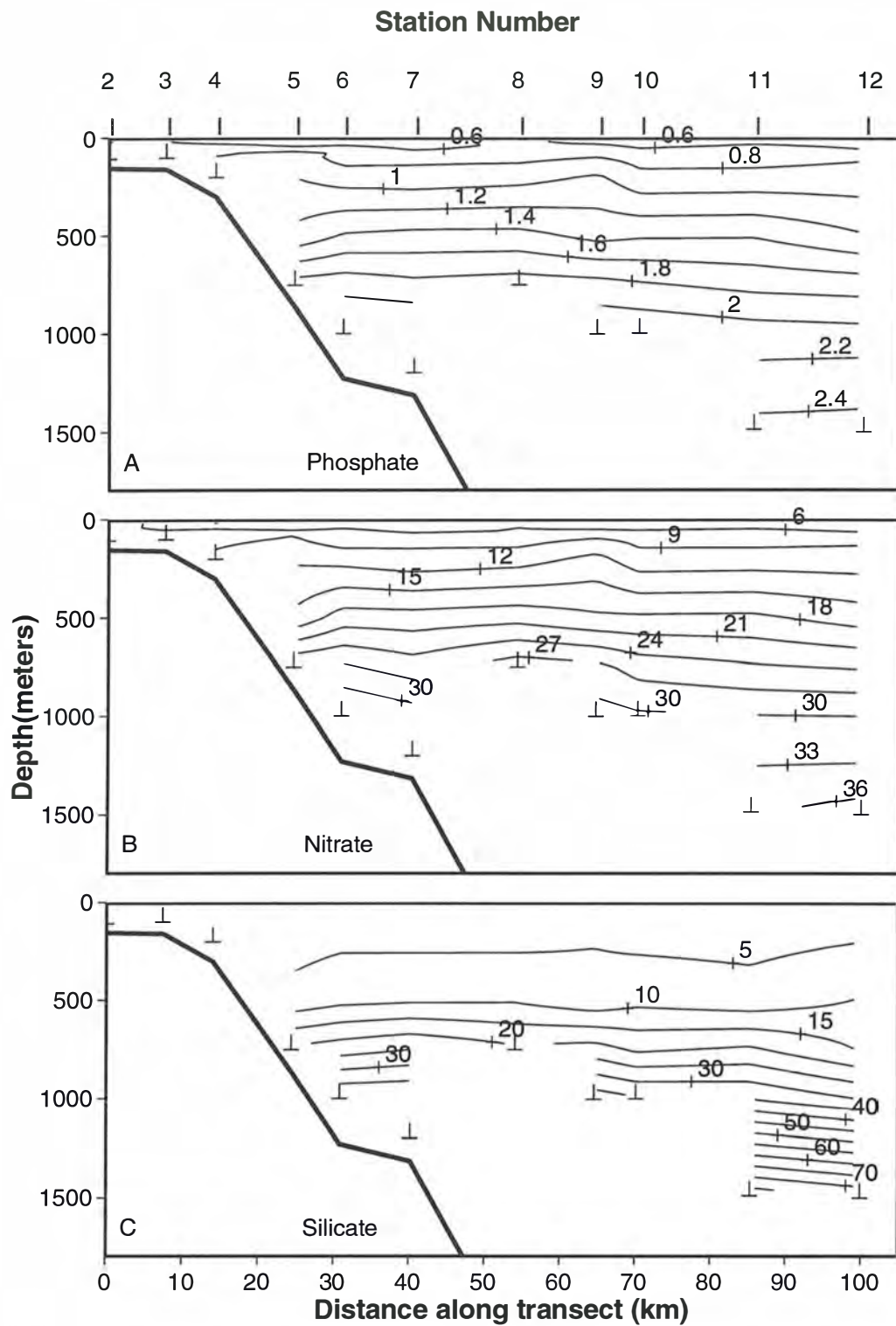

Fig. 51. Contour plots of (A) Phosphate (μM), (B) Nitrate (μM), and (C) Silicate (μM), on a vertical section (0-250 m) along the central transect, cruise SS4/92, November 1992.

Station Number


Fig. 52. Contour plots of (A) Phosphate (μM), (B) Nitrate (μM), and (C) Silicate (μM), on a vertical section (0-250 m) along the central transect, cruise SS4/92, November 1992.

Station Number

Fig. 53. Contour plots of (A) Dissolved Oxygen (μM), (B) Chlorophyll a (μg L^{-1}) and (C) PSA Total Particle Volume (10^5 μm^3 L^{-1}), on a vertical section (0-250 m) along the central transect, cruise SS4/92, November 1992.

91

On the eastern transect, the deep DO and nutrient concentrations domed upwards along with temperature and salinity at stations 34, 35, with a dramatic DO minimum extended upwards to 100 m (Fig. 54, 55). In the top 200 m, nutrients and DO showed evidence of upwelling at the shelf break, and depletion in surface waters focused on stations 34 and 35, associated with peak surface temperatures (Fig. 56, 57). There was some evidence of nutrient depletion on the shelf. Only DO and silicate indicated subsurface upwelling below stations 34 and 35. Peak chlorophyll concentrations occurred at the inshore station on the shelf (>2.3 µg L^{-1}) and at stations 34, 35 (>2.8 µg L^{-1}) (Fig. 57B). Maxima in PSA total particle volume coincided with those in chlorophyll a (Fig. 57B,C).

Overall on this cruise, there was a strong effect of phytoplankton production on the nutrient and oxygen distributions. Nutrients were depleted and DO elevated within phytoplankton blooms, with peak chlorophyll a concentrations exceeding 2 µg l^{-1}. However, the location of these blooms varied across transects. On the western transect, blooms occurred just inshore of the shelf break front, and over the cold, fresh feature 50 km from the shelf break. Chlorophyll a was lower in the saline pool, despite high nutrients and shallow stratification. In the central transect, the principal bloom occurred on the outer edge of the saline pool, above a subsurface salinity front. In the eastern transect, peak chlorophyll a occurred on the shelf, and above the dome feature on the outer edge of the warm saline pool. It is difficult to identify an immediate cause for these differences, especially given that conditions of elevated surface nutrients and shallow mixed layers appeared to favour blooms throughout all three transects. Silicate was the only nutrient which seemed to be potentially limiting, and it was only depleted in blooms.
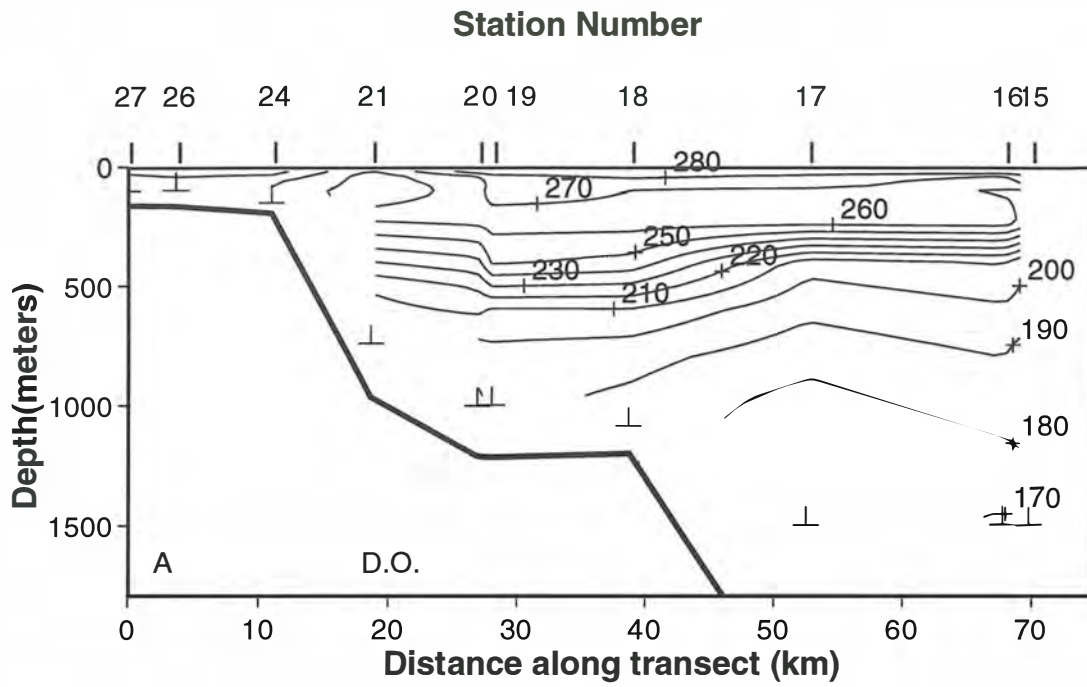
Station Number
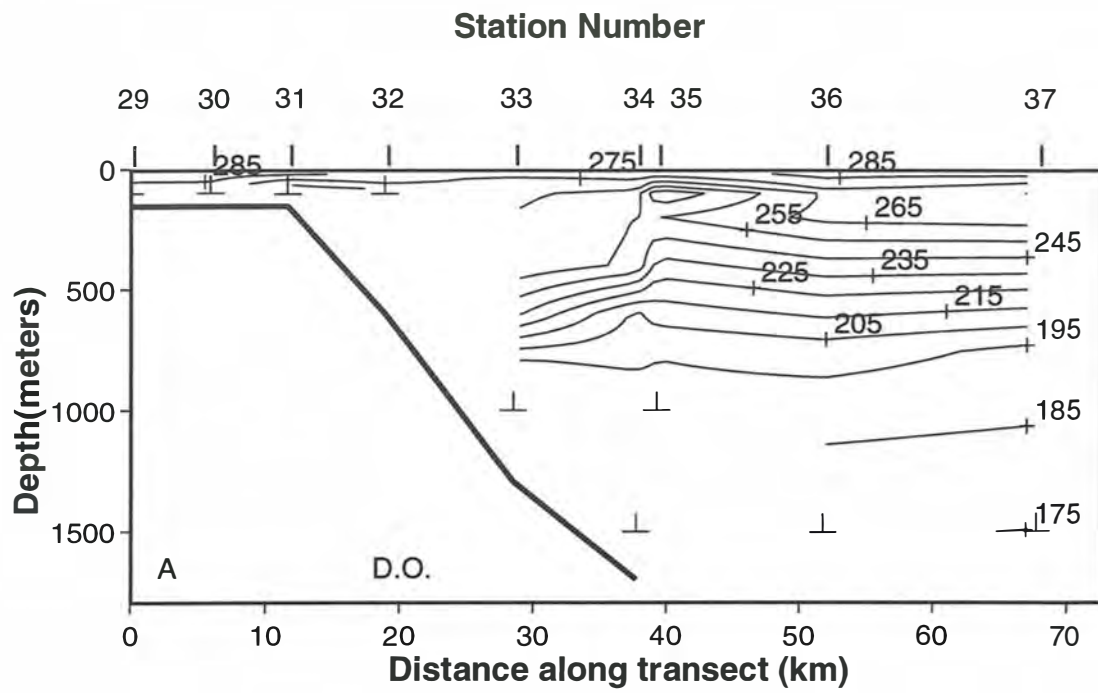
Fig. 54. Contour plots of Dissolved Oxygen (μM) on a vertical section along the eastern transect, cruise SS4/92, November, 1992.

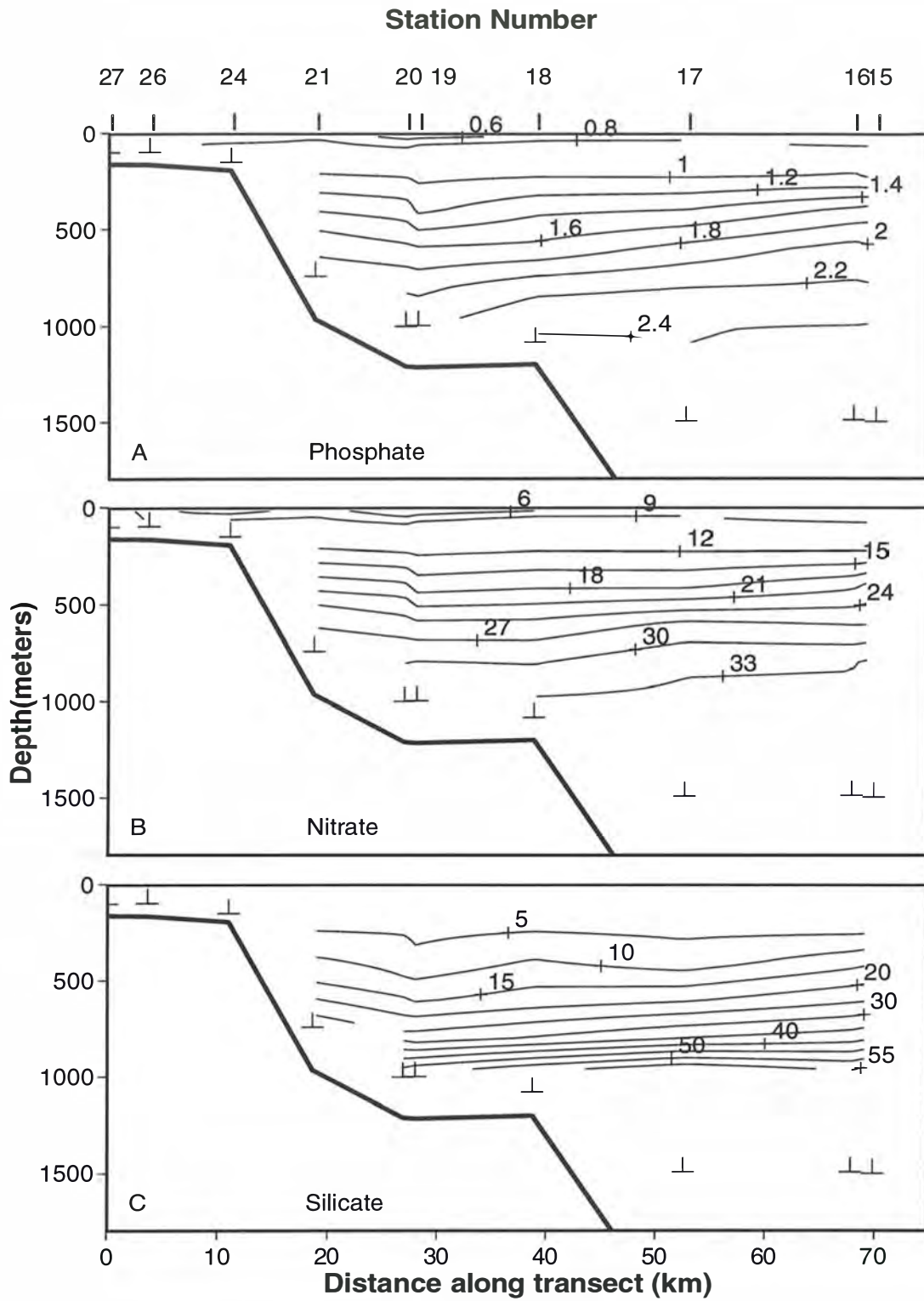Fig. 55. Contour plots of (A) Phosphate (µM), (B) Nitrate (µM), and (C) Silicate (µM), on a vertical section along the eastern transect, cruise SS4/92, November,1992.

Station Number
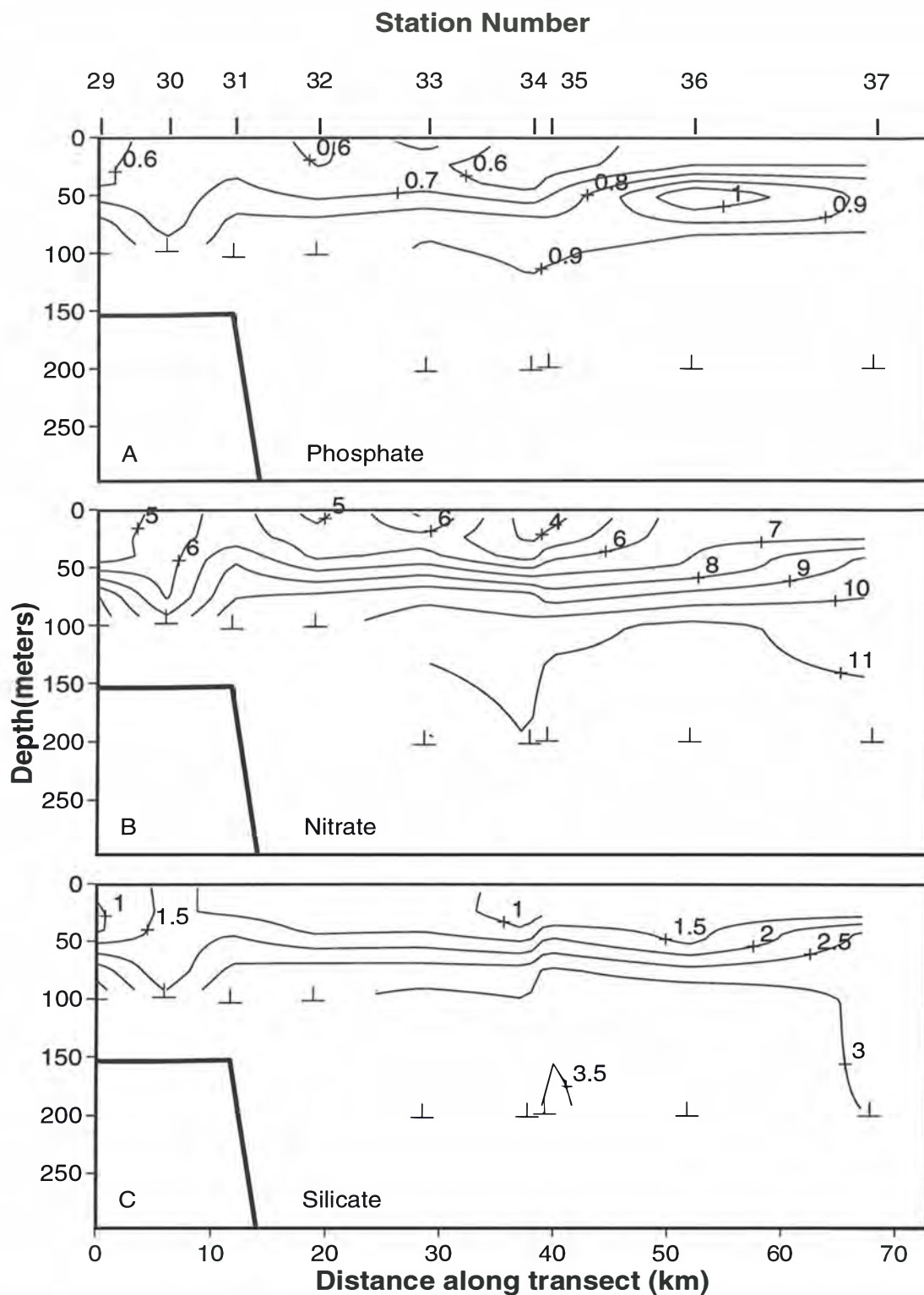
Fig. 56. Contour plots of (A) Phosphate (μM), (B) Nitrate (μM), and (C) Silicate (μM), on a vertical section (0-250 m) along the eastern transect, cruise SS4/92, November,1992.

Station Number

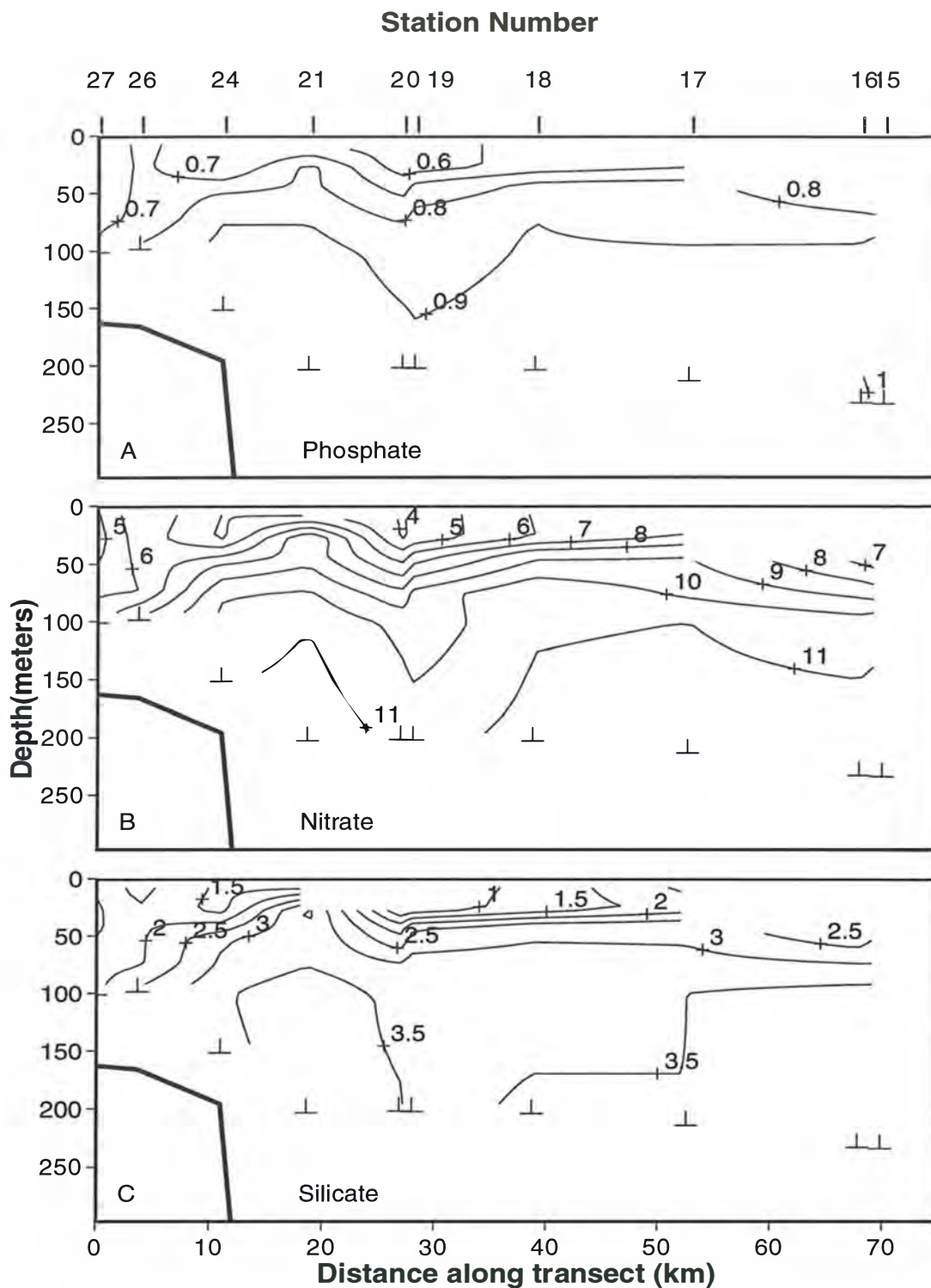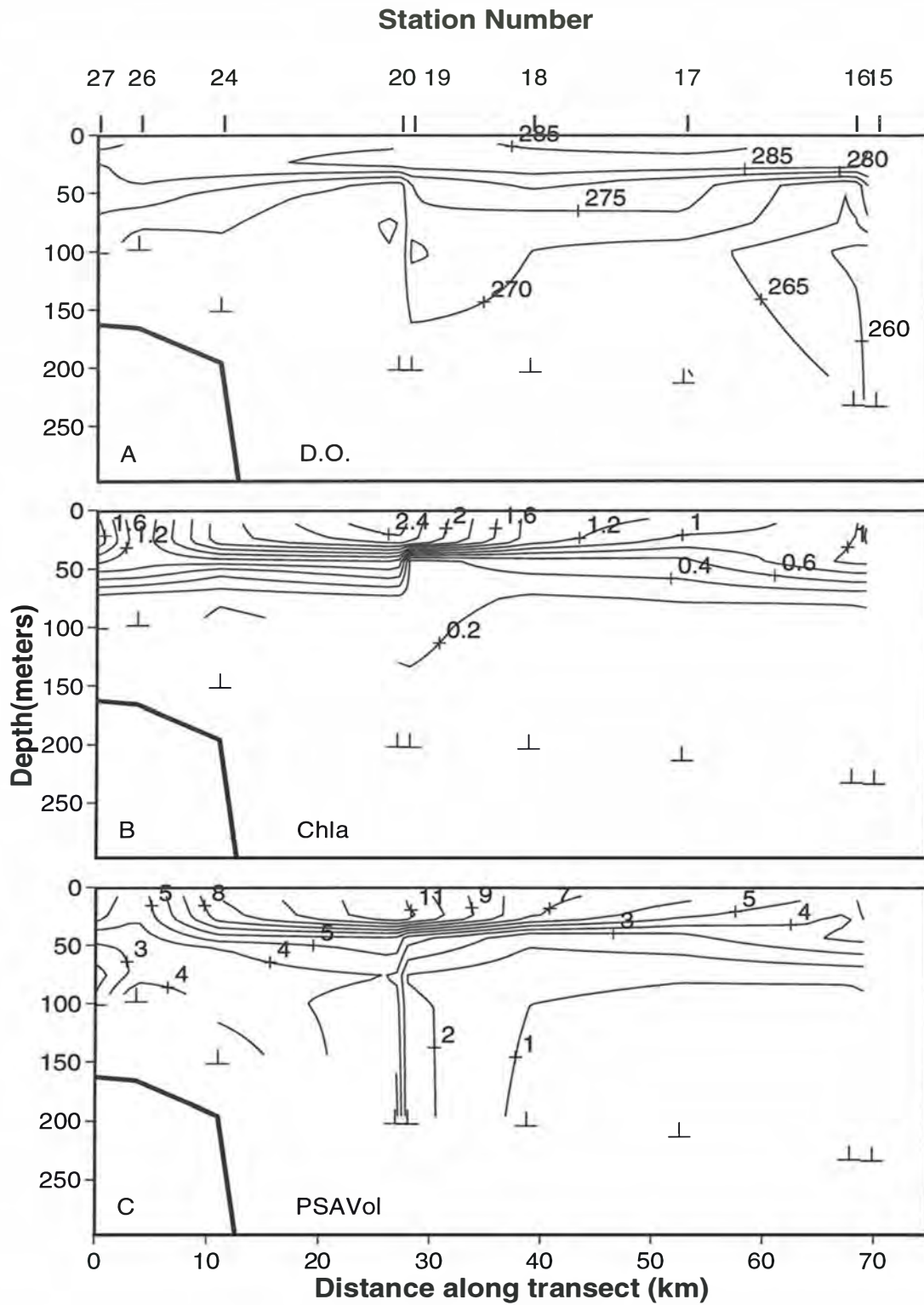Fig. 57. Contour plots of (A) Dissolved Oxygen (μM), (B) Chlorophyll a (μg L^{-1}) and (C) PSA Total Particle Volume (10^5 μm^3 L^{-1}), on a vertical section (0-250 m) along the eastern transect, cruise SS4/92, November 1992.

CRUISE SS3/93, APRIL, 1993.

On the western transect, the deep DO section showed relatively high and uniform DO values within SAMW, and a strong decrease in DO in AAIW (Fig. 58). DO values in SAMW increased at the offshore end of the transect, below the surface front near Station 25, from 230 to ca 270 μM, and at the inshore end, over the upper slope, from 230 to 250 μM. Nitrate, phosphate and silicate showed relatively little horizontal structure below 200 m, except that contours deepened along with temperature and salinity contours at the continental slope (Fig. 59). Within the top 80 m, the dominant signal in DO and nutrients occurred at the offshore front (Fig. 60, 61). Here, associated with the transition to polar water, DO increased from 250 to 280 μM, nitrate from 3 μM to 10 μM, and phosphate from 0.5 to 0.9 μM. Interestingly, silicate showed no response to this front at all, and surface silicate values were less than 2.5 μM throughout. Nitrate and phosphate values in the mixed layer were lower over the inshore half of the transect (slope and shelf). Between 40 and 120 m, nitrate, phosphate and DO contours behaved similarly to temperature and salinity contours, with evidence of upwelling at the shelf break, and over the mid-slope.

The relatively deep mixed layer, and the presence of mixed layer nitrate values around 2 μM over much of the transect, reflect autumn erosion of the base of the mixed layer. Chlorophyll values were highest in the mixed layer over the shelf and slope, and mixed layer values exceeded 0.4 μg L^{-1}, with two broad maxima greater than 0.6 μg L^{-1}, over the shelf break, and from 50 to 70 km offshore of the shelf-break (Fig. 61). The offshore maximum extended throughout a deeper (60 m) mixed layer. There was a pronounced minimum in chlorophyll at station 25 in the offshore front, and some indication of a shallow subsurface chlorophyll maximum in the colder water south of this front.
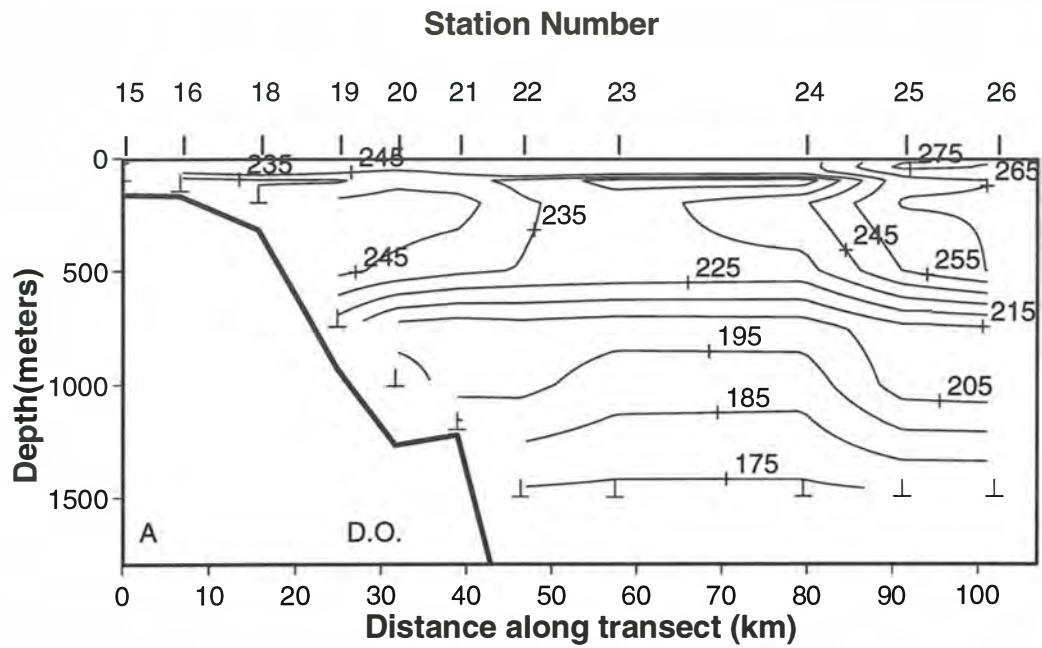
Fig. 58. Contour plots of Dissolved Oxygen (μM) on a vertical section along the western transect, cruise SS3/93, April 1993.

Station Number
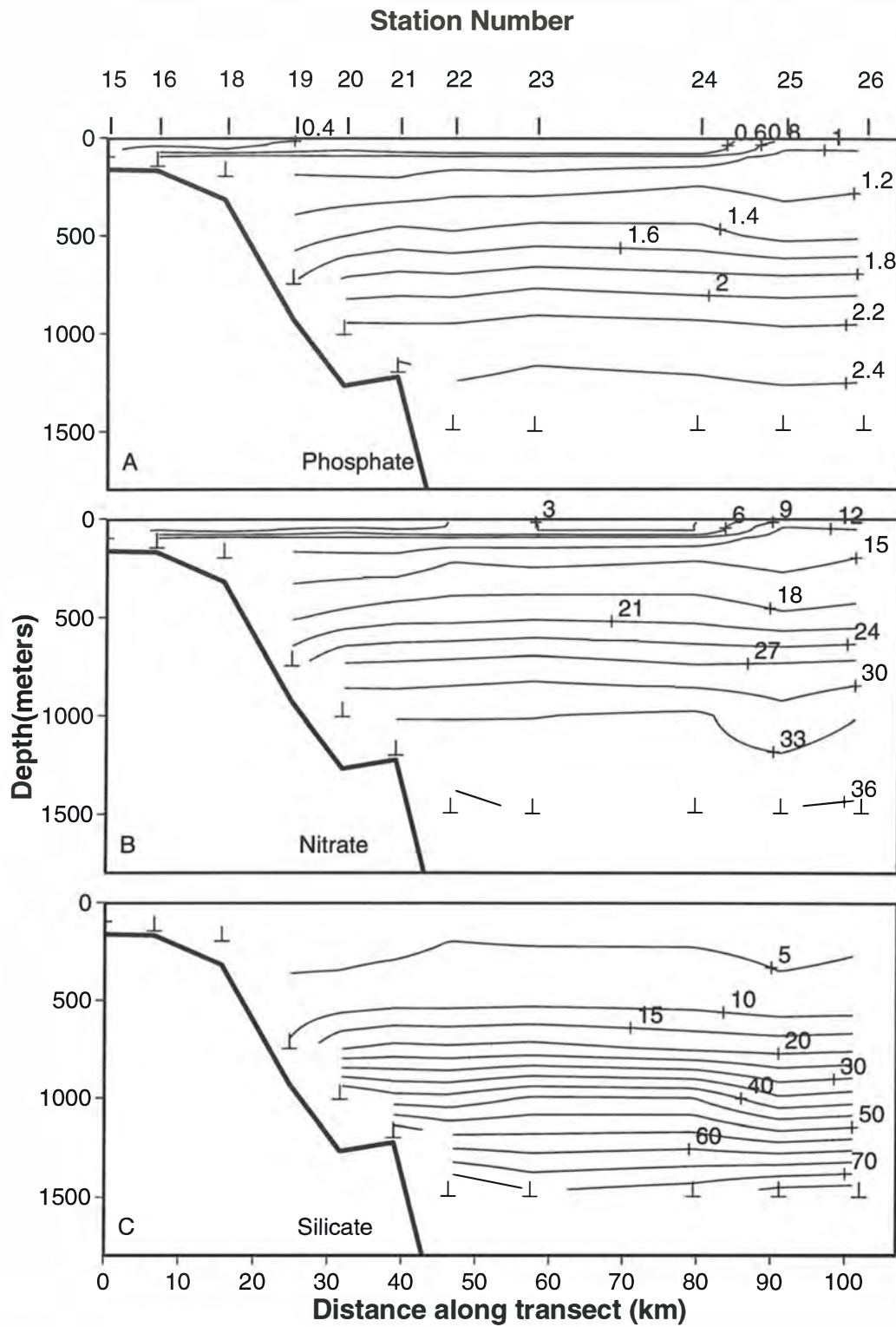
Fig. 59. Contour plots of (A) Phosphate (µM), (B) Nitrate (µM), and (C) Silicate (µM), on a vertical section along the western transect, cruise SS3/93, April, 1993.
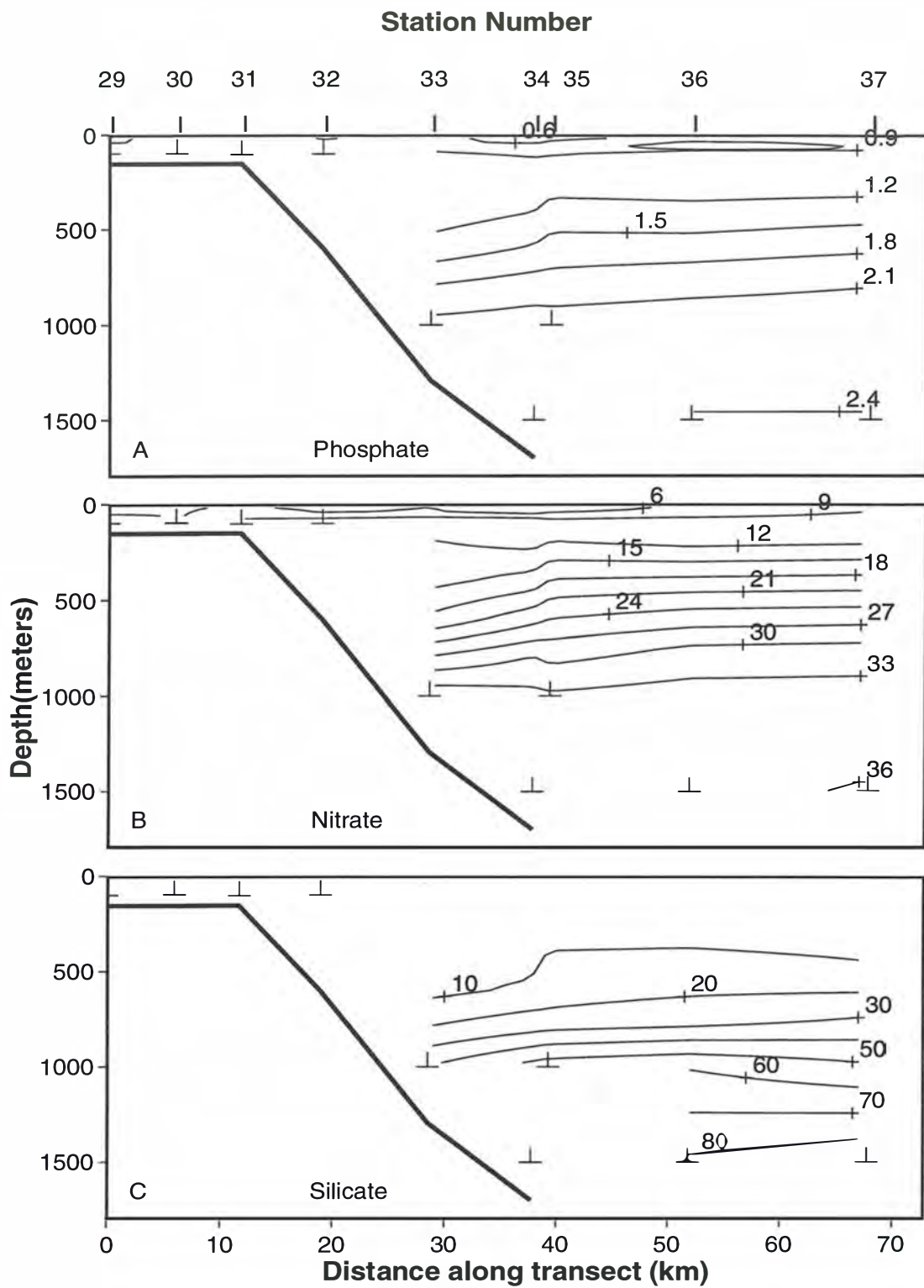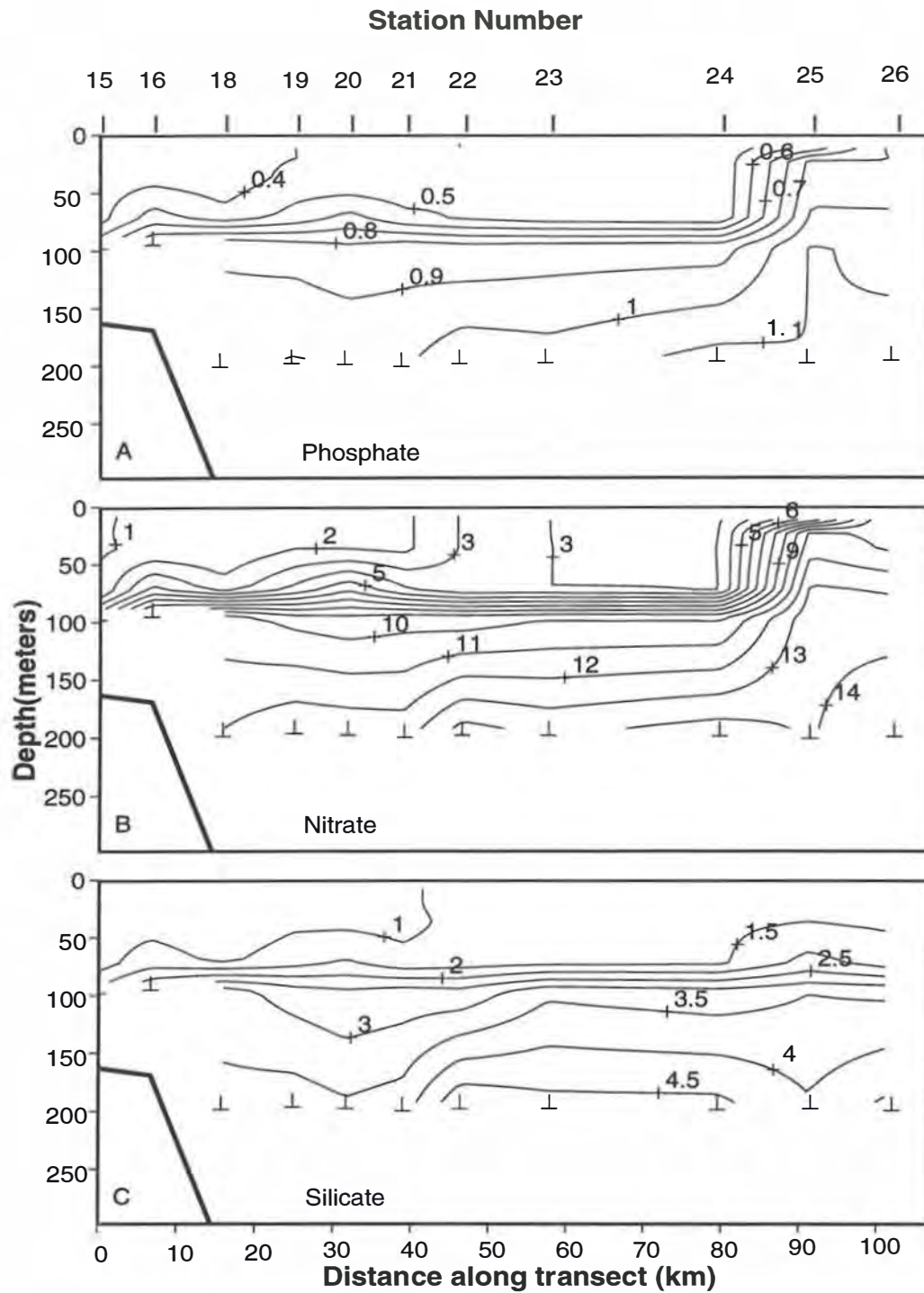
Fig. 60. Contour plots of (A) Phosphate (μM), (B) Nitrate (μM), and (C) Silicate (μM), on a vertical section (0-250 m) along the western transect, cruise SS3/93, April, 1993.

Station Number
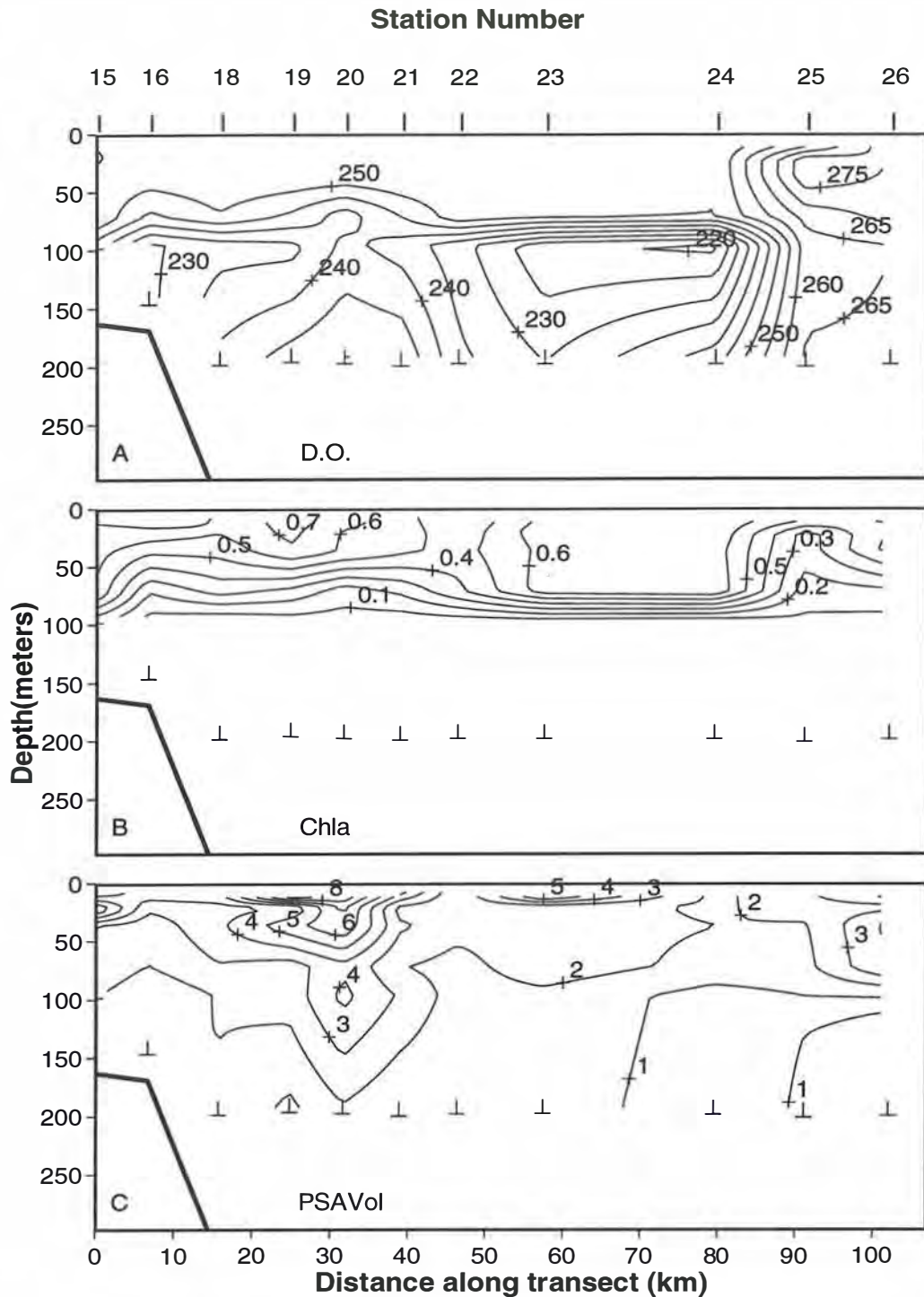
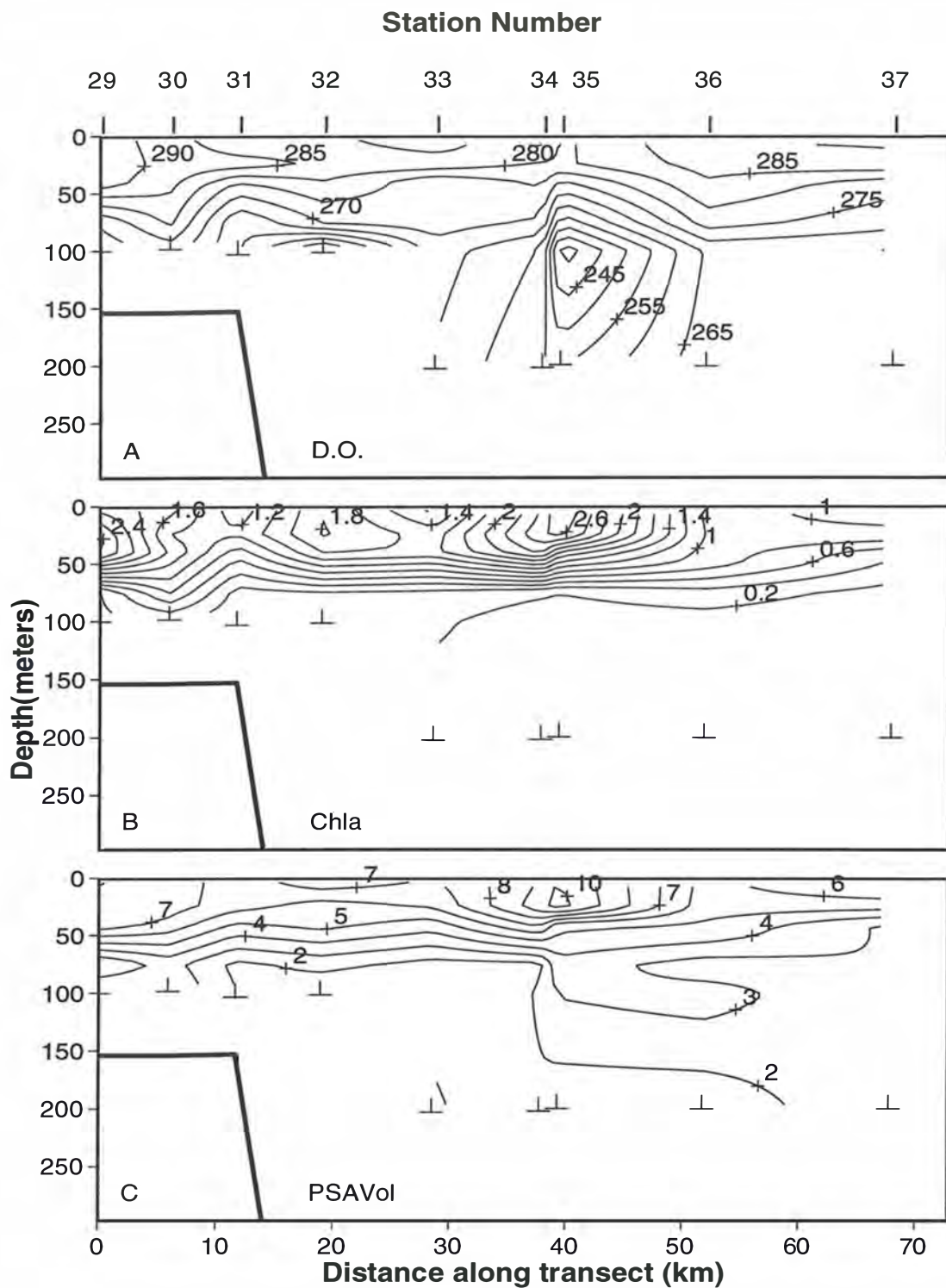

Fig. 61. Contour plots of (A) Dissolved Oxygen (μM), (B) Chlorophyll a (μg L⁻¹) and (C) PSA Total Particle Volume (10^5 μm^3 L⁻¹), on a vertical section (0-250 m) along the western transect, cruise SS3/93, April 1993.

On the central transect, DO values in mode water were about 210 to 220 µM, considerably lower than on the western transect, except for an increase at station 6 on the slope (Fig. 62). Nitrate, phosphate and silicate values all decreased at the upper slope (Fig. 63). Within the upper 80 m, DO showed little vertical structure, and values were low (240 to 250 µM), consistent with the higher temperatures (Fig. 65A). Nitrate, phosphate and silicate also showed little vertical or horizontal structure, with nitrate values between 1 and 2 µM, and silicate values between 1 and 1.5 µM (Fig. 64). The presence of detectable nitrate in such warm, saline water again suggests recent injection of nitrate due to autumn mixing. Below 80 m, the horizontal structure in nutrients and DO was dominated by apparent subsurface uplift at the shelf break, and at station 8, ca 35 km from the shelf break. This structure was very similar to that observed on the inner half of the western transect.

Chlorophyll a values were relatively high throughout the mixed layer (>0.6 µg L^{-1}), with maximum values (0.9 µg L^{-1}) occurring at the shelf break (Fig. 65B). The highest particle volume occurred offshore of this chlorophyll maximum, in the warm saline core at station 6 (Fig. 65C).

Overall on this cruise, nutrient levels were elevated in the mixed layer, compared with summer values, presumably due to mixed layer deepening and erosion of the nutracline. Between the mixed layer and 150 m, there was evidence of upwelling of nutrients at the shelf break and over the mid-slope on both transects. Chlorophyll a values were generally low on the western transect, with mixed layer values ranging from 0.4 to 0.6 µg L^{-1}, but moderate (0.6 to 0.9) on the central transect.

Station Number
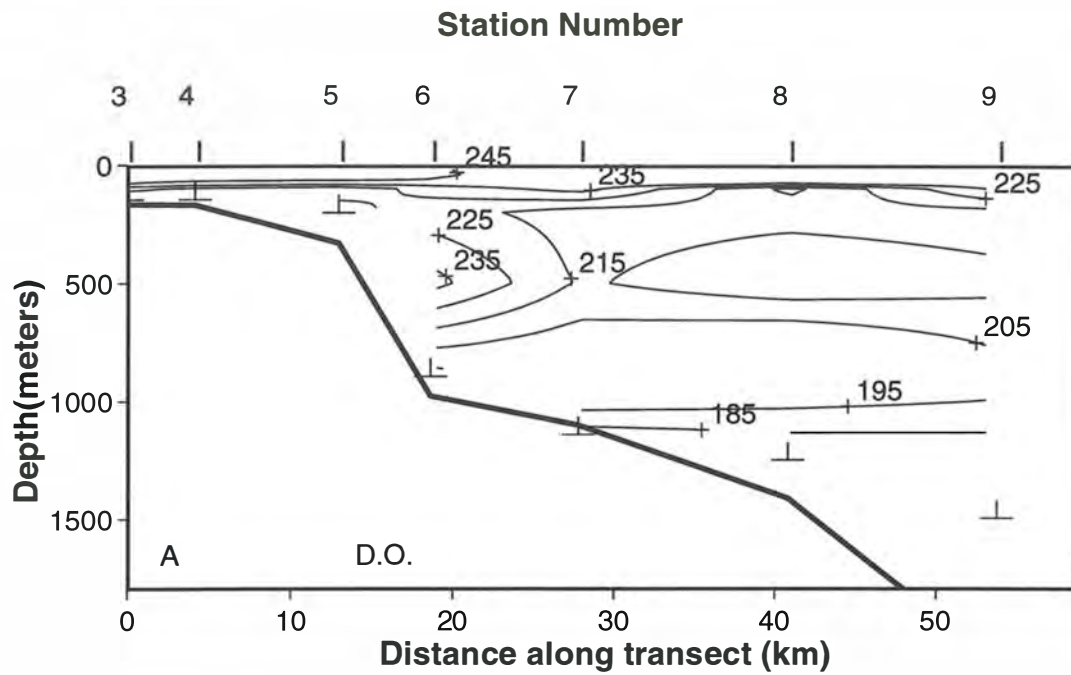
Fig. 62. Contour plots of Dissolved Oxygen (μM) on a vertical section along the central transect, cruise SS3/93, April 1993.

Station Number
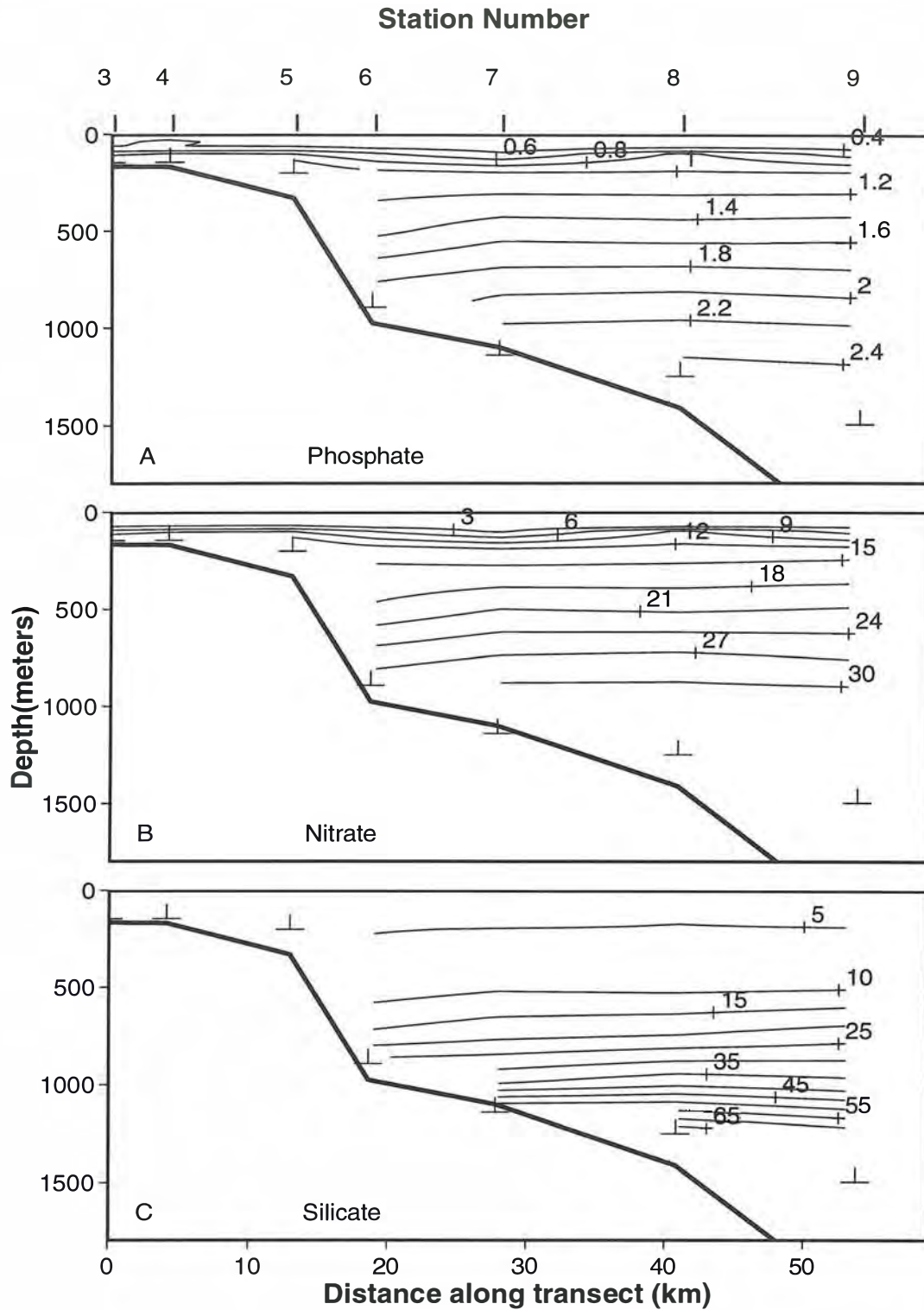
Fig. 63. Contour plots of (A) Phosphate (μM), (B) Nitrate (μM), and (C) Silicate (μM), on a vertical section along the central transect, cruise SS3/93, April, 1993.

Station Number
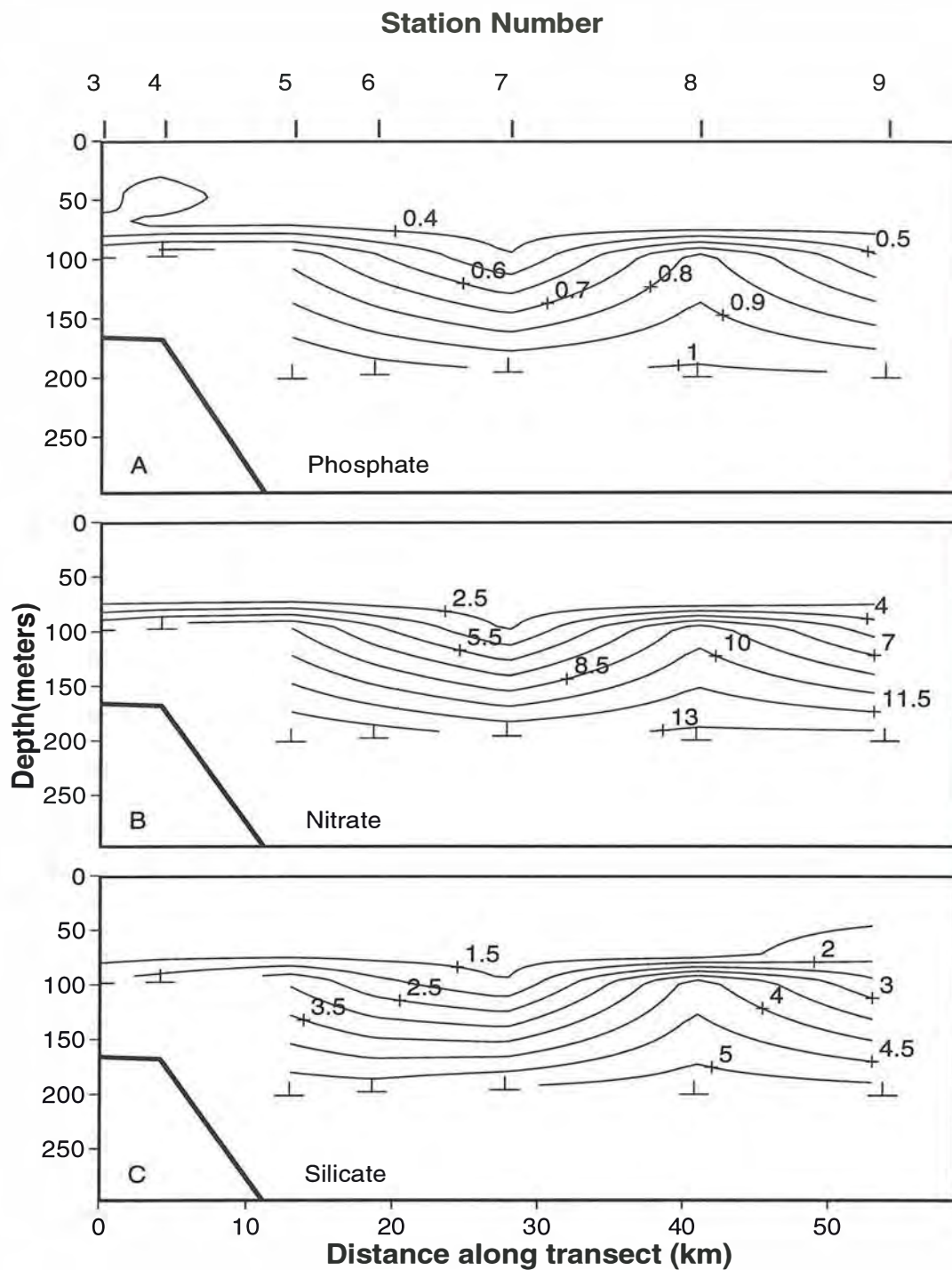
Fig. 64. Contour plots of (A) Phosphate (μM), (B) Nitrate (μM), and (C) Silicate (μM), on a vertical section (0-250 m) along the central transect, cruise SS3/93, April, 1993.

105
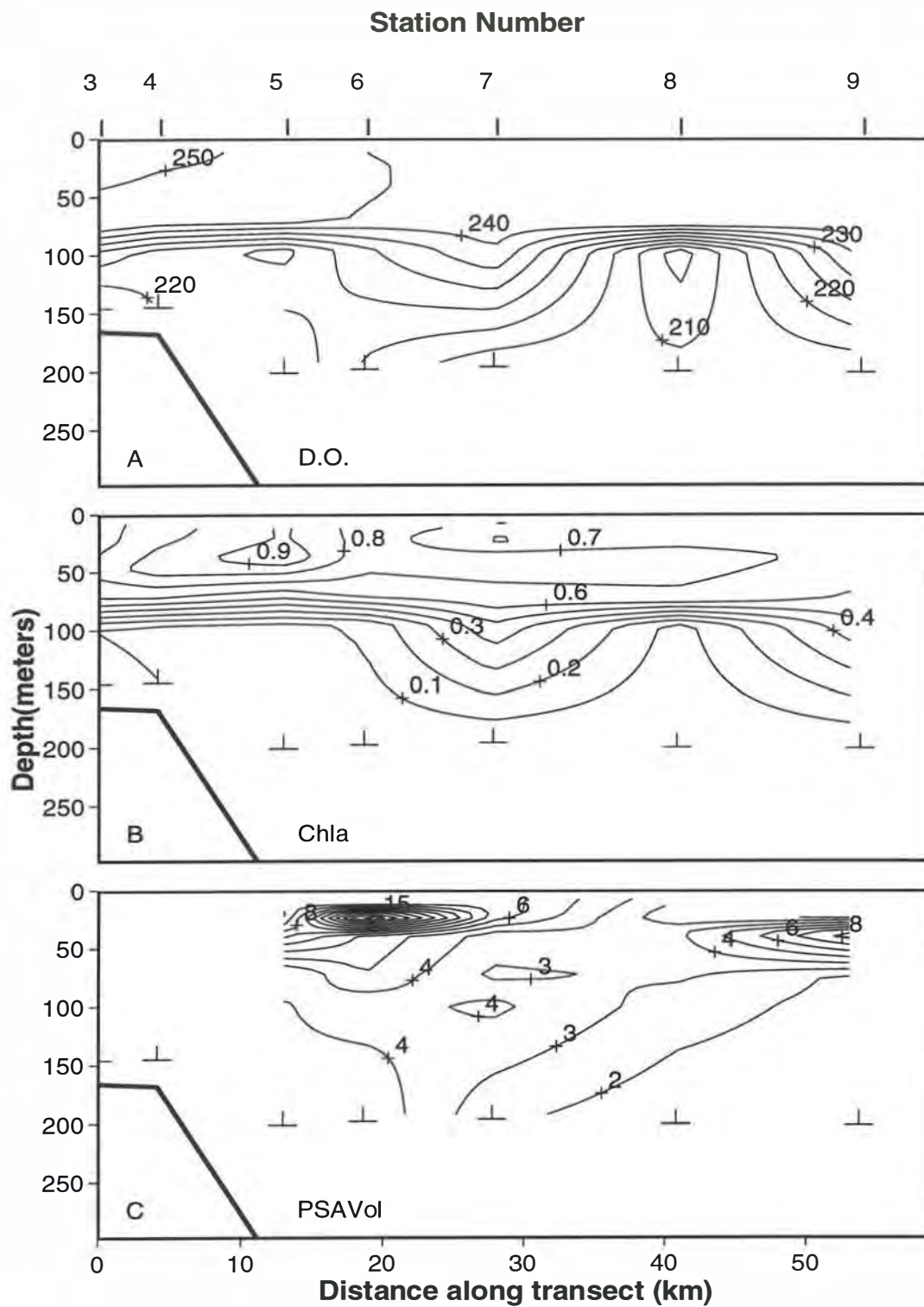
Fig. 65. Contour plots of (A) Dissolved Oxygen (μM), (B) Chlorophyll a (μg L^{-1}) and (C) PSA Total Particle Volume (10^5 μm^3 L^{-1}), on a vertical section (0-250 m) along the central transect, cruise SS3/93, April 1993.

PvsI VARIATION: DIEL CYCLE.

Although mixed layer depths varied among cruises and stations, there was little evidence of any systematic difference in PvsI parameters in the depth range 0 - 40 m. Observations within this depth range were averaged to provide a "mixed layer" value at each station. We then looked for systematic variation in these parameters within cruises, either with time of day, or mixed layer depth. In order to compare observations from all PvsI experiments, both "short" and "full", the estimates from "short" experiments were converted to equivalent estimates from "full" experiments by applying the regression relationships derived earlier (see Table 3, METHODS). Moreover, where "full" experiments showed photoinhibition, the parameter P^B_s was converted to an equivalent P_m, by applying the formulae given in the Methods section.

This analysis showed, somewhat surprisingly, that a large proportion of the variance in values of P_m within cruises could be explained by diel variation. We fitted a sinusoidal diel variation by regressing $P_m(t)$ on $\cos(2\pi t/24)$ and $\sin(2\pi t/24)$, where t is local time in hours. These multiple regressions were highly significant for all 4 cruises. This relationship can be written alternatively as:

$$P_m(t) = \overline{P_m} + A \cos(2\pi(t-\tau)/24),$$

where A is the amplitude of the diel signal, and τ is the time of maximum potential photosynthetic rate. The results obtained are shown in Table 4.

TABLE 4. REGRESSION RESULTS FOR DIEL VARIATION OF PHOTOSYNTHETIC PARAMETER P_m.

CRUISE	$\overline{P_m}$	A	τ	SIGNIFICANCE	R^2
SS2/91	3.99	0.97	10.4	<.001	0.67
SS1/92	4.94	1.24	8.2	0.018	0.44
SS4/92	4.29	1.45	9.7	<.001	0.57
SS3/93	3.62	1.43	10.2	0.003	0.66

Diel variation explained from 44 to 67% of the variance in "mixed layer" P_m within cruises. The phase of the diel signal was highly consistent among cruises, with maximum values of P_m occurring in the morning, between 0800 h and 1100 h, and a decline during the afternoon to minimum values in the evening. The daily-averaged values, $\overline{P_m}$, vary significantly among cruises or seasons, but the amplitude of the seasonal variation is comparable to the diel variation. The maximum value of $\overline{P_m}$ was observed in summer (SS1/92), and the minimum value in autumn (SS3/93).

There was no significant diel variation in α in any cruise. The summary statistics for α are given in Table 5.

TABLE 5. SUMMARY STATISTICS FOR α (mg C (mg Chl a)$^{-1}$ h^{-1} (μmol m^{-2} s^{-1})$^{-1}$)

CRUISE	MEAN	STD. ERR.	STD. DEV.
SS2/91	0.081	0.002	0.008
SS1/92	0.091	0.004	0.017
SS4/92	0.042	0.003	0.014
SS3/93	0.043	0.003	0.010

Note that the differences in mean values between cruises are highly significant. High values of α were observed in summer (SS1/92), and in winter (SS2/91), and low values in spring and fall. There was no significant dependence of either parameter on mixed layer depth within cruises.

In considering the depth-dependence of PvsI parameters below 40 m, we focused on the 75 m estimates from both "short" and "full" experiments. We looked for any systematic dependence of these parameters on time of day or mixed layer depth, and considered both the 75 m values, and the ratio of 75 m values to mixed layer values.

For SS3/93, $P_m(75)$ showed some evidence of diel variation with the right phase, although this was not statistically significant (R^2 = 0.32, Prob. =.15). $P_m(75)/$ $P_m(ml)$ showed much less diel variation (R^2 = 0.14, Prob. = .47). Results for SS1/92 were similar, with significant diel variation in $P_m(75)$ (Prob. = 0.04), and no significant diel variation in $P_m(75)/$ $P_m(ml)$ (Prob. = 0.63). For these two cruises, we can reasonably assume that $P_m(75)$ covaries on a diel basis with mixed layer values, and represent the effect of depth by a mean ratio. In fact, for both of these cruises, this mean ratio is not significantly different from 1.0. This is not too surprising for SS3/93, where autumn mixing produced mixed layer depths approaching 75 m at many stations. It is rather surprising for the summer station, where mixed layer depths were generally less than 75 m.

For SS2/91, $P_m(75)$ has a highly significant diel cycle (Prob. = 0.0009), but $P_m(75)/$ $P_m(ml)$ also has a significant cycle (Prob. = 0.03). This is primarily due to the fact that the diel cycle at 75 m has a smaller relative amplitude than the cycle in the mixed layer (A / $\overline{P_m}$ = 0.15 cf 0.24). Although some stations on this cruise had very deep winter mixed layers (> 200 m), a large number of stations showed mixed layer depths less than 75 m. The mean of the ratios $P_m(75)/$ $P_m(ml)$ was 0.95, and not significantly different from 1. On SS4/92, $P_m(75)$ showed less diel variation than $P_m(75)/$ $P_m(ml)$, though neither was significant. Here, it may be most reasonable to assume that $P_m(75)$ showed no systematic diel variation. This could be due to high light attenuation and relatively shallow

mixed layers in the spring bloom. The mean ratio $P_m(75)/ P_m(ml)$ for SS4/92 was very low (0.47), suggesting that the population at 75 m was effectively isolated from the mixed layer population.

Although differences in the relationship between $P_m(75)$ and $P_m(ml)$ between cruises appear to be related to mixed layer depth, there was no significant correlation between $P_m(75)$ or $P_m(75)/ P_m(ml)$ and mixed layer depth within cruises.

Values of $\alpha(75)/ \alpha(ml)$ showed no significant diel variation on any cruise. The summary statistics for this ratio by cruise are shown in Table 6.

TABLE 6. SUMMARY STATISTICS FOR THE RATIO $\alpha(75)/ \alpha(ml)$ BY CRUISE.

CRUISE	MEAN	STD. ERR.	STD. DEV.
SS2/91	1.02	0.04	0.19
SS1/92	1.37	0.13	0.44
SS4/92	0.99	0.07	0.30
SS3/93	1.13	0.07	0.26

Values of $\alpha(75)/ \alpha(ml)$ are on average close to 1.0 on SS2/91 and SS3/93, where average values of $P_m(75)/ P_m(ml)$ were close to 1.0. However, on the summer cruise SS1/92, where $P_m(75)/ P_m(ml)$ was close to 1.0, $\alpha(75)/ \alpha(ml)$ was significantly greater than 1, suggesting isolation of the 75 m population from the mixed layer (consistent with summer stratification), and strong light limitation. In contrast, values of $\alpha(75)/ \alpha(ml)$ on SS4/92 were close to 1.0, whereas values of $P_m(75)/ P_m(ml)$ were low.

Establishing a significant diel cycle in the PvsI parameter P_m has important ramifications, both for interpreting the field observations, and for modelling primary production. Except at the 24 h diel stations, PvsI experiments were conducted whenever the station was reached. Having established a diel cycle in P_m, we can correct the experimental estimate, P_m(observed), for time of day t, and obtain an estimate of the daily mean value for that location, by:

$$P_m(\text{corrected}) = P_m(\text{observed}) \cdot \overline{P_m} / (\overline{P_m} + A \cos (2\pi(t-\tau)/24)).$$

These corrected values were used in subsequent examination of spatial pattern in P_m and I_k within cruises. The diel cycle in P_m was also incorporated into subsequent production modelling.

MODELLING PRIMARY PRODUCTION.

The approach adopted in this study of measuring PvsI parameters, as opposed to measuring *in situ* or simulated *in situ* column production, was designed to provide a data set which would allow extrapolation beyond the immediate light conditions of the day of the experiment, to monthly or seasonal production estimates. The consistency in PvsI parameters observed within cruises, noted in the previous section, provides an encouraging basis for this extrapolation. The production model used for each station combines in a straightforward way the PvsI parameters, the observed chlorophyll a profile, an estimate of surface irradiance, and the empirical relationships between attenuation coefficient Kd and chlorophyll a derived earlier.

The model calculates daily production at depth z as:

$$P(z) = \int_0^{24} P^B(z,t) \cdot Chla(z) dt$$

where:

$$P^B(z,t) = P_m^B(z,t) \cdot (1 - e^{-\alpha(z) \cdot I(z,t)/P_m^B(z,t)})$$

(or the equivalent equation with photoinhibition), and

$$I(z,t) = I(0,t) \cdot e^{-\int_0^z Kd(z')dz'}.$$

The surface light intensity I(0,t) was calculated using equations for clear sky irradiance given by Kirk (1983), and a cloud transmission factor derived from estimates of monthly mean irradiance produced by Bishop (Bishop and Rossow, 1991), based on cloud statistics from the International Satellite Cloud Climatology Project. The time integration was carried out numerically at 6 minute time intervals, and at 1 m depth intervals. The photosynthetic parameters were linearly interpolated between observation depths, while Chl a(z) and consequently Kd(z) were based on calibrated fluorescence profiles. Vertically integrated column production values were calculated for two intervals: surface to mixed layer depth, and mixed layer depth to 100 m. Where the mixed layer exceeded 100 m, production was calculated to 100 m only. Vertically integrated chlorophyll a was calculated over the same depth intervals for comparison with production.

Estimates of daily production were calculated using the theoretical clear sky irradiance for the day of observation, modified by the monthly mean cloud factor for that month. These can be thought of as mean or typical production

values for the observed biomass, photosynthetic parameters and time of year. These estimates have been extrapolated to monthly and seasonal estimates by applying the appropriate monthly mean cloud factors to theoretical clear sky irradiance.

The estimates based on estimated values of P_m and α should be thought of as estimates of gross production, as the PvsI curves were fitted allowing for a non-zero (and usually negative) y-axis intercept. The ^{14}C technique does not provide a reliable estimate of phytoplankton respiration rates. A simple common assumption is that respiration is 10% of P_m. We have calculated net production rates under this assumption, to provide a rough indication of the possible effects of respiration.

PvsI PARAMETERS AND COLUMN PRODUCTION: SEASONAL AND SPATIAL VARIATION.

WINTER: JULY 1991, SS2/91.

On the winter cruise, there was remarkably little variation in mixed layer values of P_m and α within the study region, especially given the strong contrast in physical and chemical properties between the Zeehan Current water mass and water masses inshore and offshore from it (Fig. 66). Values of P_m ranged from 3 to 5 mg C (mg Chl a)$^{-1}$ h^{-1}, and values of α from 0.06 to 0.09 mg C (mg Chl a)$^{-1}$ h^{-1} (μmol m^{-2} s^{-1})$^{-1}$. Values of I_k ranged from 40 to 60 μmol photons m^{-2} s^{-1}. These relatively low values for I_k suggest that all populations were adapted to low winter light levels.

Total column chlorophyll in the top 100 m in winter ranged from 15 to 30 mg Chl a m^{-2}, with lowest values in Zeehan Current Water (Fig. 67). The proportion contained within the mixed layer ranged from ca 10% in the shallow mixed layers on the western transect, to 100% in the deep mixed layers of the Zeehan Current water mass. Estimated gross column production in the top 100 m was lowest in winter, with values ranging from ca 200 to 400 mg C m^{-2} d^{-1}. Values were highest offshore on the central and eastern transect, and lowest in the deeply mixed Zeehan Current water mass on the eastern transect (Fig. 67). Estimated net column production for the top 100 m was quite low throughout the region, typically about 100 mgC m^{-2} d^{-1}, and close to zero at an offshore station on the eastern transect. This reflects the combined effect of winter mixing, and low surface irradiance and short daylength.

111
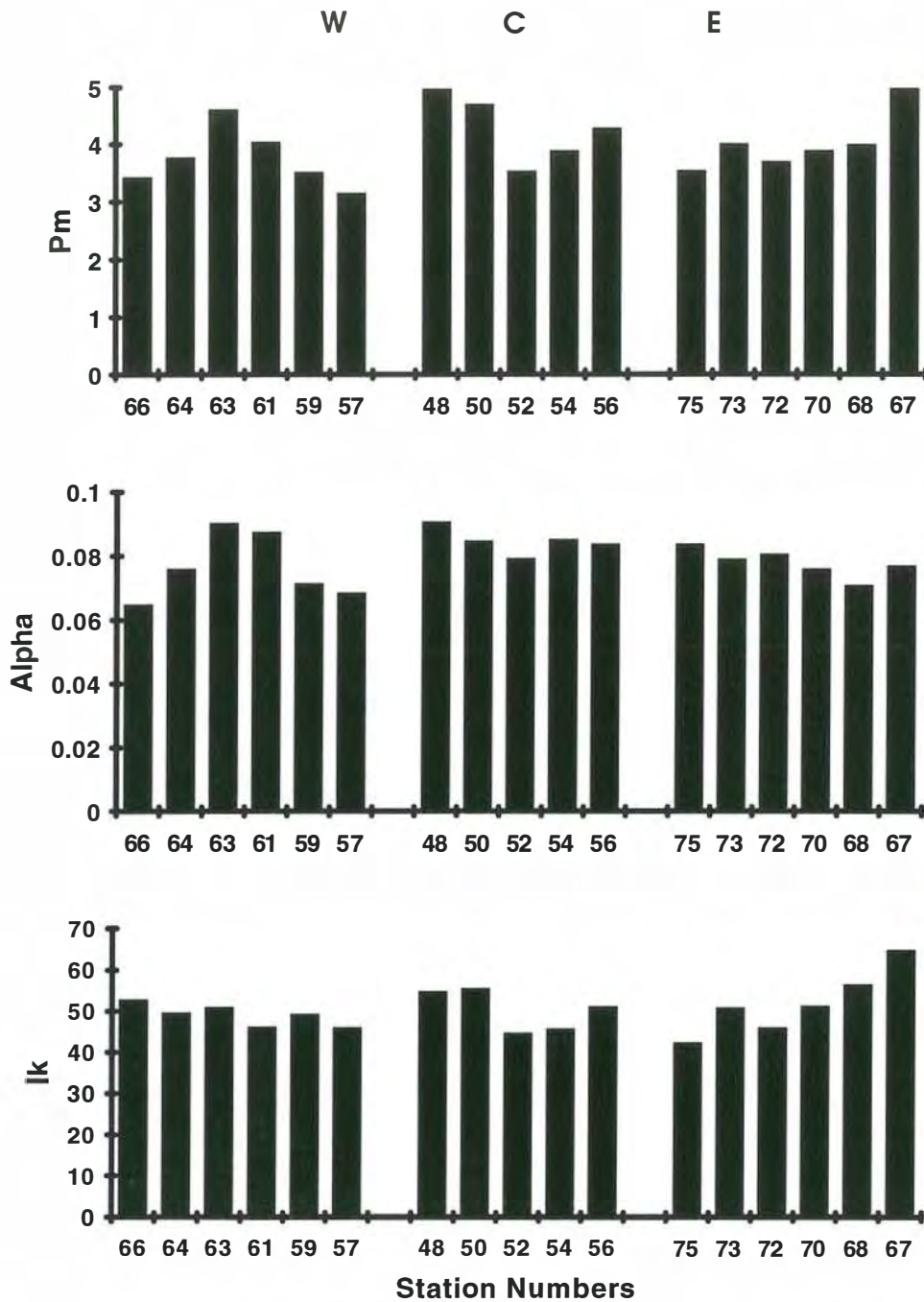
Fig. 66. Photosynthetic parameters P_m (mg C (mg Chl a)$^{-1}$ h^{-1}), α (mg C (mg Chl a)$^{-1}$ h^{-1} (μmol m^{-2} s-1)$^{-1}$), I_k (μmol m^{-2} s^{-1}) vs station number by transect on cruise SS2/91.
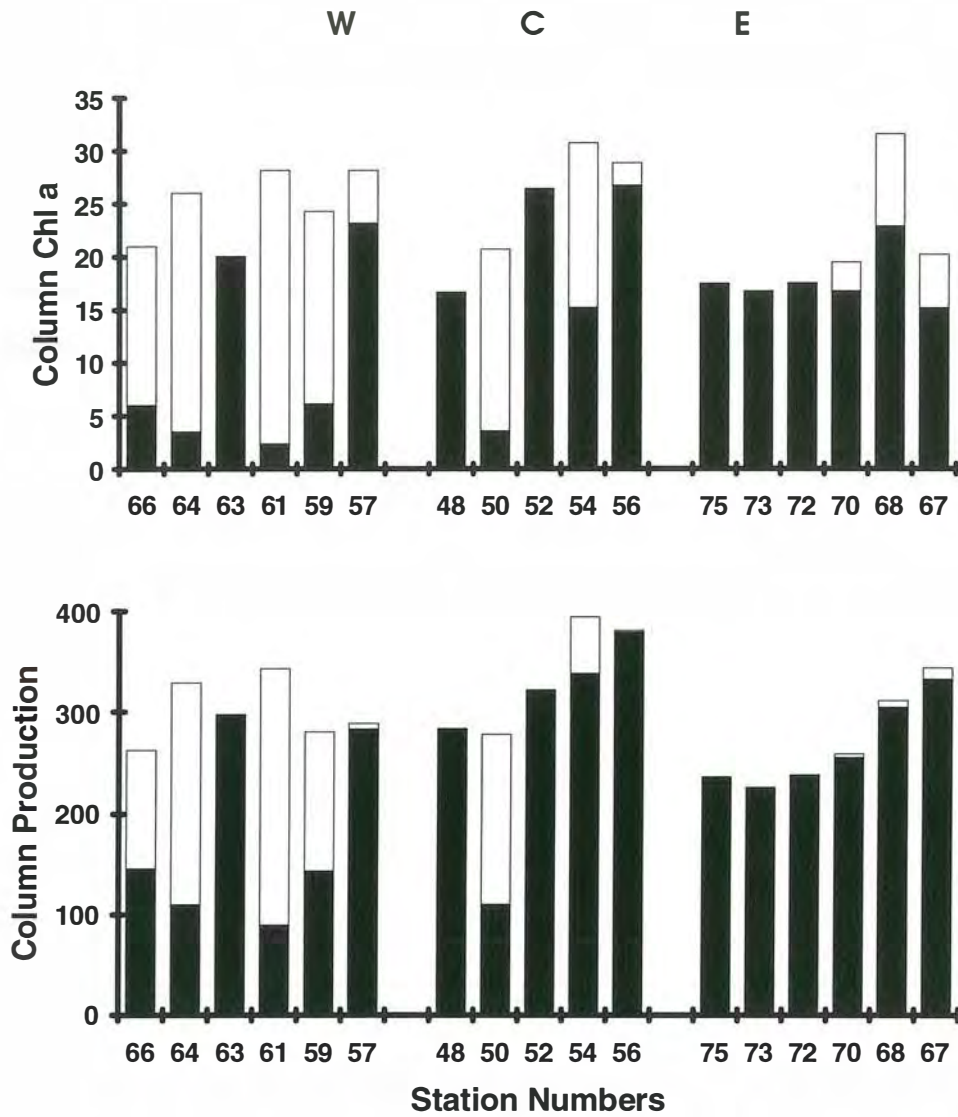
Fig. 67. Column biomass (mg Chl a m^{-2}) and column production (mg C m^{-2} d^{-1}) in the mixed layer (solid bar) and from 0 to 100 m (total bar) by station and transect on SS2/91.

SPRING: NOVEMBER 1992, SS4/92.

In spring, there was much more variation in mixed layer photosynthetic parameters, perhaps reflecting the different light histories of populations subjected to different degrees of seasonal stratification. Values of P_m generally ranged from ca 3 to 5 mg C (mg Chl a)$^{-1}$ h^{-1}, with one value of 7 (Fig. 68). Values of α were generally lower in spring, ranging from 0.02 to 0.05 mg C (mg Chl a)$^{-1}$ h^{-1} (μmol m^{-2} s^{-1})$^{-1}$, with lowest values observed on the western transect, over the shelf and mid-slope. Values of I_k were correspondingly larger, being generally around 100 μmol photons m^{-2} s^{-1}, but approaching 200 μmol photons m^{-2} s^{-1} in the shallow mixed layers at the inshore stations on the western transect (Fig. 68). The lower values of α and larger values of I_k are consistent with photoadaptation to the higher surface irradiance, long daylengths and shallow mixed layers of November.

Chlorophyll a concentrations were much higher in spring, and column values for the top 100 m were generally between 50 and 100 mg Chl a m^{-2}, with a peak value at the shelf break on the western transect of 140 mg Chl a m^{-2} (Fig. 69). The proportion contained in the mixed layer varied widely, from ca 20% in some stratified inshore stations, to ca 80% in stations with deep mixed layers. Estimated values of gross column production were very high, generally exceeding 1000 mg C m^{-2} d^{-1}. On the central and eastern transects, values were relatively independent of distance from shore, and about 1500 mg C m^{-2} d^{-1} (Fig. 69). On the western transect, values were lower (ca 1000 mg C m^{-2} d^{-1}) except for stations at the shelf break and offshore, with the offshore estimate reaching 2500 mg C m^{-2} d^{-1}. Estimates of net column production were also high, ca 800 - 1200 mg C m^{-2} d^{-1} on the central and eastern transects. On the western transect, net column production was about 600 mg C m^{-2} d^{-1} on the slope, 1300 mg C m^{-2} d^{-1} at the offshore station, but ca zero at the shelf break station 4, because of the large biomass of chlorophyll between 25 and 50 m, below the mixed layer (Fig. 69).
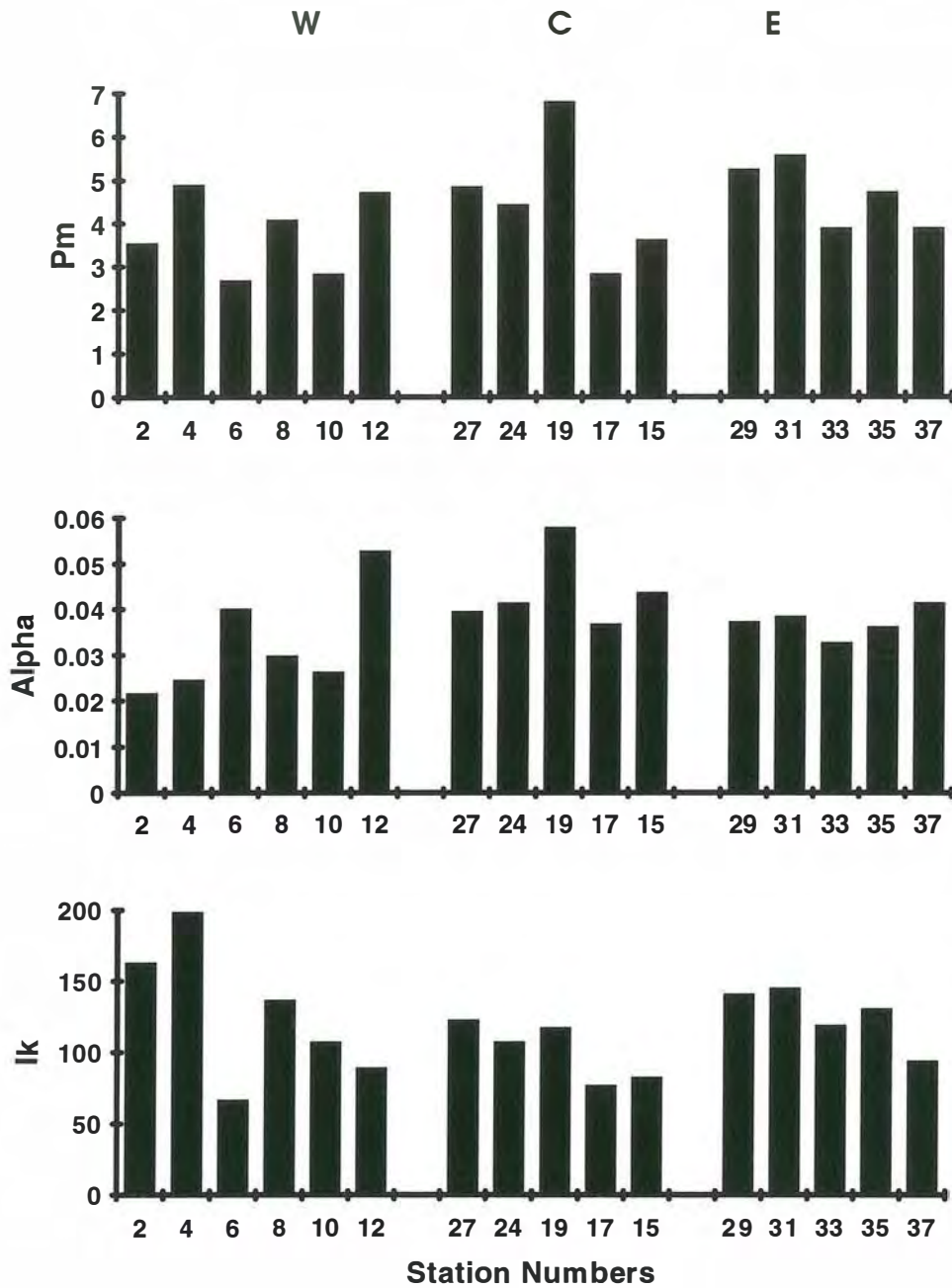
Fig. 68. Photosynthetic parameters P_m (mg C (mg Chl a)$^{-1}$ h^{-1}), α (mg C (mg Chl a)$^{-1}$ h^{-1} (μmol m^{-2} s-1)$^{-1}$), I_k (μmol m^{-2} s^{-1}) vs station number by transect on cruise SS4/92.

Fig. 69. Column biomass (mg Chl a m^{-2}) and column production (mg C m^{-2} d^{-1}) in the mixed layer (solid bar) and from 0 to 100 m (total bar) by station and transect on SS4/92.

SUMMER: FEBRUARY 1992, SS1/92.

In summer, values of P_m and α were again relatively constant (ca 4 mg C (mg Chl a)$^{-1}$ h^{-1} and 0.08 mg C (mg Chl a)$^{-1}$ h^{-1} (μmol m^{-2} s^{-1})$^{-1}$ respectively) with higher values observed in the slope waters (EAC water) on the central transect (Fig. 70). Values of I_k varied between 40 and 60 μmol photons m^{-2} s^{-1}. The high values of α and low values of I_k seem rather surprising for summer conditions. However, mixed layer depths were generally greater on the summer cruise than on the spring cruise. There is no evidence that the low values of nitrate observed in EAC water led to lower photosynthetic capacity.

Column chlorophyll a was relatively constant on the western transect (ca 50 mg Chl a m^{-2}), and somewhat lower on the central transect, except at the offshore station (Fig. 71). Column production was quite high and relatively constant over both transects, ranging from 1000 to 1400 mg C m^{-2} d^{-1}. Most of the chlorophyll, and almost all the production, occurred in the mixed layer, except at one offshore station on the western transect (Fig. 71). Net column production was generally high and constant in summer, reflecting the moderate concentration of biomass in mixed layers of moderate depth. Values ranged from 500 to 900 mg C m^{-2} d^{-1}.

AUTUMN: APRIL 1993, SS3/93

In autumn, values of P_m were lower and rather uniform, about 3 mg C (mg Chl a)$^{-1}$ h^{-1}. Values of α were also low and uniform, about 0.04 mg C (mg Chl a)$^{-1}$ h^{-1} (μmol m^{-2} s^{-1})$^{-1}$, with the exception of one high value (0.06 mg C (mg Chl a)$^{-1}$ h^{-1} (μmol m^{-2} s^{-1})$^{-1}$), at the offshore station on the western transect, in polar water (Fig. 72). Values of I_k were consequently relatively high, about 80 - 90 μmol photons m^{-2} s^{-1} , except again for the polar water station, where I_k was ca 50 μmol photons m^{-2} s^{-1}. It is rather difficult to explain why values of I_k should be higher in autumn than in summer, given the deeper mixed layers and lower surface irradiance in autumn.

Column chlorophyll a values ranged from 35 to 55 mg Chl a m^{-2} on the western transect, and were generally higher (50 to 70 mg Chl a m^{-2}) on the central transect (Fig. 73). Gross column production was moderate and relatively constant, typically about 700 mg C m^{-2} d^{-1}. Almost all the production occurred in the mixed layer (Fig. 73). Estimates of net column production were quite low, reflecting the relatively deep distribution of chlorophyll, and low α. On the western transect, values ranged from 200 to 350 mg C m^{-2} d^{-1}, except for the offshore station, where lower biomass and higher α combine to give a larger ratio of net to gross production. On the central transect, net production was very low, approaching zero at the shelf break, and ca 150 mg C m^{-2} d^{-1} over the slope.
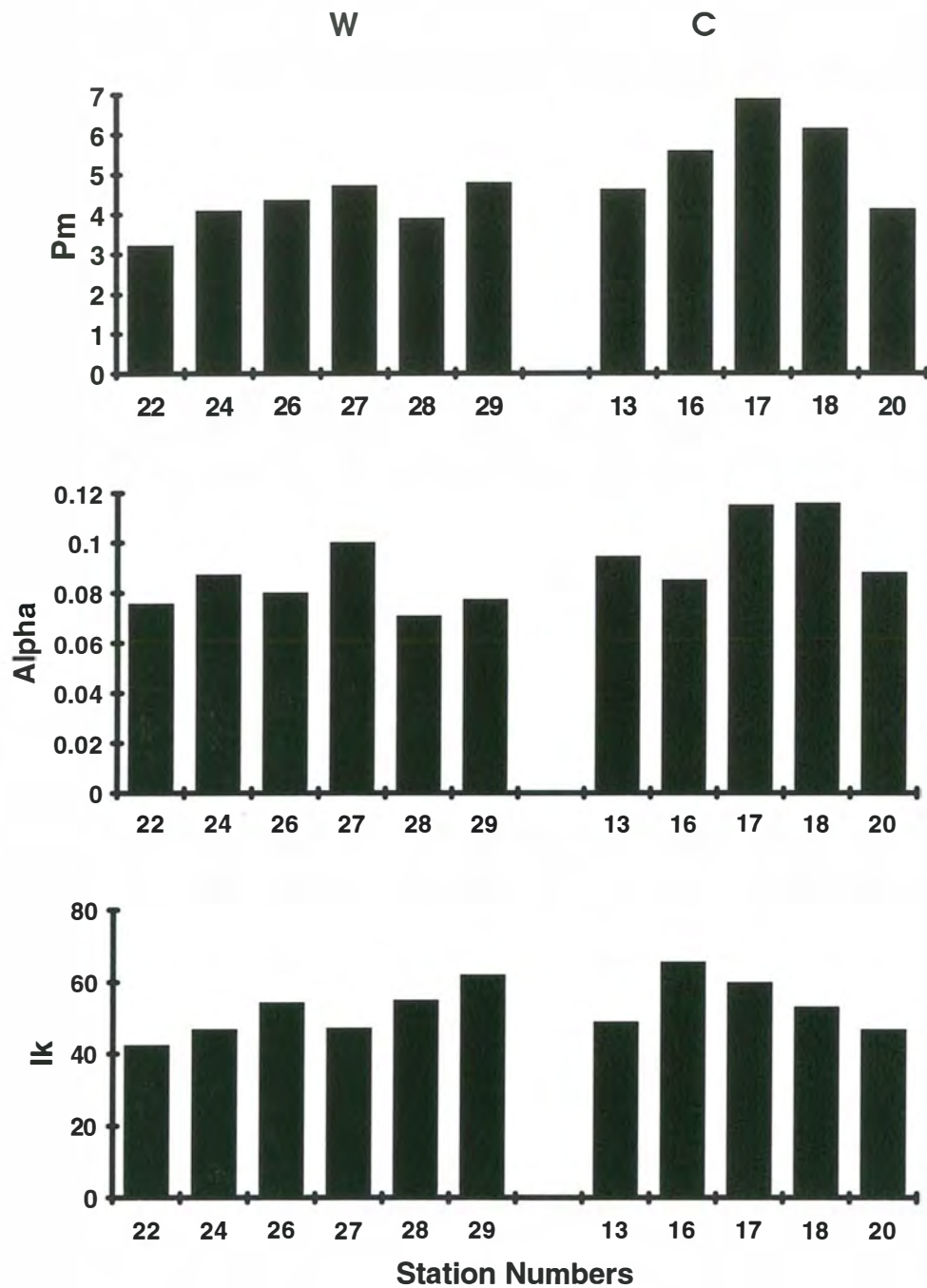
Fig. 70. Photosynthetic parameters P_m (mg C (mg Chl a) $^{-1}$ h^{-1}), α (mg C (mg Chl a)$^{-1}$ h^{-1} (μmol m^{-2} s-1)$^{-1}$), I_k (μmol m^{-2} s^{-1}) vs station number by transect on cruise SS1/92.
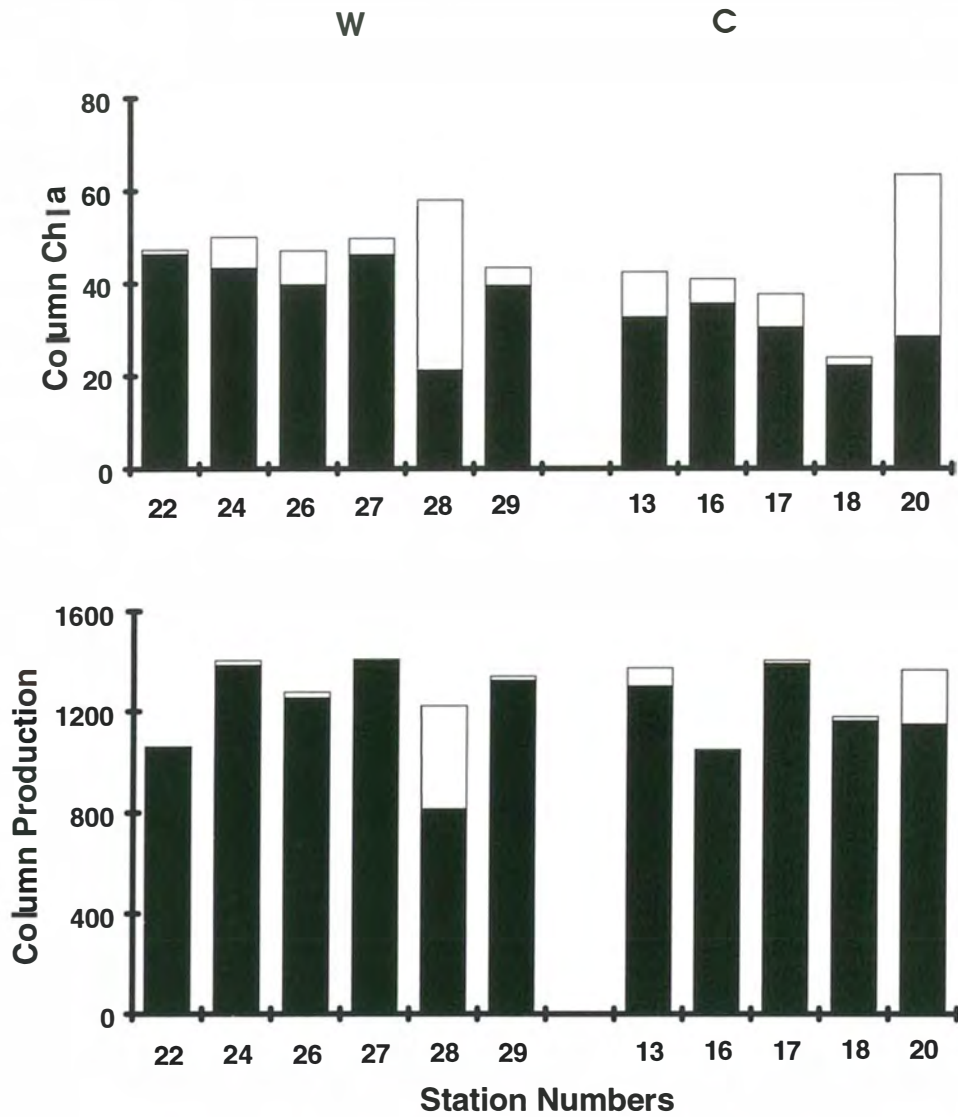
Fig. 71. Column biomass (mg Chl a m^{-2}) and column production (mg C m^{-2} d^{-1}) in the mixed layer (solid bar) and from 0 to 100 m (total bar) by station and transect on SS1/92.
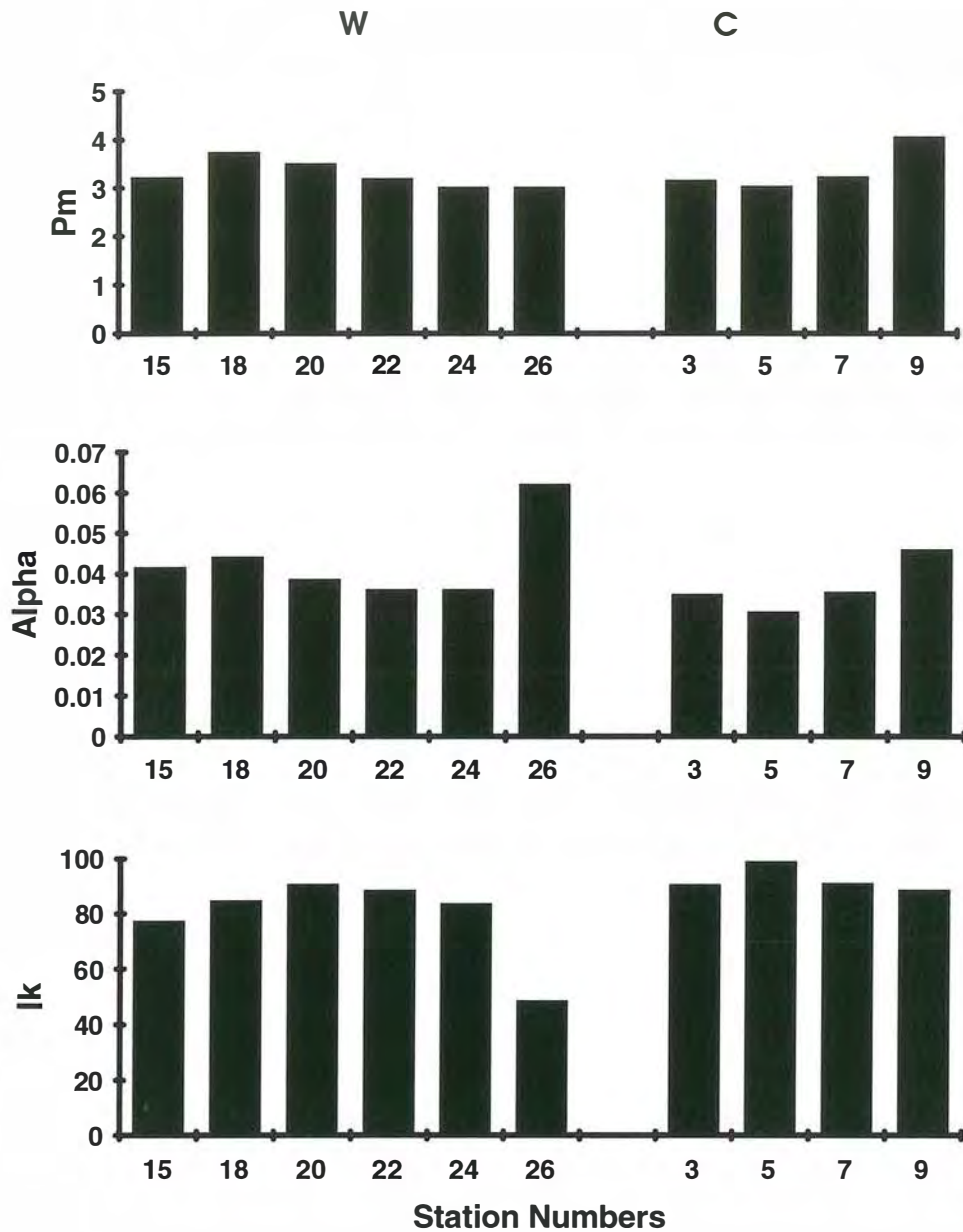
Fig. 72. Photosynthetic parameters P_m (mg C (mg Chl a)$^{-1}$ h^{-1}), α (mg C (mg Chl a)$^{-1}$ h^{-1} (μmol m^{-2} s-1)$^{-1}$), I_k (μmol m^{-2} s^{-1}) vs station number by transect on cruise SS3/93.
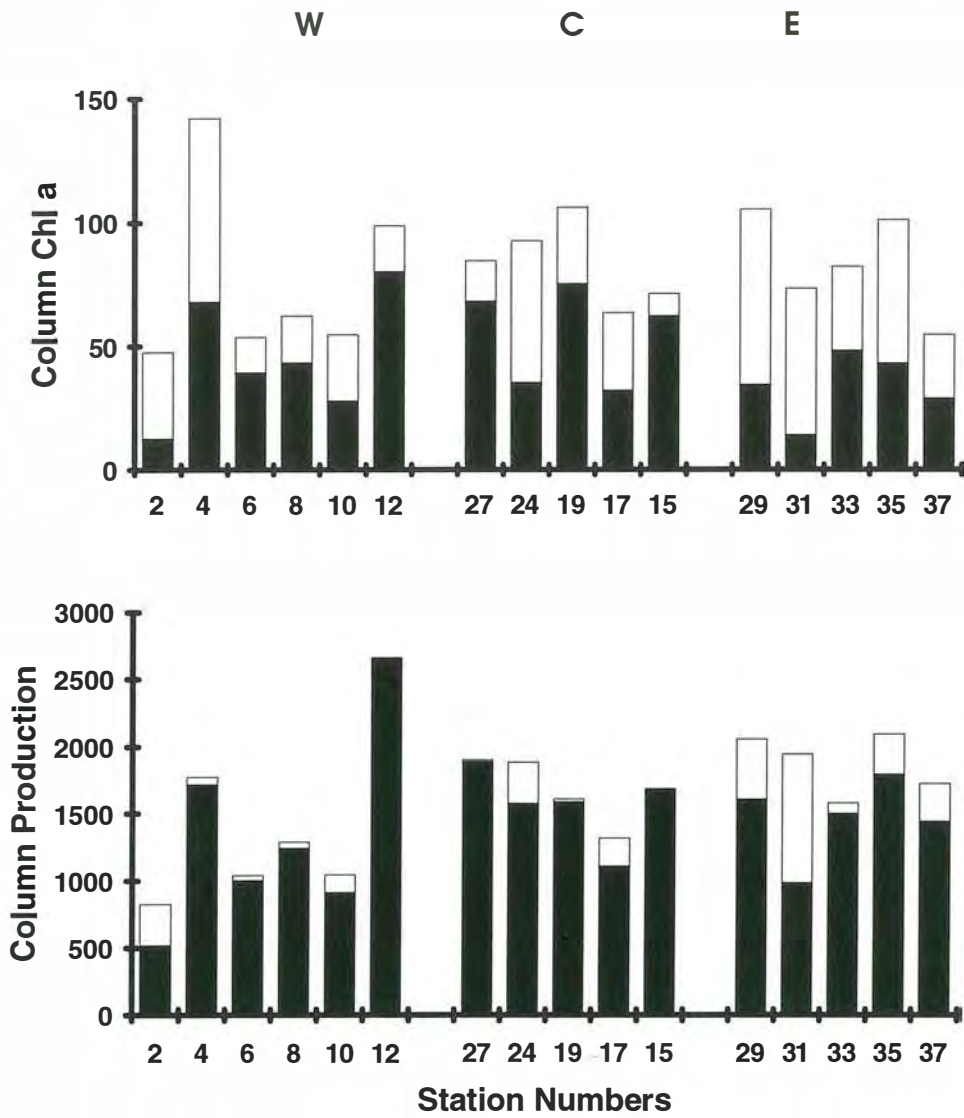
120
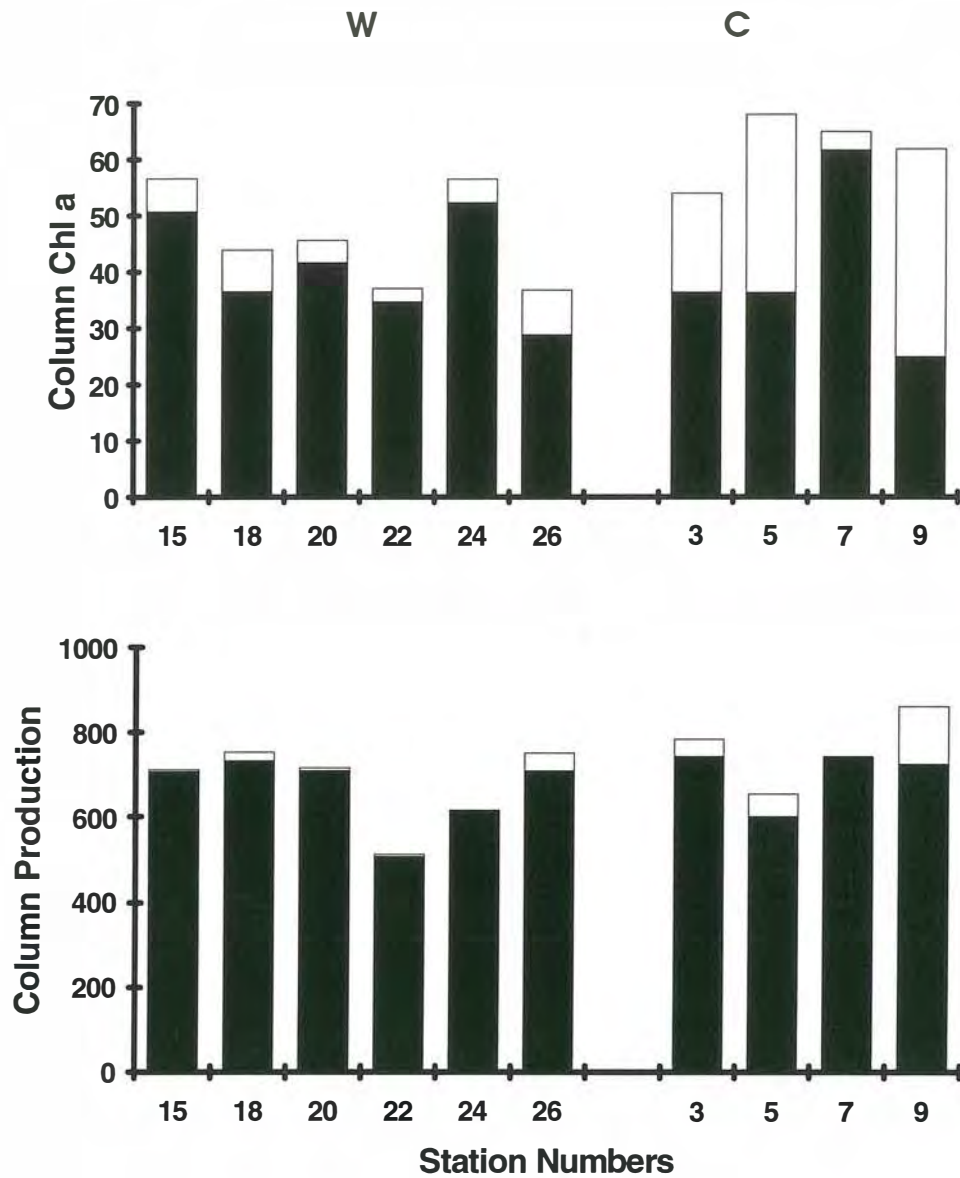
Fig. 73. Column biomass (mg Chl a m^{-2}) and column production (mg C m^{-2} d^{-1}) in the mixed layer (solid bar) and from 0 to 100 m (total bar) by station and transect on SS3/93.

NITRATE TURNOVER TIMES IN THE EUPHOTIC ZONE AND MIXED LAYER.

Turnover times for nitrate in the mixed layer and the euphotic zone (taken as 0 - 100 m) were calculated for all productivity stations, based on the estimated column production, and an assumed C:N Redfield ratio of 106:16 by atoms (Redfield, 1934). These turnover times were calculated assuming all production is based on nitrate; ie an f-number of 1. In practice, production is supported by both nitrate ("new" nitrogen) and ammonia ("regenerated" nitrogen), so that the real f-number, defined as the ratio of nitrate uptake to total N uptake, will be less than 1 (Eppley and Peterson, 1979), and the turnover times for nitrate correspondingly longer.

In July 1991, mixed layer depths varied significantly, with shallow mixed layers (10-20 m) on the western transect, and very deep mixed layers (up to 200 m) in Zeehan Current water on the shelf and upper slope. Turnover times for nitrate were generally 50 days or greater for the euphotic zone and for the mixed layer, except in the shallow mixed layers on the western transect, where turnover times were 10 to 20 days (Fig. 74A). These low turnover times reflect the fact that nitrate concentrations were not particularly high in the mixed layer in early winter (ca 2 μM), and production levels were still quite high in surface waters. Nitrate concentrations were still only ca 2 μM in the deep mixed layers of the Zeehan Current water mass on the central and eastern transects, but turnover times were long (ca 100 days) because of the mixed layer depth. At these nitrate levels, one would generally expect f-numbers to be high, perhaps around 0.5.

In February 1992, mixed layer depths were predominantly between 40 and 70 m, with two stations in the range 20 - 30 m. Turnover times for nitrate in the mixed layer were less than 10 days at all stations, and effectively zero at stations on the central transect where mixed layer nitrate was undetectable (Fig. 74B). One would expect ammonium to be the dominant nitrogen source for phytoplankton in these oligotrophic conditions, and f-numbers may be very low (ca 0.1) in those EAC waters where nitrate is undetectable. At stations on the western transect, where mixed layer nitrate concentrations were between 1 and 2 μM, one would expect f-numbers to be larger. Continued production at the levels observed on this cruise would then require resupply of nitrate to the mixed layer on time scales of 20 to 30 days. Turnover times for nitrate in the top 100 m were generally between 20 and 40 days, reflecting the elevated nitrate concentrations in the nitracline.
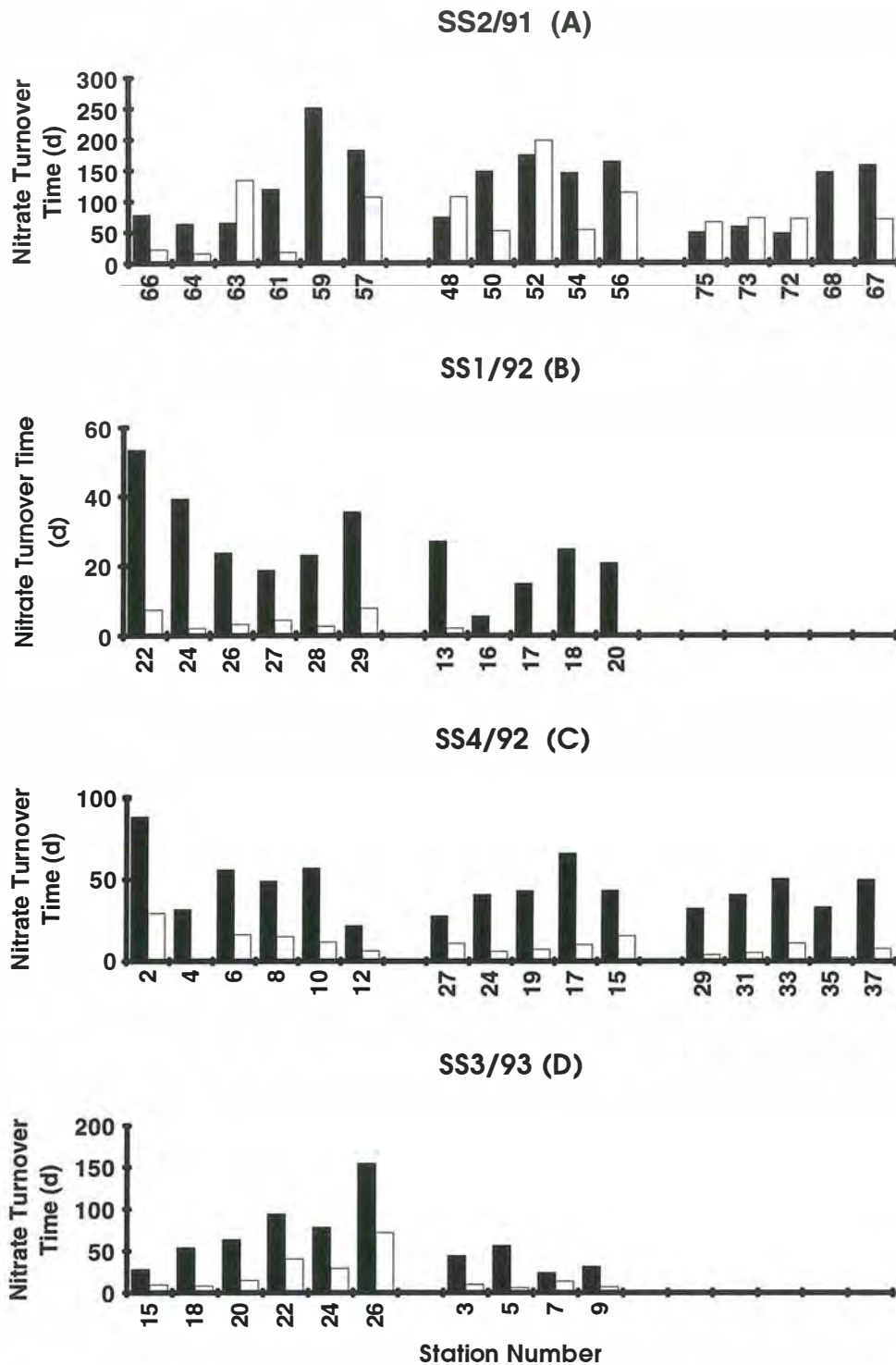
Fig. 74. Turnover times for nitrate in the mixed layer (open bars) and 0 - 100 m (closed bars), by cruise and transect, based on estimated daily carbon fixation rates, assuming Redfield C:N uptake ratio, and f-number of 1. Transects from left to right are western, central, and eastern where available.

In November 1992, mixed layer depths were generally shallow, between 20 and 40 m. Surface nitrate values were high at this time (ca 4 - 6 µM), but phytoplankton biomass and production were also very high, so that mixed layer turnover times were quite short, of the order of 5 to 15 days (Fig. 74C). In this situation (early spring bloom), one would expect nitrate to be the dominant nitrogen source, so that the time to nitrate depletion may be of similar order (ie 5 to 15 days). This sets a bound on the likely duration of the spring bloom, unless episodes of wind mixing and mixed layer deepening, followed by renewed stratification, resupply nitrate and extend the period of the bloom.

In April 1993, mixed layer depths were generally in the range 40 to 60 m, as autumn cooling and mixing began. Nitrate levels in surface water were low (1 - 3 µM), except in the cold intrusion at the offshore end of the western transect. Turnover times in the mixed layer were generally short (< 20 days), except at the offshore end of the western transect (Fig. 74D). One would expect f-numbers to be moderate in these conditions, but the turnover times are unlikely to be relevant, since cooling and mixed layer deepening continue through April and May.

Over all four cruises, nitrate concentrations in surface waters were generally greater than 1 µM, except in the EAC water in summer. One would expect a relatively high contribution of new (nitrate-based) production to total production under these circumstances. If a high f-number is assumed, calculated turnover times for nitrate in the mixed layer are generally low, of order 5 to 30 days, except in deep winter mixed layers. This suggests that nitrate is being resupplied to the mixed layer on time scales of weeks, either by vertical mixing, or by horizontal or vertical advection associated with boundary currents and mesoscale circulation.

ESTIMATES OF ANNUAL, REGIONAL PRODUCTION.

Estimates of daily primary production at each station were extrapolated to seasonal estimates using the observed PvsI parameters and biomass profiles, seasonal changes in theoretical clear sky irradiance, and monthly cloud factors calculated from Bishop's data (Bishop and Rossow, 1991). It was assumed that the spring and autumn observations applied to fairly narrow transitional regimes: these were extrapolated to the months of October, November, December, and March, April, May respectively. Winter and summer observations were extrapolated to the months of May - October, and December - March respectively. There is a choice in the overlap months of October, December, March and May. Two estimates of annual production were calculated. In the first, it was assumed that the spring and autumn conditions applied only to the months of measurement (November and April). In the second, it was assumed that the spring and autumn conditions applied for a period of three months each.

To allow results from different cruises to be combined, stations were grouped into shelf (< 300 m), slope (300 - 1500 m), and deep (1500 - 2500 m). Results are presented only for the western and central transects, as the eastern transect was not sampled in summer or autumn. Estimates of both gross and net production were calculated.

TABLE 7. ESTIMATES OF ANNUAL GROSS AND NET PRIMARY PRODUCTION (g C m^{-2}), CALCULATED ASSUMING SPRING AND AUTUMN CONDITIONS APPLIED FOR PERIODS OF 1 MONTH (1) OR 3 MONTHS (2).

	WESTERN TRANSECT			CENTRAL TRANSECT		
	SHELF	SLOPE	DEEP	SHELF	SLOPE	DEEP
GROSS PRODN 1	283	317	307	335	316	345
GROSS PRODN 2	312	308	300	379	350	369
NET PRODN 1	153	185	169	192	165	189
NET PRODN 2	123	174	164	183	156	187

Overall, estimates of annual gross production were relatively consistent between and within transects. Estimates were slightly lower on the western transect (ca 310 g C m^{-2}) than on the central transect (ca 330 g C m^{-2}), and showed no consistent onshore - offshore trend. Extending the spring and autumn observations over three months increased annual gross production by about 10 % on the central transect, but had little effect over the slope and deep water on the western transect. Extending the spring and autumn observations decreased estimates of net production in all regions, and decreased net production relative to gross production from ca 55% to ca 45% on the central transect and western shelf.

As might be expected, winter production contributed little to the annual total. The months October through April accounted for 79 to 83% of annual gross production, and 79 to 89% of annual net production.

SEASONAL CHANGES IN COLUMN NITRATE.

Seasonal nitrate depletion occurs primarily in the top 100 m, although deep winter mixing may extend this signal to 200 m or more. Nutrient sampling was such that reasonably reliable estimates can be given for the top 100 m for almost all stations, but not for the 100 to 200 m interval in a large number of cases. This discussion therefore focuses on changes in the top 100 m.

Western transect

Central transect
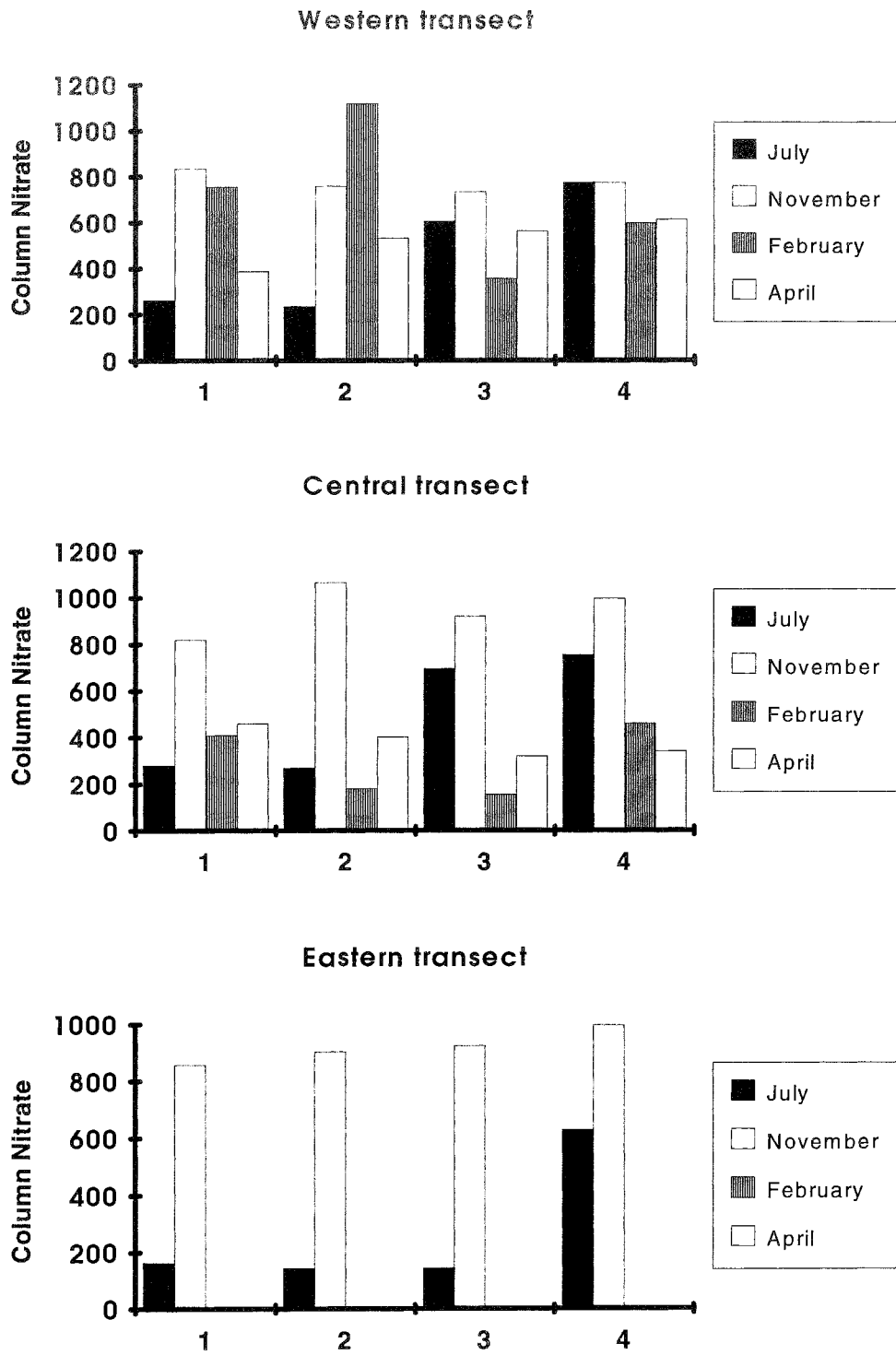
Eastern transect

Fig. 75. Column nitrate from 0 to 100 m (mmol m^{-2}) by season in 4 bathymetric depth ranges: (1) 0 - 300 m, (2) 300 - 1000 m, (3) 1000 - 2000 m, (4) 2000 - 3000 m.

126

On the western transect, on the shelf and upper slope, maximum column nitrate occurred in spring and summer (ca 800 - 1100 mmol m^{-2}), and minimum (ca 200 mmol m^{-2}) in winter (Fig. 75). This was due to the influence of low-nitrate Zeehan water in July, 1991, and the strong subsurface upwelling of high nitrate water onto the slope and upper shelf in February 1992. Offshore, the seasonal range was much smaller (ca 400 to 700 mmol m^{-2}), and the maximum occurred in winter and spring.

Throughout the central transect, the maximum column nitrate (800 to 1100 mmol m^{-2}) occurred in spring (Fig. 75). On the shelf, the minimum (250 mmol m^{-2}) occurred in winter (Zeehan influence), but over the slope, the minimum (150 mmol m^{-2}) occurred in summer (EAC influence). Offshore, the minimum (300 mmol m^{-2}) occurred in autumn, but this was close to summer levels.

The eastern transect was sampled only twice, in winter and spring (Fig. 75). Winter values were very low (150 mmol m^{-2}) over the shelf and slope, due to Zeehan Current water. Spring values were uniformly very high throughout the transect (800 - 1000 mmol m^{-2}).

The seasonal range in column nitrate (maximum - minimum) over the shelf and slope varied between 500 and 900 mmol m^{-2}, except at offshore stations on the western transect, where the range was reduced to less than 200 mmol m^{-2}. In a simple 1-D seasonal model of nitrogen cycling, one would assume that nitrate is depleted seasonally by local phytoplankton uptake, and then resupplied by vertical mixing in winter. The seasonal change in column nitrate would then provide a minimum estimate of new production and export of organic matter (minimum, because additional nitrate could be resupplied by mixing during the spring and summer). At Redfield ratios, changes in column nitrate of 500 to 900 mmol m^{-2} are equivalent to 3.3 to 6.0 mol C m^{-2}, or 40 to 70 g C m^{-2}. Comparison with Table 7 suggests that estimates of new production based on seasonal changes in column nitrate could account for 25 to 40% of net primary production.

Unfortunately, it is clear from the oceanographic data that we cannot safely interpret changes in column nitrate on the basis of a 1-D seasonal model. The data show seasonal intrusions into the study area of nitrate-depleted subtropical water associated with the Leeuwin, and with the EAC, as well as nitrate-enriched SubAntarctic water. At least part of the observed seasonal decreases in column nitrate may be due to horizontal advection, rather than *in-situ* production. On the other hand, calculations based on the seasonal cycle do not allow for additional new production supported by injection of nitrate into the surface layer in summer through vertical mixing and mesoscale upwelling.

SEDIMENT TRAP RESULTS.

The moored sediment trap collected a sequence of 21 sediment flux samples, each corresponding to ca 1 week, over the period from 9 November, 1992 to 10 April, 1993. According to the primary production model, most of the annual primary production occurs in this period. Samples were divided into < 1 mm and > 1 mm fractions before analysis. We present results for the < 1 mm fraction first.

A striking feature of the sediment trap results is the seasonal variation within the trap period, with high fluxes in November and early December, low fluxes in late December and January, and high fluxes again in February and early March. The total particle flux varies from a peak of ca 60 mg dry wt m^{-2} d^{-1} in early December and February - March, to a minimum of ca 15 mg dry wt m^{-2} d^{-1} in late January (Fig. 76A). Carbonate typically constitutes about 70% of the flux by weight, while the contribution of organic matter is only 10 - 20% (Fig. 77). The organic carbon flux ranges from ca 0.2 to 0.8 mmol C m^{-2} d^{-1}, and this is quite comparable to the carbonate carbon flux (ca 0.2 to 0.9 mmol C m^{-2} d^{-1}) (Fig. 76B,C).

Fluxes of nitrogen and phosphorus showed a somewhat similar seasonal pattern to carbon flux (Fig. 78A,B), although variation sample to sample was larger, particularly for phosphorus, where this might be explained partly by larger standard errors for replicate analyses. The seasonal pattern for silicate (biogenic opal) flux (Fig. 78C) showed an interesting contrast to that for carbon and nitrate. Fluxes were high and covaried with organic carbon in the spring (November, early December), dropped to very low levels in the early summer, but recovered only slightly in the February and March period, when organic matter flux increased to spring levels. This is entirely consistent with a classical seasonal succession in temperate phytoplankton communities, in which the spring community is dominated by diatoms, and the summer community by flagellates which do not contain silica.

The C:N ratios in organic matter showed no systematic seasonal variation (Fig. 79A), apart from one high value (associated with large standard errors) in March. Values generally exceeded the Redfield ratio of 6.6, and were typically around 20. N:P ratios showed considerable variation, but were also generally higher than the Redfield ratio of 16:1, with a majority of values exceeding 40 (Fig. 79B). It is generally accepted that remineralization of P and probably N in sedimenting organic matter occurs more rapidly and therefore shallower than C, and it is therefore not unexpected to find high ratios of C:N and N:P in deep trap material. The N:Si ratios were low (ca 0.4) in the spring, but increased systematically to ca 1.5 in summer (Fig. 79C).
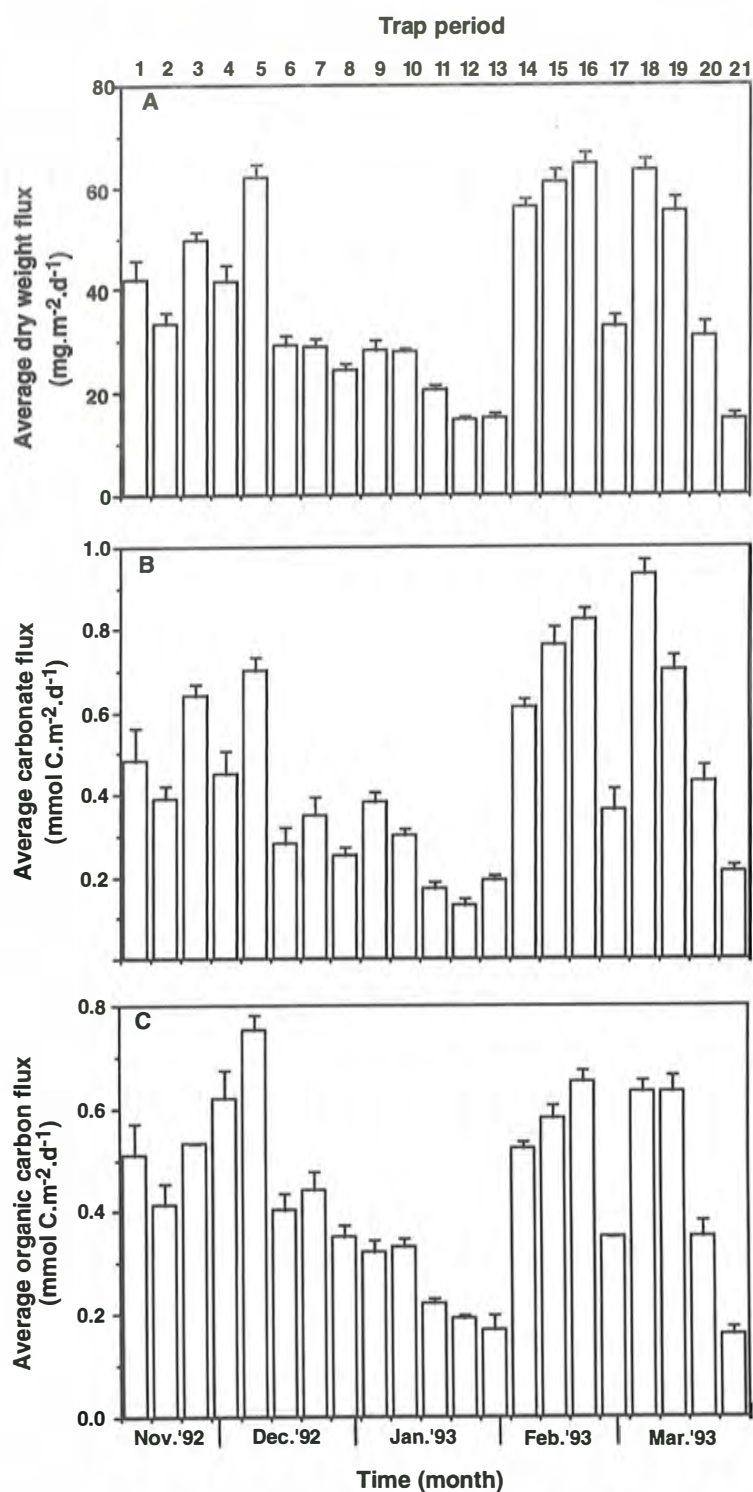
Fig. 76. Particulate fluxes (< 1 mm fraction) vs sample period / time for the moored sediment trap. (A) Dry weight; (B) carbonate carbon; (C) organic carbon.

Trap period
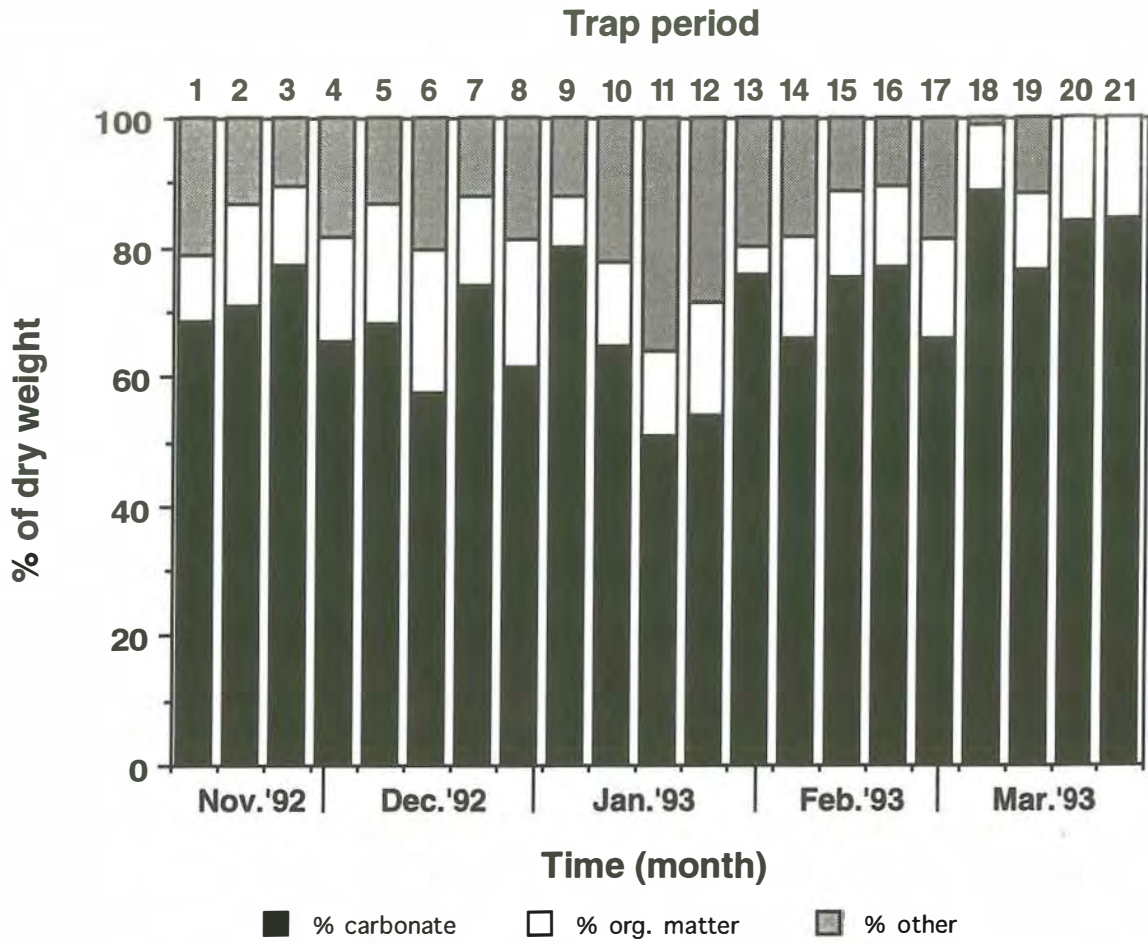
Fig. 77. Composition (% dry weight) of particulate flux (<1 mm fraction) vs sample number / time for the moored sediment trap.
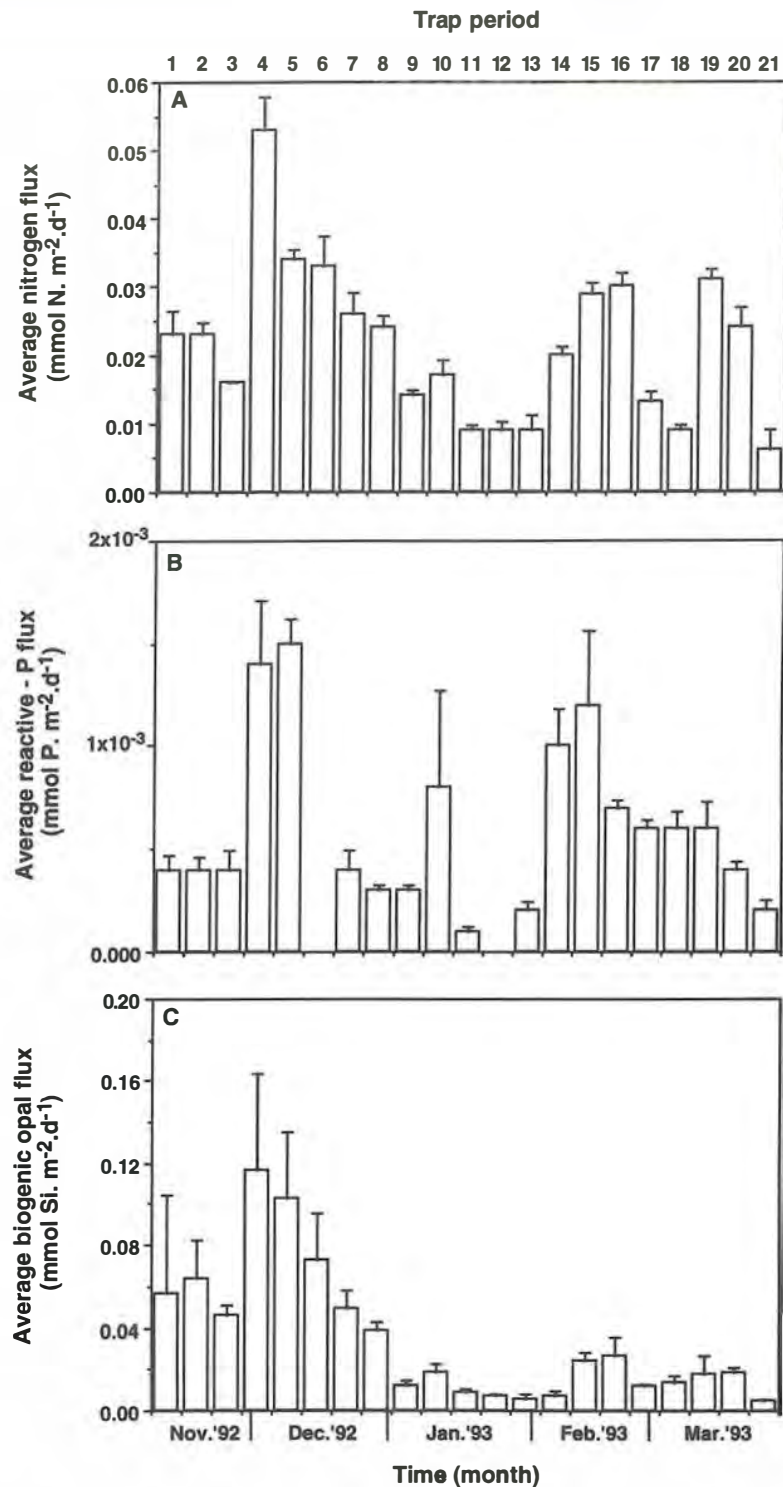
Fig. 78. Particulate fluxes (< 1 mm fraction) vs sample period / time for the moored sediment trap. (A) Organic nitrogen; (B) reactive phosphorus; (C) biogenic silica.
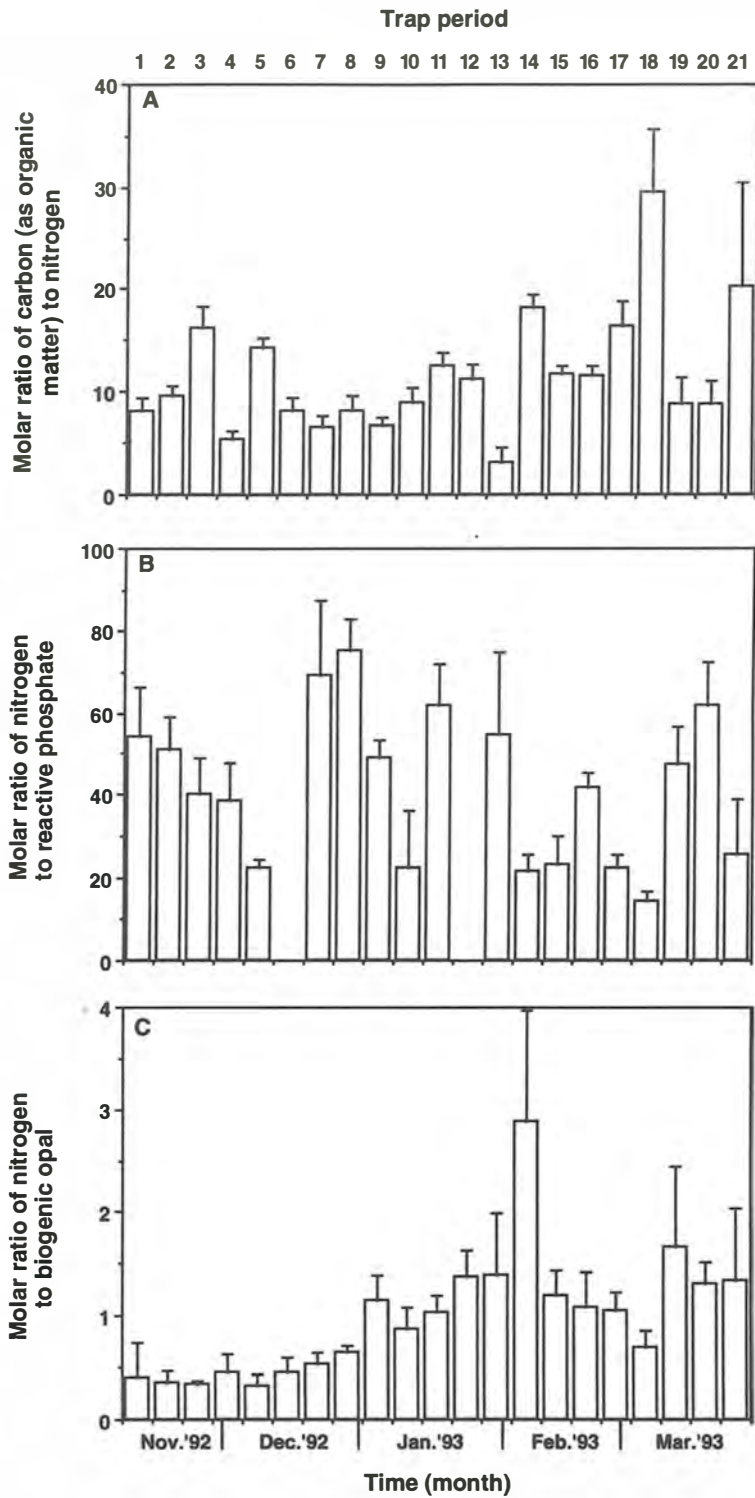
Fig. 79. Composition (molar ratios) of organic particulate flux (< 1 mm fraction) vs sample period / time for the moored sediment trap. (A) carbon:nitrogen; (B) nitrogen:phosphorus; (C) nitrogen:biogenic silica.

Trap period
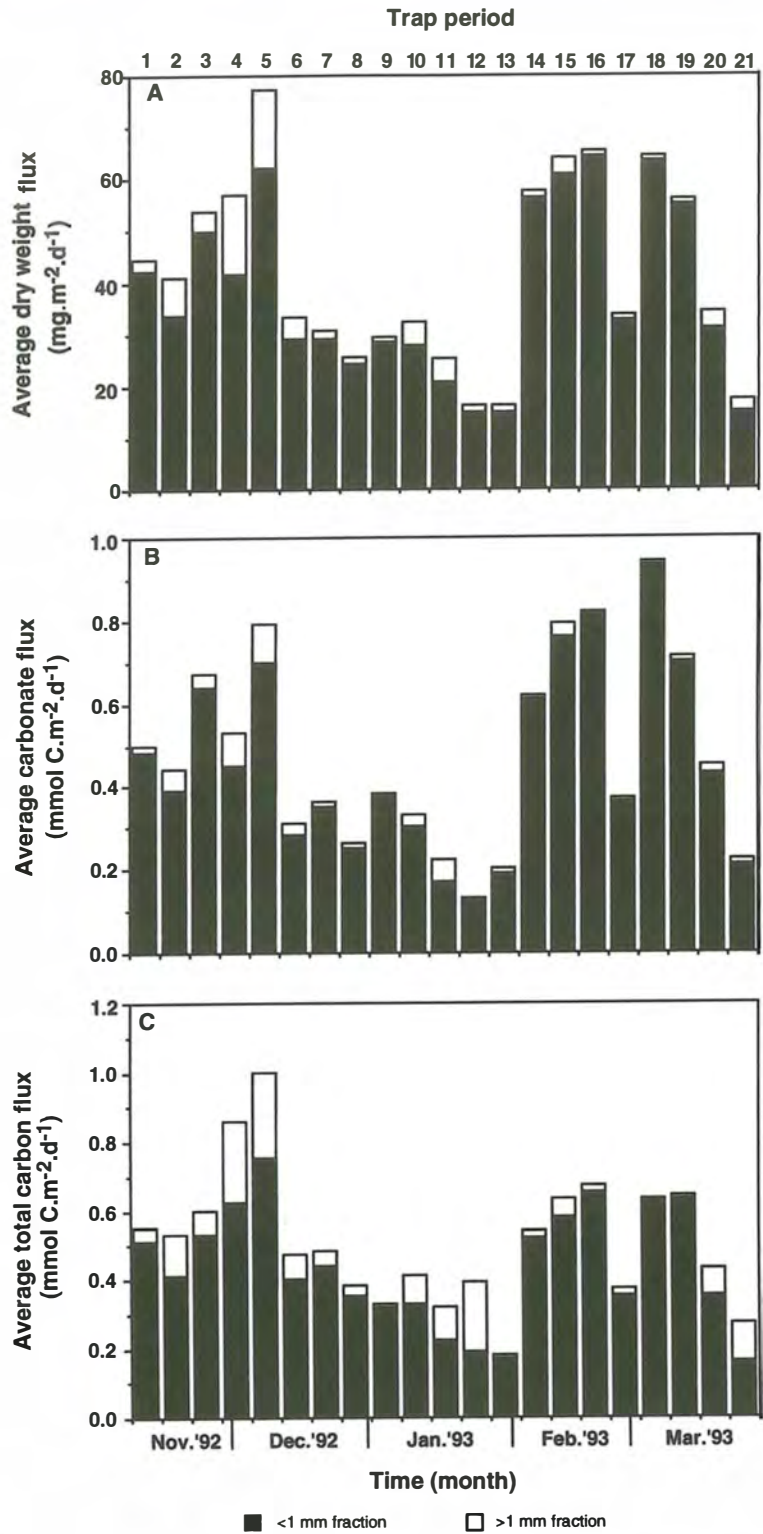
Fig. 80. Particulate fluxes (< 1 mm and > 1 mm fraction) vs sample period / time for the moored sediment trap. (A) Dry weight; (B) carbonate carbon; (C) organic carbon.

133
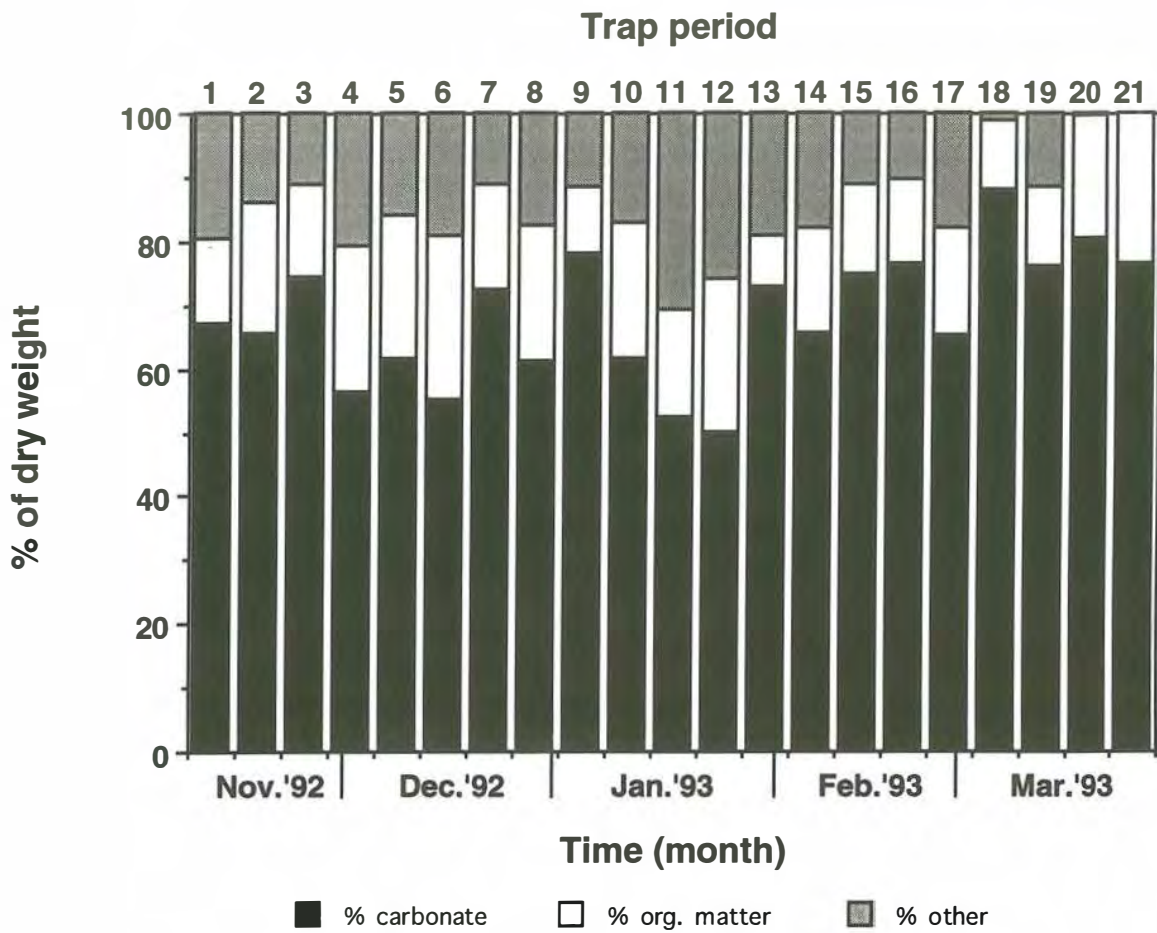
Fig. 81. Composition (% dry weight) of particulate flux (<1 mm fraction and > 1 mm fraction) vs sample number / time for the moored sediment trap.
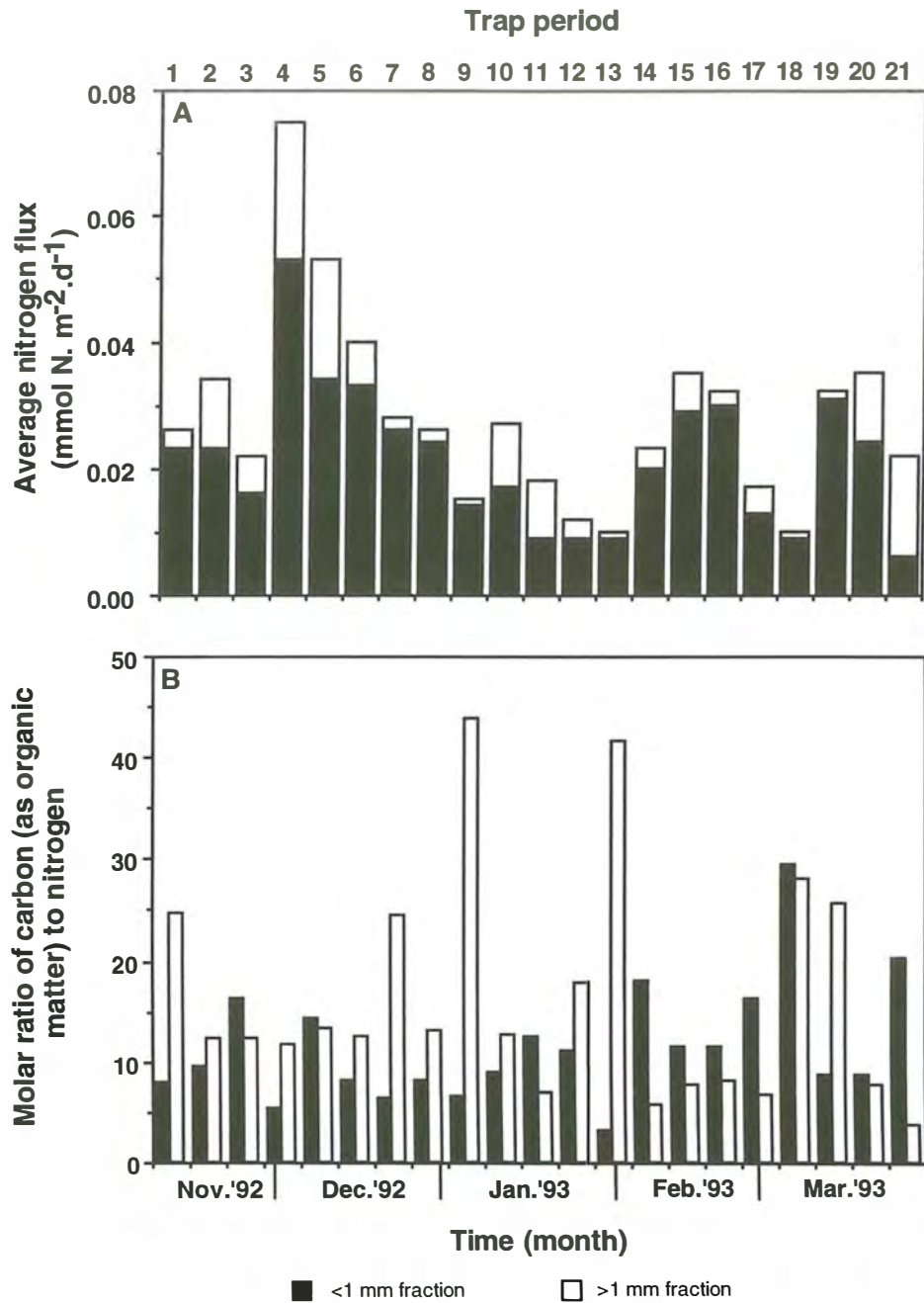
Fig. 82. Organic nitrogen flux (A) and molar ratio of organic carbon:nitrogen (B) (both < 1 mm and > 1 mm fractions) vs sample period / time for the moored sediment trap.

The > 1 mm fraction made a relatively small contribution to the total flux (as dry weight) throughout most of the deployment period (Fig. 80A), except in early December when it represented ca 20% of the total flux. The same comments apply to organic carbon fluxes: the > 1 mm fraction generally represented <10% of the total, except in early December and mid-January when it constituted 30 to 40% (Fig. 80B). The percent contribution of the > 1mm fraction to carbonate flux was much lower, peaking at ca 10% in early December (Fig. 80C). Including the > 1 mm fraction, the organic carbon flux peaked at ca 1.0 mmol C m^{-2} d^{-1} in early December. Combining the < 1 mm and > 1 mm fractions did not make a major difference to the relative composition as a % of dry weight, although the contribution of the organic matter generally increased slightly (Fig. 81). The nitrogen flux associated with the > 1 mm fraction covaried with the organic carbon flux (Fig. 82A, B). The C:N ratios in the > 1 mm fraction were significantly lower than in the < 1 mm fraction, and averaged ca 10 or less, apart from a few extreme values. C:N ratios in the > 1 mm fraction were also noticeably lower, and close to Redfield ratios, in February and March.

TABLE 8. TOTAL FLUXES, AND ELEMENTAL RATIOS OF TOTAL FLUXES, OVER THE DEPLOYMENT PERIOD OF THE MOORED SEDIMENT TRAP (9 NOVEMBER 1992 - 31 MARCH 1993).

FLUX PROPERTY	<1mm	>1mm	TOTAL
Dry Weight (mg m^{-2})	5374	527	5900
Carbonate (mmol C m^{-2})	64.5	3.5	68.0
Organic carbon (mmol C m^{-2})	61.9	10.6	72.5
Total nitrogen (mmol N m^{-2})	3.05	0.94	3.99
C:N in organic matter (by moles)	20.3	11.3	18.2
Reactive Phosphate (mmol P m^{-2})	0.078	N/A	N/A
Biogenic Opal (mmol Si m^{-2})	4.91	N/A	N/A
N:P (by moles)	38.8	N/A	N/A
N:Si (by moles)	0.62	N/A	N/A

For the slope region on the central transect, ca 75% of net annual production occurred during the November - March deployment period of the moored trap. One would expect the total fluxes recorded over the trap deployment period to represent 75% or more of annual sediment flux. (Other studies have shown that the proportion of primary production exported tends to increase with production rates.) The total organic carbon flux over the deployment period represented only 72 mmol C m^{-2}, or ca 0.85 g C m^{-2}. Approximately 85% of this occurred in the < 1 mm fraction. The C:N ratio in total organic matter was 18.2 (by moles) and significantly higher (20.3) in the < 1 mm fraction than in the > 1 mm fraction (11.3), suggesting that the <1 mm fraction may contain more refractory material (Table 8). The N:P ratio in the < 1 mm fraction was much

higher than Redfield (39 cf 16), suggesting that the small proportion of material which is refractory enough to reach 950 m has very little P compared with N. The N:Si ratio in the < 1 mm fraction was 0.62, but this is less meaningful, as it represents an average of high Si material in the spring and early summer, and low Si material in late summer.

Free-floating sediment traps were deployed on the November, 1992 and April 1993 cruises, at either end of the moored trap deployment period, and the results are given in Table 9. The fluxes measured in the shallow free-floating traps are significantly larger than those measured in the deep moored trap at the beginning and end of the deployment period. Dry weight fluxes at 200 m in November and April were respectively 15 and 10 times those measured in the first and last samples of the moored trap. The corresponding ratios for carbonate fluxes were ca 10 in November, and 5 in April. However, organic C, N and P fluxes from the free-floating traps at 200 m were 1-2 orders of magnitude higher than those from the first moored trap sample in November. Ratios of organic C : carbonate were much higher in free-floating traps, while C:N ratios were lower.

In an open ocean environment, one would expect particle fluxes to be higher, and composition to be indicative of fresher organic material, at 200 m than at 950 m. However, one would also expect the fluxes in the deep free-floating traps at 650 m to be lower than fluxes at 200 m. Instead, fluxes of organic C, N and P measured by free-floating traps at 200 m and 650 m were almost identical (Table 9).

We have attempted to correct for one potential source of error in free-floating trap data. During trap deployment and recovery, some of the saline solution in the trap is replaced by seawater. Experiments suggest that ca 2/3 of the trap contents or 3 l may be replaced in this way. As the entire trap contents were filtered, any particulate matter in this seawater would have been counted as sediment. In the worst case, one could assume that all this replacement water had the high particulate content characteristic of surface waters. On the April cruise, particulate samples were collected in the mixed layer at the deployment site, and particulate C and N measured. Based on these measurements we have calculated a maximum possible contamination by C and N from surface water: the correction (Table 9) reduces organic C by ca 25% and N by 30 - 50%. In November, 1992, the particulate carbon and nitrogen was estimated by applying the C:Chl a and N:Chl a values from April (72 mg C (mg Chl a)[-1] and 25 mg N (mg Chl a)[-1] respectively) to the measured values of Chl a in November. (The April ratios should if anything represent an overestimate when applied to the spring bloom conditions in November.) The resulting corrections again reduced organic C by ca 30% and N by ca 50%. It is noteworthy that the organic C, N

and P fluxes in November were ca 4 to 8 times higher than those in April, and mixed layer chlorophyll was 4 times higher in November.

Correcting for possible surface water contamination does not change the conclusion that fluxes measured by the free-floating traps at 650 m were similar in magnitude to those measured at 200 m. This is inconsistent with a 1-dimensional picture of particle dynamics in an open ocean, as organic matter is formed in surface waters, and grazing and microbial action should remove organic carbon and nitrogen as matter sinks. However, fluxes need not necessarily decrease with depth in a complex 3-D shelf-slope system. In a major study of carbon exchange on the east coast of the USA (SEEP-II, Niscaye *et al*, 1994), the vertical pattern of particle flux was dominated by horizontal transport, both cross-slope and long-slope. The carbon and other biogenic particle fluxes measured by sediment traps moored at the 1000 m contour actually increased with depth by ca 3 times from 130 m to 400 m, and 2 times from 400 m to 990 m (Biscaye and Anderson, 1994). The trap at 990 m was only 10 m above the bottom, and fluxes there could have been affected by resuspension, but the flux at 400 m should not have been affected by resuspension.

TABLE 9. FLUXES FROM FREE-FLOATING SEDIMENT TRAPS DEPLOYED IN NOVEMBER 1992, AND APRIL 1993. * FOR DETAILS OF CORRECTION, SEE TEXT.

DEPLOYMENT	NOV 92	NOV 92	APRIL 93	APRIL 93
Depth	200 m	650 m	200 m	650 m
Dry weight (mg m^{-2} d^{-1})	639	626	190	252
CO$_3$:organic matter:other (by weight)	41:45:14	45:43:12	30:47:23	40:50:10
Organic C (mmol C m^{-2} d^{-1})	20.4	19.3	3.33	3.58
Carbonate (mmol C m^{-2} d^{-1})	4.8	5.2	0.97	2.25
Corrected* organic C (mmol C m^{-2} d^{-1})	14.6	13.5	2.48	2.73
Total N (mmol N m^{-2} d^{-1})	3.7	2.9	0.51	0.66
Corrected* total N (mmol N m^{-2} d^{-1})	2.0	1.2	0.26	0.41
Reactive P (mmol P m^{-2} d^{-1})	0.06	0.05	0.008	0.007
Organic C:N (by moles)	7.3	6.7	6.5	5.4
Corrected* C:N (by moles)	7.3	11.3	9.5	6.7
N:P by moles	61.7	58	63.8	65.4

The similarity of fluxes at 200 m and 650 m south of Tasmania suggests that a 1-D model is not appropriate, and that horozontal transport of particulate material either cross-slope or long-slope is important. We do not have sufficient sediment trap data to shed more light on this process. In fact, we are still faced with a major anomaly in comparing the free-floating traps with the deep

moored traps, as the latter measured organic carbon fluxes ca 10 to 25 times smaller than those collected by the free-floating trap at 650 m. Our moored trap was located ca 100 m above the bottom, and was less likely to be affected by resuspension than the SEEP-II traps. However, we must still explain an extremely high loss rate of organic matter flux between 650 m and 950 m. It is possible that the trap fluxes are really dominated by horizontal transport, in which case we must propose a circulation which carries high concentrations of slowly sinking material past the 650 m layer, with relatively little of this material reaching the 950 m level. Alternatively, we must propose a very high particle removal efficiency by the grazing and microbial community between 650 and 950 m. The final possibility is that the collection efficiencies of the moored and free-floating traps are widely different.

PRIMARY PRODUCTION, SEDIMENT FLUX AND EXPORT EFFICIENCY.

The unusual vertical patterns within the sediment trap data set cast some uncertainty over attempts to relate carbon flux at depth to primary production in the overlying water. If we accept the 200 m free-floating trap data, we have corrected carbon flux estimates of 14.6 mmol C m^{-2} d^{-1} and 2.5 mmol C m^{-2} d^{-1} in November and April respectively. Based on data from the PvsI stations conducted during the trap deployment, daily gross primary production at the deployment site was 224 mmol C m^{-2} d^{-1} in November, and 83 mmol C m^{-2} d^{-1} in April. The corresponding estimates of daily net primary production were 118 mmol C m^{-2} d^{-1} in November and 35 mmol C m^{-2} d^{-1} in April. Thus, in November, the flux of carbon through 200 m represented 6.5 % of gross primary production, and 12.3 % of net primary production. The corresponding values for April were 3.0% and 7.1 %.

If sediment fluxes had been measured at the base of the mixed layer or euphotic zone, one could interpret these percentages as export ratios or f-numbers. As f-numbers, the figures of 12 % and 7.1 % are very low, given that nitrate is elevated in surface layers. Unless a considerable fraction of the organic flux is remineralised between 100 and 200 m, we are forced to conclude that the export efficiency from the euphotic zone is low, and that most of the primary production is based on regenerated nitrogen. The VERTEX experiments in the oligotrophic eastern Pacific yielded a relationship between organic carbon flux POC, primary production PP and depth z of the form (Pace et al, 1987):

$$POC = 3.523 \ z^{-0.734} \ PP \ .$$

This gives a ratio of organic carbon flux to primary production of 12% at 100 m and 7.2% at 200 m, agreeing quite closely with the results obtained here. Again, it is surprising that results obtained on the Tasmanian slope in a high nutrient

environment should correspond so closely to results from an oligotrophic gyre. In another analysis of VERTEX sediment fluxes as a function of depth by station, Martin *et al* (1987) presented organic carbon fluxes at 200 m corresponding to 1.9 to 11.5% of primary production, with most values above 5%. The exponents fitted for decrease in flux with depth corresponded at most stations to a decrease in flux between 100 and 200 m by a factor of 1.7 to 2.0.

Given these low export efficiencies, the observed nitrogen fluxes at 200 m give much lower turnover times for nitrogen in surface waters than those calculated earlier based on primary production and high f-numbers. For November 1992, the corrected N flux at 200 m of 2.0 mmol N m^{-2} d^{-1}, and the column total nitrate above 200 m of 1730 mmol m^{-2}, yield a turnover time of 865 days. If we apply the depth-flux relationships from VERTEX, the N flux at 100 m is probably ca twice that at 200 m. This implies a turnover time for the top 100m, with 780 mmol N m^{-2}, of 195 days. In April, the corresponding figures at 200 m are 0.26 mmol N m^{-2} d^{-1} and 1430 mmol N m^{-2}, giving a turnover time of 5500 days. The column total of 440 mmol N m^{-2} above 100 m, with the VERTEX depth correction, yields a turnover time of 850 days. These low fluxes and long turnover times suggest again that N cycling within the top 100 to 200 m is very efficient, and that there is no need to postulate high vertical fluxes of nitrate across 200 m to support primary production.

It should be noted that the sediment traps measure carbon and nitrogen export as sinking organic detritus only. There may be significant seasonal export as dissolved organic carbon. It is also possible that diel vertical migration by zooplankton provides an additional export mechanism which bypasses the sediment traps.

The free-floating traps at 650 m recorded fluxes almost exactly equal to those measured at 200 m. Based on the VERTEX results, one would expect the 650 m fluxes to be ca 2 to 3 times smaller. As noted above, observations on the continental slope of the eastern USA showed higher sediment fluxes at intermediate depths than at shallow depths, and this was attributed to horizontal export of particulate material off the shelf at intermediate depths. We cannot rule out a phenomenon of this kind. However, any mechanism which explains high relative fluxes at 650 m must then be reconciled with the extremely low fluxes observed in the moored trap at 950 m.

If horizontal transport does make a significant contribution to particle flux at 650 m, this raises the question as to whether a simple vertical picture of carbon flux provides an appropriate basis for a trophodynamic model. It is conceivable that primary production on the shelf makes a significant contribution to secondary production on the slope. We are not in a position on the basis of this study to quantitatively evaluate primary production on the whole shelf (we only sampled the outer shelf), or its contribution to the slope. However, we note that

the SEEP-II study found that export efficiency from the shelf was quite low: only about 5% of the carbon produced on the shelf was exported (Biscaye *et al*, 1994). We found that primary production per unit area on the outer shelf was generally comparable to that over the slope (Table 7). The shelf off Southern Tasmania is ca 50 km wide, comparable to the slope. Taken together, these observations suggest that the surface production over the slope is more important in a vertically integrated sense. However, this does not rule out the possibility that production on the shelf is more efficiently transferred to depth over the slope by downslope currents. The role of other vertical and horizontal transfer mechanisms will be dealt with in the following section.

The organic carbon flux estimates from the moored trap in the first and last samples were ca 0.6 and 0.3 mmol C m^{-2} d^{-1} respectively. Based on the VERTEX results, one would expect these to be ca 3 to 5 times lower than fluxes at 200 m. In fact, they are ca 25 and 8 times smaller respectively. They are equivalent to only 0.5% and 0.9% respectively of estimated net primary production during the November and April cruises near the mooring site. The total organic carbon flux over the deployment period of ca 72 mmol C m^{-2} represented only .65% of the estimated net primary production over the slope on the central transect during this period.

The carbonate fluxes measured in the moored trap at 950 m were roughly equal to organic carbon fluxes (as moles carbon). The carbonate fluxes at 200 m were about 1/4 the organic carbon fluxes. If we assumed carbonate was preserved between 200 and 950 m, this would imply that organic carbon had been reduced by ca 4 times, which would be consistent with reductions over this depth observed in other locations. However, the carbonate fluxes at 200 m were 10 times those at 950 m in November, and 4 times in April. The carbonate : organic carbon ratio at 200 m is consistent with a commonly accepted value of 20%. The free-floating flux estimates could be overestimated as a result of surface water contamination, but only by a factor of 2 or less. This suggests that carbonate is still apparently disappearing between 200 and 950 m. If carbonate is in fact preserved over this depth range, it suggests a difference in collection efficiency between free-floating traps and the moored trap.

To sum up, the sediment trap results leave us with a number of surprising and in some cases inconsistent results. The fluxes measured by free-floating traps at 200 m are consistent in terms of export efficiency with results measured by the VERTEX experiment in the oligotrophic northeast Pacific, but suprisingly low given the high nutrient, biomass and primary production on the Tasmanian slope, especially in the spring bloom period. Relative to those at 200 m, the fluxes measured by the free-floating traps at 650 m are anomalously large, showing little or no systematic decrease from 200 m to 650 m. Taken at face value, these suggest a strong contribution of horizontal particle transport across or along the slope. However, the fluxes measured by the moored sediment trap

at 950 m are very low, being smaller in proportion to the 200 m fluxes than fluxes at comparable depths in the oligotrophic ocean. The carbonate data suggest that the moored trap may be less efficient at collecting material than the free-floating traps.

TROPHODYNAMIC MODELS

A VERTICALLY-INTEGRATED VIEW OF THE PELAGIC COMMUNITY.

We consider first a vertically integrated view of the trophic structure over the slope, without regard to the mechanisms of vertical transfer. The primary production estimates developed in the preceding sections are ca 300 to 350 g C m^{-2} y^{-1}(gross), or 160 g C m^{-2} y^{-1} (net). The net estimate is almost certainly low, as it is based on an assumed respiration rate of 10% P_m, and this is too high in light-limited populations. A figure of ca 200 g C m^{-2} y^{-1} would be a reasonable best estimate of net primary production.

Annual average estimates of mesozooplankton biomass (Terauds, Appendix 1) are ca 1 g C m^{-2}, with minimum values of ca 0.5 g C m^{-2} in winter. For these large zooplankton, estimates of consumption have generally fallen into the range of 10 to 20% of body weight per day, or ca 40 to 80 times biomass per year. The resulting estimates of phytoplankton consumption by mesozooplankton are ca 40 to 80 g C m^{-2} y^{-1}. This represents quite a significant proportion of estimated net primary production, given that microzooplankton are now generally believed to consume the major share of phytoplankton production in most marine systems, and that mesozooplankton often feed on microzooplankton as well as phytoplankton. Estimates of gross growth efficiency for large crustacean zooplankton are generally about 25%; combined with the consumption rates, this implies annual production : biomass ratios of about 10 to 20 (Parsons and Takahasi, 1973). This in turn leads to estimates of annual production by mesozooplankton of 10 to 20 g C m^{-2} y^{-1}.

The mesozooplankton discussed by Terauds are predominantly crustaceans, and do not include the large gelatinous zooplankton (salps and pyrosomes). These were sampled by the mid-water trawl, and are discussed briefly by Williams (Appendix 2). Based on his wet weight estimates, and literature values for carbon content, the typical biomass appears to be ca 0.1 g C m^{-2}. This is a rather uncertain figure, and there is generally much less information available on consumption and growth efficiency for these organisms. If we assume the same values as for other mesozooplankton, then their contribution is relatively small: ca 4 to 8 g C m^{-2} y^{-1} consumption, and ca 1 to 2 g C m^{-2} y^{-1} production. However, there is a considerable possibility that both sampling methods and trophic assumptions underestimate their role. Gelatinous zooplankton may also be important because they filter fine particulates, and can feed at the lowest

trophic level, but are large enough to figure in the diets of top predators (Bulman, Appendix 4).

Estimates of micronekton biomass and composition (predominantly fish, but including small squid and large crustaceans) are given by Williams (Appendix 2). The mean annual biomass based on trawl estimates is ca 0.1 g C m^{-2}. However, Koslow et al (1995) have reviewed these estimates, based on intercomparison of acoustic data and trawl data, and concluded that the trawl efficiency is low, of order 4 - 14 %, depending on the approach taken to the acoustic data. After correcting for trawl efficiency, estimates of mean annual biomass are increased to ca 1 to 2.5 g C m^{-2}. We assume a P/B ratio of 0.25, based upon Banse and Mosher's (1980) relationship for fish: P/B = 0.38 M$^{-0.26}$, where M is body size in g wet weight, and assuming a mean body size between 3 and 10 g. This implies annual production of micronekton of ca 0.25 to 0.6 g C m^{-2} y^{-1}. If we assume a gross growth efficiency for micronekton of 15%, annual consumption by micronekton should be ca 1.5 to 4 g C m^{-2} y^{-1}. The myctophids, gonostomatids, and sternoptychids that dominated the midwater community are predominantly planktivores, and presumably feed primarily at the third trophic level. Their estimated consumption represents from ca 10 to 50 % of estimated annual production by mesozooplankton. Some mesozooplankton production is presumably consumed by large pelagics. It is also be true that some micronekton are feeding at higher trophic levels (Williams and Terauds, Appendix 3), and that the effective consumption of zooplankton is therefore larger.

These results are summarised in Table 10.

TABLE 10. SUMMARY OF ESTIMATES OF BIOMASS, ANNUAL CONSUMPTION AND PRODUCTION FOR PRINCIPAL TROPHIC COMPONENTS INVOLVED IN LINKS TO DEMERSAL FISHES.

TROPHIC COMPONENT	TROPHIC LEVEL	BIOMASS g C m^{-2}	CONSUMPTION g C m^{-2} y^{-1}	PRODUCTION g C m^{-2} y^{-1}
Phytoplankton	1	1.2 - 5	300	200
Mesozooplankton	2/3	0.5-1.5	40-80	10-20
Salps, pyrosomes	2/3	0.1	4-8	1-2
Micronekton	3/4	1-2.5	1.5 - 4	0.25-0.6

VERTICAL TRANSFER PROCESSES.

The figures discussed so far refer to the whole water column, and ignore the issue of the vertical separation of primary production in surface waters from mesopelagic and demersal consumption, and the processes involved in vertical transfer. The study has provided information on a variety of transfer processes.

First, the sediment trap data taken at face value indicate a substantial annual flux of ca 15 g C m^{-2} y^{-1} out of the upper 200 m and through the 650 m layer. However, according to the deep moored trap, less than 10% of this reaches the sediment. This sedimenting particulate detritus through 650 m can be regarded as primary production from the point of view of the mesopelagic community, although its C:N ratio indicates that its nutritional quality is probably inferior to fresh surface material.

Second, the mesozooplankton data (Terauds, Appendix 1) indicate that the mesozooplankton community can be divided into two major components. A set of diel migrators predominantly occupies the top 500 m: these are unlikely to directly contribute to flux through 500 m. The seasonal migrators, especially Neocalanus tonsus, do contribute a direct flux of material through 500 m. Terauds' minimum estimate of this flux is 0.5 g C m^{-2} y^{-1}, based on the peak seasonal biomass observed below 500 m: however, if this downward migration occurs over a period of time, and the population below 500 m is subject to predation, the true flux may be considerably higher, perhaps 1 g C m^{-2} y^{-1}.

Third, a large fraction of the micronekton community (ca 60%) undergoes large diel migrations, from below 500 m to above 500 m, and appears to feed on mesozooplankton in the top 300 m at night (Williams, Appendix 2). This diel migration can potentially result in transfer of a large fraction of micronekton production from the upper water column to depth. If we assume that 50% of the production of this migrating micronekton community is consumed below 500 m, this represents an effective annual transfer of ca 0.1 to 0.2 g C m^{-2} y^{-1} of micronekton production.

In comparing these fluxes, we have to remember that a flux of material at a lower trophic level must be discounted by a net trophic transfer efficiency in considering its contribution to demersal carnivores. If we assume a net transfer efficiency of 10% per trophic level, we can crudely intercompare the net effect of these different processes (Table 11). Interestingly, all three processes appear to contribute about the same amount of production at the tertiary level.

TABLE 11. VERTICAL FLUX THROUGH 500 m DUE TO DIFFERENT PROCESSES, AND ITS CONTRIBUTION TO PRODUCTION AT DIFFERENT TROPHIC LEVELS.

Process	Primary g C m^{-2} y^{-1}	Secondary g C m^{-2} y^{-1}	Tertiary g C m^{-2} y^{-1}
Particle flux	15	1.5	0.15
Seasonal migration of mesozooplankton		1.0	0.10
diel migration of micronekton			0.1-0.2

DEMERSAL CONSUMPTION AND PRODUCTION

The estimates of demersal fish biomass from the trawl site are quite low. The typical background biomass is about 0.05 g C m^{-2} (Bulman, Appendix 4). Based on an earlier study (Bulman and Koslow 1992) and further enzyme studies Bulman (pers. comm.), the annual consumption by this background level of demersal fish is ca 0.1 to 0.25 g C m^{-2} y^{-1}. This level of consumption is consistent with the estimates of micronekton production, and vertical transfer of tertiary production, given above.

However, it is well known that random demersal trawling greatly underestimates the biomass of demersal stocks, especially orange roughy, because of their highly aggregated nature. The virgin biomass of orange roughy in the stock(s) spawning off northeastern Tasmania and fished off southern Tasmania is estimated to be 200,000 t, based on the catch history and egg and acoustic biomass surveys (SE Fishery Stock Assessment, 1994). This estimate is 14-fold higher than the biomass estimate from swept-area trawl surveys conducted in 1988-89 (Koslow et al. 1994), presumably because orange roughy aggregate on pinnacles and other ground that was not covered in the trawl survey. This biomass estimate cannot be too far wrong: landings since 1989 of orange roughy have been 158,000 t.

The density of orange roughy and other demersal species from trawling carried out in the present study was reduced from that obtained in 1988-89 (1.06 cf 4.82 g m^{-2}), which may be due to effects of fishing or differences in sampling location between studies. Because trawling in the present study was not conducted on pinnacles, the density estimate in our trophodynamic calculations should be based on the virgin biomass of orange roughy spread over the available habitat between 700 and 1200 m in the southeastern fishery region (4000 km^2): 50 g m^{-2}, or 2.5 g C m^{-2}, assuming a 5% conversion from wet weight to carbon (Wiebe et al. 1975). Approximately 1200 km^2 of this area is off southern Tasmania, where the fish appear to reside primarily when feeding. The density in this region may have been as high as 125 g m^{-2} or 6.25 g C m^{-2}. Because the biomass of orange roughy appears to outweigh that of non-aggregated species, the trophodynamic model will assess the production requirements of this species alone.

The daily food requirements of orange roughy are approximately 1% of body weight, based on estimates from feeding rate in the field (Bulman and Koslow 1992) and from levels of metabolism approximated by concentrations of the metabolic enzyme LDH. The annual food requirement is therefore approximately 9-23 g C m^{-2} y^{-1}, depending upon the area over which the roughy are assumed to be distributed.

145

This consumption estimate exceeds by 1 to 2 orders of magnitude both the average areal estimates of local micronekton production on the slope (Table 10), and the estimates of vertical transfer at the appropriate trophic level (Table 11). Of course, the densities of orange roughy in feeding aggregations on pinnacles are many orders of magnitude higher again. It is obvious that local production over pinnacles cannot support feeding aggregations, and that they are effectively harvesting food organisms out of the mesopelagic layer as it is advected past. The significance of the findings in this study is that the source area from which this advected mesopelagic community is drawn must be much larger than the area of the slope, again by 1 to 2 orders of magnitude.

It is possible in principle for there to be a micronekton community concentrated over the slope, and dependent on transport of zooplankton or particulate matter from offshore. However, the fact that the pelagic community appears to be in approximate balance with local primary production, and that the trophic break occurs between micronekton and orange roughy, suggests strongly that this does not occur, and that mesopelagic prey are advected over the slope as part of a roughly balanced pelagic community. Given the complexity of the circulation over the slope, it is not clear exactly what the larger source area ultimately supporting roughy is, or whether the surface production processes observed in this study apply there. Orange roughy feed on prey in Antarctic Intermediate Water from 700 m to 1200 m. However, given the extensive diel migrations undertaken by micronekton, and the time taken for AntarcticIntermediate Water to reach the slope, it would certainly be wrong to suggest a link to Antarctic Intermediate source waters. It is worth recalling that the Tasmanian slope occurs within the relatively productive SubTropical Convergence Zone. In this study, the annual primary production estimates for the offshore zone (deeper than 2000 m) were comparable to those for the slope and shelf (Table 7), and may be representative of production values over a much wider area.

REFERENCES

Airey, D. and G. Sanders (1987) Automated analysis of nutrients in seawater. *CSIRO (Australia) Marine Laboratories Report No. 166*

Banse, K. and Mosher, S. 1980. Adult body mass and annual production/biomass relationships of field populations. Ecological Monographs, 50: 355-379.

Biscaye, P.E., C.N. Flagg and P.G. Falkowski (1994). The Shelf Edge Exchange Processes experiment. SEEP-II: an introduction to hypotheses, results and conclusions. *Deep-Sea Research,* **41**, 231-252.

Biscaye, P.E. and R.F. Anderson (1994). Fluxes of particulate matter on the slope of the southern Middle Atlantic Bight: SEEP-II. *Deep-Sea Research*, **41**, 459-510.

Bishop, J.K. and W.B. Rossow. (1991) Spatial and temporal variability of global surface solar irradiance. *Journal of Geophysical Research*, **99** (C9), 16839-16858.

Blaber, S.J.M. and Bulman C.M. (1987). Diets of fishes of the upper continental slope of eastern Tasmania: content, calorific values, dietary overlap and trophic relationships. *Marine Biology,* **95**, 345-356.

Bulman, C.M. and S.J.M. Blaber (1986) Feeding ecology of Macruronus novaezelandie (Hector) (Teleostei: Merlucciidae) in south-eastern Australia. *Australian Journal Marine Freshwater Research*, **37**, 621-639.

Bulman and Koslow (1992). Diet and food consumption of a deep-sea fish, orange roughy *Hoplostethus atlanticus* (Pisces: Trachichthyidae), off southeastern Australia. *Marine Ecology Progress Series,* **82**, 115-129.

Bulman et al. 1995 Orange roughy surveys in SE Australia. *CSIRO Marine Laboratories Report.* (in press).

Chavez, F. P. (1989). Size distribution in the central and eastern tropical Pacific. *Global Biogeochemical Cycles* **3**, 27-35.

Chavez, F.P. and R. T. Barber (1987) An estimate of new production in the equatorial Pacific. *Deep-Sea Research* **34**, 1229-1243.

Clementson L.A., G.P. Harris, F.B. Griffiths and D.W. Rimmer (1989) Seasonal and interannual variability in chemical and biological observations in Storm Bay, Tasmania. I: physics, chemistry and the biomass and abundance of components of the food chain. *Australian Journal of Marine and Freshwater Research*, **40**, 25-38.

Cullen J.J., M.R. Lewis, C.O. Davis, and R.T. Barber (1992) Photosynthetic characteristics and estimated growth rates indicate grazing is the proximate control of primary production in the Equatorial Pacific. *Journal of Geophysical Research* **97**, C1, 639-654.

Eppley, R.W. and B.J. Peterson (1979) Particulate organic matter flux and planktonic new production in the deep ocean. *Nature*, **282**, 677-680.

Gunn, J.S., B.D. Bruce, D.M. Furlani, R.E. Thresher and S.J.M. Blaber (1989). Timing and location of spawning of Blue Grenadier, Macruronus novaezelandie (Teleostei: Merlucciidae) in Australian coastal waters. *Australian Journal of Marine and Freshwater Research,* **40**, 97-112.

Harris G.P., G.G. Ganf and D.P. Thomas (1987) Productivity growth rates and cell size distributions of phytoplankton in the SW Tasman Sea: implications for carbon metabolism in the photic zone. *Journal of Plankton Research*, **9**, 1003-1030.

Harris, G.P., P. Davies, M. Nunez and G. Meyers (1988). Interannual variability in climate and fisheries in Tasmania. *Nature*, **333**, 754-757.

Harris G.P., F.B. Griffiths and D.P. Thomas (1989) Light and dark uptake and loss of ^{14}C: methodological problems with productivity measurements in oceanic waters. *Hydrobiologia*, **173**, 95-105.

Harris G.P., F.B. Griffiths, L.A. Clementson, V. Lyne and H. Van Der Doe (1991). Seasonal and interannual variability in physical processes, nutrient cycling and the structure of the food chain in Tasmanian shelf waters. *Journal of Plankton Research*, **13** (supplement), 109-131.

Harris, G.P., F.B. Griffiths and L.A. Clementson (1992). Climate and the fisheries off Tasmania - interactions of pphysics, food chains and fish. *South African Journal of Marine Science*, **12**, 585-597.

Harris, G.P., G.C. Feldman and F.B. Griffiths (1993) Global oceanic production and climate change. pp237-270 In: Barale, V. and P.M. Schlittenhardt (ed),

Ocean Colour: Theory and Applications in a Decade of CZCS Experience, Kluwer Academic, Dordrecht.

Honjo, S. (1980) Material fluxes and modes of sedimentation in the mesopelagic and bathypelagic zones. *Journal of Marine Research*, **38**, 53-97.

Honjo, S. and S.J. Manganini (1992) Biogenic particle fluxes at the 34°N 21°W and 48°N 21°W stations, 1989-1990: methods and analytical data compilation. *Woods Hole Oceanographic Institution Technical Report No.* **92-15**, 77 pp.

Jeffrey S.W. and G.F. Humphrey (1975) New spectrophotometric equations for determining chlorophylls a, b, c_1 and c_2 in higher plants, algae and natural phytoplankton. *Biochemie und Physiologie der Pflanzen*, **167**, S. 191-194.

Jorgenson, S.E. (1979*). Handbook of Environmental Data and Ecological Parameters.* International Society for Ecological Modelling, Copenhagen.

Kirk, J.T.O. (1983). *Light and Photosynthesis in aquatic ecosystems.* Cambridge University Press, Cambridge, 401 pp.

Knauer, G.A., J.H. Martin and K.W. Bruland (1979) Fluxes of particulate carbon, nitrogen and phosphorus in the upper water column of the northeast Pacific. *Deep - Sea Research*, **26**, 97-108.

Koslow, J.A., C.M. Bulman, and J.M. Lyle. 1994. The mid-slope demersal fish community off southeastern Australia. *Deep-Sea Research,* **41**, 113-141.

Koslow, J.A., R.J. Kloser and A. Williams (1995) Pelagic biomass and community structure over the mid-continental slope off southeastern Australia based upon acoustic and midwater trawl survey. (MS submitted to *Marine Ecology Progress Series*).

Lewis, M.R. and J.C. Smith (1983). A small volume, short-incubation time method for measurement of photosynthesis as a function of incident irradiance. *Marine Ecology Progress Series* **13**, 99-102.

Major G.A., G. Dal Pont, J. Kyle and B. Newell (1972) Laboratory techniques in marine chemistry. *CSIRO (Australia) Division of Fisheries and Oceanography Report No. 51*.

Martin, J.H., G.A. Knauer, D.M. Karl and W.W. Broenkow (1987) VERTEX: carbon cycling in the northeast Pacific. *Deep - Sea Research*, **34**, 267-285.

May, J.L. and S.J.M. Blaber (1989) Benthic and pelagic biomass of the upper continental slope off eastern Tasmania. *Marine Biology*, **101**, 11-25.

McCartney, M.S. (1977) SubAntarctic mode water. pp103-119 In: Angel, M.V. (Ed), *A Voyage of Discovery*, Pergamon Press, N.Y.

McCartney, M.S. (1982) The subtropical recirculation of mode waters. *Journal of Marine Research*, **40** (Suppl.), 427-464.

Pace, M.L., G.A. Knauer, D.M. Karl anfd J.H. Maretin. (1987) Primary production, new production and vertical flux in the eastern Pacific Ocean. *Nature*, **325**, 803-804.

Parsons, T.R. and M. Takahashi. 1973. Biological Oceanographic Processes. Pergamon Press, N.Y. 186 pp.

Platt T., C.L. Gallegos and W.G. Harrison (1980) Photoinhibition of photosynthesis on natural assemblages of marine phytoplankton. *Journal of Marine Research*, **38**, 687-701.

Redfield, A.C. (1934) On the proportions of organic derivations in sea water and their relation to the composition of plankton. pp 177-192 In: *James Johnstone Memorial Volume*, Liverpool University Press, Liverpool.

Riley G.A. (1956) Oceanography of Long Island Sound, 1952-54. II. Physical oceanography. *Bulletin of The Bingham Oceanographic Collection,* **15**, 15-46.

Wiebe, P.H. S. Boyd, and J.L. Cox. 1975. Relationships between zooplankton displacement volume, wet weight, dry weight, and carbon. *Fishery Bulletin,* **73,** 777-786.

Wright, S.W., S.W. Jeffrey, R.F.C. Mantoura, C.A. Llewellyn, T. Bjørnland, D. Repeta and N. Welschmeyer (1991) Improved HPLC method for the analysis of chlorophyll and carotenoids from marine phytoplankton. *Marine Ecology Progress Series*, **77**, 183-196.

Young, J.W. and S.J.M. Blaber (1986). Feeding ecology of three species of mid-water fishes associated with the continental slope of eastern Tasmania, Australia. *Marine Biology*, **93**, 147-156.

BENEFITS

This work should primarily benefit the South-east Trawl fishery. The work was originally identified in correspondence between FRDC and Division of Fisheries as strategic research, to provide a better understanding of the ecosystem underlying the fishery, and to support long-term sustainable development. The key outcomes were to be in the areas of trophodynamic links and stock-stock interactions, and impacts of climate variability on deep-water stocks.

A key scientific conclusion from the study is that the key deep-water stocks are unlikely to be supported by vertical flux of material from local surface production (either as sinking particulates or via vertical migration). Instead, they appear to depend primarily on advection of food organisms such as micronekton and zooplankton in mesopelagic layers past the pinnacles on which commercial stocks congregate. In an open system of this kind, one would expect trophodynamic stock-stock interactions to be less significant than would be the case in a closed system limited by the ecological transfer efficiency of local surface production. Competition among deep-water stocks for food could still occur in principle through sequential depletion of prey as they are advected through the slope system. In order to address this question, a follow-up study comparing slope communities with offshore communities is required.

Contrary to the popular conception of the deep ocean as invariant, there is mounting evidence of significant variability in the deep sea on time scales ranging from tidal/daily to seasonal and interannual. The evidence is derived from sources as various as reports from deepwater fishermen of short-term changes in currents and fish availability; photographic time series showing the rapid sedimentation to the ocean floor of spring blooms; and apparent decadal-scale variability in recruitment to deepwater fisheries, such as orange roughy. To begin to examine the causes of recruitment variation or changes in fish availability to deepwater fisheries, it is critical to understand the primary sources of production to these fisheries. The present study indicates that future investigations of variability in southeast Australian deepwater fisheries need to focus primarily upon the factors driving variability in currents and the availability and production of prey species at intermediate water depths, and upon broad or far-field changes in surface ocean production and climatology.

The study identified strong impacts of seasonal and interannual changes in ocean circulation upon the physical and chemical environment in surface waters. These in turn produced large variations in primary production in, and particulate carbon export from, surface waters. There was significant change in deep water physical properties extending down to 1000 m, associated both with seasonal / interannual forcing, and in at least one case with a mesoscale feature. Significant changes were observed in the mesopelagic community from cruise to

cruise, but it is difficult to attribute these to either seasonal or interannual forcing. However, if the deep-water stocks feed on advected prey as hypothesized, then one might well expect the abundance of prey and the behaviour and distribution of stocks to vary with circulation patterns and broad-scale changes in the mesopelagic community. At least some of the surface interannual variation observed took place over broad areas of the Sub-Tropical Convergence Zone, and could well result in broad-scale shifts in mesopelagic zooplankton and micronekton production and abundance.

INTELLECTUAL PROPERTY

There is no commercially significant intellectual property arising from the FRDC funded research.

FURTHER DEVELOPMENT

This research has led to a shift in paradigm concerning the trophodynamic basis of the deep-water trawl fishery which in turn suggests further lines of investigation. The key need is for combined physical - biological studies to establish better the nature of the physical coupling between the slope and offshore waters, and the magnitude and nature of the biological fluxes which it drives. A high-resolution physical model of the circulation over the slope region and its interaction with the large-scale flow patterns in the surrounding oceans may be a basic requirement: this could emerge from the Division of Oceanography Exclusive Economic Zone modelling program. Studies of the plankton and nekton communities in offshore waters both upstream and downstream of the slope are needed to complete the biological picture. This could be done at scales ranging from individual pinnacles to the Tasmanian slope as a whole. The acoustic techniques developed in this study and in SET biomass assessment projects could potentially provide the spatial and temporal resolution required. Moored acoustic and other instrumentation could provide time series data on both physical and biological variables with greatly improved temporal coverage and resolution, and serve to quantify fluxes and monitor seasonal and interannual change. The detailed oceanographic and biological data collected on this cruise provides an ideal basis for interpreting the data which would be collected in such a follow-up study.

STAFF

Cathy Bulman
Pru Bonham
Lesley Clementson
Gary Critchley
Gwen Fenton
Sandra Garland
Brian Griffiths
Rudi Kloser
Tony Koslow
Mark Lewis
Don McKenzie
John Parslow
Chris Rathbone
Aleks Teraud
Alan Williams

FINAL COST

Statement of Receipts and Expenditure follows.

OTHER CONTRIBUTIONS:

ARC grant to Fenton and Koslow:
1992-93: $43800
1993-94: $42000.

DISTRIBUTION LIST

Tasmanian Fishing Industry Council

Tasmanian Sea Fisheries

National Fishing Industry Council
Unit 1, 6 Phipps Pl, Deakin, Act 2600

National Fishing Industry Training Council
GPO Box 2851AA, Melbourne, Vic 3001.

CSIRO Division Fisheries Library
GPO Box 1538, Hobart, Tas 7001

APPENDIX 1.

ZOOPLANKTON ON THE MID-SLOPE: VERTICAL DISTRIBUTION AND THE TRANSFER OF ENERGY.

ALEKS TERAUDS, CSIRO DIVISION OF FISHERIES.

Zooplankton on the mid-slope : Vertical distribution and the transfer of energy.

Draft of contribution to Parslow FRDC report

Aleks Terauds, CSIRO Division of Fisheries

MATERIALS and METHODS

The vertical distribution of the major calanoid and euphausiid species inhabiting the mid-slope was determined in terms of abundance and biomass. In addition, the developmental stage of several calanoid species were identified and the adults were sexed. The occurrence of diurnal and seasonal migration was tested by the application of three-way ANOVA and community partitioning was further examined by multivariate methods.

The study site was located approximately 150 km off the south coast of Tasmania (Figure 1). This site was chosen as it is representative of the mid-slope environment that supports major fisheries in this region. The bottom depth throughout this area varied from approximately 900m to 1300m with several seamounts that rose to depths of 600 to 400 m. Areas where the bottom depth varied considerably, including seamounts were avoided during trawling.

Sampling was performed in February 1992 (Summer), November 1992 (Spring), April 1993 (Autumn) and August 1993 (Winter) and was restricted to day and night. All sampling was done using the CSIRO Fisheries Research Vessel *Southern Surveyor*. Sampling within one hour of dusk and dawn was avoided as this is the time of maximum vertical movement of migrating species (Longhurst, 1981). Two day replicates and two night replicates were obtained from all seasons except for Autumn. Due to inclement weather conditions, only a single daytime tow was accomplished during the autumn sampling. Replicate tows were usually carried out consecutively.

The EZ net was used for all sample collection. The EZ net is a multiple opening-closing net system (BIONESS-Bedford Institute Oceanography Net and Environmental Sensing System- see Sameoto, 1979 for construction details and schematic diagrams) which is capable of obtaining samples from discrete depth strata. Discrete 100 m samples were taken between the surface and 900 m during each tow

Figure 1
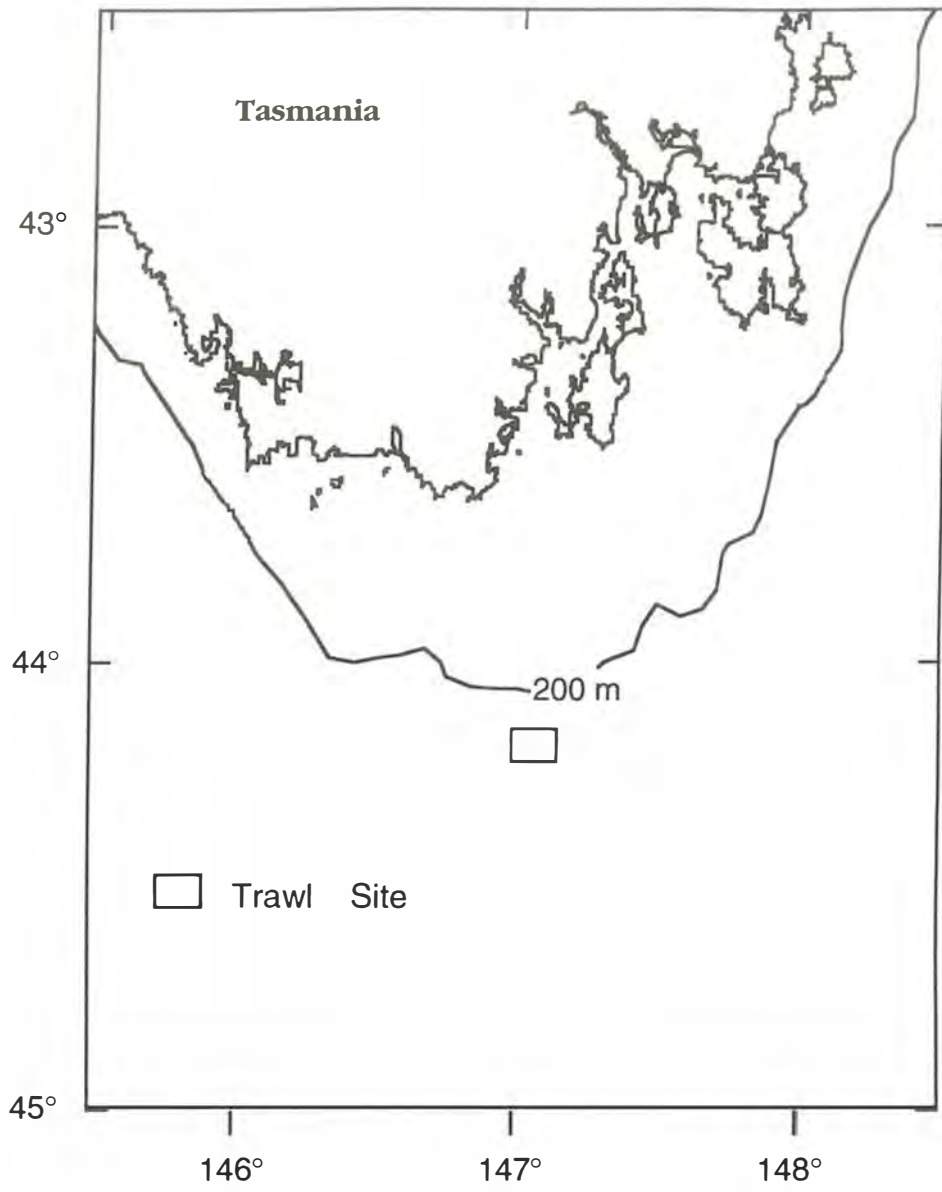
After the final 100 m depth stratum had been sampled, the net as brought onboard and each net was washed down into the hard cod-ends to ensure no specimens were left in the nets. The cod-ends were then removed and processed immediately. Shipboard processing involved splitting the sample with a Folsom Plankton Splitter (McEwan *et al.*, 1954). After splitting, one half of the sample was placed in pre-combusted foil and frozen at -20 °C. The other half of the split was preserved in a buffered 4% formalin-seawater solution. The time that each net sampled a single depth stratum varied and ranged from ten to thirty minutes. Biomass tends to be higher in shallower depths (Raymont, 1983; Vinogradov and Tseitlein, 1983; Rodriguez and Mullin, 1986) and thus sampling time was reduced in the upper 200 m relative to the deeper tows. The amount of time that each net fished a specific depth stratum was a tradeoff between minimising time spent in the water and obtaining a representative sample from that depth. It was desirable to decrease the total tow time as this reduced the time the nets remained in the water and damage to organisms already collected. The volume of water filtered through each net was calculated by the use of flowmeters on the EZ net.

Many samples were in poor condition at the time of processing. Sample condition appeared to decrease with increasing time spent in the water and thus samples from the deeper waters were often in considerably worse condition than those from the surface water tows of the same station. The speed at which the net was towed also seemed to have a significant bearing on the condition of the samples. The ideal tow speed for this net is approximately 3 knots (Sameoto *et al.*, 1980) and samples from tows executed at this speed were in better condition than those from higher speed tows. Unfortunately, in rough or windy weather, boat speed had to be increased to maintain steerage and consequently the condition of the collected samples often suffered.

Post sampling processing
Abundance

Each sample was sorted into two sub-samples, one containing zooplankton less than 5 mm and the other containing zooplankton greater than or equal to 5 mm. Sorting samples into size classes has been shown to increase the precision with which zooplankton in samples can be enumerated (Alden *et al.*, 1983).

All subsamples containing the small zooplankton (<5 mm) needed to be split further using the Folsom Plankton splitter. The displacement volume of splits

was also periodically checked to ensure variation between splits was not significant. The number of times a sample was split ranged from once in the smaller samples up to 10 times in the larger spring samples. The aim was to obtain a count of at least 75 for the most abundant species as this reduces the error inherent in enumeration of samples split with the Folsom Plankton Splitter (Alden *et al.*, 1983). After splitting the samples were sorted in filtered seawater and the major species were identified and counted. Many of the small size class samples were in poor condition and the majority contained many unidentifiable pieces of plankton. Only specimens that could be conclusively identified were counted. The sex and stage of some species were also ascertained.

After counting, the abundances were corrected for the splitting factor using the following equation :

$$N = n/(1/2^K) \qquad\qquad (1)$$

where K equals the number of splits (including shipboard split). Abundances were then converted to numbers per 1000m^3 using the volume filtered readings obtained from the EZ net.

Biomass
After the sample had been split into two size classes the displacement volume of each was determined (Ahlstrom and Thrailkill, 1963). This value was then standardised to ml per 1000 m^3 using volume filtered readings obtained from the EZ net.

To ascertain the biomass of each species at the different depths it was necessary to determine the dry weight of individual specimens. Only the biomass of the major calanoid and euphausiid species was examined. A number of authors have suggested that dry weight contains less variability than other measures of biomass used in the past such as wet weight or displacement volume (Ahlstrom and Thrailkill, 1963; Beers, 1976). Only specimens from the preserved samples could be used for dry weight determination as it was not possible to sort the frozen sample and obtain specimens in good condition.

Sample condition was important for selection of individuals for measurement of dry weight. Net damage to zooplankton was evident in many samples and although these species could be identified to species, their internal contents, legs and other appendages were often at least partially missing. Specimens that were in good condition were obtained from the preserved samples and dried at

60°C for 48 hours. They were then weighed individually on a Mettler ME30 microbalance that was accurate to ± 0.001 mg. Between 15 and 25 individuals of each stage or sex were weighed for most species. Some species were very rarely found in good condition and thus fewer replicates of these specimens were weighed. In some species, the early stages were consistently found in poor condition and the weights of these were estimated using length weight relationships.

Several authors have demonstrated that the preservation of zooplankton in buffered formalin-seawater solutions has a significant effect on the biomass of the preserved specimens (e.g. Omori, 1978; Omori and Ikeda, 1984; Williams and Robins, 1982; Bottger and Schnack, 1986). Therefore, in order to obtain a more realistic picture of the biomass of species at different depths in the present study, it was assumed that all copepods and euphausiids lost 35% and 21% of their body weight respectively and the observed weights were adjusted accordingly. These values are averages of losses that have been reported in the literature (see review by Bottger and Schnack, 1986). These corrected weights were then used in conjunction with the abundance data to calculate the biomass of each species at different depths. Subsequently, the contribution of seasonal migrators to the flux of carbon through the water column could also be calculated.

The abundance and biomass values (per 1000m^3) were transformed according to the following equation.:

$$X' = \log_{10}(X+1) \qquad (2)$$

enabling the variation in the smaller samples to be examined in conjunction with the larger samples. The +1 term was included so that zero values could still be used in the transformation.

Statistical Analyses

A three way ANOVA was used in an attempt to clarify the interactions and effects of depth, season and time on the distribution of biomass of the major species. The null hypothesis for each species can be represented by :

> H_O : The vertical distribution of biomass is consistent over a yearly cycle (factor=season), over a daily cycle (factor=time) and throughout the water column (factor=depth).

The effect of three way interaction between these three factors was tested as was the effect of the two-way interaction between each of the factors. The statistical evidence was interpreted in the following way : If the two way interaction between season and depth is observed to have a statistically significant effect then this can be interpreted as evidence of seasonal migration (if the biomass profiles are in agreement). Similarly, if the interaction of time and depth is observed to be significant then this may be interpreted as evidence in support of diurnal vertical migration. The statistical evidence provided by these two way interactions can only be considered useful if three criteria are met. Firstly there must be no significant three way interaction between the depth, season and time, secondly, the plot of studentised residuals should show no distinct trend and thirdly, the normal probability plot should show that the residuals are distributed normally

As biomass data were used to establish vertical distribution patterns it was also used in the multivariate analyses. The biomass data was examined using both the stations (i.e. season/depth) as variables and the species as variables. These two types of analyses were classified as "Q-mode analysis" and "r-mode" or "inverse" analysis by Field *et al.* (1982). The biomass data were transformed using the same transformation cited earlier. Field *et al.* (1982) suggested that this type of transformation was necessary to scale down the effect of abundant species so they do not swamp the other data, and recommended its use for biomass data. These authors also recommended the use of the Bray-Curtis Dissimilarity Measure (Bray and Curtis, 1957) in analysis of biomass data as it is a robust measure, is not affected by joint absences and gives more weight to abundant species when comparing samples than to rare ones. For these reasons the Bray-Curtis measure was adopted in the present study.

Hierarchical agglomerative cluster analysis was performed on the dissimilarity matrices, formed by applying the Bray-Curtis formula. The method used is termed UPGMA (unweighted pair-group method average) and forms clusters based on the unweighted arithmetic average linkage between groups (Legendre and Legendre, 1983). This method is thought to be the most conservative and rarely gives rise to spurious groupings or misclassification (Clifford and Stephenson, 1975). The analysis was performed on the entire data set, without differentiating between day and night samples.

RESULTS

Relative abundance and biomass by species

Figures 2-17 illustrate the abundance and biomass of the 14 major species of calanoid copepods and euphausiids relative to each other. These figures are useful to examine the dominant species in each depth stratum during different seasons.

Throughout the year calanoids of the *Pleuromamma* genus were numerically abundant in several depth strata but due to their small size were not large contributors to the biomass. Conversely, the three species of euphausiid accounted for a high proportion of the biomass in various depth strata although their numbers were relatively low. The calanoid *Neocalanus tonsus* was an important component of the deeper waters throughout the year, particularly in spring and winter. Other seasonal migrators including *Eucalanus hyalinus* and *Rhincalanus nasutus* were also present in large numbers in deeper waters at certain times of the year. *Calanus australis* was numerically dominant in surface waters during summer and was also present in high numbers in some lower strata. Due to the small size of this calanoid large numbers were necessary before it made a significant contribution to the biomass. The calanoid *Metridia lucens* was numerically abundant during spring and winter.

Gross Biomass Variation

The variation in displacement volume of both the small and the large size samples is illustrated by Figures 18-25. The values are plotted on a logarithmic scale, due to increasing standard deviation with mean (cf Zar, 1984).

There is a general trend for zooplankton biomass, particularly the smaller size class, to increase in the upper 300m at night. Clearest evidence of this was observed during spring and summer. Biomass of all size classes was highest in the upper 200 m during spring and during the night in summer, while the lowest values were observed during winter. The biomass of both size classes changed little below 500 m on both a daily and seasonal basis. This contrasts with the results of previous studies (e.g. Longhurst and Williams, 1979; Raymont, 1983; Koppleman and Weikert, 1992) which demonstrated that biomass generally decreases with increasing depth.

Nematoscelis megalops   Pleuromamma quadrangulata

Euphausia spinifera   Pleuromamma abdominalis

Euphausia similis   Subeucalanus longiceps

Euchirella rostrata   Rhincalanus nasutus

Metridia spp   Eucalanus hyalinus

Metridia lucens   Calanus australis

Pleuromamma gracilis   Neocalanus tonsus

Key to Figures 2-17
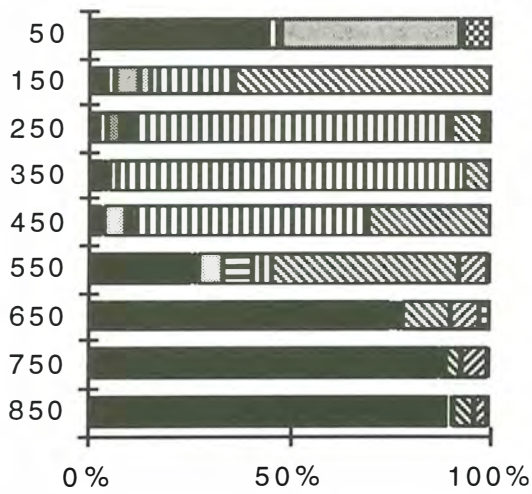
DEPTH (m)

Figure 2 Spring, Day, Abundance
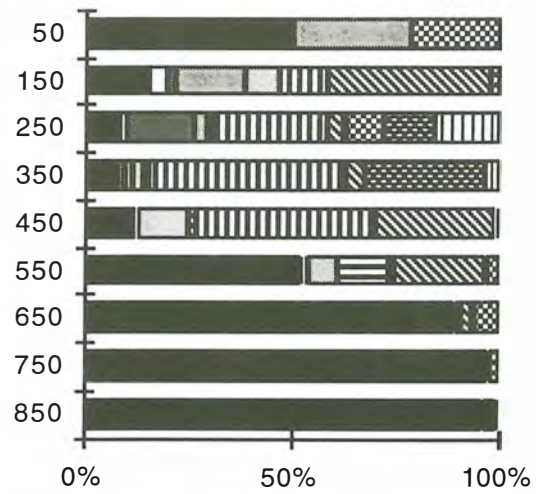
Figure 3 Spring, Day, Biomass
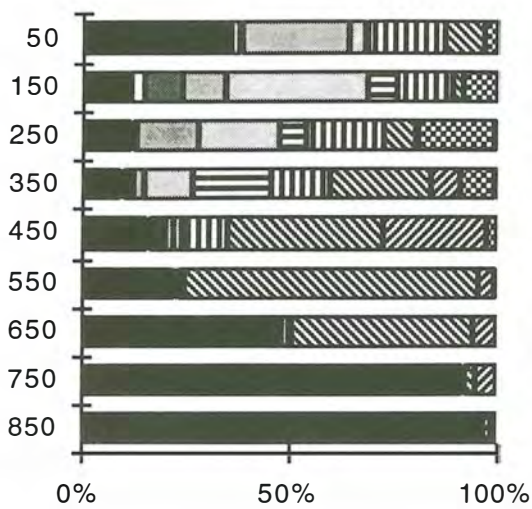
Figure 4 Spring, Night, Abundance
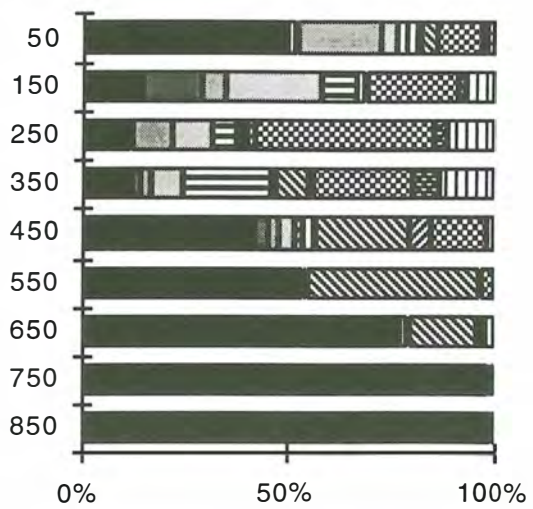
Figure 5 Spring, Night, Biomass

ABUNDANCE(%)

BIOMASS (%)
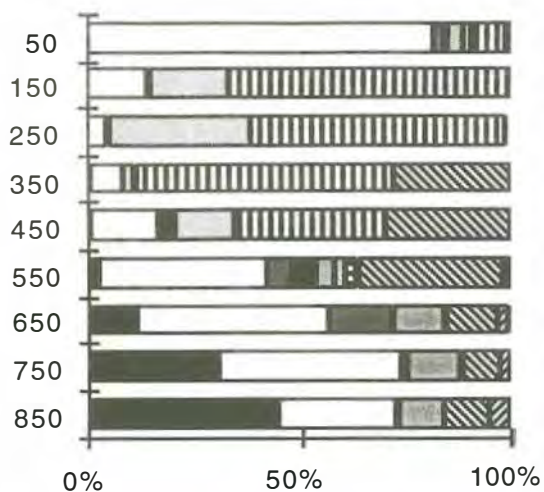
Figure 6 Summer, Day, Abundance
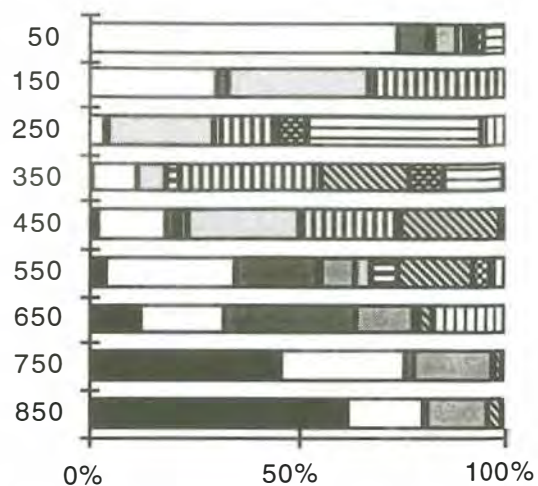
Figure 7 Summer, Day, Biomass
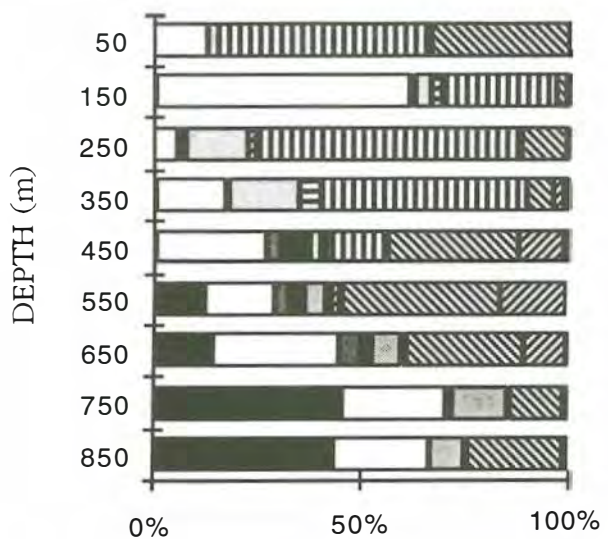
Figure 8 Summer, Night, Abundance
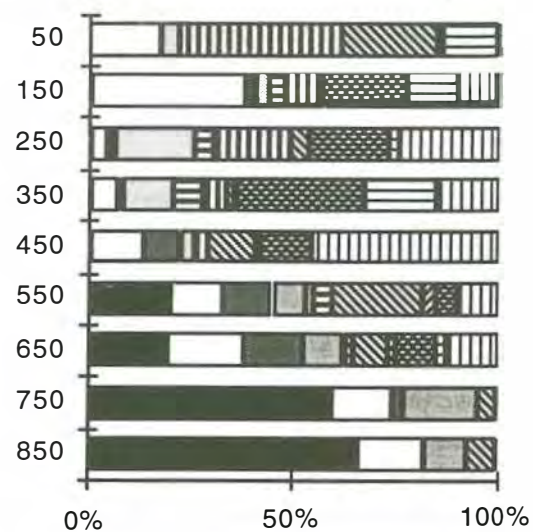
Figure 9 Summer, Night, Biomass
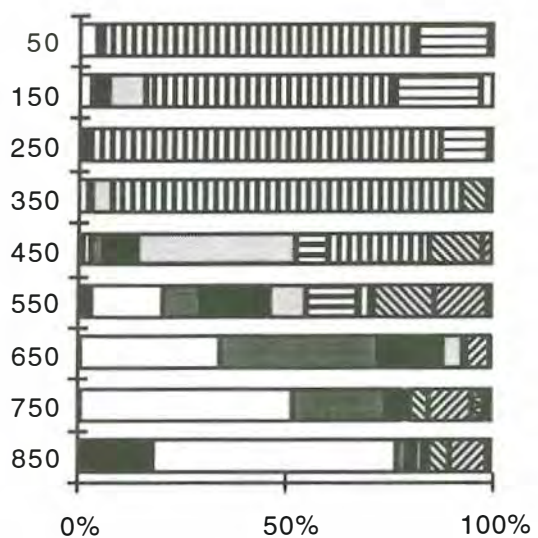
Figure 10 Autumn, Day, Abundance
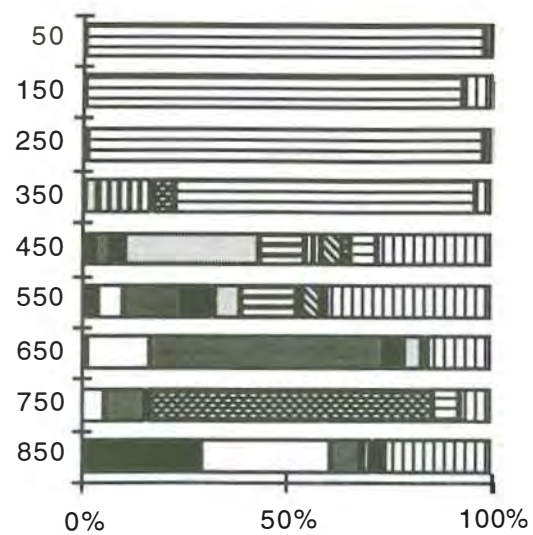
Figure 11 Autumn, Day, Biomass

DEPTH (m)
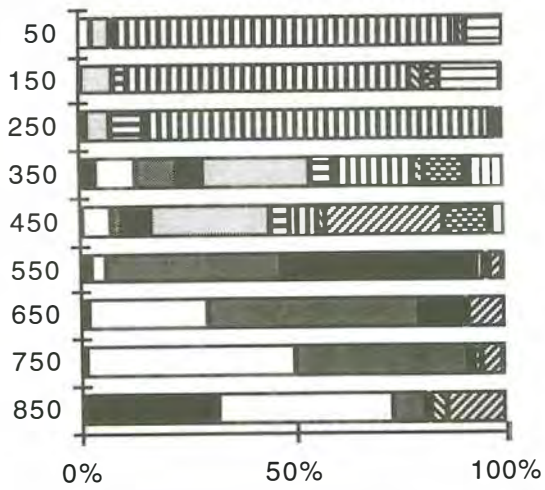
ABUNDANCE (%)

BIOMASS (%)

Figure 12 Autumn, Night, Abundance
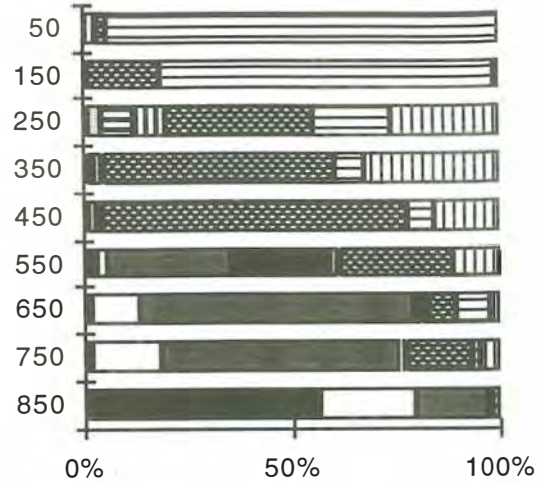
Figure 13 Autumn, Night, Biomass
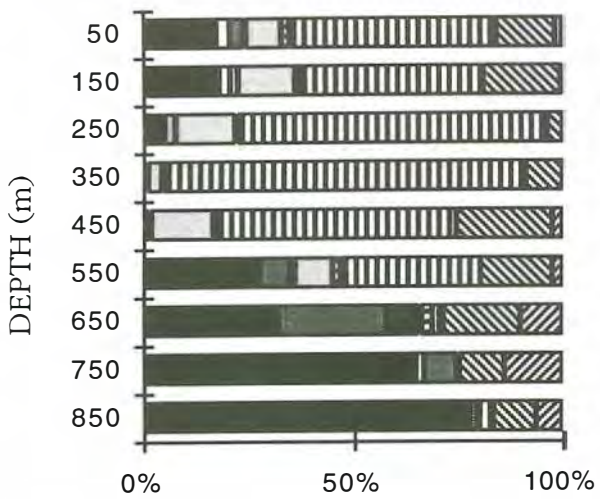
Figure 14 Winter, Day, Abundance
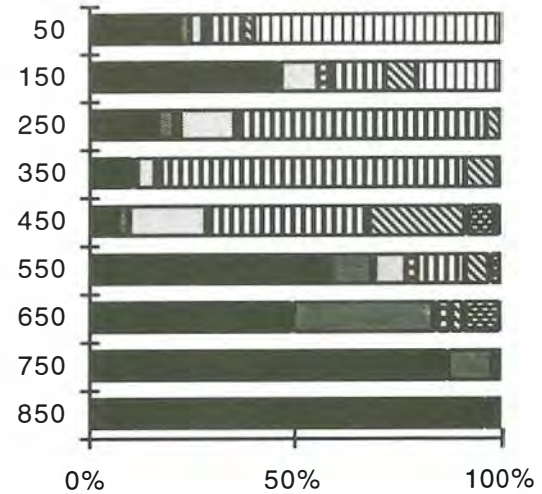
Figure 15 Winter, Day, Biomass
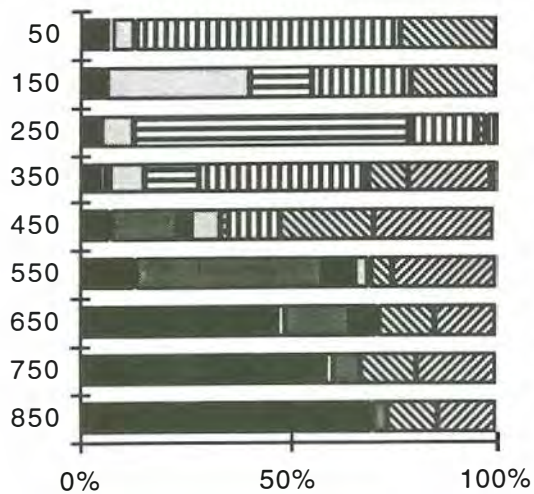
Figure 16 Winter, Night, Abundance
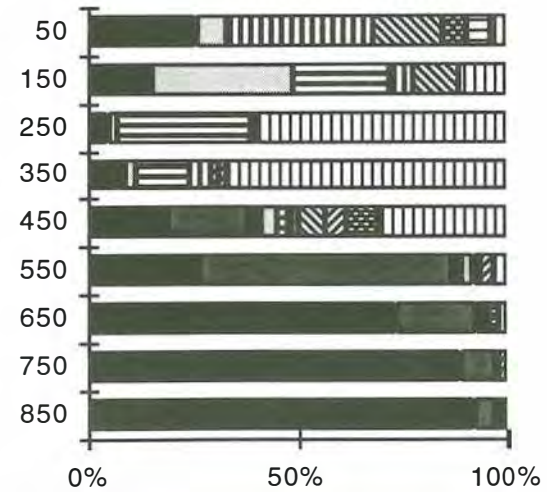
Figure 17 Winter, Night, Biomass

DEPTH (m)

ABUNDANCE (%)

BIOMASS (%)

Figure 18 : Spring Day
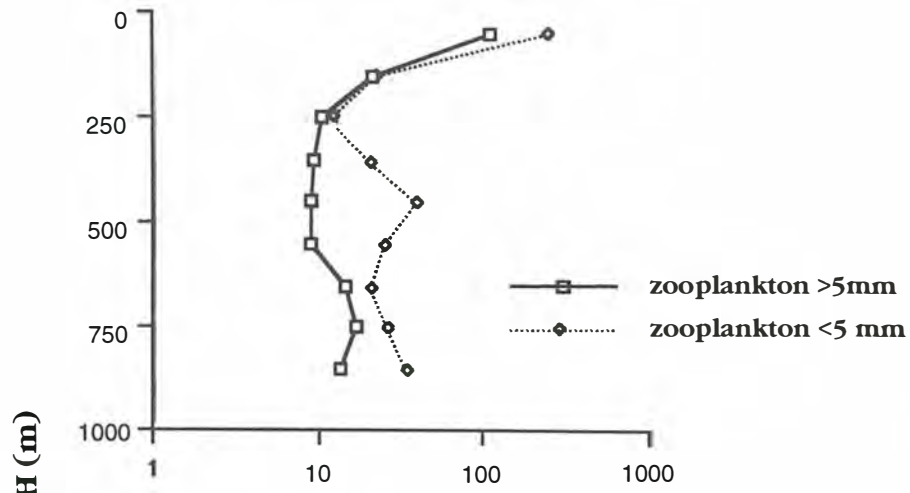
Figure 19 : Spring, Night
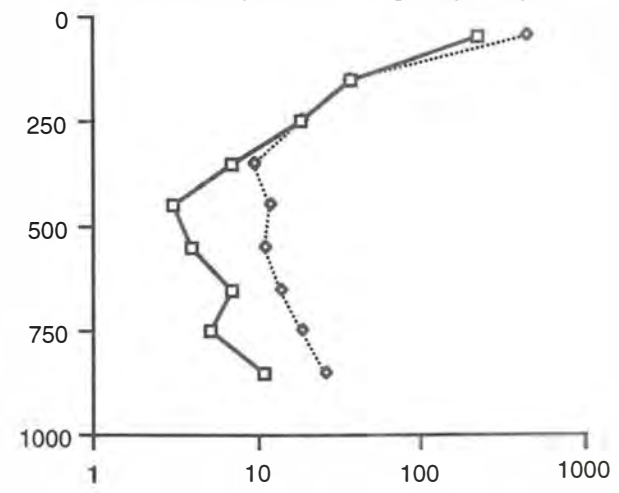
Figure 20 : Summer, Day

Figure 21 : Summer, Night

zooplankton >5mm

zooplankton <5 mm
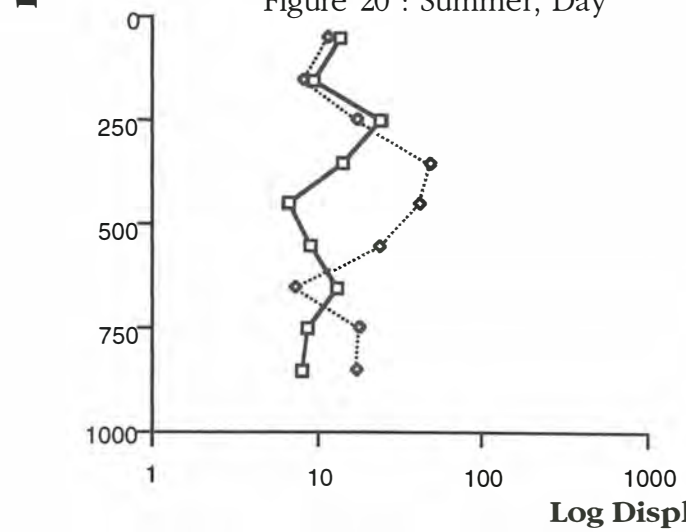
DEPTH (m)

Log Displacement volume (ml.1000m-3)
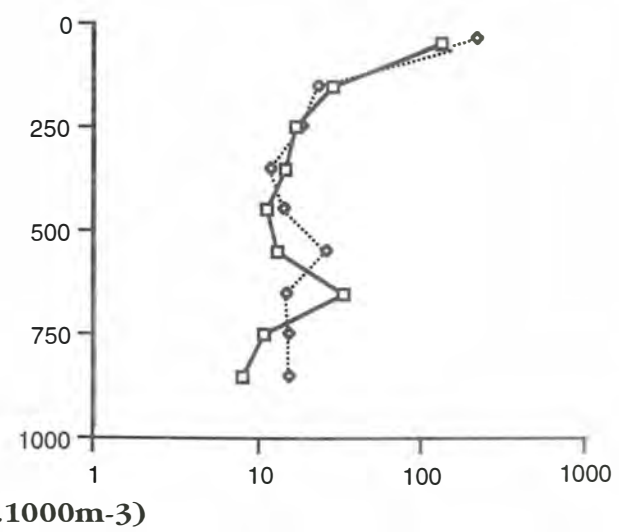
Figure 18 -21: Variation in displacement mvolume with depth
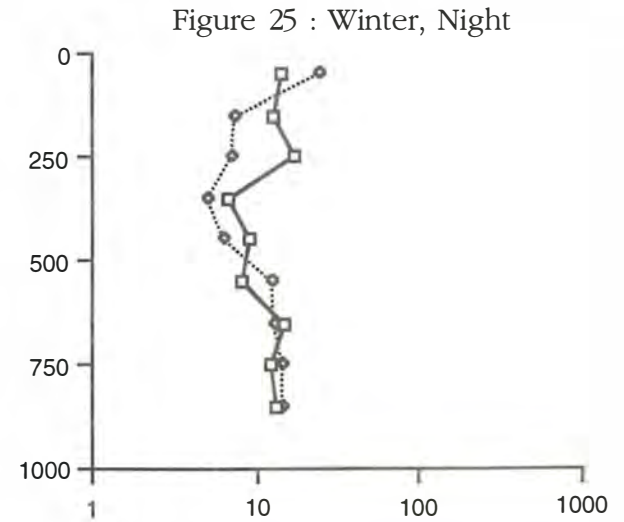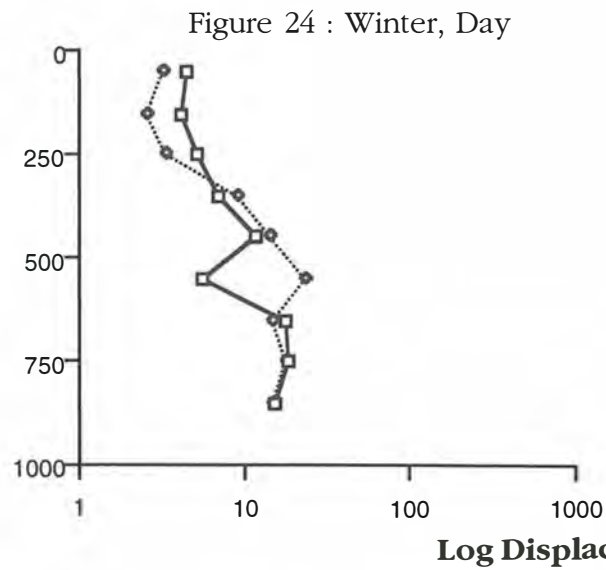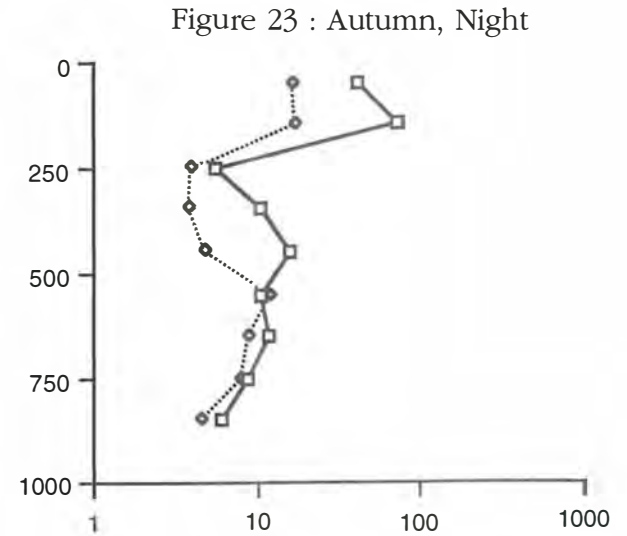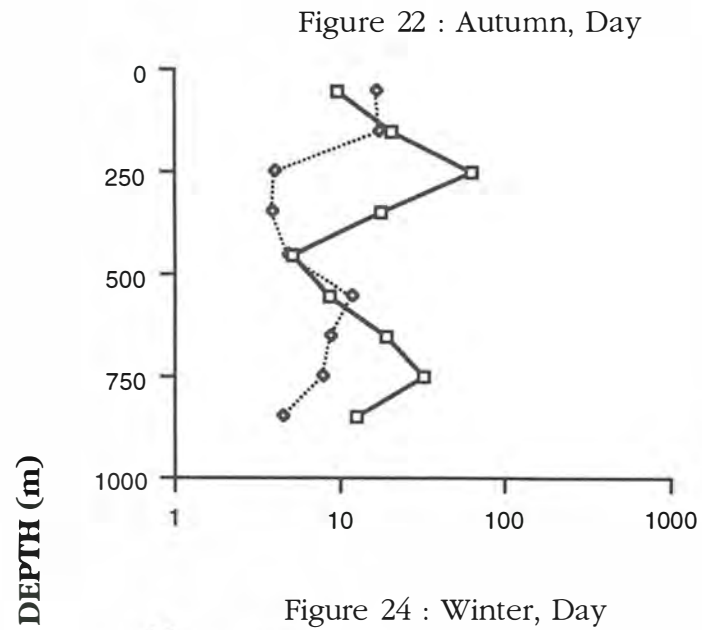
Figures 22-25 Variation in displacement volume (ml.1000m-3) with depth

Community Structure

The major species could be divided loosely into three main groups; seasonal migrators, diurnal migrators and non-migrators.

The biomass of seasonal migrators tended to increase in the upper 100 m depth strata during spring. This was possibly in response to increased food abundance in the upper water layers during the spring phytoplankton bloom . Figure 26 illustrates the daily and yearly movements of the calanoid *Neocalanus tonsus*, a typical seasonal migrator. This figure clearly shows the movement of biomass into deeper waters after spring, the predominance of the C5 stage at this depth during summer and autumn, the maturation of this stage into adults during winter and the subsequent appearance of earlier stages which move into shallower waters during spring to feed. Other species that appeared to perform seasonal migrations on the mid-slope region include; *Calanus australis*, *Eucalanus. hyalinus*, *Rhincalanus nasutus* and *Subeucalanus longiceps*. The application of three-way ANOVA provided strong evidence that the depth distribution of the above species changed significantly ($p < 0.001$) on a seasonal basis, supporting the hypothesis that they are seasonal migrators.

The biomass of species that exhibited diurnal migration was generally concentrated in the upper 500 m of the water column throughout the year. Unlike the seasonal migrators, there is no *en masse* movement of a large proportion of the population into deeper water after spring. In general the species classified as diurnal migrators show a relatively consistent pattern of migratory movements throughout the year. Figure 27 illustrates the daily and yearly movements of *Pleuromamma gracilis* a typical seasonal migrator. Clearly biomass increases in shallower waters during the night and is higher in deeper waters during the day. Other species on the mid-slope that were included in this category include *Pleuromamma abdominalis*, *P. quadrangulata*, *Metridia lucens* and *Euphausia similis*. The three-way ANOVA provided strong evidence that the depth distribution of four species of calanoid changed significantly ($p < 0.001$) on a daily basis, supporting the evidence obtained from the biomass distribution graphs. Due to non-normal distribution of the data, no statistical evidence could be obtained for *Euphausia similis*.

There was only a small number of species inhabiting the waters of the mid-slope region that did not exhibit some form of seasonal or diurnal vertical movement. There was only weak evidence that the euphausiids *N. megalops* and *E. spinifera*, and the calanoids *Metridia* spp. and *Euchirella rostrata* moved vertically on a
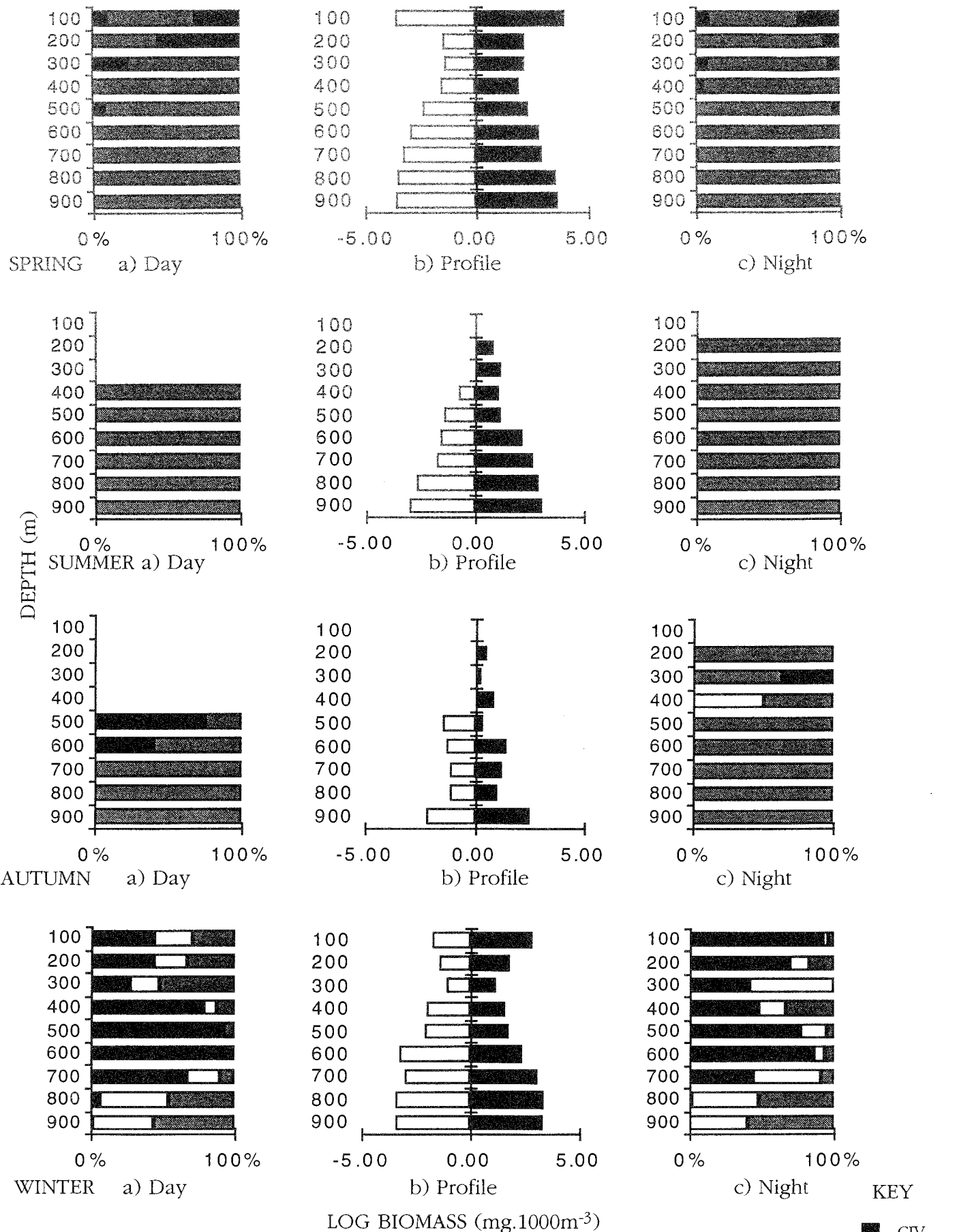
Figure 26 *Neocalanus tonsus*
a) & c) composition of depth strata in terms of developmental stage and sex of adults
b) total variation in biomass of species in mg.1000-3 at night (shaded)and night (unshaded).
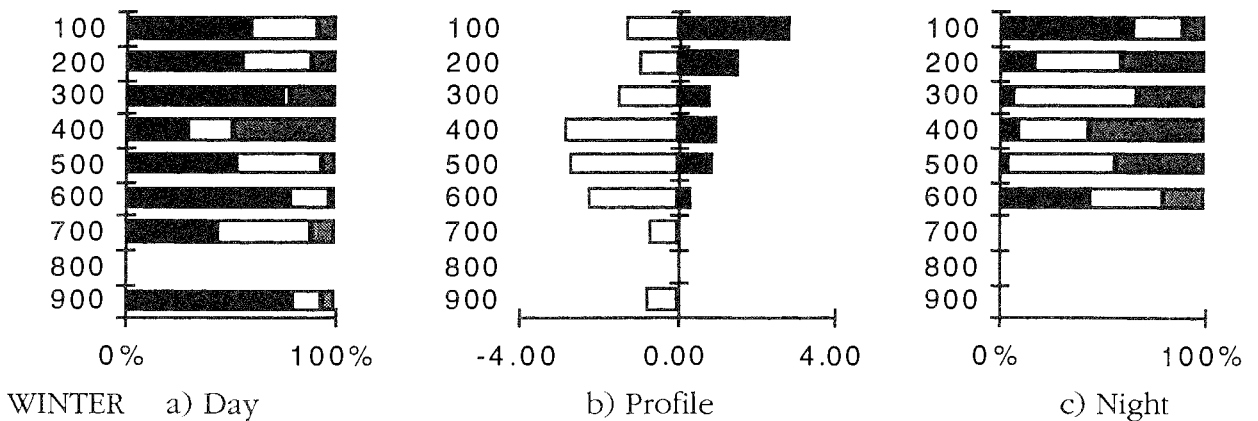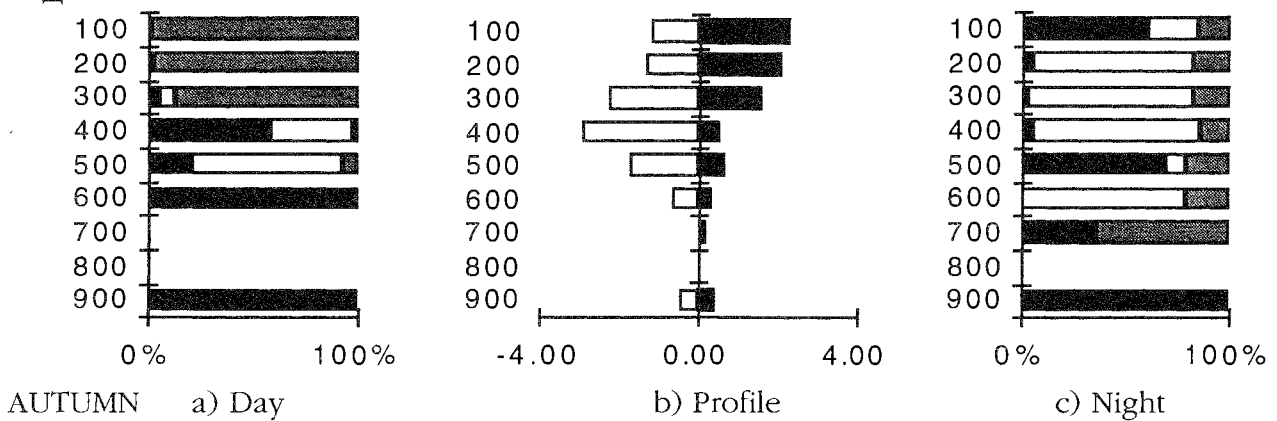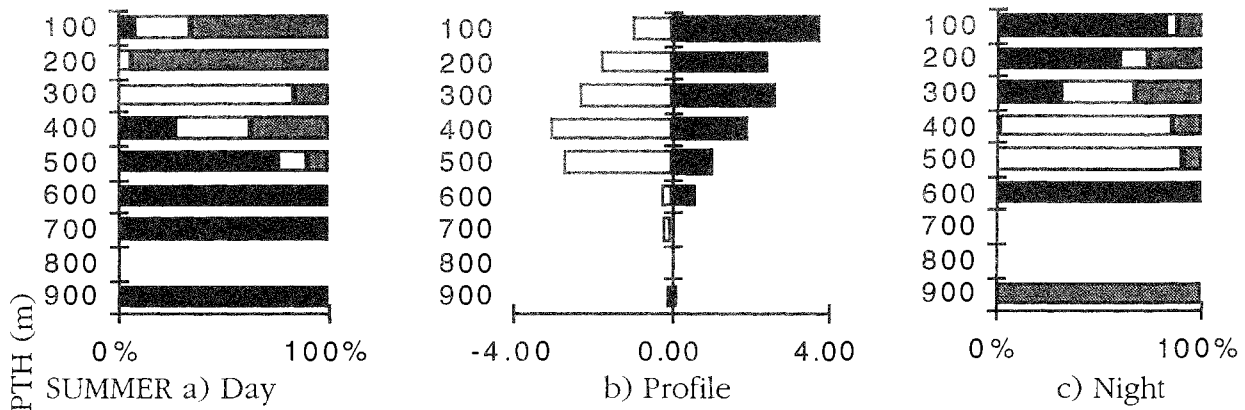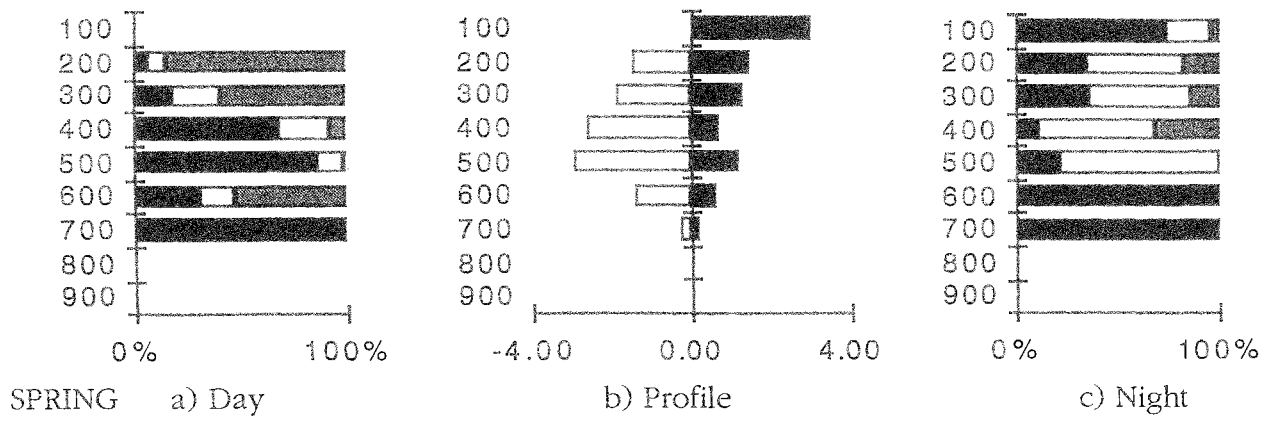
Figure 27 *Pleuromamma gracilis*
a) & c) composition of depth strata in terms of developmental stage and sex of adults
b) total variation in biomass of species in mg.1000-3 at night (shaded)and night
(unshaded).

KEY

CV
male
female

regular basis. There were some difficulties in conclusively identifying the vertical movements of the euphausiids due to net avoidance.

Analysis of the biomass distribution data using multivariate methods yielded results that were consistent with the above results. The UPGMA cluster analysis using species as variables and formed from a matrix of Bray-Curtis dissimilarities showed that two main clusters were present. The first cluster formed consists of all *Pleuromamma* species and the euphausiids *E. Similis* and *N. Megalops*. The second cluster consists of *N. tonsus*, *M. lucens*, *C. australis* and *S. longiceps*. These two groups are very similar to the groups of diurnal and seasonal migrators outlined earlier. The broad and abundant distribution of *M. lucens* is likely to be responsible for its inclusion in the seasonal migrators cluster. The Q-mode analysis or using stations as variables showed that stations could be broadly divided into two main clusters. The first consisted mainly of stations that were below 500 m and the second consisting largely of those stations above 500 m.

There does appear reasonable evidence from these analyses to support the hypothesis that the zooplankton on the mid-slope can be segregated into two major sub-groups. These groups can be loosely dived into seasonal migrators and diurnal migrators. Cluster analysis suggests that these groups are primarily separated by depth and that the depth discontinuity occurs at approximately 500m.

Seasonal migrators and the transfer of energy

The biomass distribution data (e.g. Figure 26) showed that seasonal migrators could potentially facilitate the movement of material to deeper waters. Table 1 shows that the calanoid *N. tonsus* comprises 99 % of the biomass of seasonal migrators in the deeper waters during late spring. The life history of *N. tonsus* is such that all this biomass moved to deeper waters during spring and will remain there for the rest of the year. Thus, this seasonal movement represents a potential energy transfer of 0.4066 gC $m^{-2}y^{-1}$ to the deeper waters. In addition, the other seasonal migrators, excretory processes, and the production of the next generation at depth all potentially increase the contribution of seasonal migrators to the flux of energy to deeper waters.

Table 1 : Contribution of seasonal migrators to biomass below 500 m (gC.m^{-2})

Species	Spring (D)	Spring (N)	Summer (D)	Summer (N)	Autumn (D)	Autumn (N)	Winter (D)	Winter (N)
N.tonsus	0.4611	0.4066	0.0770	0.1181	0.0084	0.0156	0.3686	0.2442
C.australis	0.0010	0.0001	0.0505	0.0503	0.0214	0.0145	0.0017	0.0016
E. hyalinus	0.0001	0.0002	0.0192	0.0250	0.0389	0.0514	0.0616	0.0519
R.nasutus	0.0000	0.0001	0.0003	0.0001	0.0037	0.0088	0.0013	0.0012
S.longiceps	0.0022	0.0040	0.0288	0.0342	0.0007	0.0000	0.0000	0.0000
Total (gC m-2)	**0.4644**	**0.4109**	**0.1758**	**0.2277**	**0.0732**	**0.0903**	**0.4332**	**0.2989**

REFERENCES

Ahlstrom, E. H. and Thrailkill, J. R. 1963. Plankton volume loss with time of preservation. *Californian Cooperative Fisheries Investigative Report.* **9**, 57-73.

Beers, J. 1976. Determination of zooplankton biomass. In *Zooplankton fixation and preservation.* Ed by H. F. Steedman, pp 35-84. UNESCO Press, Paris.

Bottger, R. and Schnack, D. 1986. On the effect of formaldehyde fixation on the dry weight of copepods. *Meeresforshung.* **31**, 141-152.

Bray, J. R. and Curtis, J. T. 1957. An ordination of the upland forest communities of Southern Wisconsin. *Ecological Monographs.* **27**, 325-349.

Clifford, H. T. and Stephenson, W. 1975. *An Introduction to Numerical Classification*. Academic Press, New York

Field, J. G. , Clarke, K. R. and Warwick, R. M. 1982. A practical strategy for analysing multispecies distribution patterns. *Marine Ecology Progress Series.* **8**, 37-52.

Koppelman, R. and Weikert, H. 1992. Full depth zooplankton profiles over the deep bathyal of the NE Atlantic. *Marine Ecology Progress Series*. **86**, 263-272.

Legendre, L. and Legendre, P. 1983. *Numerical Ecology.* Elsevier Publishing Company, New York.

Longhurst, A. R. 1981. *Analysis of Marine EcoSystems.* Acedemic Press, London.

Longhurst, A. and Williams, R. 1979. Materials for plankton modelling : Vertical distribution of Atlantic zooplankton in summer. *Journal of Plankton Research.* **1**, 1-28.

McEwan, G. F., Johnson, M. W. and Folsom, T. R. 1954. A statistical study of the performance of the Folsom Plankton Splitter, based upon test observations. *Archiv fuer Meteorologie Geophysik und Bioklimatologie Serie A.* **7**, 502-527.

Omori, M. 1978. Some factors affecting on dry weight, organic weight, and concentrations of carbon and nitrogen in freshly prepared and preserved zooplankton. *Internationale Revue gesamt Hydrobiologia.* **63**, 261-269.

Omori, M. and Ikeda, T. 1984. *Methods in Zooplankton Ecology*. John Wiley and Sons, New York

Raymont, J. E. G. 1983. *Plankton and Productivity in the Oceans.* Pergamon Press, Oxford.

Rodriguez, J. and Mullin, M. M. 1986. Diel and interannual variation in size distribution of oceanic zooplankton biomass. *Ecology*. **67**, 215-222.

Sameoto, D. D. 1979. Bedford Institute of Oceanography Net and Environmental Sensing System (BIONESS) construction details. *Fisheries and Marine Services Technichal Report*. **903**, 14 pp.

Vinogradov, M. E. and Tseitlin, V. B. 1983. Deep sea pelagic domain (Aspects of bioenergetics). In *Deep-Sea Biology*. Ed by G. S. Rowe, pp 123-165. John wiley and Sons, New York.

Williams, R. and Robbins, D. B. 1982. Effects of preservation on wet weight, dry weight, nitrogen and carbon contents of *Calanus helgolandicus* (Crustacea, Copepoda). *Marine Biology*. **71**, 271-281.

Zar, J. H. 1984. *Biostatistical analysis*. Prentice Hall, New Jersey.

APPENDIX 2.

COMPOSITION, VERTICAL DISTRIBUTION AND ABUNDANCE OF MICRONEKTON OVER THE MID-SLOPE REGION OFF SOUTHEASTERN AUSTRALIA, AND TROPHIC LINKS WITH THE BENTHOPELAGIC FISH ORANGE ROUGHY, *HOPLOSTETHUS ATLANTICUS*

ALAN WILLIAMS, CSIRO DIVISION OF FISHERIES.

COMPOSITION, VERTICAL DISTRIBUTION AND ABUNDANCE OF MICRONEKTON OVER THE MID-SLOPE REGION OFF SOUTHEASTERN AUSTRALIA AND TROPHIC LINKS WITH THE BENTHOPELAGIC FISH ORANGE ROUGHY, *HOPLOSTETHUS ATLANTICUS*

ALAN WILLIAMS, CSIRO DIVISION OF FISHERIES

INTRODUCTION

Off southeastern Australia and around New Zealand extraordinarily large concentrations of benthopelagic fishes occur over the mid-slope region in depths between 700 and 1200 m. The most abundant species, which supports large commercial trawl fisheries in both regions, is the orange roughy, *Hoplostethus atlanticus* Collett, 1889. Recent estimates put the size of the *H. atlanticus* stock off SE Australia at about 2×10^5 t (1995 SEF Stock Assessment Report) making it one of the largest fishery resources in Australian waters.

High fish abundance over the mid-slope relative to shallower depths has been reported previously in the North Atlantic Ocean where it was attributed to the exploitation of mesopelagic prey which occur in high abundance at corresponding depths (Gordon & Duncan 1985; Mauchline 1990). Clark et al. (1989) noted that the highest benthopelagic fish concentrations occurred where topography intersected mesopelagic layers and suggested that retaining close proximity to the bottom was important for pelagic foragers. Our observations of mid-slope dynamics around the orange roughy fishing ground off southeastern Australia are consistent with these features: a prominent mesopelagic layer is seen by echosounder in depths of about 650-800 m and orange roughy are aggregated around seamounts which intersect or peak in this depth range. Dietary studies confirm that mesopelagic fishes and, to a lesser extent, decapod crustaceans and cephalopods are the main constituents in the diet of adult orange roughy (Bulman & Koslow 1982, Roscecchi et al. 1988).

A major project to identify and quantify the food chain supporting large concentrations of benthopelagic fishes over the mid-slope and to assess its dependence on oceanographic forcing was undertaken during 1992 and 1993. The project site was within the orange roughy fishing grounds off Tasmania in southeastern Australia. In this paper, one of a series resulting from this study (see this report), we provide a description of the mesopelagic micronekton overlying this region. The composition of the micronekton, its structure and biomass is examined with reference to the implications for energy flow to mid-slope benthopelagic fishes, in particular *H. atlanticus*. It is the first study of the mesopelagic micronekton over the cool-temperate Australian mid-slope region and first study in Australian waters to provide discrete depth data over a wide range of depths (0-900 m). Previous ecological studies of mesopelagic fishes or the oceanic micronekton in Australian waters are few.

MATERIALS AND METHODS

Field collections. Samples of mesopelagic fauna were collected during four seasonal cruises from the CSIRO Division of Fisheries research vessel FRV

Southern Surveyor in February 1992 (summer), November 1992 (spring), April 1993 (autumn) and July 1993 (winter). The study area for the larger mid-slope trophodynamics project, which involved a range of oceanographic and biological sampling, was off the southern coast of Tasmania adjacent to the main commercial fishing grounds for orange roughy. Pelagic trawling was conducted within the study area in a rectangle bounded by latitudes 44°11'S and 44°14'S and longitudes 147°06'E and 147°18'E. Within this area of approximately 36 square miles the bottom depth ranged from about 1000 to 1400 m.

Samples were collected using a large pelagic trawl fitted with an opening/closing, five-net cod-end system based on the Multiple Plankton Sampler of Pearcy et al. (1977). The trawl rig was fished from twin warps using 50 m sweeps and Polyvalant trawl doors. Trawl design was based on the International Young Gadoid Pelagic Trawl (IYGPT), but was larger overall and of heavier construction. Combination rope was used in the net headline and foot-rope and selvedges were overbound to support the additional drag of the cod-end system. The cross-sectional area of the net mouth when fishing, as measured by hydroacoustic sensors, was about 105 m^2. Mesh sizes in the trawl was 100 mm in the wings, 100 mm reducing to 20 mm in the body and 10 mm in the extension; cod-ends were 7 mm with a short 0.5 mm mesh detachable bucket at the end. Opening and closing of the cod-ends was controlled by a remote pre-set electro-mechanical timer mounted on the cod-end frame. The timer was coupled to a net-tripping mechanism which sequentially release hinged bars tensioned by elastic shock cords. Release of each bar effected the closure of one cod-end net and opening of the next. Net geometry, the height of the gear off bottom and depth below the surface, and the spread of the trawl doors were monitored using the Scanmar trawl sensor system.

Sampling was based on contiguous oblique tows to maximise the efficiency of the sampling gear, and because they provide a better estimate of abundance than tows along horizontal horizons (Pearcy et al. 1977). During each trawl the net took one oblique sample as the gear descended to fishing depth and four depth stratified samples as the net ascended. An even rate of ascent was achieved by monitoring the net depth sensor. Strata of approximately 100 m depth were selecting on the basis of the resolution needed for assessing distributional limits in previous studies (Badcock and Merrett 1976), the depth range of current interest (0–900 m), and because only four depth-stratified samples could be taken per trawl. Thus, the following eight depth strata were sampled: (0-100 m, 100-200 m, 200-300 m, 300-400 m, 400-525 m, 525-650 m, 650-775 m, 775-900 m). Each stratum was sampled twice per day and night during four seasons giving a total of 128 samples. Tow duration was longer in deeper strata to compensate for lower catch rates: tows times were 30 mins for strata between 0 and 200 m, 40 mins between 200 and 650 m and 60 mins in deeper strata. Trawling was at a speed of 2.5- 3 knots. Sampling was timed to avoid a two hour period at sunset and at sunrise; the time of civil twilight (sun at 6° below the horizon) was taken as the mid-point. No account of moon phase or cloud cover was made.

Specimen processing. On deck, net cod-ends containing catches were immersed in seawater ice slurry immediately after detachment from the trawl rig. Each sample was then coarsely sorted in a tray of chilled seawater to remove gelatinous zooplankton and large fish and cephalopod specimens, and to

separate fish, cephalopod and crustaceans. Specimens were preserved in a neutral-buffered 10% seawater formaldehyde solution as soon as possible after sorting. Following preservation, specimens were washed in water and transferred through an alcohol series (to reduce shrinkage) into 70% ethanol prior to examination. Specimens were identified to species, enumerated and weighed. Taxonomy of fishes relied on several unpublished keys in addition to standard works. The most important of these was a key to the species of Myctophidae known from Australian waters provided by Dr John Paxton of the Australian Museum, Sydney.

Some rationalisation of the catch components was necessary to account for their great disparity of sizes. Large-sized fish and squid, whose relatively small numbers accounted for a disproportionately high fraction of overall biomass, were separated from micronektonic animals. Similarly, the gelatinous zooplankton, which comprised only two dominant species, was also treated as a separate, single category because it constituted nearly three times the biomass of the micronekton. Large numbers of macro-zooplankton, primarily euphausiids, were also retained by the fine mesh codends. However, because animals of this size were not sampled quantitatively by our gear they were excluded from this analysis. The plankton was sampled with a 10-net opening/ closing EZ net as part of this project and is treated in a separate paper (Terauds, this report).

Data analysis. Catches in each seasonal/day or night/ depth stratum were standardised to unit volume by calculating the volume of water filtered by the net. Volume filtered was calculated from the net mouth area x tow speed x distance travelled (based on the ship's GPS positions). Catches were not standardised with respect to the filtration efficiency of the net or catchability coefficients for different species since no data were available to assess these parameters. Abundance data were transformed using the natural logarithm to stabilise variance. Variance in abundance due to effects of season, time of day and depth and their interaction components were analysed using an analysis of variance (ANOVA) model. A split plot design was used because strata were sampled in groups of four per trawl.

RESULTS

COMPOSITION OF TRAWL CATCHES

Overall, about 546 kg of material was taken in the 128 samples. The micronekton made up about 22% of total biomass and 31% of total numbers. Fishes predominated in the micronekton (Fig. 1a, making up about 90% of biomass and 77% of numbers (Table 1), and were the most speciose component with 137 species from 33 families. Cephalopods and crustaceans constituted comparatively small and similar fractions of biomass although, due to the relatively small size of many species, crustaceans were more numerous (Table 1).

Table 1 Catch composition of primary components

Component of catch	Total sample		Micronekton	
	% Wt	% Nos.	% Wt	% Nos.
Micronekton				
Fish	19.3	24.2	89.4	77.4
Cephalopods	1.0	0.7	4.7	2.2
Crustaceans	1.3	6.4	5.9	20.4
Other groups				
Gelatinous zooplankton	59.8	21.6	—	—
Large fish	12.3	0.1	—	—
Large cephalopods	5.7	0.1	—	—
Macrozooplankton	0.6	46.9	—	—
Total	100.0	100.0	100.0	100.0

Gelatinous zooplankton was the single largest fraction of catches in wet weight biomass (Fig. 1b). It made up 60% of overall biomass and 22% of overall numbers (Table 1), predominantly due to the pyrosome *Pyrosoma* sp. (56% biomass, 51% numbers) and the large salp *Thetys* sp. (29% biomass, 26% numbers). Small salps and siphonophores, which were mostly damaged and unidentifiable, made up the remaining fraction.

Figure 1a Seasonal micronekton biomass
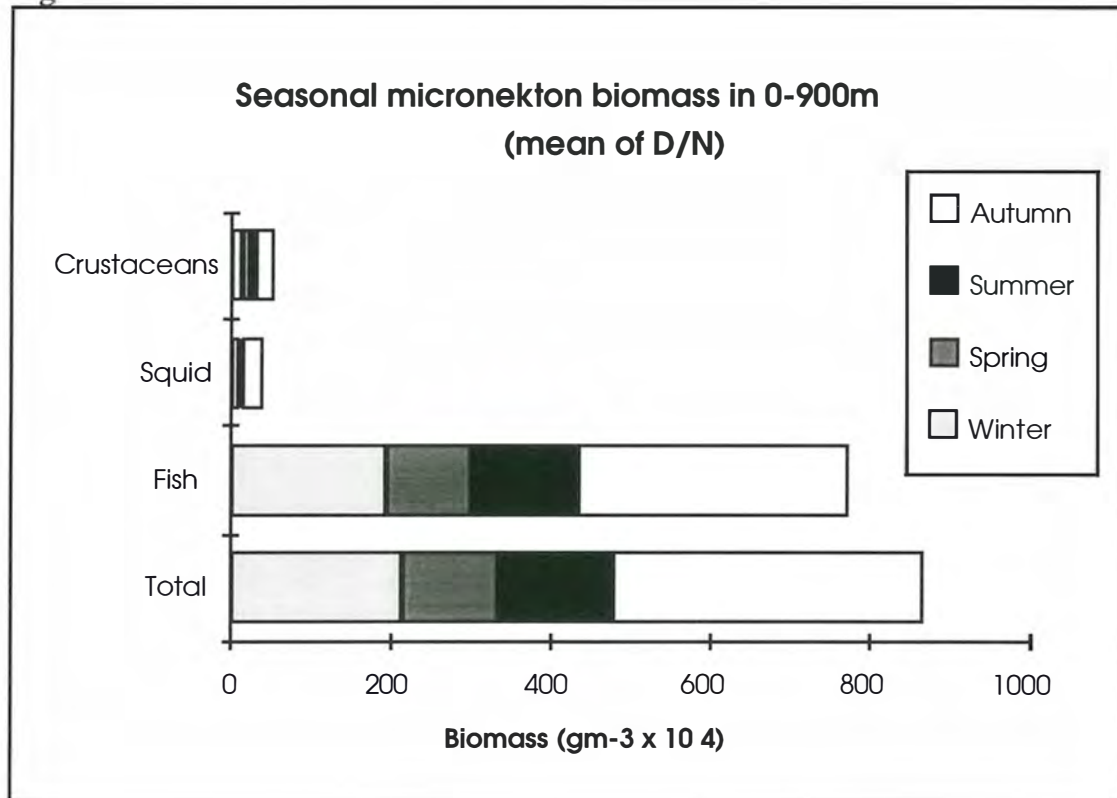
Large fishes and cephalopods were also caught in appreciably large quantities (Fig. 1b). Twelve species of large epipelagic, mesopelagic and benthopelagic fishes represented 39% of total fish biomass but only 0.4% of fish numbers. Similarly, three species of large pelagic squid comprised 85% of squid biomass but made up only 14% of total squid numbers.

Figure 1b Seasonal biomass of gelatinous zooplankton and large animals
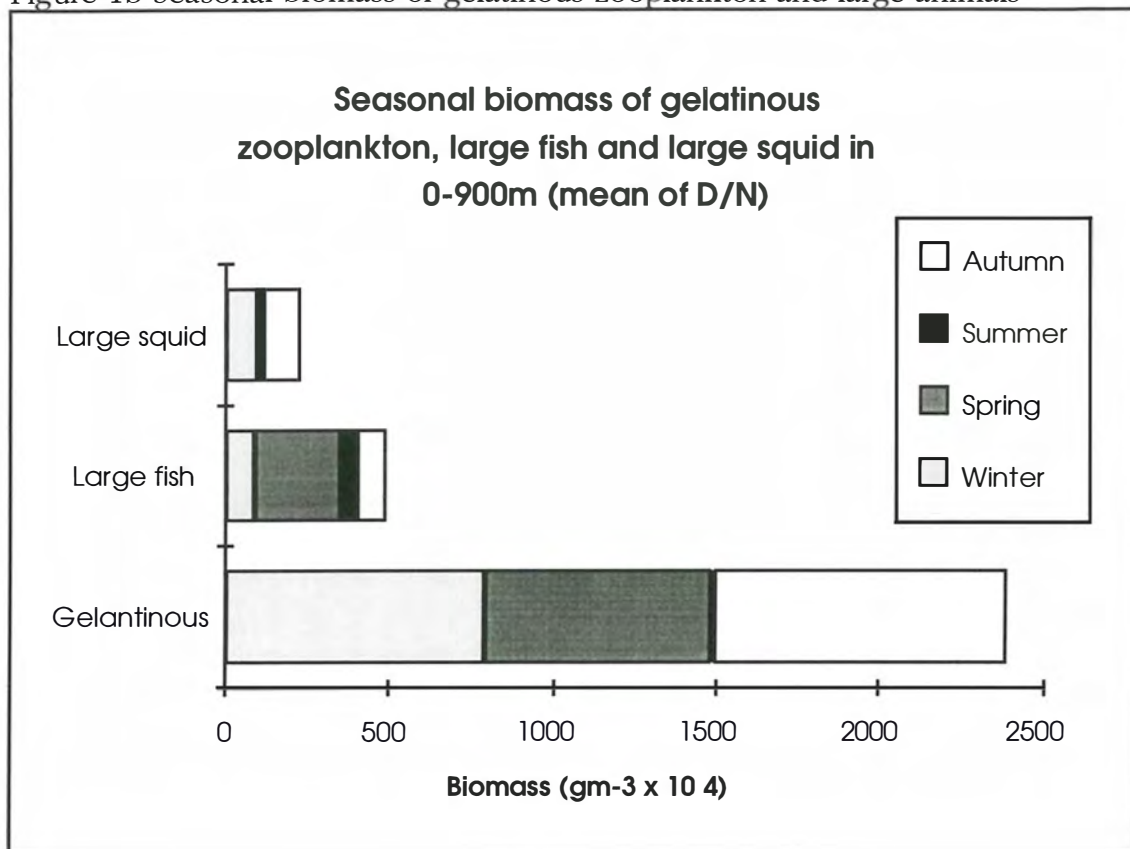
The ten top ranked families comprised 90% of micronekton biomass with the same top nine making up 96% of numbers (Table 2). These comprised seven families of fishes (Myctophidae, Gonostomatidae, Sternoptychidae, Seariidae, Bathylagidae, Notosudidae and Chauliodidae), two crustacean families (Sergestidae and Oplophoridae), and a single squid family (Lycoteuthidae). Within these families the most abundant species together comprised over three quarters of overall micronekton biomass and nearly two thirds of numbers (Table 2).

As a single family, the Myctophidae (lanternfishes) was conspicuous in being top-ranked in biomass (48%) and numerical abundance (61%) (Table 2). With 49 species it was also the most speciose family (Table 2). Within this family the same species of lanternfish (*L. australis*, *S. barnardi*, *D. danae*, *L. proceros* and *H. hanseni*) ranked in the top five in both biomass and numbers (Table 3).
Also prevalent was the Gonostomatidae (lighthouse fishes) which ranked second in biomass (17%) and third in numbers (7%). Although represented by nine species in our collections, its high ranking was mostly attributable to one species, *P. argenteus*. This was also the case for the remaining highly ranked fish and squid families where a single species accounted for most biomass and/ or

numbers in each case (Table 2). In both dominant families of crustaceans, no single species was dominant.

Overall, however, relatively few species were present in high abundance. Plots of cumulative percentage contribution to the total catch (biomass and numbers) by species show a high proportion of rare species. About 90% of both biomass and numbers are made up by about 20% of species. In fact, because species level differentiation was not possible for all groups, e.g. within the Astronesthidae or Melanostomidae, the number of rare species is underestimated.

Table 2 Dominant families and species of micronekton (by biomass)

Family	Rank Wt.	% Wt.	Cum. % Wt.	Species	Rank Wt.	% Wt.	Cum. % Wt.
Myctophidae (lanternfishes)	1	48.16	48.16				
				Lampanyctus australis	2	12.93	12.93
				Symbolophorus barnardi	3	8.86	21.79
				Diaphus danae	4	8.65	30.44
				Lampichthys proceros	6	3.92	34.36
				Hygophum hanseni	9	2.38	36.73
				Diaphus hudsoni	12	1.75	38.49
				Lampanyctus intricarius	14	1.68	40.16
Gonostomatidae (lighthouse fishes)	2	17.25	65.41				
				Photichthys argenteus	1	15.58	55.75
Sternoptychidae (hatchet fishes)	3	5.94	71.35				
				Argyropelecus gigas	5	5.39	61.13
Searidae (tube shoulders)	4	3.71	75.06				
				Persparsia kopua	7	3.70	64.84
Sergestidae	5	3.32	78.38				
				Sergestes (Sergia) potens	13	1.71	66.55
Lycoteuthidae	6	3.61	81.99				
				Lycoteuthis cf diadema	8	3.61	70.15
Bathylagidae (deepsea smelts)	7	3.04	85.03				
				Melanolagus bericoides	10	1.89	72.04
Oplophoridae	8	1.88	86.91				
				Acanthephyra quadrispinosa	24	0.58	72.62
				Acanthephyra pelagica	25	0.58	73.20
Notosudidae (wearyfishes)	9	1.81	88.72				
				Scopelosaurus sp.	11	1.80	75.00

Chauliodontidae   10   1.59 90.31
(viperfishes)   *Chauliodus sloani*   15   1.59 76.59

PATTERNS OF DISTRIBUTION AND BIOMASS

COMBINED MICRONEKTON

Mean annual micronekton biomass, based on data from all seasons, clearly showed a night-time translocation of biomass to the epipelagic zone due to the movement of vertical migrators (Fig. 3). Estimates of overall water column biomass in 0-900 m were similar during the night and day and ranged from 196 gm^{-3} x 10^4 (2.41 gm^{-2}) in day catches to 237 gm^{-3} x 10^4 (2.57 gm^{-2}) at night (Table 4).

Figure 3 Mean annual micronekton biomass
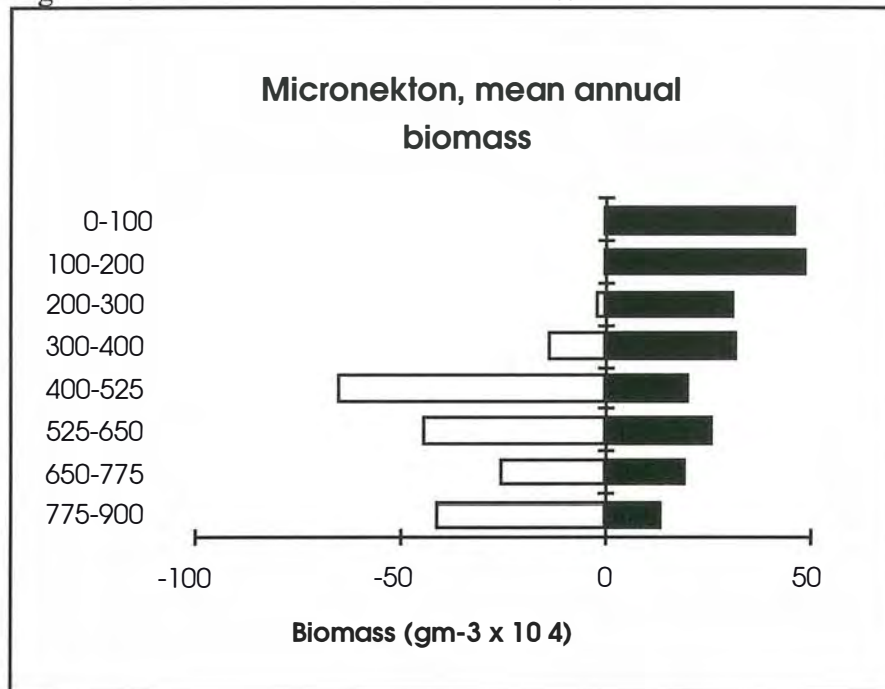
Table 4 Mean annual micronekton biomass

Depth (m)	Day gm-3 x 10 4	Night gm-3 x 10 4	Day gm-2	Night gm-2
775-900	41.7	13.5	0.52	0.17
650-775	25.9	19.4	0.32	0.24
525-650	44.7	26.1	0.56	0.33
400-525	65.6	20.3	0.82	0.25
300-400	14.6	31.5	0.15	0.32
200-300	2.7	31.2	0.03	0.31
100-200	0.4	48.5	0.00	0.49
0-100	0.7	46.2	0.01	0.46
Total	196.3	236.7	2.41	2.57
Stratum mean	24.5	29.6	0.30	0.32

The catch of combined micronektonic fishes, cephalopods and crustaceans, summed through the water column, was lowest in spring, higher in summer, peaked in autumn before declining in winter. Tests on the ANOVA model log transformed data showed the only significant ($P<0.05$) component of seasonal variation was the contrast between autumn and the other three seasons . The vertical distribution of micronekton biomass varied significantly between depth strata and between day and night due to vertical migration. These sources of variation were significantly different in all seasons ($P<0.001$) but, for the micronekton as a whole, vertical and day/ night distributions did not vary significantly between seasons.

The greatest variability in vertical distribution occurred between day and night in 0-300 m: in this depth range catches were significantly higher ($P<0.05$) at night than during the day in all seasons. In 300-400 m, significantly higher ($P<0.05$) night vs day time biomass was also observed in winter and spring. Below 400 m, daytime biomass was significantly greater than nighttime ($P<0.05$) only in 400-525 m in autumn and in 775-900 m in summer. Significantly higher ($P<0.05$) nighttime catches were taken in 0-400 m in autumn compared to the other seasons.

No other comparisons of biomass between day and night in a given depth stratum, or in adjacent strata in either day or night, were significantly different from each other. However, some trends in the data were apparant: in each season except spring, night catches in the surface 200m were higher than between 200 and 400m. Below 400m, catches were greater in the day than at night in all strata in every season. Below 525 m, nighttime biomass was lowest in the deepest stratum (775-900m) but there was no consistent trend in the decrease of biomass with depth. No trend was evident below 400 m during daytime either.

Since fishes made up the majority of the micronekton biomass in all seasons (Fig. 1a), patterns of overall fish distribution showed no significant departures from those described for the combined micronekton (Fig. 4). Similarly, micronektonic crustacean biomass displayed few departures from patterns of combined micronekton abundance. Their biomass was significantly higher ($P<0.01$) in autumn, negligable in all 0-200 m daytime samples but present in all strata at night in all seasons. Micronektonic crustacea caught above 400 m during the day only during autumn. Patterns of vertical distribution below 400 m showed no consistent trend with depth or between seasons. Data for the dominant species, *Sergestes (Sergia) potens* is given in the following section.

Catches of micronektonic cephalopods were dominated by a single squid species, *Lycoteuthis* cf *diadema*, which comprised 3.6% of total micronekton biomass and 77% of micronektonic cepahalopods. It was significantly more abundant in autumn ($P<0.01$) in 0-200 m at night and 300-525 m during the day than in any other catches. However, apart from the daytime winter catch in 400-650 m, it was taken in only small quantities. Among the other micronektonic cephalopod species only the cranchid squid *Teuthowenia pellucida* made up more than 2% of micronekton biomass. It represented 0.6% of total micronekton biomass and 17% of cephalopod biomass, but was caught only intermittently.

DOMINANT MICRONEKTON SPECIES

To determine what patterns underlay the overall pattern of micronekton distribution and abundance, the 20 dominant individual micronekton species (ranked by weight) were examined individually (Fig. 5). This group (18 fishes, 1 crustacean and 1 squid) which represented 80% of total micronekton biomass, is also used for analysis of assemblage structure because it closely mirrored the distribution of total micronekton. It slightly underestimated biomass only in the strata containing a relatively high proportion of low abundance species. Thus, less biomass is represented in the shallowest daytime stratum, in which small sternoptichids (*Vinciguerria* species and *Maurolicus mulleri*) and epipelgic juveniles of a variety of taxa (principally stromateoids, monacanthids and morids) were found, and in the deepest stratum where low abundance stomiiform fishes such as melanostomiatids are most prevalent.

All dominant species were caught in each season, but there was no consistent pattern to seasonal abundance. Relatively large catches of several dominant species contributed to the peak micronekton biomass observed in autumn, although it was driven principally by the top four ranked fishes, *P. argenteus*, *L. australis*, *S. barnardi* and *D. danae*. The catches of several species fluctuated greatly between seasons: *S. barnardi* was the most abundant species in autumn catches but was relatively scarce in the other seasons. In common with *L. diadema* and *H. hanseni* it was virtually absent in spring.

Figure 4 Day/ night micronekton biomass by season and depth (shaded bars = night)

Micronekton, spring

Micronekton, summer

Micronekton, autumn
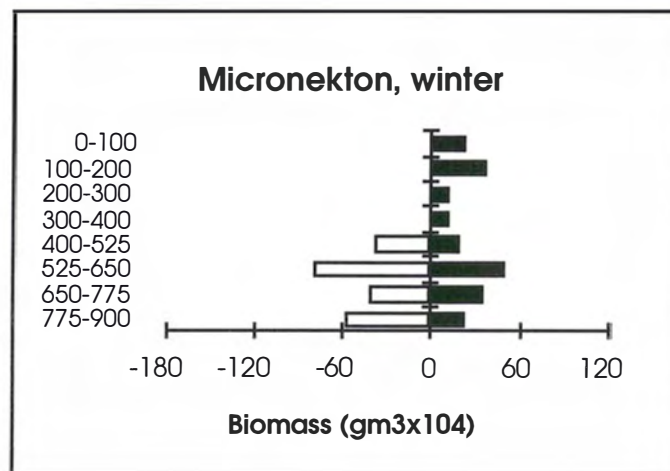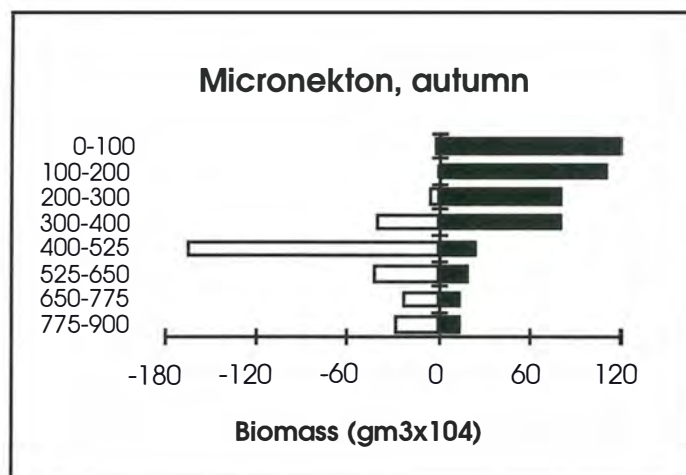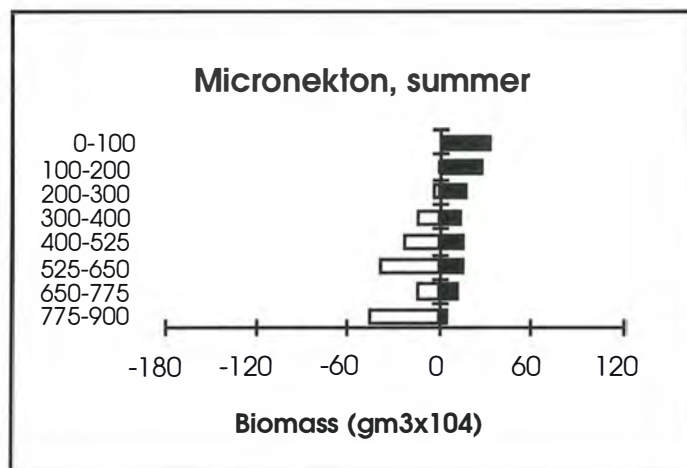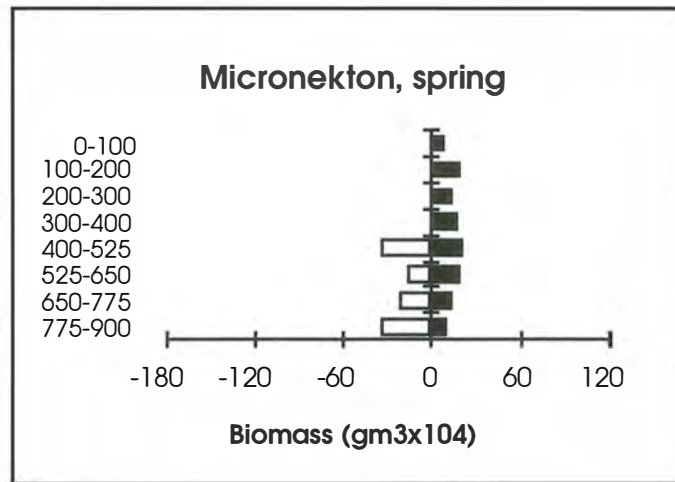
Individual species varied greatly in their daytime/ nighttime residence depth ranges and in their degree of vertical migration. Vertical residence ranges, in combined seasonal data, were typically greater than 200 m during the day and night (Fig. 5). This was also true in each season for top ranked species (*P. argenteus*, *L. australis*, *Symbolophorus*, *D. danae* and *A. gigas*) where residence depths were examined in each season. Indication of a shallower residence range in summer was seen in some species, e.g. *P. argenteus*, *L. australis*. Nighttime ranges varied greatly from around 200 m in *H. hanseni*, to 900 m in *L. australis*.

A range of vertical migration patterns was evident among the dominant species (Fig. 5). Eight of the ten dominant myctophids showed some degree of upwards movement at night. Migrations involved wholesale translocation of a species, e.g. *H. hanseni*, or a graded migration where daytime and nighttime ranges overlapped, e.g. *L. australis*. Nyctoepipelagic migrators (those moving to the surface 200 m) included *L. proceros*, *E. paucirastra* and *Symbolophorus boops* with deep daytime residence depths and *S. barnardi*, *D. danae* and *H. hanseni* with predominantly intermediate daytime ranges. *Lampanyctus australis* and *Diaphus hudsoni* appeared to be partial migrators where most biomass remained below the epipelagic zone. No evidence of migration was apparant in *Electrona risso* from intermediate depths or in *Lampanyctus intracarius*, a deep mesopelagic species. A corresponding variety of migration patterns was also evident among the non-myctophid fishes. The single dominant cephalopod, *L. diadema*, was caught intermittently but showed clear evidence of nyctoepipelagic migration in autumn when most specimens were taken. The dominant crustacean, *Sergestes (Sergia) potens*, appeard to be a deep living, partial migrator with some individuals reaching the epipelatic zone.

LARGE FISHES AND CEPHALOPODS
Large fishes, which were caught infrequently and in low numbers, were predominantly the two deep mesopelagic stromateoid fishes, *Tubbia tasmanica* and *Tetragonurus cuvieri*. In total only 79 individuals of large fish species were caught: 1 *Apristurus* sp. C (Scyliorhinidae), 5 *Centroscymnus crepidater,* 1 *Etmopterus baxteri,* 1 *E. puscillus* (Squalidae), 1 *Macruronus novaezelandiae.* (Merluccidae), 4 *Coryphaenoides subserrulatus* (Macrouridae), 1 *Allocyttus verrucosus* (Oreosomatidae), 1 *Aphanopus* sp., 1 *Trichiurus* sp. (Trichiuridae), 1 *Centrolophus niger,* 1 *Schedophilus huttoni,* 35 *Tubbia tasmanica* (Centrolophidae), and 26 *Tetragonurus cuvieri* (Tetragonuridae).
Large fishes were caught deeper than 200 m, most below 525 m, with more taken at night than during the day. The relatively high biomass of large fish taken in spring in 525-900 m coincided with the trawl passing in close proximity to a small seamount previously uncharted in the study area.
Large squids were also caught infrequently and in low numbers, and were represented by three taxa: 15 *Histioteuthis miranda* (Histiotheuthidae), 52 *Nototodarus gouldi* and 12 *Todarodes* sp. (Ommastrephidae). Catches were low in spring, zero in summer but relatively large in autumn and winter. The total nighttime catch was significantly larger that the daytime catch.

GELATINOUS ZOOPLANKTON
Data for the gelatinous zooplankton show few consistent patterns and, due to an inconsistency in the data collection during the first cruise, the summer data are not presented. A significantly higher total daytime vs nighttime catch was taken in the other three seasons but the vertical distribution of biomass was makedly different. In winter and spring biomass was greatest between 200 and 525 m whereas in autumn large catches were taken in the suface 100 m and between 300 and 400 m. The only large nighttime catches were taken in the surface 100 m in winter and spring indicating vertical migration of some fraction of the gelatinous zooplankton.

DISCUSSION

COMPOSITION OF THE MESOPELAGIC MICRONEKTON

The mesopelagic micronekton overlying the mid-slope region off southern Tasmania is dominated in terms of both wet weight biomass and numbers by two components: gelatinous organisms and fishes. Most species were uncommon or rare with only the two common gelatinous organisms, *Pyrosoma* sp. and *Thetys* sp., and the two most abundant fishes, *P. argenteus* and *L. australis* individually making up more than 10% of overall biomass. Micronektonic cephalopods were scarce, with only one species, *L. diadema*, amongst the dominant 20 species. Similarly, decapod crustaceans constituted a relatively small proportion of biomass; only *S. potens* was among the dominant 20 species.

The distributional ranges of dominant species over the mid-slope region are broadly defined by or encompass the Sub-tropical Convergence (STC) zone in a range of latitudes from about 40-50°S (McGinnis 1982, Paxton et al. 1989). Few expatriate species from adjacent neritic, sub-tropical or sub-antarctic waters were identified. *Lampanyctodes hectoris*, the dominant component of the micronekton in shelf-break and upper slope waters off eastern Tasmania was infrequently caught. A few expatriate species including *Electrona carlsbergi, Gymnoscopelus microlampus and Protomyctophum* sp. were caught in low numbers.

SPATIAL STRUCTURE

The high degree of structural complexity within the mesopelagic micronekton community was evident from the broad ranges and markedly different patterns of vertical distribution of individual species, and from the layered and clumped distributions of scatterers commonly seen in echo-recordings. These patterns changed daily with the nighttime ascent of vertical migrators fundamentally changing both the distribution of biomass and the species composition through the water column. The degree of vertical migration varied greatly, ranging from a wholesale shift in daytime/ nighttime residence depths in some species through to no apparent migration of others (Fig. 5). Vertical migration to varying levels in the surface 900 m was undertaken by mid-depth species and deep mesopelagic species with daytime residence depths below 650 m.

Despite this underlying complexity, analysis of the species composition of samples and the distributions of multiple species showed some well defined and consistent depth related patterns. Among dominant species, distribution patterns corresponded to epipelagic, mid-depth and deep mesopelagic regions. During the day when the surface 400m was virtually devoid of any of the dominant species, only broad mid-depth and deep mesopelagic assemblages could be seen in the species groupings. At night, nyctoepipelagic and mid-depth assemblages were clearly differentiated, while a deep mesopelagic assemblage showed some separation of the deepest living species from the remainder. A significant finding was the presence of deep mesopelagics, including several dominant species, among the nyctoepipelagic migrators.

Dietary studies have shown that many mid-slope benthopelagic fishes are predators of the mesopelagic micronekton (Mauchline & Gordon 1984; Clark 1985). Orange roughy, the dominant benthopelagic slope fish off southeastern Australia, has been consistently found to be a generalist predator on mesopelagic fishes, cephalopods and crustaceans (Bulman and Koslow 1992; Rosecchi et al. 1988; Gordon and Duncan 1987). Utilisation of the mesopelagic fauna by benthopelagic fishes was proposed by (Gordon & Duncan 85) as the reason for the maximum biomass of benthopelagic fish occurring at mid-slope depths in the Rockall Trough region. Mauchline & Gordon (1991) showed that at mid-slope depths (800-1550 m) in the Rockall Trough, there is the highest potential for vertical and horizontal impingement of mesopelagic micronekton onto the slope itself. Based on analysis of prey and predator feeding depths, these authors concluded that the availability of mesopelagic animals to benthopelagic predators in the Rockall Trough was due mostly to vertical impingement where the vertical distribution of pelagic prey is truncated at the seafloor. Thus, energy flux to benthopelagic predators was predominantly a process of vertical transfer.

Off New Zealand, where populations of some benthopelagic fishes, including orange roughy, occur in considerable quantities, Clark et al. (1989) noted that benthopelagic fish concentrations often coincide with areas where bottom topography interrupts deep scattering layers. This would appear to indicate that horizontal impingement was an important source of prey for benthopelagic fishes on the New Zealand mid-slope region. Impingement processes demonstrate that spatial overlap of benthopelagic predator and mesopelagic prey does occur, and clearly concentration of prey items occurs at impingement sites. However, simple impingement does not adequately explain the highly aggregated spatial distribution of orange roughy or its extraordinarily high biomass in mid-slope depths. Other mechanisms are needed to explain these phenomena.

One possibility is that orange roughy undertake extensive vertical migrations to shallow mesopelagic depths (<525 m) where overall micronekton biomass is highest. This hypothesis is difficult to test, however, demersal catch data, echosounder observations, and the vertical distribution of prey species are consistent with only limited migrations being undertaken. The extent of migrations by orange roughy during pelagic foraging cannot be estimated directly because this species is rarely captured in pelagic trawls. It is noteworthy that, despite being the dominant benthopelagic fish in our study area, no orange roughy were present in the 128 samples taken during this study. Our experience over several years of research and commercial trawling in southeastern Australia, and that of Rosecchi et al. (1988), is that orange roughy can be caught on the bottom at all times of the day. It therefore seems unlikely that extensive or diel vertical migration in search of prey is undertaken. Soundings from around seamounts off Tasmania where most of the commercial catch is taken show what are believed to be orange roughy schools forming vertical and lateral plumes extending up to 100 m into mid-water. Such plumes frequently occur between 700 and 900 m and therefore correspond to depths where a relatively high daytime abundance of mesopelagic micronekton occurs. It seems likely that excursions into mid-water around seamounts are undertaken whilst foraging but there is no evidence from catches or soundings to support extensive vertical

migration, such as those undertaken by merluccid fishes over the upper slope (Blaber & Bulman 1987). It should be noted, however, that the absence of orange roughy in pelagic trawl catches does not discount the possibility that more extensive vertical migration does occur. The species has a marked avoidance response to cameras and other sampling gears (Koslow et al. 1995) and therefore may easily avoid pelagic trawls.

An alternative hypothesis to explain the maintenance of high orange roughy biomass is that advective processes bring prey onto the mid-slope. Prey advection or 'dynamic horizontal impingement' into critical areas could also explain the aggregated distribution of orange roughy around seamounts. Support for this hypothesis is provided by two observations. First, higher (daytime) abundances of known prey species overlap the primary residence depth range of orange roughy (700-1200 m) than occur in shallower depths. Secondly, our estimate of overall micronekton biomass appears to be too low to provide the required energetic input for this species.

Prey species (Bulman and Koslow 1992; Rosecchi et al. 1988) include vertical-migrating and non-migratory species from the mesopelagic as well as the benthopelagic realm. Daytime/ nighttime vertical distributions of this suite of species indicated a relatively high abundance in 775-900 m compared to shallower strata. Whether this represents modal abundance remains unclear because we have no vertical distribution data below 900 m. Many of these prey species are known to have vertical distributions that extend into bathypelagic depths e.g. *C. sloani, M. niger, C. subserrulatus*. However, the abundance of the pelagic micronekton characteristically decreases generally/markedly below 1000 m. In the Myctophidae, the highest unidentified component of orange roughy diets, relatively few species extend are significantly abundant below 1000 m.

The spatial concentration of orange roughy biomass is remarkable. Surveys of the southeastern Australian mid-slope between 1987 to 1989 (Bulman et al. 1995) showed that orange roughy were widely dispersed over flat, 'trawlable' ground, being present in 97% of 376 demersal trawl samples between 700 and 1200 m. However, the subsequent development of commercial fishing grounds showed that orange roughy were also found in dense aggregations around seamounts. Off Tasmania, it is the dominant species on seamounts peaking between ~700 and 1000 m and has its highest biomass in this depth range. Interestingly, most of the commercial catch is taken from aggregations around isolated seamounts and not from the continental margin itself. Based on the estimated flat ground biomass (~15 x 10³ tonnes) (Bulman et al. 1995) and the estimate of virgin stock biomass off Tasmania (~200 x 10³ tonnes) (1994 SEF Stock Assessment Report), it may be surmised that most orange roughy exist in aggregations. Prior to commercial exploitation such concentrations may have represented greater than 90% of total biomass. The isolated peaks of seamounts therefore seen to provide a critical habitat for this species. We suggest that a key factor is their intrusion into relatively dense layers of the deep mesopelagic micronekton.

Calculations of mesopelagic fish, crustacean and cephalopod biomass indicate that they form too low a component of in situ vertical flux to support the energy requirements of orange roughy populations. Total water column micronekton

biomass in 0-900 m was estimated at only 2.41-2.57 gm^{-2}. Koslow (this report) calculated that the mid-slope input required to support orange roughy appears to be many times greater.

REFERENCES

Blaber, S.J.M. and Bulman C.M. (1987). Diets of fishes of the upper continental slope of eastern Tasmania: content, calorific values, dietary overlap and trophic relationships. Marine Biology 95, 345-356.

Bulman and Koslow (1992). Diet and food consumption of a deep-sea fish, orange roughy *Hoplostethus atlanticus* (Pisces: Trachichthyidae), off southeastern Australia. Marine Ecology Progress Series 82, 115-129.

Bulman et al. 1995 Orange roughy surveys in SE Australia. CSIRO Marine Laboratories Report. (in press).

Clark, M.R. (1985a). The food and feeding of seven fish species from the Campbell Plateau, New Zealand. New Zealand Journal of Marine and Freshwater Research, 19, 339-363.

Clark, M.R. (1985b). Feeding relationships of seven fish species from the Campbell Plateau, New Zealand. New Zealand Journal of Marine and Freshwater Research, 19, 365-374.

Clark, M. R., King, K.J. and McMillan (1989). The food and feeding relationships of black oreo, Allocyttus niger, smooth oreo, Pseudocyttus maculatus, and eight other fish species from the continental slope of the south-west Chatham Rise, New Zealand. Journal of Fish Biology, 35, 465-484.

Gordon, J.D.M. and Duncan, J.A.R. (1985). The ecology of the deep-sea benthic and benthopelagic fish on the slopes of the Rockall Trough, northeastern Atlantic. Progress in Oceanography, 15, 37-69.

Gordon, J.D.M. and Bergstad, O.A. (1992). Species composition of demersal fish in the Rockall Trough, North-Eastern Atlantic, as determined by different trawls. Journal of Marine Biology, 72, 213-230.

Koslow, J.A. (1994). A trophodynamic approach to the ecology of the mid-slope community off southeast Australia. Proceedings of the Australian Society for Fish Biology, Sorrento, Western Australia, August, 1993

Koslow, J.A., Bulman, C.M. and Lyle, J.M. (1994). The mid-slope demersal fish community off south-eastern Australia. Deep-Sea Research. (In press).

Mauchline, J (1990). Aspects of production in a marginal oceanic region, the Rockall Trough, northeastern Atlantic Ocean. Reviews in Aquatic Sciences, 2, 167-183.

Mauchline. J. and Gordon, J.D.M. (1984). Occurrence and feeding of berycomorphid and percomorphid teleost fish in the Rockall Trough. Journal Cons. int. Explor. Mer, 41, 239-247.

Rosecchi, E., Tracey, D.M. and Webber, W.R. (1988). Diet of orange roughy, *Hoplostethus atlanticus* (Pisces: Trachichthyidae), on the Challenger Plateau, New Zealand. Marine Biology 99, 293-306.

APPENDIX 3.

DIETS OF FIVE ABUNDANT MICRONEKTONIC FISHES FROM THE MID-SLOPE REGION OFF SOUTHEASTERN AUSTRALIA

ALAN WILLIAMS AND ALEX TERAUDS, CSIRO DIVISION OF FISHERIES

DIETS OF FIVE ABUNDANT MICRONEKTONIC FISHES FROM THE MID-SLOPE REGION OFF SOUTHEASTERN AUSTRALIA

ALAN WILLIAMS AND ALEX TERAUDS, CSIRO DIVISION OF FISHERIES

INTRODUCTION

Five dominant fish species were selected for dietary analysis; criteria for selection were primarily a high relative abundance (weight and numbers) in the mesopelagic micronekton and being present in all seasonal samples. *Photichthys argenteus* (Photichthyidae) was the top ranked species by weight, whilst three myctophids, *Lampanyctus australis*, *Diaphus danae* and *Hygophum hanseni*, ranked one to three in overall numerical abundance and in the top nine species by weight. *Chauliodus sloani* (Chauliodontidae), ranked tenth by weight and known to be a frequent constituent of the diet of *H. atlanticus* (Bulman and Koslow 1992), was chosen as a representative of the deep mesopelagic fauna.

METHODS

Fishes were selected for study from catches which contained 20 or more individuals to permit meaningful assessment of size range within a depth stratum. Length (to the nearest mm) and blotted wet weight (to the nearest g) were recorded for each fish but only specimens which showed no evidence of net feeding or regurgitation (prey evident in oesophagus or buccal cavity) were dissected. Prior to the removal of the stomach, fish sex was also recorded. Stomach fullness (estimated on a scale of 0-4), overall prey digestion stage (estimated on a scale of 0-3) and the wet weight of the total contents were recorded. The identity and relative proportion of all constituent items was assessed and converted to wet weight per prey category based on its proportion of total contents. Subsequently, the stomach contents were air dried at 60°C in a biological drying oven and reweighed (to 1 mg) on a Mettler microbalance to yield dry weight for total contents and each prey category.

PRELIMINARY RESULTS

In total, 460 *P. argenteus*, 821 *L. australis*, 516 *D. danae*, 316 *H. hanseni* and 57 *C. sloani* were examined.

Calanoids and euphausiids predominated in the diets of the myctophids, with the calanoids *Neocalanus tonsus* and species of the genus *Pleuromamma* , and euphausiids from the genus *Euphausia* being most prevalent (Tables 1-5). The vertical distributions of major zooplankton species were strongly correlated with depth (Terauds, this report). Prey vertical distribution agreed well with the nighttime vertical distributions of these three myctophids. Thus, the nyctoepipelagic species, *D. danae* and *H. hanseni*, had larger proportions of shallower living zooplankton species in their diets.

The diet of *D. danae* appeared to vary throughout the year, although some prey species were always present. The major prey items were calanoid copepods, primarily species of *Pleuromamma*. Euphausiids were also relatively common, becoming the dominant prey item during autumn. During the other seasons, however, smaller prey items such as calanoids and to a lesser extent, ostracods predominated.

Although the stomachs of *H. hansenii* showed a tendency to be relatively full, the level of digestion was also high. As a result, the identification of prey items to species level was difficult and general 'remains' categories were often the best level of resolution possible. As was seen in *D. danae*, calanoids, especially *N. tonsus* and *Pleuromamma* species, and euphasiids, were important components of the diet. Again some seasonal variation in diet was observed with *Pleuromamma* becoming more common in summer and winter, with euphausiids predominating in autumn.

Neocalanus tonsus and euphausiid species were the major components in the diet of *L. australis*. Qualitative observations indicated that this species consumed a larger class of prey items than *D. danae* and *H. hanseni*. The presence of decapods and the relatively high abundance of euphausiids also provides evidence that this species preferentially feeds on larger prey items. The range of prey consumed by *L. australis* appeared to be larger than that of *D. danae* and *H. hanseni*, however, this may be a consequence of examining a larger number of stomachs. In addition, it was possible to identify many prey items to species level because of their frequently low degree of digestion. Euphausiids also predominated in the diet of *L. australis* during autumn. Fish scales were commonly found in the stomachs of *L. australis*– something not seen in *D. danae* and *H. hanseni*. Scales were probably gulped into the stomachs of these fish whilst in the cod-ends of the net, perhaps indicating an increased activity or robustness compared to *D. danae* and *H. hanseni*.

Photichthys argenteus was unlike the species of myctophid studied in that calanoids did not form a large component of the diet. Fish appeared to be important and fish remains were a relatively common component of the stomachs examined. Overall, this species appeared to prefer larger prey items. The presence of gammariid amphipods in several stomachs indicates that some individuals were be benthic or benthopelagic feeders. The contents of most stomachs were well digested and subsequently identifications could rarely be made to species level. In addition, >50% of stomachs were empty and, despite our pre-dissection scrutiny, it is likely that this was due to regurgitation after capture.

Relatively few stomachs from *Chauliodus sloani* were examined meaning that fewer inferences about its diet can be made. It was obvious, however, that the diet of *C. sloani* differed significantly from the other four species examined. It appeared to feed primarily on fish, with few crustacean remains found in any of the stomachs. Prey items were also relatively large. These observations are consistent with the infrequent feeding on large prey commonly seen in deep mesopelagic stomiiform fishes.

Table 1 Percentage occurrence of prey items in *Photichthys argenteus*

Photichthys argenteus
% occurrence of prey
items

	Spring	Summer	Autumn	Winter
No. fish examined	61	97	131	171
No. stomachs with contents	36	65	95	60
Amphipods				
Hyperiidea	5.6	3.1	1.1	3.3
Gammariidea		6.2		1.7
Parathemisto (Hyperiidea)			1.1	
Calanoid copepods				
Unidentifiable calanoid	5.6	7.7	2.1	1.7
Calanoid remains	5.6	4.6	4.2	8.3
Neocalanus tonsus	2.8	1.5		1.7
Paraeucheata spp.		4.6		
Paracalanus spp.		1.5		
Pleuromamma spp.	5.6	15.4	1.1	5.0
Pleuromamma gracilis		4.6	1.1	
Pleuromamma abdominalis		6.2		
Pleuromamma remains	5.6	4.6	8.4	
Metridia lucens		7.7		
Heterorhabdus spp.		1.5		
Eucalanus hyalinus		1.5		
Scottocalanus spp.	2.8			
Decapods				
Decapoda		1.5		
Decapod remains				1.7
Pasiphae spp.				1.7
Gennadas spp.			2.1	3.3
Sergestid prawn		1.5		
Euphausids				
Euphausiidacea		13.8	9.5	5.0
Euphausiid remains	27.8	21.5		13.3
Nematoscelis megalops		1.5		3.3
Euphausia spinifera		3.1	32.6	
Euphausia similis (var armata)	2.8		1.1	5.0
Fishes				
Unidentified fish				5.0
Fish remains			2.1	1.7
fish scales	11.1	27.7	4.2	3.3
fish lenses	2.8		1.1	3.3
Chauliodus larvae		1.5		

Myctophidae	2.8		1.1	
Other groups				
Gelatinous zooplankton		3.1		1.7
Bivalvia				3.3
Gastropoda				1.7
Ostracoda	16.7	12.3	2.1	5.0
Pyrosoma		1.5		3.3
Larvacean	2.8			
Chaetognatha		3.1		
Stomach lining	19.4	6.2	6.3	8.3
Crustacean remains	33.3	24.6	37.9	25.0
Unidentifiable remains	22.2	16.9	15.8	25.0

Table 2 Percentage occurrence of prey items in *Lampanyctus australis*

Lampanyctus australis % occurrence of prey items	Spring	Summer	Autumn	Winter
No. fish examined	162	128	238	293
No. stomachs with contents	145	105	221	247
Amphipods				
Hyperiid remains			0.5	0.8
Hyperiidea	3.4	2.9	0.9	2.8
Gammariidea		1.0	0.5	
Phronimidae (Hyperiidea)				0.4
Phronima sedentaria				1.2
Parathemisto (Hyperiidea)	1.4	1.9	0.5	
Hyperiidae (Hyperiidea)	1.4			0.4
Lanceola spp.		1.0		
Calanoid copepods				
Unidentifiable calanoid	14.5	17.1	2.7	15.4
Calanoid remains	9.7	12.4	4.1	17.8
Neocalanus tonsus	22.1	16.2	0.5	17.8
Candacia spp.		1.9		0.4
Paraeucheata spp.	2.1	9.5	1.4	2.8
Paraeuchaeta biloba	0.7			1.2
Rhincalanus nasutus	0.7			0.4
Pleuromamma spp.	4.1	6.7	1.8	7.3
Pleuromamma gracilis			0.5	2.8
Pleuromamma abdominalis	2.8		0.5	4.5
Pleuromamma quadrangulata	2.1	1.9		0.4
Pleuromamma xiphias			0.5	1.6
Pleuromamma remains	5.5	8.6	1.4	21.5
Metridia lucens	1.4	4.8		1.2
Heterorhabdus spp.		1.9		
Eucalanus hyalinus		1.9		
Scottocalanus spp.			1.8	
Neocalanus gracilis				0.4
Lucicutia spp.		1.0		
Gaetanus spp.		1.9		
Gaetanus latifrons		1.0		

	1	2	3	4
Subeucalanus longceps		1.0		
Megacalanus princeps	2.8	1.0		
Euchirella rostrata	2.1			
Calanus australis			1.4	
Decapods				
Decapoda	0.7			
Pasiphae spp.				0.4
Gennadas spp.	1.4		1.4	1.6
Sergestid prawn	0.7			
Euphausids				
Euphausiidacea		10.5	18.6	8.5
Euphausiid remains	33.1	46.7	62.9	21.1
Nematoscelis megalops	2.1	9.5	5.9	9.7
Euphausia spinifera	0.7	4.8	24.0	0.8
Euphausia similis (var armata)		2.9	21.3	4.9
Euphausiid furcilia remains			0.5	
Euphausiid furcilia	15.9	8.6	6.8	1.2
Euphausia spp.			0.9	
Fishes				
Unidentified fish		1.0	0.5	0.4
Fish remains			0.5	
Maurolicus mulleri				0.4
fish scales	35.9	54.3	9.0	17.0
Myctophidae				0.4
Other groups				
Gelatinous zooplankton				0.4
Bivalvia				0.8
Ostracoda	9.7	9.5	0.5	7.7
Pyrosoma		1.0		
Polychaeta				0.4
Stomach lining	1.4		0.9	6.5
Crustacean remains	19.3	13.3	9.0	19.0
Unidentifiable remains	4.8	1.0		11.7

The great variety and seasonal peaks in the occurrence of particular prey species indicated that these fishes were opportunistic rather than preferential feeders. Feeding appeared to be on abundant species in certain size classes rather than on specific prey species. Further analysis and comparison with the zooplankton distribution data is needed to further evaluate this observation.

Table 3 Percentage occurrence of prey items in *Hygophum hanseni*

Hygophum hanseni
% occurrence of prey items

	Spring	Summer	Autumn	Winter
No. fish examined	4	25	173	114
No. stomachs with contents	3	20	129	102
Amphipods				
Hyperiidea			0.8	2
Parathemisto (Hyperiidea)			1.6	
Calanoid copepods				
Unidentifiable calanoid	33	10	0.8	11.8
Calanoid remains		15	3.9	16.7
Neocalanus tonsus	33			14.7
Candacia spp.				2
Paraeucheata spp.		5	0.8	9.8
Paraeuchaeta biloba			0.8	1
Pleuromamma spp.			0.8	8.8
Pleuromamma gracilis		5	3.1	9.8
Pleuromamma abdominalis			0.8	2
Pleuromamma remains		45	33.3	44
Metridia lucens			0.8	
Calanus australis			1.6	
Candacia curta				2
Decapods				
Decapoda				1
Euphausids				
Euphausiidacea			5.4	6.9
Euphausiid remains		30	38.8	32.4
Nematoscelis megalops				1
Euphausia spinifera			6.2	
Euphausia similis (var armata)			5.4	3
Euphausiid furcilia		20	9.3	10.8
Euphausia spp.			3.1	
Euphausiid nauplii			1.6	
Fishes				
fish scales		10	2.3	
Myctophidae				1
Other groups				
Gastropoda				2
Ostracoda		5	1.6	3
Stomach lining				3.9
Crustacean remains	100	40	17.8	19.6
Unidentifiable remains			0.8	3

Table 4 Percentage occurrence of prey items in *Diaphus danae*

Diaphus danae
% occurrence of prey items

	Spring	Summer	Autumn	Winter
No. fish examined	60	291	0	165
No. stomachs with contents	60	279	0	151
Amphipods				
Amphipoda		0.4		
Hyperiid remains	1.7			1.3
Hyperiidea	5.0	4.3		2.0
Gammariidea		0.4		
Phronimidae (Hyperiidea)	1.7			
Parathemisto (Hyperiidea)	3.3	0.7		
Hyperiidae (Hyperiidea)		0.7		1.3
Calanoid copepods				
Unidentifiable calanoid	20.0	9.0		6.6
Calanoid remains	10.0	10.4		20.5
Neocalanus tonsus	11.7	0.4		6.6
Candacia spp.	1.7	1.4		
Paraeucheata spp.		4.3		2.0
Paraeuchaeta biloba				0.7
Paracalanus spp.				1.3
Rhincalanus nasutus	1.7			0.7
Pleuromamma spp.	10.0	10.4		10.6
Pleuromamma gracilis	1.7	6.1		14.6
Pleuromamma abdominalis	5.0	4.3		6.0
Pleuromamma quadrangulata		0.7		2.0
Pleuromamma xiphias		1.1		0.7
Pleuromamma remains	1.7	30.8		33.8
Metridia lucens	5.0	3.9		2.6
Calanoides microcarinatus				0.7
Heterorhabdus spp.	1.7	1.1		
Eucalanus hyalinus		0.7		
Scottocalanus spp.		0.4		
Neocalanus gracilis		0.4		
Lucicutia spp.		0.4		
Gaetanus spp.		1.4		
Euchirella rostrata	1.7			
Calanus australis		1.8		
Euchirella latirostris		0.4		
Gaetanus minor		0.4		
Aetideus spp.		0.7		
Cyclopoids				
Cyclopoid	1.7			0.7
Oncaea spp.				1.3
Decapods				
Decapod remains		0.4		

Gennadas spp.		0.4	
Euphausids			
Euphausiidacea	3.3	6.8	
Euphausiid remains	60.0	40.9	13.9
Nematoscelis megalops	1.7	0.7	2.0
Euphausia spinifera		9.0	
Euphausia similis (var armata)		1.4	1.3
Euphausiid furcilia remains		0.7	
Euphausiid furcilia	11.7	7.9	3.3
Euphausia spp.		4.3	
Fishes			
Hygophum hansenii		0.4	
Fish remains	1.7	1.1	1.3
fish scales	18.3	33.0	13.2
fish eggs		0.4	2.0
fish lenses		0.7	
Other groups			
Bivalvia	1.7		
Gastropoda	3.3	1.8	7.9
Mollusca		0.4	
Ostracoda	46.7	5.7	13.2
Pyrosoma	1.7		
Larvacean	1.7	0.7	
Chaetognatha		0.4	2.0
Polychaeta			0.0
Stomach lining	8.3	2.9	4.0
Crustacean remains	38.3	30.5	7.9
Unidentifiable remains	10.0	3.6	23.2

Table 5 Percentage occurrence of prey items in *Chauliodus sloani*

Chauliodus sloani
% occurrence of prey items

	Spring	Summer	Autumn	Winter
No. fish examined	3	15	26	13
No. stomachs with contents	0	5	8	4
Lampichthys proceros			12.5	
Hygophum hanseni			12.5	50
Myctophidae		40	37.5	
Stomiiform fish remains			12.5	50
Fish remains		40	37.5	

APPENDIX 4.

SEASONAL BIOMASS AND DISTRIBUTION OF THE DEMERSAL FISH COMMUNITY OF THE MID-SLOPE OFF SOUTHERN TASMANIA

CATHY M. BULMAN, CSIRO DIVISION OF FISHERIES

SEASONAL BIOMASS AND DISTRIBUTION OF THE DEMERSAL FISH COMMUNITY OF THE MID-SLOPE OFF SOUTHERN TASMANIA

C. M. BULMAN
CSIRO DIVISION OF FISHERIES

METHODS

In each of the four trophodynamic cruises, a series of demersal trawls was made over a 24 h period. Tows of between half and one hour duration were made every four hours. The fish caught were identified to species, weighed and enumerated. Biological samples and information were obtained from selected species.

For each species, catch weights were summed across all tows. The mean biomass for each species was calculated by dividing the total catch weight by the total area swept by the net over all tows. The proportion of each species in the total catch was also calculated.

RESULTS

During the winter cruise, 55% of the overall demersal fish biomass for all cruises was caught: catches from the other three cruises were one third to one fifth of the winter cruise (Table 1). Orange roughy, *Hoplostethus atlanticus*, dominated the winter catches (Figs 1 & 2); 55% of the biomass was roughy (Fig 2), and 82% of all roughy caught were from this cruise. Its biomass was more than three times greater than any other species in any other cruise. Overall it was the most abundant species (Table 2). *Alepocephalus* spp., *Coryphaenoides subserrulatus*, *Etmopterus baxteri* and *Centroscymnus crepidater* were also relatively abundant species during winter, each representing between 3-10% of the winter biomass. The mean fish biomass was 1.057 $g.m^{-2}$.

Table 1. Biomass of demersal fish caught in deep water (1000m) off southern Tasmania, 1991-1993.

	2/91 (WINTER)	1/92 (SUMMER)	4/92 (SPRING)	3/93 (AUTUMN)	TOTAL
Overall fish biomass ($g.m^{-2}$)	2.037	0.365	0.932	3.188	1.057
Total weight caught (kg)	1755.9	347.51	549.87	530.47	3183.76
No. tows	9	5	11	7	32

Halargyreus johnstonni was an important component in the summer, comprising 22% of the biomass which was slightly greater than *H. atlanticus*. *Alepocephalus* spp. and *C. subserrulatus* were also still abundant (Fig 2). *Allocyttus verrucosus* was also abundant. The mean fish biomass during summer was about 20% of that in winter (Table 1).

Diastobranchus capensis dominated spring and autumn catches, (25% and 19% by weight (Fig 2)). It was also most abundant in spring when 46% of the overall eel catch was caught. *H. atlanticus, Alepocephalus* spp. and *E. baxteri* were major components of the biomass also (Figs 1 & 2). Fish biomass in spring was about 80% that of the winter.

Allocyttus verrucosus was caught mostly in autumn (50% of overall warty dory catch) although it only contributed less than 10% of the species composition (Fig 2). The other oreo dories were even less common. *H. atlanticus* was much less important in this season than in any other. *D. capensis* was the most prominent species in autumn, followed by *H. johnstonni, C. subserrulatus, Alepocephalus* spp., and *A. verrucosus*. Mean fish biomass was 0.88 gm^{-2}.

The combined *Alepocephalus* spp. catch was between 10-17% by weight of the catches of all cruises (Table 2). The ratios of the two species varied but may have been due to identification problems.

Coryphaenoides subserrulatus was the most common whiptail (Table 2). It was abundant during winter and autumn but its proportion in catches remained at about 10% in all except the spring cruise (2%) (Fig 2). Other whiptails comprised less than 1% of all catches (Table 2).

Sharks (dogfish) were also a major component of the catches, usually between 10-15% of the biomass (Fig 1 & 2, Table 2). The actual species composition differed from cruise to cruise.

Table 2. Overall species composition and biomass

SPECIES	% BIOMASS	BIOMASS (10^3 GM-2)
Hoplostethus atlanticus	36.89	389.92
Diastobranchus capensis	9.38	99.14
Alepocephalus sp. 1	8.22	86.86
Coryphaenoides subserrulatus	7.44	78.67
Halargyreus johnstonii	6.96	73.51
Etmopterus baxteri	4.76	50.30
Centroscymnus crepidater	4.52	47.76
Alepocephalus sp. 2	3.56	37.68
Allocyttus verruccosus	3.38	35.70
Macrourus carinata	2.72	28.70
Deania calcea	1.98	20.94

SPECIES	% BIOMASS	BIOMASS (10^3 GM^{-2})
Centroscymnus owstoni	1.66	17.51
C. coelolepis	1.42	15.00
Neocyttus rhomboidalis	0.78	8.24
Pseudocyttus maculatus	0.44	4.67
Coelorinchus kaiyomaru	0.31	3.31
Coryphaenoides serrulatus	0.31	3.27
Allocyttus niger	0.10	1.05
Coelorinchus kermadecus	0.07	0.75
Epigonus robustus	0.05	0.55
E.lenimen	0.05	0.53
Coelorinchus innotabilis	0.02	0.18
Others	4.99	52.74

3

APPENDIX 5.

DIETS OF THE MAJOR DEMERSAL FISH SPECIES OF THE MID-SLOPE OFF SOUTHERN TASMANIA

CATHY M. BULMAN, CSIRO DIVISION OF FISHERIES

DIETS OF THE MAJOR DEMERSAL FISH SPECIES OF THE MID-SLOPE OFF SOUTHERN TASMANIA

C. M. BULMAN
CSIRO DIVISION OF FISHERIES

METHODS

The diets of 23 species were examined. A maximum of 20 stomachs were removed from each species in each tow. They were either preserved in 10% formalin if small or frozen if large. Specimens whose stomachs were everted were ignored. The contents of the stomachs were identified to lowest taxon, enumerated, weighed, dried at 60°C and re-weighed. The calorific contents of some prey items were determined using a Parr bomb calorimeter.

RESULTS

Analysis of the data is incomplete and only a quantitative view is given here.

Table 3. Diets of demersal fish species of southern Tasmania.

SPECIES	SS2/91 (WINTER)	SS1/92 (SUMMER)	SS4/92 (SPRING)	SS3/93 (AUTUMN)
Centroscymnus crepidater	Unid fish P. argenteus C. sloani Serrivomer Lampanyctus sp. M. niger A. pelagica Squid	Unid fish	Chauliodus Unid fish Gnathophausia L. procerus	no data
Deania calcea	Myctophid-size fish	no data	no data	no data
Centroscymnus owstoni	Coryphaenoides or morid Squid	no data	no data	salp
Centroscymnus coelolepis			Unid fish	Unid fish Cetacean
Diastobranchus capensis	L. australis Unid fish Mysid	Unid fish Unid crust	Sergia Squid E. baxteri Gnathophausia Unid fish Centrolophid	Unid fish Squid

SPECIES	SS2/91 (WINTER)	SS1/92 (SUMMER)	SS4/92 (SPRING)	SS3/93 (AUTUMN)
Etmopterus baxteri	Unid fish I. fasciola Gnathophausia Squid	Ceratoid H. atlanticus	Squid Fish Serrivomer	Squid Fish
Alepocephalus sp 1	Pyrosoma Fish	Pyrosoma	Pyrosoma	Pyrosoma
Alepocephalus sp. 2		Pyrosoma	Pyrosoma	Pyrosoma
Lepidion microcephalus	Unid fish Squid	no data	no data	no data
Macruronus novaezelandiae	Myctophidae	no data	no data	no data
Macrourus carinata	C. subserrulatus			
Coelorinchus innotabilis	Eurythenes Penaeidae	no data	no data	Unid crustacea
C. serrulatus	L. australis Penaidae Unid fish crab	Mysid	Amphipoda Squid Unid fish	Unid fish Crustacea incl crabs Squid
C. subserrulatus	Unid & calanoid copepods Mysid Myctophidae Holothurian Gammarids Polychaeta	Mysid Unid fish	Neocalanus Euchaeta Squid Unid fish Sergestes Unid crust	Crustacea-copepods Mysid Unid fish
C. kaiyomaru	Polychaeta fish Copepods	Unid fish	Gammarid Gennadas Isopod Polychaeta Unid molluscs Copepods	Polychaeta Amphipod
C. kermadecus			Ampihpoda Fish	Unid crustacea
Hoplostethus atlanticus	Boreomysis Gnathophausia Caridae Bathylagus Chauliodus Lampanyctus Gammaridae	Gnathophausia Eurythenes Lipkius Sergia Coelorinchus	Amphipoda Mysid Unid fish Sergia Lyssianassidae C. subserrulatus Squid	Unid crustacea Unid fish Sergestes sp. Acanthephyra sp

5

SPECIES	SS2/91 (WINTER)	SS1/92 (SUMMER)	SS4/92 (SPRING)	SS3/93 (AUTUMN)
	Unid fish		Neoscopelus Eurythenes	
Neocyttus rhomboidalis	Pyrosoma Pandalidae	Pyrosoma		no data
Pseudocyttus maculatus	Pyrosoma	Pyrosoma Unid fish	Squid	no data
Allocyttus verrucosus	Amphipoda Mysid Chauliodus Unid fish Squid	Unid fish Mysid Squid Ostracoda Amphipoda	Unid fish Unid crustacea Squid Mysid	Unid fish Unid crustacea Squid Mysid
Epigonus lenimen			Neocalanus	Unid crustacea Pyrosoma
E. robustus			Neocalanus	Unid crustacea Pyrosoma
Tetragonurus cuvieri			Pyrosoma	

Small pelagic fishes such as myctophids were eaten largely by sharks, *Diastobranchus capensis*, *Macruronus novaezelandiae*, *Hoplostethus atlanticus* and *Allocyttus verrucosus* . Carid and penaeid prawns also contributed to these fishes' diets. Smaller fishes, such as the whiptails, relied more heavily on prawns and smaller crustaceans. Pyrosoma was a major, and often, the only dietary item of several species; *Neocyttus rhomboidalis, Pseudocyttus maculatus, Alepocephalus* spp., and *Epigonus* spp. Squid was a minor component of *H. atlanticus* diets and also of *D. capensis* , *Etmopterus baxteri,* and *A. verrucosus.* Only *Coelorinchus innotabilis* and *H. atalnticus* ate species which were benthic such as the Lyssianassid *Eurythenes* sp. and small molluscs.